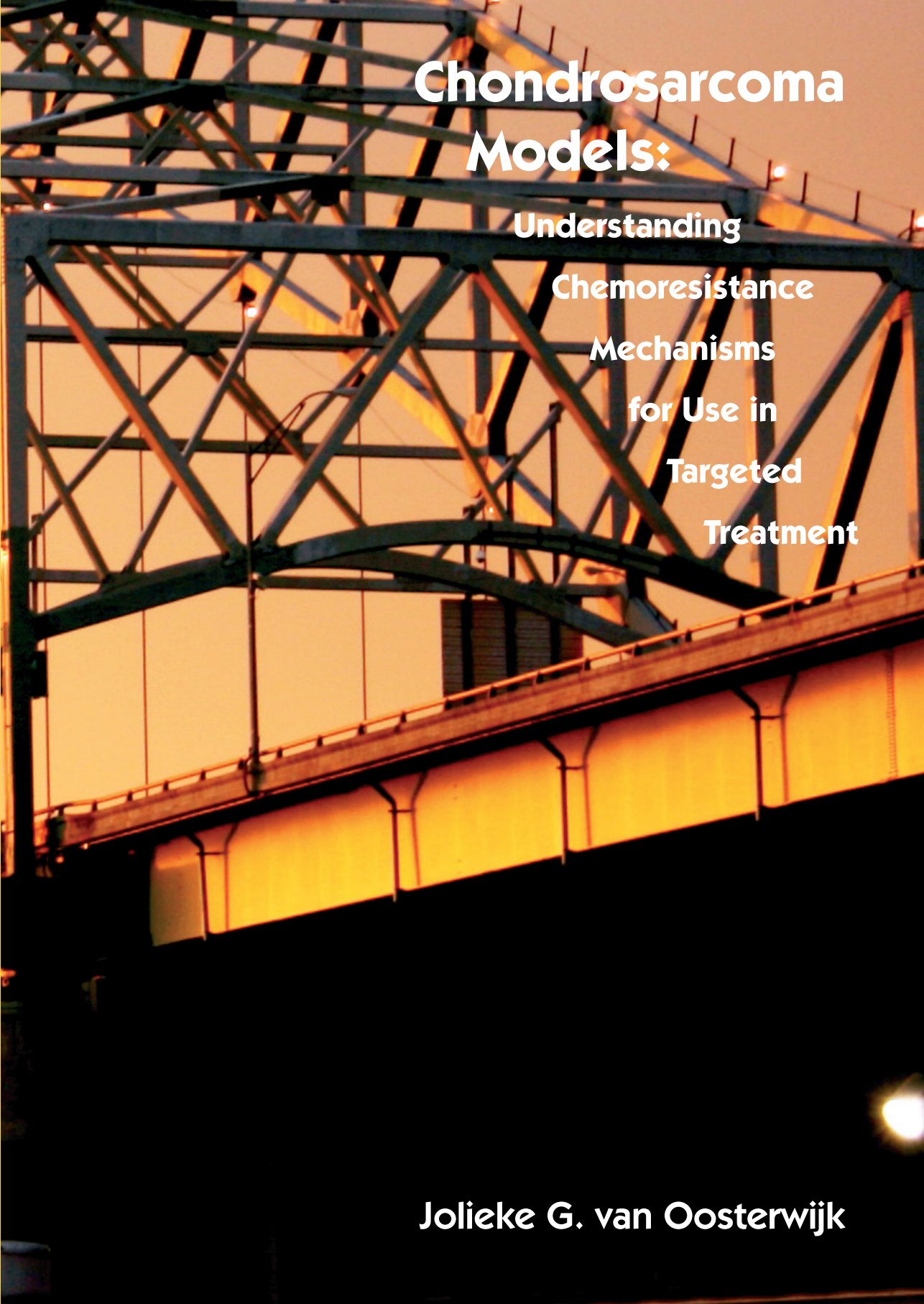

Chondrosarcoma Models:

Understanding Chemoresistance Mechanisms for Use in Targeted Treatment

Jolieke G. van Oosterwijk

CHONDROSARCOMA MODELS: UNDERSTANDING CHEMORESISTANCE MECHANISMS FOR USE IN TARGETED TREATMENT

The work presented in this thesis was financially supported by EuroBoNet, a European Commission granted network of Excellence for studying the pathology and genetics of bone tumors (917-67-315), EuroSARC, a European Commission granted FP7 clinical trials network (278742), and the Dutch Cancer Society (UL2010-4873).
Cover art: Photograph taken by J.G. van Oosterwijk of the "Hernando de Soto", or "M", bridge from Memphis, TN, to Arkansas. Editing by Thijs van Himbergen.
Printed by: Drukkerij Mostert en van Onderen, Leiden, the Netherlands.

CHONDROSARCOMA MODELS: UNDERSTANDING CHEMORESISTANCE MECHANISMS FOR USE IN TARGETED TREATMENT

Proefschrift

ter verkrijging van
de graad van Doctor aan de Universiteit Leiden,
op gezag van Rector Magnificus prof.mr. C.J.J.M. Stolker,
volgens besluit van het College voor Promoties
te verdedigen op dinsdag 19 november 2013
klokke 13.45 uur

door

Jolieke Gerdy van Oosterwijk
geboren te Leiden
in 1984

Promotiecommissie
Promotor:Prof. dr. J.V.M.G. Bovée
Overige leden:Prof. dr. P.C.W. Hogendoorn
Prof. dr. A.J. Gelderblom
Prof. B. van de Water
Prof. dr. J.-Y. Blay (Université Claude Bernard Lyon I, Centre Léon Bérard, France)

Voor Opa

Chapter 1

General Introduction

I. Primary Chondrosarcoma

Primary bone tumors are rare, constituting 0.2% of all reported neoplasms (1). Malignant cartilage tumors of bone are classified as chondrosarcomas. After osteosarcoma, primary chondrosarcoma is the second most frequent high grade bone tumor in humans, and is most common in adults between the 3rd and 6th decade of life. Conventional chondrosarcoma is the most common variant, and constitutes about 85% of all chondrosarcomas (fig 1) (2).
Chondrosarcomas frequently occur in the bones of the pelvis, ribs and bones of the extremities, and are much more rare in the skull or small bones of the hands and feet. Patients often present with persistent swelling and/ or pain. Using conventional imaging, a radiolucent lesion with ring-like opacities can be observed due to calcifications, MRI imaging is helpful to determine matrix calcification and soft-tissue involvement. A central chondrosarcoma typically arises in the metaphysis or epiphysis and dynamic contrast enhanced MRI is a helpful tool in identifying malignancy. In the diagnosis of a peripheral chondrosarcoma, arising on the surface of the bone, an MRI scan can be particularly helpful as a cartilage cap >1.5-2cm is an indicator of malignancy (3;4). Histologically, conventional chondrosarcomas are divided into 3 grades (5). As the former grade I chondrosarcoma (CSI) (6) was rarely reported to metastasize, in the 2013 WHO classification CSI is reclassified as atypical cartilaginous tumor (ACT), being of the intermediate, locally aggressive category and will here be referred to as ACT/ CSI. High grade chondrosarcomas that are more prone to metastasize, are classified as grade II (CSII) and grade III (CSIII) chondrosarcoma (2).
An important predictor for local recurrence is the margin status upon resection. The most important predictor of metastases is histological grade. So far no molecular markers have been identified that are independent from and better than histological grading, and correct assessment of histological grade requires an experienced pathologist. An ACT/ CSI will show ample hyaline cartilaginous matrix surrounding the cells that have small hyperchromatic nuclei, whereas CSII and CSIII will show increased cellularity, nuclear atypia, and nuclear size. Grade III lesions are more cellular than grade II lesions with high mitotic count, more myxoid matrix and spindle cell changes at the edge of the lobuli. The distinction between a benign enchondroma and an ACT/ CSI can prove difficult and a high interobserver variability has been established (7-9). For clinical management, the distinction between ACT/ CSI and CSII is more important, which is less subjected to interobserver variability (8). In ACT/ CSI, curettage with local adjuvans is showing good long term results with <6% local recurrence rate (10) and currently has a 5 year survival rate of 83%. In CSII and CSIII, en-bloc resection is required and wide resection margins are necessary to prevent local recurrence, as 13% of local recurrences show an increase in histological grade. The combined 5 year survival rate for CSII/ CSIII is 53% (2;5;10;11).

II. Secondary chondrosarcoma arising in benign cartilaginous tumors

Enchondroma and secondary central chondrosarcoma

A conventional chondrosarcoma arising from a pre-existing benign precursor lesion is classified as a secondary chondrosarcoma (fig 1). Enchondromas are benign cartilaginous lesions arising in the medullary cavity of the bone. Enchondromas are most common in the short tubular bones where they can cause palpable swellings, and less common in the long tubular bones and flat bones, in which case these lesions are mostly asymptomatic and often incidentally detected in radiographs. The majority of enchondromas are detected between the second to fifth decade of life and are solitary. Occasionally involvement of more than one bone or multiple lesions in one bone are observed, indicating enchondromatosis. The most common enchondromatosis subtypes are Ollier disease (multiple enchondromas often in a unilateral distribution) or Maffucci syndrome (multiple enchondromas combined with (spindle cell) hemangiomas) (12;13).

Recently, mutations in *isocitrate dehydrogenase -1* (*IDH1*) or *-2* (*IDH2*) were identified in 87-93% of enchondromas (14-16). IDH mutations were originally discovered in glioblastomas (17), and the molecular mechanism in tumor formation is currently being elucidated. Both IDH1 and IDH2 are mitochondrial enzymes in the tricarboxylic acid (TCA) cycle and are dependent on NADP+. Under normoxic conditions, NADPH and α-ketoglutarate is produced, the latter crucial in preventing the stabilization of HIF-1α (18). IDH mutations lead to a shift in the TCA cycle favoring the production of the oncometabolite D-2-hydroxyglutarate (D2HG) (19-22). The increased D2HG production has been reported to contribute to tumor formation through epigenetic mechanisms such as impairment of histone and DNA demethylation (23-25). As α-ketoglutarate and D2HG show a high degree of structural homology, they share the same substrates. Accumulation of D2HG can inhibit the histone demethylases, as well as the TET family of methylcytosine hydroxylases, otherwise activated by α-ketoglutarate (26-28). Aberrant DNA methylation patterns have been observed in IDH mutant primary tumors (23;28-31) including enchondromas (14). Using a knock-in approach, a heterozygous IDH1 R132H mutation was introduced into a human colorectal cancer cell line, inducing genome-wide histone and CpG methylation, along with a change in gene expression, supporting the causative role of IDH mutations in tumorigenesis (32). Moreover, IDH induced hypermethylation has been shown to block cell differentiation in hematopoetic stem/progenitor cells and adipocytes (24;28).

Prolyl hydroxylases, responsible for the degradation of HIF1/2α proteins and maturation of collagen proteins, are also dependent on α-ketoglutarate. The role of D2HG in creating a "pseudohypoxic" state by preventing the proteosomal degradation of HIF1α is still under debate (27;33), but IDH1 R132H knock-in mutant mice were shown to have decreased ROS levels and stabilization of HIF1α proteins. Though IDH1 mutations were under a brain-specific promoter, the same

study showed collagen maturation to be perturbed after IDH1 R132H knock-in and to be attributed to D2HG accumulation (34).
The role of IDH mutations and the induced epigenetic changes resulting from D2HG accumulation in the progression from enchondroma to atypical cartilaginous tumor/CSI still remains to be determined (fig 1). Enchondromas were found to be mosaic, harboring both wildtype cells and IDH mutant cells (14). Moreover, IDH mutations were found in 38-70% of primary and 85-88% of secondary chondrosarcomas (14;16;35). In enchondromatosis the risk factors for malignant transformation include age and location. Enchondromas located in the long tubular bones and flat bones were reported to give rise to chondrosarcomas in 45% and 50% of Ollier and Maffucci patients, respectively. Although enchondromas are most common at the short tubular bones, malignancy at this location occurred in only 15% of Ollier patients, and in none of the Maffucci patients. Patients with enchondromas in both the long and short tubular bones were most prone to develop chondrosarcomas, showing 46% and 62% incidence in Ollier and Maffucci patients, respectively (2;36).

Osteochondroma and secondary peripheral chondrosarcoma
Secondary peripheral chondrosarcomas arise from osteochondromas, benign cartilage capped bony projections arising on the surface of the bone. Patients usually present in the first three decades of life with a, usually asymptomatic, persistent hard mass. In approximately 15% of patients multiple lesions can be found, characteristic of multiple osteochondromas (previously called multiple hereditary exostoses), a hereditary autosomal dominant syndrome (37) caused by germline mutations in *exostosin-1* (*EXT1*) or *-2* (*EXT2*) (fig 1). In sporadic osteochondromas, somatic homozygous deletions of *EXT1* can be found (37;38). EXT is a glucosyltransferase important in the synthesis of heparan sulfate, a proteoglycan essential for IHH diffusion in the growth plate (39).
Chondrocytes mature in a matrix rich environment and are dependent on the proteoglycan-mediated diffusion of morphogens through their extracellular matrix. The morphogen Indian hedgehog (IHH) and parathyroid hormone-related protein (PTHrP) control the cells in the hypertrophic and proliferating zones, through a negative feedback loop (40;41). Impaired IHH signaling and retention of PTHrP can lead to an increase in proliferating chondrocytes and inhibition of differentiation. Recently, osteochondromas were shown to be mosaic, containing both wildtype and *EXT* mutant cells (42;43), and secondary peripheral chondrosarcomas have been shown to arise from the wildtype *EXT* cells as they no longer contain *EXT* mutations (fig 1) (44). The *EXT* mutations of their neighboring cells, however, are thought to create an environment in which the wildtype cells are prone to developing yet unknown (epi-)genetic changes (fig 1) (45). Though no longer containing *EXT* mutations, loss of inhibitory feedback of IHH on PTHrP and BCL-2 was shown to correlate with progression from osteochondroma to peripheral chondrosarcoma (46;47).

In central chondrosarcoma, EXT and its downstream pathways have been studied as well. Despite wildtype *EXT*, aberrant IHH signaling is found, along with retention of PTHrP in high grade central chondrosarcomas (48;49), suggesting an EXT independent mechanism towards tumorigenesis. Reports about the suitability of the hedgehog pathway as a therapeutic target in central chondrosarcoma are conflicting, as targeting the hedgehog pathway with triparanol led to reduction in tumor growth in mouse xenografts (48), but cyclopamine was effective in only 1 of 6 cell lines (50).
Malignant transformation to secondary peripheral chondrosarcoma is found in ~1% of solitary osteochondromas, whereas in patients with multiple osteochondromas progression to secondary peripheral chondrosarcoma is reported in ~5% of cases (2).

III Rare chondrosarcoma subtypes
The rare chondrosarcoma subtypes include dediffferentiated chondrosarcoma (10%), mesenchymal chondrosarcoma (3%), and clear cell chondrosarcoma (2%).

Dedifferentiated chondrosarcoma
A dedifferentiated chondrosarcoma is histologically comprised of two clearly defined compartments; a highly cellular high grade anaplastic or undifferentiated component juxtaposed to a usually low grade chondrosarcoma. In addition to pain and swelling, patients can present with paresthesia and pathological fractures due to cortical destruction by the tumor. Upon imaging, an ill-defined lesion can be observed, and the irregular calcification showing both ring-like cartilaginous components and a high grade lytic permeable component can indicate the presence of a dedifferentiated component (51). Dedifferentiated chondrosarcoma shows a relentless clinical course and a large retrospective study revealed that survival is highly dependent on presence of metastasis at diagnosis. Patients presenting with metastases have a 2 year survival rate of only 10%, compared to a 28% 10 year survival in patients presenting without metastasis (52).
As dedifferentiated chondrosarcoma histologically shows two clearly defined regions, genetic markers were investigated to determine whether the two compartments are derived from a common origin (53;54). Recently, IDH mutations were found in 54% of dedifferentiated chondrosarcomas, and were not mutually exclusive with TP53 mutations (14;53). As identical IDH and TP53 mutations as well as loss of p16 expression has been found in the two different components this is suggestive of a common clonal origin and thought to be early events contributing to its histogenesis (fig 1) (53;54). Immunohistochemically, distinct pathway activation such as PTHLH expression (55) as well as different loss of heterozygosity patterns (54) can be observed, suggesting an early diversion of the two components (fig 1). MYC (56) and MDM2 (53) amplification have only been

reported in the dedifferentiated component and are therefore likely to be late events occurring after the separation of the two components
As the prognosis is dependent on the dedifferentiated component, research aims at identifying pathways distinctly activated in this component for the development of therapeutic strategies.

Mesenchymal chondrosarcoma
Mesenchymal chondrosarcoma shows a mixture of undifferentiated cells with islands of well differentiated hyaline cartilage. Mesenchymal chondrosarcoma shows a widespread skeletal distribution, including the craniofacial bones, and primary soft tissue localization is reported in approximately 20-30%. Patients present with pain and swelling, occasionally of sudden onset, but most often present for at least one year (57). Due to its aggressive course, long term follow up is recommended. Tumor localization in the jaw or metastasis at time of presentation is a bad indicator for prognosis, whereas young age appears to be a good prognostic factor (58;59). Upon imaging, mesenchymal chondrosarcoma presents as an ill-defined, lytic lesion, often with cortical destruction, in most cases resembling high grade conventional chondrosarcoma (57).
Mesenchymal chondrosarcomas were recently shown to carry the HEY1-NCOA2 fusion gene (60), and a HEY1-NCOA2 negative lesion was found to carry an IRF2BP2-CDX1 fusion gene (fig 1) (61). Mesenchymal chondrosarcomas have not been found to carry IDH mutations, and mutations in TP53, p16, or MDM2 are also found to be rare events (53;62;63). However, Rb pathway dysregulation was found in 70% of mesenchymal chondrosarcomas (53).

Clear cell chondrosarcoma
Clear cell chondrosarcoma represents a low grade chondrosarcoma showing clear cells with a distinct membrane surrounded by a hyaline cartilaginous matrix. Clear cell chondrosarcoma is most common on the epiphyseal ends of long bones, and shows the best prognosis with a mortality of 15%. The most common presenting symptom is pain, and upon imaging a well defined lytic lesion in the epiphysis of a long bone is observed, occasionally showing a sclerotic rim. The best curative option is en-bloc excision with clear margins. Clear cell chondrosarcoma is the only subtype reported to have a sex preference as it occurs three times more often in men than in women (64).
Clear cell chondrosarcomas show random chromosome losses or gains, often with hemizygous involvement of the CDKN2A/p16 locus (fig 1). No involvement of IDH, TP53, or MDM2 has been reported (14;53).

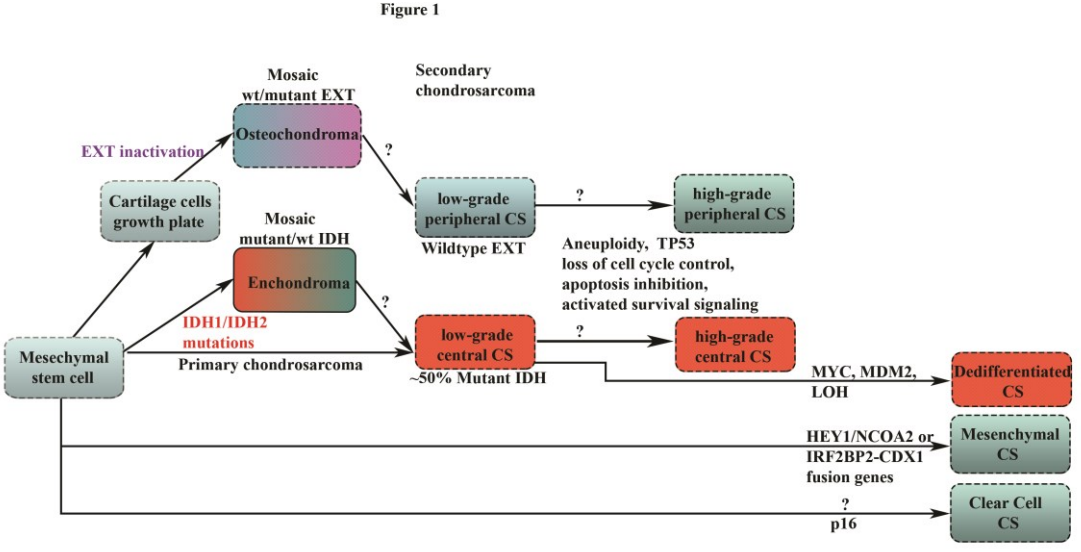

Figure 1.1. Progression model for conventional chondrosarcoma. A: In contrast to secondary chondrosarcoma, primary chondrosarcoma arises from the precursor cell without an intermittent benign lesion. EXT inactivation is observed in the benign osteochondroma. Peripheral chondrosarcomas are wildtype for EXT, and arise from the EXT wildtype cells in the osteochondroma. IDH mutations are found in enchondromas as well as low and high grade central chondrosarcomas, but only enchondromas were shown to be mosaic. Approximately 50% of low grade chondrosarcomas were shown to harbor IDH mutations. The (epi-)genetic events leading to progression from benign precursor lesion to a low grade tumor are unknown, and in progression from low grade to high grade, aneuploidy, loss of heterozygosity, as well as deregulations in the apoptosis, survival and growth plate signaling pathways are found. All these factors are likely to contribute to progression in grade and resistance to therapy. Both the cartilaginous and dedifferentiated components of dedifferentiated chondrosarcoma have been shown to harbor IDH and TP53 mutations, supporting the hypothesis of a common clonal origin. MYC and MDM2 mutations as well as loss of heterozygosity (LOH) patterns were found to differ between components, suggesting occurrence after component separation. In mesenchymal chondrosarcoma, the HEY1/NCOA2 fusion gene was recently identified, and the IRF2BP2-CDX1 fusion gene in a HEY1/NCOA2 negative lesion, indicating the mutual exclusive nature of these fusion genes. In clear cell chondrosarcoma, other than common loss of p16 protein expression, no causative mutations have been identified as of yet.

III. Chondrosarcoma model systems

Recurrent and metastatic disease as well as chondrosarcomas located at unresectable sites present a major problem, as conventional chemo- and radiotherapy have shown to be ineffective (64). In order to improve survival rates and quality of life, there is an urgent need for new therapeutic strategies in chondrosarcoma. Chemoresistance has long been attributed to the cartilaginous matrix surrounding the cells, to the relatively low mitotic rate, as well as to possible expression of multi-drug resistance genes. Increasingly, activation of various pathways are being recognized in prohibiting apoptosis and promoting cell survival in chondrosarcoma (65).

Ever since the discovery of Imatinib (11), as the prototype of targeted therapy in solid tumors, there has been an explosive growth in targeted therapies. In the preclinical search for the proper treatment strategy for chondrosarcoma, adequate model systems are invaluable. This is especially important in a rare malignancy such as chondrosarcoma, in which it is difficult to conduct large randomized clinical trials and for which it can be challenging to obtain funding from the pharmaceutical industry.

Chondrosarcoma cell lines

In cancer research, the use of cancer cell lines facilitates the study of the characteristics and behavior of cancer cells. Since the publication of the first human cell line in 1952, HeLa (66), the changes in the field of tissue culture have rapidly advanced cancer research. However, through HeLa, the community also learned about the pitfalls of cell lines. The rapid and wide dissemination of HeLa shortly after its discovery led to large scale cell line cross contamination. Today, most labs have implemented cell line typing in order to closely monitor and maintain the unique identity of each cell line (67).

Cell lines prove an especially useful tool in the search for new treatment strategies. A first step is to investigate the effect of any treatment on cell viability using basic characteristics of the cells, such as presence of ATP or mitochondrial activity. However, a limitation of such viability assays can be the lack of proof of occurrence of apoptosis. In a healthy cell, the anionic phosphatidylserines are facing the cytoplasmic side of the plasma membrane. During apoptosis, disruption of phospholipids in the cellular membrane will cause the phosphatidylserines to face outwards. Being a natural binding site for human AnnexinV, recombinant AnnexinV can be used in combination with a fluorescent label such as FITC to detect apoptosis in cells (68). Combined with live cell imaging, specific apoptosis occurrence after drug exposure can be monitored over time (69).

Real-time monitoring of cell number can also be performed with the xCelligence system (ACEA Biosciences). Providing a label-free system, based on cell density, this system uses small gold electrodes which cover the bottom of the plate. The electrodes are connected to a computer outside the incubator and as cells multiply, an increase in resistance over the electrodes can be converted into a cell index (70). Moreover, the xCelligence provides a real-time migration assay, with a 16 well-

plate containing micropores. As cells are plated on the side without electrodes, a signal will only arise once cells have started migrating (71).
Cell lines, however, are so-called 2D cultures. As chondrosarcomas histologically show cartilaginous matrix surrounding the cells, a 3D culturing system to investigate its role can be used. In 3D culturing, cells can be grown in scaffolds made to resemble the natural extracellular matrix (ECM). Correctly mimicking the ECM and controlling appropriate stimuli such as growth factors can be challenging in a system using scaffolds. A second method, widely used in oncology to examine tumor behavior, are multicellular spheroids. In this method, various approaches are applied to obtain cell spheroids, which are maintained using appropriate growth factors (72). As chondrocytes (73) were shown to create matrix in 3D culture, this model can be used to model chondrosarcoma behavior and drug response *in vivo*.

Chondrosarcoma mouse models
Ideally, drugs proven effective in cell lines are subsequently proven effective *in vivo* in rodent models before proceeding to the clinic. A stable, reproducible mouse model is advantageous for standardizing *in vivo* research. Current chondrosarcoma mouse models either show subcutaneous xenografting of tumor tissue immediately after resection from the patient, or subcutaneous injection of cell lines (74). An orthotopic model, more closely resembling the patient situation would be preferable. The pharmacokinetics of a drug need to be taken into account, as the distribution to an intra-osseous and a subcutaneous tumor can differ. In addition, subcutaneous injection could alter chondrosarcoma cell behavior through communication with surrounding cells. An orthotopic mouse model is therefore more likely to correctly predict response of the primary tumor than a subcutaneous model.
In the literature several chondrosarcoma rodent models exist. One such model is the orthotopic swarm rat chondrosarcoma model, created using cell lines derived from a chondrosarcoma that spontaneously arose in a sprague-dawley rat. However, it was recently shown that the cell lines used to create the model consist of different cytogenetic properties (75). The literature also describes an orthotopic chondrosarcoma mouse model, derived from the JJ012 cell line (76). A limitation of these methods is that the role of EXT or IDH mutations in the tumorigenesis of osteochondromas and enchondromas, respectively, cannot be investigated. Conditional *Ext1* knock out mouse models for EXT exist, and also show exostosis formation, closely resembling human osteochondromas, however, no malignant transformation to chondrosarcoma is observed in these lesions (77-79). So far, two *IDH* conditional knock-in mutant mouse model exist, specific for neural or hematopoetic progenitor cells, and in neither model has enchondroma or chondrosarcoma formation been found (34;80). As tumor size can only be assessed at time of animal sacrifice, when testing drug response, a method enabling live monitoring of tumor growth would be ideal. Using luciferase constructs, tumor growth can be monitored during the experiment with minimal stress to the animal,

as a single intra-peritoneal injection is required to activate the construct and the tumor can be visualized using a bio-imager (81).

V. Approaches to identify new treatment strategies

The hallmarks of cancer as characterized by Weinberg and Hanahan in 2000 (82), identified pathways distinctive to cancer cells which can be utilized when designing cancer therapeutics. Two of these pathways are recognized to be the apoptosis and survival pathways. Apoptosis pathways lead to an acquired capacity to evade programmed cell death. Survival pathways including tyrosine kinases can lead to a self-sufficiency in growth signals, as well as insensitivity to anti-growth signals, limitless replicative potential, sustained angiogenesis, and the acquired ability to invade distant tissue and metastasize(83;84).

Apoptotic pathways

One class of apoptotic proteins is the Bcl-2 family, and a shift favoring anti-apoptotic Bcl-2 proteins can lead to the acquired capacity to evade programmed cell death, even in the presence of death signals (fig 2).

Besides from its anti-apoptotic properties, Bcl-2 is also a player in the indian hedgehog (IHH) pathway during endochondral bone development (85). In both central and peripheral chondrosarcoma aberrant IHH signaling is observed along with retention of PTHrP. Apart from inhibiting differentiation, PTHrP also inhibits apoptosis through stimulating the expression of the anti-apoptotic protein Bcl-2, found to be overexpressed in high grade chondrosarcomas (fig 1) (46;48;49;85-89).

The four Bcl-2 homology (BH) domains are characteristic of the Bcl-2 family, enabling oligodimerization. Three classes of proteins control cell survival and regulate apoptosis. Anti-apoptotic (Bcl-2, Bcl-xl, Bcl-w) and pro-apoptotic (BAX, BAK) family members possess all four BH domains, creating a hydrophobic groove able to bind BH3-only proteins (90). Two classes of BH3 proteins exist: i) activating BH3 proteins (BID, BIM) promote the oligomerization of BAX/BAK dimers, and ii) sensitizing BH3 proteins (BAD) bind the anti-apoptoptic proteins (fig 2). Only activating BH3-only proteins have the ability to induce cytochrome C release, and can in turn be released from the anti-apoptotic proteins by the sensitizing BH3-only proteins. The upregulation of anti-apoptotic proteins as reported in cancer, leads to the sequestration of BH3-only proteins, and prohibits the formation of BAX/BAK dimers (fig 2). Without the insertion of BAX/BAK dimers, the mitochondrial membrane will not be permeabilized, with the consequential lack of cytochrome C release and caspase activation (90;91).

Inhibitors of the Bcl-2 family are based on protein-protein interactions. The first inhibitor to be discovered was HA14-1, a nonpeptidic ligand of Bcl-2 (92). The new class of inhibitors are called BH3 mimetics, specifically binding the hydrophobic BH3 groove of anti-apoptotic Bcl-2 proteins. The BH3 mimetic ABT-737 (93) has shown promising preclinical results and its orally available counterpart, Navitoclax (ABT-263) (94), is currently in clinical trials for various

malignancies, including solid tumors (95). Resistance to ABT-737 has been attributed to increased Mcl-1 expression (96), and recently, a BH3 alpha-helix mimetic was designed, JY-1-106, specifically disrupting the protein-protein interactions between Bcl-xl and Mcl-1 with Bak (97). Finally, the BH3 mimetic GX15-070, obatoclax, has been developed to bind Bcl-2, Bcl-xl, Bcl-w, and MCL-1 (98) and is currently in clinical trials.

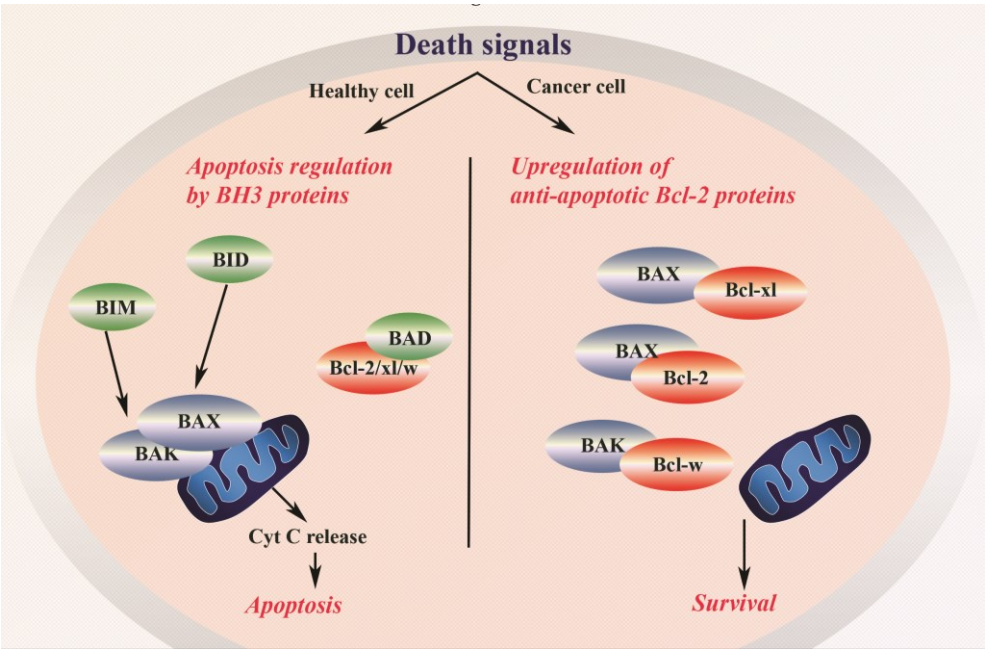

Figure 1.2. Apoptosis pathway. In a healthy cell (left panel), response to death signals such as DNA damage can occur through activation of BH3 only proteins. Two types of BH3 only proteins will allow for apoptosis to occur: sensitizing BH3 only proteins like BAD will release BAX and BAK from the anti-apoptotic Bcl-2 proteins, Bcl-2, Bcl-xl, and Bcl-w. The activating BH3 only proteins, such as BID or BIM, will then promote BAX/BAK heterodimerization and insertion into the mitochondrial membrane, upon which the mitochondrial membrane becomes permeabilized. Consequentially, cytochrome C and calcium are released and caspases are activated, leading to apoptosis. In cancer, upregulation of anti-apoptotic proteins is often found (right panel), in which case a cell becomes desensitized to the activation of BH3 only proteins. BAX and BAK remain sequestered to anti-apoptotic proteins and the mitochondrial membrane is not permeabilized. The upregulation of anti-apoptotic proteins hereby leads to survival of cells, even in the presence of death signals, such as they might occur after chemotherapy.

Survival pathways
In biochemistry, an enzyme actively transferring phosphate groups from proteins in the process of phosphorylation is called a kinase. Tyrosine kinases are kinases which become activated once phosphorylated at a specific catalytic tyrosine site (99). Of the hallmarks of cancer (82), self sufficiency of growth signals, limitless replicative potential and tissue invasion can be traced back to tyrosine kinases which play an important role in survival pathways governing cancer cell survival, proliferation, and metastasis (83;84). Using kinome profiling, tyrosine kinase pathways were found to be active in chondrosarcoma (100).
Receptor tyrosine kinases (RTK) have a cytoplasmic tyrosine kinase domain, and an extracellular ligand binding regulatory domain. As a rule, RTKs require ligand binding (typically growth factors) to undergo a conformational change allowing for dimerization and autophosphorylation, with resulting downstream signaling (101). The increased RTK signaling observed in cancer can occur through gene amplification leading to constitutive activation, or through close clustering on the membrane leading to homodimerization in absence of ligand (92). The importance of tyrosine kinase signaling in cancer has led to the development of a multitude of different tyrosine kinase inhibitors, of which 18 have now been approved by the FDA for a variety of malignancies (102).

VI. Aim and outline of the thesis

The aim of this thesis was to unravel mechanisms for chemoresistance and identify new therapeutic strategies for targeted treatment in chondrosarcoma. In order to rapidly translate results from basic research to clinical practice, pre-clinical models including chondrosarcoma cell lines and mouse models were developed.
Chapter 2 focuses on new therapeutic strategies in chondrosarcoma. As such a review of recent preclinical research is linked to ongoing or completed clinical trials in chondrosarcoma in an attempt to provide a concise overview of the current state of the art of possibilities for targeted therapy in chondrosarcoma. In light of the recent discovery of IDH mutations, and advances regarding EXT mutations, their respective roles in chondrosarcoma tumorigenesis and chemoresistance is discussed, as well as the therapeutic potential of hedgehog signaling.
In **chapters 3 and 4** the development of new chondrosarcoma model systems is described. First, the generation and characterization of three new chondrosarcoma cell lines (**chapter 3**), and second, the development of an orthotopic chondrosarcoma mouse model (**chapter 4**).

In **chapters 5-8**, mechanisms of chondrosarcoma chemoresistance are investigated. **Chapter 5** explores chemoresistance mechanisms in conventional chondrosarcoma, focusing on drug inaccessibility due to matrix hindrance, activity of multidrug resistance transporters, and overexpression of anti-apoptotic Bcl-2 proteins (45;94). The role of Bcl-2 proteins in chemoresistance of conventional (**chapter 5**) and dedifferentiated chondrosarcoma (**chapter 6**) is further examined using the BH-3 mimetic ABT-737 in combination with doxorubicin or cisplatin. As rare chondrosarcoma subtypes histologically resemble different stages of the growth plate, in **chapter 6**, immunohistochemistry is performed on tissue microarrays of rare chondrosarcoma subtypes, to examine expression levels of proteins involved in growth plate signaling pathways.
Finally, tyrosine kinase signaling pathways are investigated. Using kinome profiling, the PI3K/AKT and SRC pathway were found to be active (100), and were hypothesized to play a role in chondrosarcoma chemoresistance. In **chapter 7** we therefore combine enzastaurin (AKT inhibition) and dasatinib (SRC inhibition) with doxorubicin. As Src kinases are reported to play a role in metastasis formation (95), migration assays are performed. Hypothesizing that an upregulation in protein tyrosine kinases could well be concomitant with an upregulation of receptor tyrosine kinases, in **chapter 8** a similar approach is used to investigate the activities of receptor tyrosine kinases (RTK) in chondrosarcoma cell lines using a phospho-receptor tyrosine kinase array. The roles of RTK activation in chondrosarcoma proliferation is further examined using kinase inhibitors, with analysis of downstream pathway activation. In comparison, mTOR pathway activation is studied to investigate downstream activation of RTK signaling.
Chapter 9 will conclude with a summary of the results and an outlook to the future.

Reference List

(1) Giuffrida AY, Burgueno JE, Koniaris LG, Gutierrez JC, Duncan R, Scully SP. Chondrosarcoma in the United States (1973 to 2003): an analysis of 2890 cases from the SEER database. J Bone Joint Surg Am 2009;91(5):1063-72.

(2) Hogendoorn PCW, Bovée JVMG, Nielsen GP. Chondrosarcoma (grades I-III), including primary and secondary variants and periosteal chondrosarcoma. In: Fletcher C.D.M., Bridge JA, Hogendoorn PCW, Mertens F, editors. World Health Classification of Tumours. Pathology and Genetics of Tumours of Soft Tissue and Bone. 4 ed. 2013. p. 264-8.

(3) Fletcher C.D.M., Bridge JA, Hogendoorn PCW, Mertens F. WHO Classification of Tumours of Soft Tissue and Bone. 4 ed. 2013.

(4) Freyschmidt J, Ostertag H, Jundt G. Knörpelbildende Tumoren. Knochentumoren. 2010. p. 273-442.

(5) Evans HL, Ayala AG, Romsdahl MM. Prognostic factors in chondrosarcoma of bone. A clinicopathologic analysis with emphasis on histologic grading. Cancer 1977;40:818-31.

(6) Fletcher CDM, Unni KK, Mertens F. WHO Classification of tumours. Pathology & Genetics of Tumours of Soft Tissue and Bone. IARC Press, Lyon ed. Lyon: IARC Press; 2002.

(7) Reliability of Histopathologic and Radiologic Grading of Cartilaginous Neoplasms in Long Bones. J Bone Joint Surg Am 2007;89-A(10):2113-23.

(8) Eefting D, Schrage YM, Geirnaerdt MJ, Le CS, Taminiau AH, Bovee JV, Hogendoorn PC. Assessment of interobserver variability and histologic parameters to improve reliability in classification and grading of central cartilaginous tumors. Am J Surg Pathol 2009;33(1):50-7.

(9) Gajewski DA, Burnette JB, Murphey MD, Temple HT. Differentiating clinical and radiographic features of enchondroma and secondary chondrosarcoma in the foot. Foot Ankle Int 2006;27(4):240-4.

(10) Verdegaal SH, Brouwers HF, van Zwet EW, Hogendoorn PC, Taminiau AH. Low-grade chondrosarcoma of long bones treated with intralesional curettage followed by application of phenol, ethanol, and bone-grafting. J Bone Joint Surg Am 2012;94(13):1201-7.

(11) Gelderblom H, Hogendoorn PCW, Dijkstra SD, van Rijswijk CS, Krol AD, Taminiau AH, Bovee JV. The clinical approach towards chondrosarcoma. Oncologist 2008;13(3):320-9.

(12) Lucas DR, Bridge JA. Chondromas: enchondroma, periosteal chondroma. In: Fletcher C.D.M., Bridge JA, Hogendoorn PCW, Mertens F, editors. World Health Organization Classification of Tumours. Pathology and Genetics of Tumours of Soft Tissue and Bone. 4 ed. 2013. p. 273-4.

(13) Mertens F, Unni KK. Enchondromatosis: Ollier disease and Maffucci syndrome. In: Fletcher CDM, Unni KK, Mertens F, editors. World Health Organization Classification of Tumours. Pathology and genetics of tumours of soft tissue and bone.Lyon: IARC Press; 2002. p. 356-7.

(14) Pansuriya TC, van ER, d'Adamo P, van Ruler MA, Kuijjer ML, Oosting J, Cleton-Jansen AM, van Oosterwijk JG, Verbeke SL, Meijer D, van WT, Nord KH, Sangiorgi L, Toker B, Liegl-Atzwanger B, San-Julian M, Sciot R, Limaye N, Kindblom LG, Daugaard S, Godfraind C, Boon LM, Vikkula M, Kurek KC, Szuhai K et al. Somatic mosaic IDH1 and IDH2 mutations are associated with enchondroma and

spindle cell hemangioma in Ollier disease and Maffucci syndrome. Nat Genet 2011;43(12):1256-61.

(15) Amary MF, Damato S, Halai D, Eskandarpour M, Berisha F, Bonar F, McCarthy S, Fantin VR, Straley KS, Lobo S, Aston W, Green CL, Gale RE, Tirabosco R, Futreal A, Campbell P, Presneau N, Flanagan AM. Ollier disease and Maffucci syndrome are caused by somatic mosaic mutations of IDH1 and IDH2. Nat Genet 2011;43(12):1262-5.

(16) Amary MF, Bacsi K, Maggiani F, Damato S, Halai D, Berisha F, Pollock R, O'Donnell P, Grigoriadis A, Diss T, Eskandarpour M, Presneau N, Hogendoorn PC, Futreal A, Tirabosco R, Flanagan AM. IDH1 and IDH2 mutations are frequent events in central chondrosarcoma and central and periosteal chondromas but not in other mesenchymal tumours. J Pathol 2011;224(3):334-43.

(17) Yan H, Parsons DW, Jin G, McLendon R, Rasheed BA, Yuan W, Kos I, Batinic-Haberle I, Jones S, Riggins GJ, Friedman H, Friedman A, Reardon D, Herndon J, Kinzler KW, Velculescu VE, Vogelstein B, Bigner DD. IDH1 and IDH2 mutations in gliomas. N Engl J Med 2009;360(8):765-73.

(18) Bayley JP, Devilee P. Warburg tumours and the mechanisms of mitochondrial tumour suppressor genes. Barking up the right tree? Curr Opin Genet Dev 2010 June;20(3):324-9.

(19) Leonardi R, Subramanian C, Jackowski S, Rock CO. Cancer-associated isocitrate dehydrogenase mutations inactivate NADPH-dependent reductive carboxylation. J Biol Chem 2012;287(18):14615-20.

(20) Dang L, White DW, Gross S, Bennett BD, Bittinger MA, Driggers EM, Fantin VR, Jang HG, Jin S, Keenan MC, Marks KM, Prins RM, Ward PS, Yen KE, Liau LM, Rabinowitz JD, Cantley LC, Thompson CB, Vander Heiden MG, Su SM. Cancer-associated IDH1 mutations produce 2-hydroxyglutarate. Nature 2009;462(7274):739-44.

(21) Luchman HA, Stechishin OD, Dang NH, Blough MD, Chesnelong C, Kelly JJ, Nguyen SA, Chan JA, Weljie AM, Cairncross JG, Weiss S. An in vivo patient-derived model of endogenous IDH1-mutant glioma. Neuro Oncol 2012;14(2):184-91.

(22) Ward PS, Patel J, Wise DR, Abdel-Wahab O, Bennett BD, Coller HA, Cross JR, Fantin VR, Hedvat CV, Perl AE, Rabinowitz JD, Carroll M, Su SM, Sharp KA, Levine RL, Thompson CB. The common feature of leukemia-associated IDH1 and IDH2 mutations is a neomorphic enzyme activity converting alpha-ketoglutarate to 2-hydroxyglutarate. Cancer Cell 2010;17(3):225-34.

(23) Noushmehr H, Weisenberger DJ, Diefes K, Phillips HS, Pujara K, Berman BP, Pan F, Pelloski CE, Sulman EP, Bhat KP, Verhaak RG, Hoadley KA, Hayes DN, Perou CM, Schmidt HK, Ding L, Wilson RK, Van Den Berg D, Shen H, Bengtsson H, Neuvial P, Cope LM, Buckley J, Herman JG, Baylin SB et al. Identification of a CpG island methylator phenotype that defines a distinct subgroup of glioma. Cancer Cell 2010;17(5):510-22.

(24) Lu C, Ward PS, Kapoor GS, Rohle D, Turcan S, Abdel-Wahab O, Edwards CR, Khanin R, Figueroa ME, Melnick A, Wellen KE, O'Rourke DM, Berger SL, Chan TA, Levine RL, Mellinghoff IK, Thompson CB. IDH mutation impairs histone demethylation and results in a block to cell differentiation. Nature 2012;483(7390):474-8.

(25) Dang L, Jin S, Su SM. IDH mutations in glioma and acute myeloid

leukemia. Trends Mol Med 2010;16(9):387-97.

(26) Chowdhury R, Yeoh KK, Tian YM, Hillringhaus L, Bagg EA, Rose NR, Leung IK, Li XS, Woon EC, Yang M, McDonough MA, King ON, Clifton IJ, Klose RJ, Claridge TD, Ratcliffe PJ, Schofield CJ, Kawamura A. The oncometabolite 2-hydroxyglutarate inhibits histone lysine demethylases. EMBO Rep 2011;12(5):463-9.

(27) Xu W, Yang H, Liu Y, Yang Y, Wang P, Kim SH, Ito S, Yang C, Wang P, Xiao MT, Liu LX, Jiang WQ, Liu J, Zhang JY, Wang B, Frye S, Zhang Y, Xu YH, Lei QY, Guan KL, Zhao SM, Xiong Y. Oncometabolite 2-hydroxyglutarate is a competitive inhibitor of alpha-ketoglutarate-dependent dioxygenases. Cancer Cell 2011;19(1):17-30.

(28) Figueroa ME, Abdel-Wahab O, Lu C, Ward PS, Patel J, Shih A, Li Y, Bhagwat N, Vasanthakumar A, Fernandez HF, Tallman MS, Sun Z, Wolniak K, Peeters JK, Liu W, Choe SE, Fantin VR, Paietta E, Lowenberg B, Licht JD, Godley LA, Delwel R, Valk PJ, Thompson CB, Levine RL et al. Leukemic IDH1 and IDH2 mutations result in a hypermethylation phenotype, disrupt TET2 function, and impair hematopoietic differentiation. Cancer Cell 2010;18(6):553-67.

(29) Christensen BC, Smith AA, Zheng S, Koestler DC, Houseman EA, Marsit CJ, Wiemels JL, Nelson HH, Karagas MR, Wrensch MR, Kelsey KT, Wiencke JK. DNA methylation, isocitrate dehydrogenase mutation, and survival in glioma. J Natl Cancer Inst 2011 January 19;103(2):143-53.

(30) Laffaire J, Everhard S, Idbaih A, Criniere E, Marie Y, de RA, Schiappa R, Mokhtari K, Hoang-Xuan K, Sanson M, Delattre JY, Thillet J, Ducray F. Methylation profiling identifies 2 groups of gliomas according to their tumorigenesis. Neuro Oncol 2011;13(1):84-98.

(31) Turcan S, Rohle D, Goenka A, Walsh LA, Fang F, Yilmaz E, Campos C, Fabius AW, Lu C, Ward PS, Thompson CB, Kaufman A, Guryanova O, Levine R, Heguy A, Viale A, Morris LG, Huse JT, Mellinghoff IK, Chan TA. IDH1 mutation is sufficient to establish the glioma hypermethylator phenotype. Nature 2012;483(7390):479-83.

(32) Duncan CG, Barwick BG, Jin G, Rago C, Kapoor-Vazirani P, Powell DR, Chi JT, Bigner DD, Vertino PM, Yan H. A heterozygous IDH1R132H/WT mutation induces genome-wide alterations in DNA methylation. Genome Res 2012;22(12):2339-55.

(33) Koivunen P, Lee S, Duncan CG, Lopez G, Lu G, Ramkissoon S, Losman JA, Joensuu P, Bergmann U, Gross S, Travins J, Weiss S, Looper R, Ligon KL, Verhaak RG, Yan H, Kaelin WG, Jr. Transformation by the (R)-enantiomer of 2-hydroxyglutarate linked to EGLN activation. Nature 2012;483(7390):484-8.

(34) Sasaki M, Knobbe CB, Itsumi M, Elia AJ, Harris IS, Chio II, Cairns RA, McCracken S, Wakeham A, Haight J, Ten AY, Snow B, Ueda T, Inoue S, Yamamoto K, Ko M, Rao A, Yen KE, Su SM, Mak TW. D-2-hydroxyglutarate produced by mutant IDH1 perturbs collagen maturation and basement membrane function. Genes Dev 2012;26(18):2038-49.

(35) Schaap FG, French PJ, Bovee JVMG. Mutations in the Isocitrate Dehydrogenase Genes IDH1 and IDH2 in Tumors. Adv Anat Pathol 2013;20(1):32-8.

(36) Verdegaal SHM, Bovée JVMG, Pansuriya TC, Grimer RJ, Ozger H, Jutte PC, San-Julian M, Biau DJ, van der Geest ICM, Leithner A, Streitburger A, Klenke FM, Gouin FG, Campanacci DA,

Marec-Berard P, Hogendoorn PCW, Brand R, Taminiau AHM. Incidence, predictive factors and prognosis of chondrosarcoma in patients with Ollier disease and Maffucci syndrome; an international multicenter study of 161 patients. 2011.

(37) Bovée JVMG, Heymann D, Wuyts W. Osteochondroma. In: Fletcher C.D.M., Bridge JA, Hogendoorn PCW, Mertens F, editors. World Health Organization Classification of Tumours. Pathology and Genetics of Tumours of Soft Tissue and Bone. 4 ed. 2013. p. 273-4.

(38) Jennes I, Pedrini E, Zuntini M, Mordenti M, Balkassmi S, Asteggiano CG, Casey B, Bakker B, Sangiorgi L, Wuyts W. Multiple osteochondromas: mutation update and description of the multiple osteochondromas mutation database (MOdb). Hum Mutat 2009;30(12):1620-7.

(39) Stickens D, Brown D, Evans GA. EXT genes are differentially expressed in bone and cartilage during mouse embryogenesis. Dev Dyn 2000;218(3):452-64.

(40) Chung U-I, Lanske B, Lee K, Li E, Kronenberg HM. The parathyroid hormone/parathyroid hormone-related peptide receptor coordinates endochondral bone development by directly controlling chondrocyte differentiation. Proc Natl Acad Sci USA 1998;95:13030-5.

(41) Chung UI, Schipani E, McMahon AP, Kronenberg HM. Indian hedgehog couples chondrogenesis to osteogenesis in endochondral bone development. J Clin Invest 2001;107(3):295-304.

(42) de Andrea CE, Wiweger M, Prins F, Bovee JVMG, Romeo S, Hogendoorn PCW. Primary cilia organization reflects polarity in the growth plate and implies loss of polarity and mosaicism in osteochondroma. Lab Invest 2010;90(7):1091-101.

(43) Szuhai K, Jennes I, De Jong D, Bovée JVMG, Wiweger M, Wuyts W, Hogendoorn PCW. Tiling resolution array-CGH shows that somatic mosaic deletion of the EXT gene is causative in EXT gene mutation negative multiple osteochondromas patients. Hum Mutat 2011;32(2):2036-49.

(44) de Andrea CE, Reijnders CM, Kroon HM, de JD, Hogendoorn PC, Szuhai K, Bovee JV. Secondary peripheral chondrosarcoma evolving from osteochondroma as a result of outgrowth of cells with functional EXT. Oncogene 2011.

(45) de Andrea CE, Hogendoorn PC. Epiphyseal growth plate and secondary peripheral chondrosarcoma: the neighbours matter. J Pathol 2012;226(2):219-28.

(46) Hameetman L, Kok P, Eilers PHC, Cleton-Jansen AM, Hogendoorn PCW, Bovée JVMG. The use of Bcl-2 and PTHLH immunohistochemistry in the diagnosis of peripheral chondrosarcoma in a clinicopathological setting. Virchows Arch 2005;446:430-7.

(47) Bovee JVMG, Van den Broek LJCM, Cleton-Jansen AM, Hogendoorn PCW. Up-regulation of PTHrP and Bcl-2 expression characterizes the progression of osteochondroma towards peripheral chondrosarcoma and is a late event in central chondrosarcoma. Lab Invest 2000;80:1925-33.

(48) Tiet TD, Hopyan S, Nadesan P, Gokgoz N, Poon R, Lin AC, Yan T, Andrulis IL, Alman BA, Wunder JS. Constitutive hedgehog signaling in chondrosarcoma up-regulates tumor cell proliferation. Am J Pathol 2006;168(1):321-30.

(49) Rozeman LB, Hameetman L, Cleton-Jansen AM, Taminiau AHM, Hogendoorn PCW, Bovée JVMG. Absence of IHH and retention of PTHrP signalling in enchondromas and central chondrosarcomas. J Pathol 2005;205(4):476-82.

(50) Schrage YM, Hameetman L, Szuhai K, Cleton-Jansen AM, Taminiau AHM, Hogendoorn PCW, Bovée JVMG. Aberrant heparan sulfate proteoglycan localization, despite normal exostosin, in central chondrosarcoma. Am J Pathol 2009;174(3):979-88.

(51) Inwards CY, Hogendoorn PCW. Dedifferentiated Chondrosarcoma. In: Fletcher C.D.M., Bridge JA, Hogendoorn PCW, Mertens F, editors. World Health Organization Classification of Tumours. Pathology and Genetics of Tumours of Soft Tissue and Bone. 4 ed. 2013. p. 269-70.

(52) Grimer RJ, Gosheger G, Taminiau A, Biau D, Matejovsky Z, Kollender Y, San Julian M, Gherlinzoni F, Ferrari C. Dedifferentiated chondrosarcoma: Prognostic factors and outcome from a European group. Eur J Cancer 2007;43(14):2060-5.

(53) Meijer D, de JD, Pansuriya TC, van den Akker BE, Picci P, Szuhai K, Bovee JV. Genetic characterization of mesenchymal, clear cell, and dedifferentiated chondrosarcoma. Genes Chromosomes Cancer 2012;51(10):899-909.

(54) Bovée JVMG, Cleton-Jansen AM, Rosenberg C, Taminiau AHM, Cornelisse CJ, Hogendoorn PCW. Molecular genetic characterization of both components of a dedifferentiated chondrosarcoma, with implications for its histogenesis. J Pathol 1999;189:454-62.

(55) Rozeman LB, de Bruijn IH, Bacchini P, Staals EL, Bertoni F, Bovee JVMG, Hogendoorn PCW. Dedifferentiated peripheral chondrosarcomas: regulation of EXT-downstream molecules and differentiation-related genes. Mod Pathol 2009;22(11):1489-98.

(56) Morrison C, Radmacher M, Mohammed N, Suster D, Auer H, Jones S, Riggenbach J, Kelbick N, Bos G, Mayerson J. MYC Amplification and Polysomy 8 in Chondrosarcoma: Array Comparative Genomic Hybridization, Fluorescent In Situ Hybridization, and Association With Outcome. J Clin Oncol 2005;23(36):9369-76.

(57) Nakashima Y, de Pinieux G, Ladanyi M. Mesenchymal Chondrosarcoma. In: Fletcher C.D.M., Bridge JA, Hogendoorn PCW, Mertens F, editors. World Health Organization Classification of Tumours. Pathology and Genetics of Tumours of Soft Tissue and Bone. 2013. p. 271-2.

(58) Cesari M, Bertoni F, Bacchini P, Mercuri M, Palmerini E, Ferrari S. Mesenchymal chondrosarcoma. An analysis of patients treated at a single institution. Tumori 2007;93(5):423-7.

(59) Dantonello TM, Int-Veen C, Leuschner I, Schuck A, Furtwaengler R, Claviez A, Schneider DT, Klingebiel T, Bielack SS, Koscielniak E. Mesenchymal chondrosarcoma of soft tissues and bone in children, adolescents, and young adults: experiences of the CWS and COSS study groups. Cancer 2008;112(11):2424-31.

(60) Wang L, Motoi T, Khanin R, Olshen A, Mertens F, Bridge J, Dal CP, Antonescu CR, Singer S, Hameed M, Bovee JV, Hogendoorn PC, Socci N, Ladanyi M. Identification of a novel, recurrent HEY1-NCOA2 fusion in mesenchymal chondrosarcoma based on a genome-wide screen of exon-level expression data. Genes Chromosomes Cancer 2012;51(2):127-39.

(61) Nyquist KB, Panagopoulos I, Thorsen J, Haugom L, Gorunova L, Bjerkehagen B, Fossa A, Guriby M, Nome T, Lothe RA, Skotheim RI, Heim S, Micci F. Whole-transcriptome sequencing identifies novel IRF2BP2-CDX1 fusion gene brought about by translocation t(1;5)(q42;q32) in mesenchymal chondrosarcoma. PLoS ONE 2012;7(11):e49705.

(62) Bae DK, Park YK, Chi SG, Lee CW, Unni KK. Mutational alterations of the p16CDKN2A tumor suppressor gene have low incidence in mesenchymal chondrosarcoma. Oncol Res 2000;12(1):5-10.

(63) Park YK, Park HR, Chi SG, Kim CJ, Sohn KR, Koh JS, Kim CW, Yang WI, Ro JY, Ahn KW, Joo M, Kim YW, Lee J, Yang MH, Unni KK. Overexpression of p53 and rare genetic mutation in mesenchymal chondrosarcoma. Oncol Rep 2000;7(5):1041-7.

(64) McCarthy EF, Hogendoorn PCW. Clear Cell Chondrosarcoma. In: Fletcher C.D.M., Bridge JA, Hogendoorn PCW, Mertens F, editors. World Health Organization Classification of Tumours. Pathology and Genetics of Tumours of Soft Tissue and Bone. 4 ed. 2013. p. 273-4.

(65) Bovee JVMG, Cleton-Jansen AM, Taminiau AHM, Hogendoorn PCW. Emerging pathways in the development of chondrosarcoma of bone and implications for targeted treatment. Lancet Oncology 2005;6(8):599-607.

(66) Gey GO, Coffmann WD, Kubicek MT. Tissue Culture Studies of the Proliferative Capacity of Cervival Carcinoma and Normal Epithelium. Cancer Res 1952;12:264-5.

(67) Lucey BP, Nelson-Rees WA, Hutchins GM. Henrietta Lacks, HeLa Cells, and Cell Culture Contamination. Arch Pathol Lab Med 2009;133:1463-7.

(68) Tait JF. Imaging of apoptosis. J Nucl Med 2008;49(10):1573-6.

(69) Puigvert JC, de BH, van de Water B, Danen EH. High-throughput live cell imaging of apoptosis. Curr Protoc Cell Biol 2010;Chapter 18:Unit-13.

(70) Ke N, Wang X, Xu X, Abassi YA. The xCELLigence system for real-time and label-free monitoring of cell viability. Methods Mol Biol 2011;740:33-43.

(71) Limame R, Wouters A, Pauwels B, Fransen E, Peeters M, Lardon F, De WO, Pauwels P. Comparative analysis of dynamic cell viability, migration and invasion assessments by novel real-time technology and classic endpoint assays. PLoS ONE 2012;7(10):e46536.

(72) Page H, Flood P, Reynaud EG. Three-dimensional tissue cultures: current trends and beyond. Cell Tissue Res 2013;352(1):123-31.

(73) Reijnders CM, Waaijer CJ, Hamilton A, Buddingh' EP, Dijkstra SP, Ham J, Bakker E, Szuhai K, Karperien M, Hogendoorn PCW, Stringer SE, Bovee JVMG. No haploinsufficiency but loss of heterozygosity for EXT in multiple osteochondromas. Am J Pathol 2010;177(4):1946-57.

(74) Clark JC, Dass CR, Choong PF. Development of chondrosarcoma animal models for assessment of adjuvant therapy. ANZ J Surg 2009;79(5):327-36.

(75) Stevens JW, Patil SR, Jordan DK, Kimura JH, Morcuende JA. Cytogenetics of swarm rat chondrosarcoma. Iowa Orthop J 2005;25:135-40.

(76) Clark JC, Akiyama T, Dass CR, Choong PF. New clinically relevant, orthotopic mouse models of human chondrosarcoma with spontaneous metastasis. Cancer Cell Int 2010;10:20.

(77) Stickens D, Zak BM, Rougier N, Esko JD, Werb Z. Mice deficient in Ext2 lack heparan sulfate and develop

exostoses. Development 2005;132(22):5055-68.

(78) Zak BM, Schuksz M, Koyama E, Mundy C, Wells DE, Yamaguchi Y, Pacifici M, Esko JD. Compound heterozygous loss of Ext1 and Ext2 is sufficient for formation of multiple exostoses in mouse ribs and long bones. Bone 2011;48(5):979-87.

(79) Matsumoto K, Irie F, Mackem S, Yamaguchi Y. A mouse model of chondrocyte-specific somatic mutation reveals a role for Ext1 loss of heterozygosity in multiple hereditary exostoses. Proc Natl Acad Sci U S A 2010;107(24):10932-7.

(80) Sasaki M, Knobbe CB, Munger JC, Lind EF, Brenner D, Brustle A, Harris IS, Holmes R, Wakeham A, Haight J, You-Ten A, Li WY, Schalm S, Su SM, Virtanen C, Reifenberger G, Ohashi PS, Barber DL, Figueroa ME, Melnick A, Zuniga-Pflucker JC, Mak TW. IDH1(R132H) mutation increases murine haematopoietic progenitors and alters epigenetics. Nature 2012;488(7413):656-9.

(81) Wetterwald A, Van Der PG, Que I, Sijmons B, Buijs J, Karperien M, Lowik CW, Gautschi E, Thalmann GN, Cecchini MG. Optical imaging of cancer metastasis to bone marrow: a mouse model of minimal residual disease. Am J Pathol 2002;160(3):1143-53.

(82) Hanahan D, Weinberg RA. The hallmarks of cancer. Cell 2000 January 7;100(1):57-70.

(83) Cepero V, Sierra JR, Giordano S. Tyrosine kinases as molecular targets to inhibit cancer progression and metastasis. Curr Pharm Des 2010;16(12):1396-409.

(84) Hanahan D, Weinberg RA. Hallmarks of cancer: the next generation. Cell 2011 March 4;144(5):646-74.

(85) Amling M, Neff L, Tanaka S, Inoue D, Kuida K, Weir E, Philbrick WM, Broadus AE, Baron R. Bcl-2 lies downstream of parathyroid hormone related peptide in a signalling pathway that regulates chondrocyte maturation during skeletal development. J Cell Biol 1997;136:205-13.

(86) Bovée JVMG, Van den Broek LJCM, Cleton-Jansen AM, Hogendoorn PCW. Up-regulation of PTHrP and Bcl-2 expression characterizes the progression of osteochondroma towards peripheral chondrosarcoma and is a late event in central chondrosarcoma. Lab Invest 2000;80:1925-33.

(87) Kobayashi T, Chung UI, Schipani E, Starbuck M, Karsenty G, Katagiri T, Goad DL, Lanske B, Kronenberg HM. PTHrP and Indian hedgehog control differentiation of growth plate chondrocytes at multiple steps. Development 2002;129(12):2977-86.

(88) Posl M, Amling M, Neff L, Grahl K, Baron R, Delling G. Coexpression of PTHrP and BCL2 correlates with the degree of malignancy of chondrogenic tumors. J.Bone Miner.Res. 11, S113. 1996.

(89) Tiet TD, Alman BA. Developmental pathways in musculoskeletal neoplasia: involvement of the Indian Hedgehog-parathyroid hormone-related protein pathway. Pediatr Res 2003;53(4):539-43.

(90) Letai A, Bassik MC, Walensky LD, Sorcinelli MD, Weiler S, Korsmeyer SJ. Distinct BH3 domains either sensitize or activate mitochondrial apoptosis, serving as prototype cancer therapeutics. Cancer Cell 2002;2(3):183-92.

(91) Wyllie AH. "Where, O death, is thy sting?" A brief review of apoptosis biology. Mol Neurobiol 2010;42(1):4-9.

(92) Wang JL, Liu D, Zhang ZJ, Shan S, Han X, Srinivasula SM, Croce CM, Alnemri ES, Huang Z. Structure-based discovery of an organic compound that binds Bcl-2 protein and induces apoptosis of tumor cells. Proc Natl Acad Sci U S A 2000;97(13):7124-9.

(93) Oltersdorf T, Elmore SW, Shoemaker AR, Armstrong RC, Augeri DJ, Belli BA, Bruncko M, Deckwerth TL, Dinges J, Hajduk PJ, Joseph MK, Kitada S, Korsmeyer SJ, Kunzer AR, Letai A, Li C, Mitten MJ, Nettesheim DG, Ng S, Nimmer PM, O'Connor JM, Oleksijew A, Petros AM, Reed JC, Shen W et al. An inhibitor of Bcl-2 family proteins induces regression of solid tumours. Nature 2005;435(7042):677-81.

(94) Tse C, Shoemaker AR, Adickes J, Anderson MG, Chen J, Jin S, Johnson EF, Marsh KC, Mitten MJ, Nimmer P, Roberts L, Tahir SK, Xiao Y, Yang X, Zhang H, Fesik S, Rosenberg SH, Elmore SW. ABT-263: a potent and orally bioavailable Bcl-2 family inhibitor. Cancer Res 2008;68(9):3421-8.

(95) Rudin CM, Hann CL, Garon EB, Ribeiro de OM, Bonomi PD, Camidge DR, Chu Q, Giaccone G, Khaira D, Ramalingam SS, Ranson MR, Dive C, McKeegan EM, Chyla BJ, Dowell BL, Chakravartty A, Nolan CE, Rudersdorf N, Busman TA, Mabry MH, Krivoshik AP, Humerickhouse RA, Shapiro GI, Gandhi L. Phase II study of single-agent navitoclax (ABT-263) and biomarker correlates in patients with relapsed small cell lung cancer. Clin Cancer Res 2012;18(11):3163-9.

(96) Konopleva M, Contractor R, Tsao T, Samudio I, Ruvolo PP, Kitada S, Deng X, Zhai D, Shi YX, Sneed T, Verhaegen M, Soengas M, Ruvolo VR, McQueen T, Schober WD, Watt JC, Jiffar T, Ling X, Marini FC, Harris D, Dietrich M, Estrov Z, McCubrey J, May WS, Reed JC et al. Mechanisms of apoptosis sensitivity and resistance to the BH3 mimetic ABT-737 in acute myeloid leukemia. Cancer Cell 2006;10(5):375-88.

(97) Cao X, Yap JL, Newell-Rogers MK, Peddaboina C, Jian W, Papaconstantinou HT, Jupitor D, Rai A, Jung KY, Tubin RP, Yu W, Vanommeslaeghe K, Wilder PT, Mackerell AD, Jr., Fletcher S, Smythe RW. The novel BH3 alpha-helix mimetic JY-1-106 induces apoptosis in a subset of cancer cells (lung cancer, colon cancer and mesothelioma) by disrupting Bcl-xL and Mcl-1 protein--protein interactions with Bak. Mol Cancer 2013;12(1):42.

(98) Shore GC, Viallet J. Modulating the bcl-2 family of apoptosis suppressors for potential therapeutic benefit in cancer. Hematology Am Soc Hematol Educ Program 2005;226-30.

(99) Hunter T, Cooper JA. Protein-tyrosine kinases. Annu Rev Biochem 1985;54:897-930.

(100) Schrage YM, Briaire-de Bruijn IH, de Miranda NFCC, van Oosterwijk JG, Taminiau AHM, van Wezel T, Hogendoorn PCW, Bovée JVMG. Kinome profiling of chondrosarcoma reveals Src-pathway activity and dasatinib as option for treatment. Cancer Res 2009;69(15):6216-22.

(101) Cadena DL, Gill GN. Receptor tyrosine kinases. FASEB J 1992;6(6):2332-7.

(102) Drenberg CD, Baker SD, Sparreboom A. Integrating clinical pharmacology concepts in individualized therapy with tyrosine kinase inhibitors. Clin Pharmacol Ther 2013;93(3):215-9.

Chapter 2

Update on targets and novel treatment options for high grade chondrosarcoma

This chapter is based on the review: van Oosterwijk JG,Anninga JK, Gelderblom H, Cleton-Jansen AM, Bovée JVMG, Update on Update on targets and novel treatment options for high grade osteo- and chondrosarcoma, *Hem/Onc Clinics of North America, 2013*

Introduction

Primary bone tumors are rare and have a very specific age distribution (fig 2.1). Conventional osteosarcoma (OS) is the most frequent primary high-grade bone tumor in humans with 4 new cases per 10^6 population and year with the highest incidence in adolescence (1). The second most frequent primary bone malignancy, chondrosarcoma, accounts for approximately 3 new cases per 10^6 population and year predominantly affecting adults (2).The clinical management of unresectable and metastatic disease as well as therapy resistance remain a clinical challenge (3). This review will discuss the molecular pathways that have been identified as a result of intensive genome wide and basic biology analysis and rationale to current clinical and pre-clinical targets for therapy of these two most frequent bone sarcomas

Chondrosarcoma

Clinicopathological features

Chondrosarcomas are hyaline cartilaginous tumors most often arising in bones which develop during endochondral ossification. Incidence and location are shown in figures 1 and 2. Conventional chondrosarcoma accounts for approximately 85% of all primary chondrosarcomas (3) and prognosis is strongly correlated with histological grading. Grade I chondrosarcoma, now reclassified as an atypical cartilaginous tumor, shows low cellularity and is locally aggressive, but typically does not metastasize (2). Grade II and grade III conventional chondrosarcomas show increased cellularity with mitoses and reduced cartilaginous matrix, and a corresponding increase in metastasizing capacity alongside poor patient survival (2;4). Amongst the rare chondrosarcoma subtypes, dedifferentiated chondrosarcoma accounts for up to 10% of all chondrosarcomas and shows a dismal prognosis. Dedifferentiated chondrosarcoma is comprised of two histologically well distinctive components: a high grade dedifferentiated component, and a seemingly low grade cartilaginous component (5). Mesenchymal chondrosarcoma is considered high grade and accounts for approximately 3% of primary chondrosarcoma histologically showing undifferentiated small round cells admixed with well differentiated cartilage (6). Clear cell chondrosarcoma is considered low grade and comprises about 2% of all primary chondrosarcomas, demonstrating tumor cells with a clear, empty cytoplasm (7).

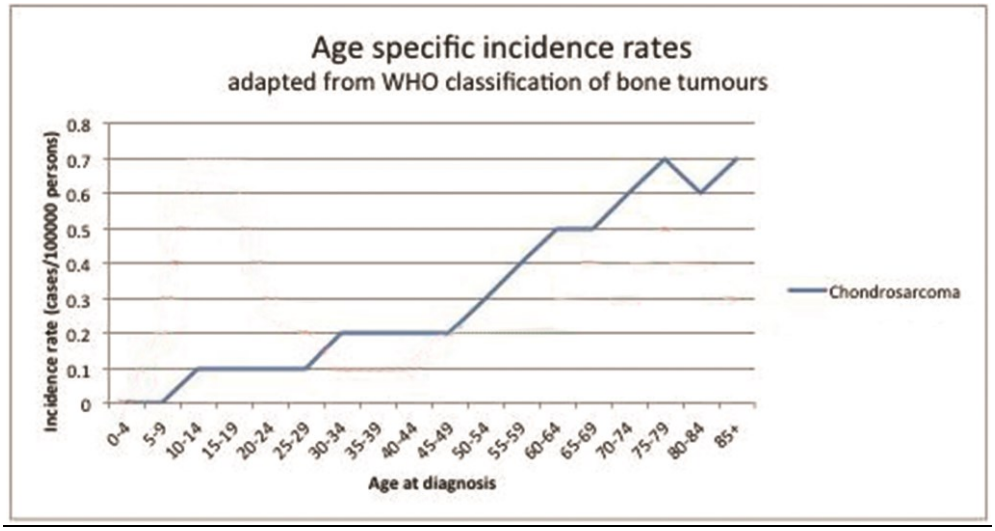

Figure 2.1. Incidence of chondrosarcoma stratified by age group. Chondrosarcoma (CS) is the second most common primary bone malignancy in humans and occurs predominantly between the 3rd and 6th decade of life. The increase in incidence observed after the 6th decade is attributed to recurrences. Adapted from WHO 2013

Current management of chondrosarcoma and resistance to therapy

The first line of treatment for chondrosarcoma is surgical resection with local adjuvant treatment such as phenol or cryosurgery, followed by filling the cavity with bone graft, showing long term local control in atypical cartilaginous tumor / grade I chondrosarcoma (8). Due to the necessity of wide resection margins to prevent recurrence in grade II and III chondrosarcoma, the patient often needs to undergo mutilating surgery. In the event of tumor location at a nonresectable site, such as in the skull or pelvis, or metastatic disease, there is still no curative treatment (3;9). Chondrosarcoma is notorious for its resistance to conventional chemo- and radiotherapy (3). Recently, a phase II study including 25 patients with chondrosarcoma using the nucleoside analog gemcitabine (657 mg/m2 on day 1 and day 8) followed by the anti-mitotic docetaxel (75 mg/m2 on day 8) over a course of 21 days, was aborted as only 2 patients showed partial response (10). In a recent study including 9 patients with dedifferentiated chondrosarcoma treated with surgery and chemotherapy (adriamycin, ifosfamide, cisplatin, and methotrexate) all patients died of metastatic disease (11). These results illustrate the high need for new targeted treatments in chondrosarcoma, as the conventional chemotherapeutics targeting the DNA machinery are not effective.

Primary chemoresistance of chondrosarcoma has long been ascribed to the phenotypic properties, such as hyaline cartilaginous matrix surrounding the cells prohibiting access to the cells, poor vascularization, and a slow division rate (12;13). As these properties are less prominent in high grade chondrosarcoma,

which typically shows less matrix, increased vascularization and increased mitotic rate, the resistance to therapy could also be due to activated anti-apoptosis or pro-survival pathways (12). Moreover, nuclear accumulation of doxorubicin was shown despite the presence of matrix and multidrug resistance pump activity. In addition, inhibition of the anti-apoptotic Bcl-2 family members was found to overcome resistance to doxorubicin and cisplatin in chondrosarcoma cell lines (14).

Targets and novel treatment options in chondrosarcoma

Over the past years advances have been made identifying multiple active pathways in chondrosarcoma, and preclinical work has led to the identification of potential targets for clinical trials (table 1). Here the recent identification of *IDH* mutations will be discussed in relation to active survival pathways and HIF1α expression found in high grade chondrosarcomas, as well as growth plate signaling pathways including anti-apoptotic signaling, and retinoblastoma pathway alterations.

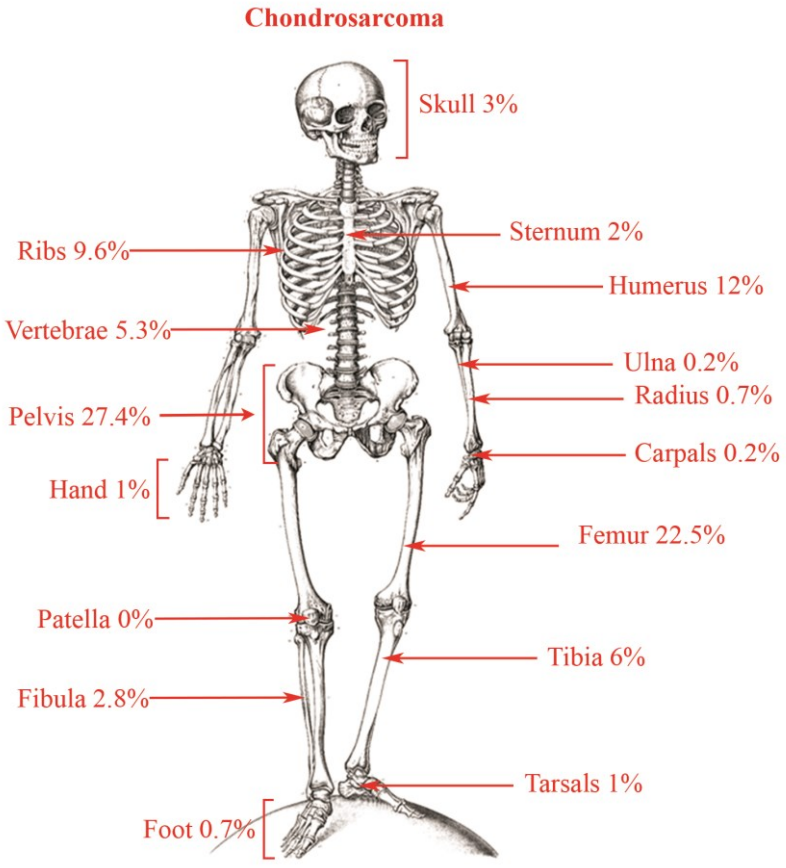

Figure 2.2. Distribution of chondrosarcoma across the skeleton.

Survival pathways: IDH mutations

Mutations in the isocitrate dehydrogenases (IDH) are found in 87% of benign enchondromas, 38-70% of primary conventional central chondrosarcoma, and 54% of dedifferentiated chondrosarcomas, but not in clear cell or mesenchymal chondrosarcomas (15-20). IDH is involved in the tricarboxylic acid cycle (Kreb's cycle) (21) and mutations in IHD1/2 lead to a diminished capacity to convert isocitrate to α-ketoglutarate (α-KG) and an acquired ability to convert αKG to D-2-hydroxyglutarate (D2HG), which is considered an oncometabolite (19;21-25).

The exact mechanism through which D2HG causes tumor formation is unknown although increasing evidence points towards epigenetic mechanisms (26-31). D2HG impairs the function of the αKG dependent dioxygenase TET2, leading to inhibition of DNA demethylation causing CpG island hypermethylation (27;32;33). Indeed, enchondromas carrying *IDH* mutations were hypermethylated (17). In addition, D2HG was shown to impair histone demethylation (33). Moreover, mutations in IDH are postulated to inhibit the prolyl/lysyl/hydroxylation of collagen proteins and thereby their maturation as an *IDH1* R132H conditional knock-in mouse model showed a reduction in collagen IV maturation (34). Finally, D2HG was postulated to induce pseudohypoxia (fig3) by inhibition of the HIF proline hydroxylases although this is controversial (22;34;35).

HIF-1α is upregulated by a multitude of malignancies to cope with reduced perfusion, and is associated with increased proliferation, VEGF production, and resistance to chemo- and radiotherapy (36-40). High grade conventional chondrosarcoma shows activation of the hypoxia pathway through HIF1α (41). Most drugs targeting hypoxia, are designed either to target VEGF, the downstream target of HIF1α, or to target the PI3K/AKT/mTOR pathway, which can induce HIF1α independent of oxygen conditions (fig 3) (36;42).

Survival pathways: PI3K, AKT, mTOR, VEGF

The PI3K/AKT pathway is often upregulated in cancer and can either inhibit apoptosis, or promote cell proliferation (fig 3) (43). Active AKT signaling was shown in chondrosarcoma(44) and the PI3K/AKT pathway has been shown to be involved in proliferation in mesenchymal chondroprogenitor cells (45). In chondrocytes, the PI3K/AKT can be activated by the chondrogenic transcription factor SOX9 (46), which is also expressed in chondrosarcoma (47;48). SOX9 siRNA in a chondrosarcoma cell line (SW1353) induced apoptosis which could be rescued by PTEN expression (46). Mutations in the tumor suppressor *PTEN* are rare in chondrosarcoma (49). Perifosine, an AKT inhibitor inhibiting AKT membrane recruitment, showed 17% decrease in tumor size in one chondrosarcoma patient after two cycles (Steinert, CTOS 2006). A larger phase II study was conducted including patients with chemoinsensitive sarcomas but has not posted results (NCT00401388).

Mechanistic TOR (mTOR) is a point of convergence of many pathways involved in protein synthesis and cell proliferation, including the PI3K/AKT pathway (fig

3). The first suggestion of activation of the mTOR pathway was in mesenchymal chondrosarcoma, showing strong cytoplasmic p-AKT, p-mTOR, and PDGFR-alpha staining (50). In an adjuvant rat orthotopic Swarm Rat chondrosarcoma model, everolimus alone or in combination with doxorubicin after curettage showed inhibition of mTORC1 and decreased cell proliferation, however, the combination with doxorubicin showed an antagonistic effect with activation of the mTORC2 pathway (51). Allosteric inhibitors of the mTOR pathway, rapalogs, (rapamycin (sirolimus), everolimus, and temsirolimus) have limited efficacy in the clinic, but show high synergy with dual PI3K/mTOR inhibitors such as BEZ235 (52). A clinical trial with temsirolimus and liposomal doxorubicin included chondrosarcoma patients (NCT00949325). While awaiting the results of this trial, a study including ten patients with unresectable chondrosarcoma who were treated with sirolimus and cyclophosphamide showed a disease control rate of 70% (53). However, the resistance to rapalogs observed in other malignancies is suggestive that in chondrosarcoma a strategy including dual PI3K/mTOR inhibitors such as BEZ235 should be considered for future clinical trials.
Activated Src signaling can also lead to HIF1α expression (fig 3) (12;54;55) and promote cell survival. Src signaling was shown to be elevated in chondrosarcoma (44), and the tyrosine kinase inhibitor dasatinib showed a decrease in cell proliferation in 7 out of 9 cell lines (44). However, in a phase II study no objective response was obtained with dasatinib single agent (70mg bid as starting dose) in chondrosarcoma patients (Schuetze CTOS 2010).
Activation of survival pathways can be through stimulation of the receptor tyrosine kinases by IGF-1 or PDGF. IGF-1 pathway activation was shown to be involved in chondrosarcoma proliferation, migration, apoptosis (56) (57;58), as well as progression to malignancy (58). Activation of the PDGF pathway has been shown to be related to worse prognosis in chondrosarcoma (59-61). Inhibition with imatinib, however, showed no effect in vitro in four chondrosarcoma cell lines (44), and in a clinical study including 26 patients no objective response was measured (62). HIF1α expression is suggested to result in increased VEGF expression in chondrosarcoma (40). Sunitinib and pazopanib are tyrosine kinase inhibitors, targeting multiple kinases including both PDGF and VEGF. In combination with proton beam radiation, sunitinib was reported to achieve complete symptomatic relieve and durable response in a patient with metastatic clear cell chondrosarcoma (63). A clinical study with pazopanib is currently recruiting chondrosarcoma patients (NCT01330966).

Developmental pathways: Hedgehog
In osteochondroma, a benign cartilaginous tumor at the surface of bone that can give rise to secondary peripheral chondrosarcoma, mutations in the genes encoding either *exostosin -1* (*EXT1*) or -2 (*EXT2*) have been identified (64). *EXT1* and *EXT2* are involved in the biosynthesis of heparan sulfate proteoglycans, which are necessary for the diffusion of the morphogen Indian Hedgehog (IHH) (65).

Recently, osteochondromas were shown to contain a mixture of both *EXT* mutant as well wildtype tumor cells (with functional EXT), and the latter were shown to be the precursor cells of peripheral chondrosarcoma (66) since peripheral chondrosarcoma have functional EXT, pointing towards a pathogenesis in chondrosarcoma independent of EXT.

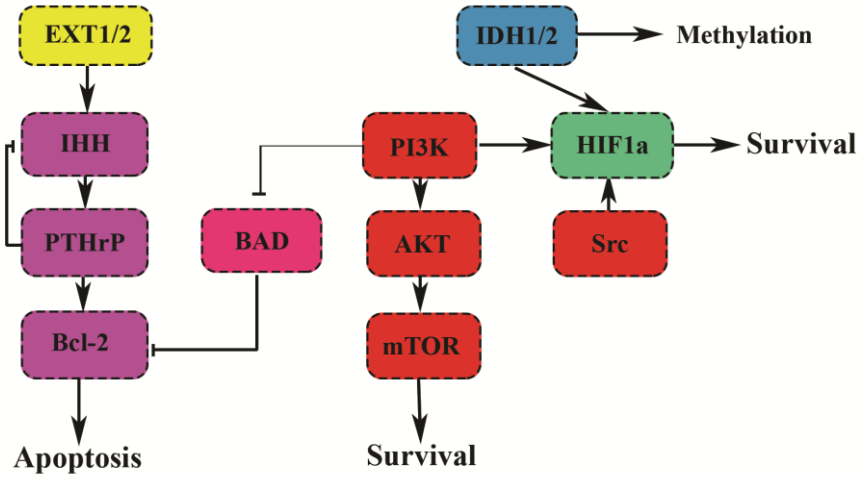

Figure 2.3. Apoptosis and survival pathways. EXT1/2: exostosin 1/2, IHH: Indian hedgehog, PTHrP: parathyroid protein, Bcl-2: B-cell lymphoma 2, BAD: Bcl-2 associated protein 2, IDH1/2: isocitrate 1/2, PI3K: phosphoinositide 3-kinase, AKT (PKB: Protein kinase B), mTOR: mammalian target of rapamycin, HIF1a: hypoxia inducible factor 1a, Src: sarcoma.

IHH is part of a negative feedback loop with parathyroid hormone-related protein (PTHrP), creating a tight balance between proliferation and differentiation (fig 3) (for review see (67;68)). Aberrant hedgehog signaling is also found in central chondrosarcoma (69;70), despite absence of *EXT* mutations. Blocking of the hedgehog pathway with triparanol was shown to be effective (70), but reports on the effect of cylopamine are conflicting (69-71).

A recent randomised phase II clinical trial with IPI-926 (saridegib), a potent cyclopamine analogue (72), for patients with metastatic or locally advanced conventional chondrosarcoma was terminated as the primary endpoint, progression-free survival, was not met (NCT01609179). A second trial is currently ongoing with vismodegib, a cyclopamine-competitive SMO-inihibitor

(NCT01267955). Preliminary results show stable disease in 4 out of 17 patients (Italiano, ASCO 2012). In osteochondroma, primary cilia were found to retain their normal length but lose their orientation contributing to loss of chondrocyte directionality (73) while 70-100% of human enchondromas and chondrosarcomas were found to lack primary cilia (74). In lft88-/- mice lacking primary cilia increased hedgehog signaling and enchondroma and chondrosarcoma formation, was observed. As cyclopamine depends on the primary cilia for SMO accumulation, chondrosarcoma cells lacking primary cilia were unresponsive to cyclopamine treatment (74). These results support the role for IHH in initiation of chondrosarcoma, and suggest that when inhibiting the hedgehog pathway in chondrosarcoma targets should be carefully selected.

Developmental pathways: Anti-apoptosis

The anti-apoptotic protein Bcl-2 is under direct regulation of PTH1R and is upregulated in chondrosarcoma (fig 3) (75). Moreover, Bcl-xl, another anti-apoptotic protein belonging to the Bcl-2 family was shown to be overexpressed in 18 chondrosarcoma tissues (76), indicating a specific defense mechanism contributing to chemoresistance in chondrosarcoma. siRNA against Bcl-2, Bcl-xl, and XIAP showed an enhanced sensitivity to doxorubicin and radiation (77;78), and treatment with the BH-3 mimetic ABT-737, was shown to synergistically overcome resistance to doxorubicin and cisplatin (14). Another anti-apoptotic protein, not related to the Bcl-2 family, survivin, was also found to be highly expressed in chondrosarcoma (79;80) and inhibition experiments in 2 cell lines resulted in overcoming resistance to doxorubicin (79). These data point towards an effective defense mechanism in which chondrosarcoma cells prevent programmed cell death in response to stress signals such as DNA damage.

Treatment with dulanermin (rhApo2L/TRAIL), a death receptor 4 (DR4) and 5 (DR5) agonist, showed complete remission in one patient (81), and treatment with apomab, a DR5 agonist, showed a 20% reduction in measureable disease in one chondrosarcoma patient (82), but showed no efficacy in a follow up phase 2 trial with 90 chondrosarcoma patients (NCT00543712). These (pre-) clinical results combined with this promising result with dulanermin show that restoring the defect in the apoptotic machinery could prove strong therapeutic potential in chondrosarcoma. However, since multiple anti-apoptotic proteins are upregulated in chondrosarcoma, a multi-targeted approach may be more effective, considering that dulanermin, targeting both DR4 and DR5, was more effective than apomab, targeting only DR5.

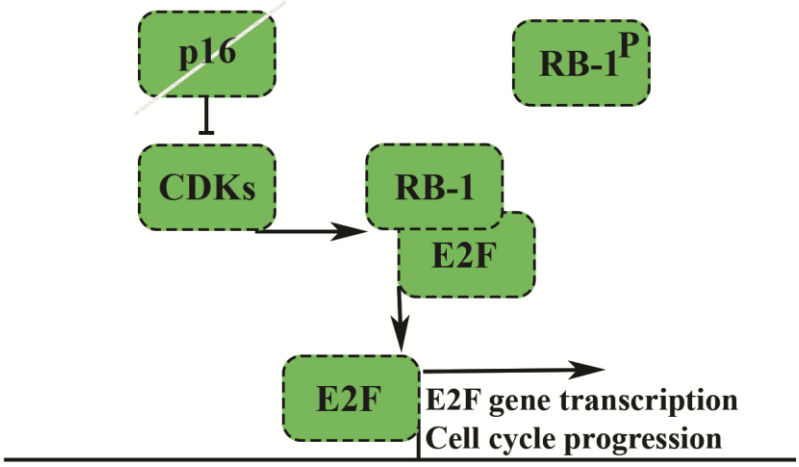

Figure 2.4. RB-1 pathway: p16 is a tumor suppressor and inhibits the cyclin dependent kinases (CDKs). Upon loss of p16, active CDKs phosphorylate RB-1 and release it from the E2F transcription factors, allowing for E2F target gene transcription and uncontrolled cell cycle progression.

Retinoblastoma signaling

The retinoblastoma protein pRb is a tumor suppressor controlling the cell cycle. In the absence of $p16^{INK4A}$, RB-1 is released from E2F transcription factors such as histone deacetylases (HDAC) and cell cycle progression and gene transcription can occur (fig 4) (83). Recently *Rb* was shown to be required for hypertrophic chondrocyte differentiation, and $Rb^{c/c}/p107^{-/-}$ mice were shown to develop enchondromas, indicating an important role for cell cycle regulation during tumor development (84).

Ninety-six percent of conventional central high grade chondrosarcoma show alterations in the retinoblastoma pathway (85); not only through loss of the tumor suppressor *CDKN2A/p16* (86;87) along with elevated *CDK4* (88) but also through amplifications of *CDK6* and *E2F3* (89). In dedifferentiated chondrosarcoma p16 aberrations were found to be common (85%) and associated with loss of chromosome 9p (16) or promoter methylation (90). In mesenchymal and clear cell chondrosarcoma p16 alterations are found in 70% and 95% of the cases, respectively (16). Inhibition of CDK4 using shRNA against CDK4 was found to inhibit cell proliferation in three central chondrosarcoma cell lines (85). In a phase I dose defining study of the HSP90 inhibitor alvespimycin, one chondrosarcoma

patient showed CR (>6months stable disease) with reduction in CDK4 levels (91), supporting further exploration of HSP90 or CDK4 inhibitors in chondrosarcoma.
On close proximity to the *CDKN2* locus on chromosome 9 is the methylthioadenosine phosphorylase (*MTAP*), an enzyme vital for the recycling of adenine and methionine synthesis. Deletions involving the MTAP locus (9p21) have been reported in 50% of chondrosarcoma cases (89;92-94). In MTAP deficient cells, adenine and methionine are not metabolized rendering these cells more sensitive to selective inhibition of de novo purine synthesis. Permetrexed disodium is a multitargeted anti-folate preventing the formation of precursor purine and pyrimidine nucleotides (95). A phase II trial with permetrexed disodium, has been performed in patients with metastatic or locally advanced chondrosarcoma (NCT00107419). No results have been posted yet.

Other therapies: COX-2 and aromatase inhibitors
Estrogen signaling plays a role in skeletal maturation and was found to be active in all chondrosarcoma subtypes (96-98). Even though initial results were promising (96;99), a recent retrospective series including 6 patients with locally advanced or metastatic chondrosarcoma treated with aromatase inhibitors did not show an increase in PFS compared to historically untreated patients (98). The prostaglandin synthase cyclooxygenase-2 (COX-2) is upregulated during inflammation, but also in for example colorectal, breast and prostate cancer (100). COX-2 upregulation was shown in chondrosarcoma (101;102) and to be associated with poor survival (103). COX-2 inhibition with celecoxib showed decreased cell viability in 4 chondrosarcoma cell lines, however, in chondrosarcoma xenografts, a relapse was observed after 6 weeks (102). The negative results obtained with aromatase inhibitors in patients and COX-2 inhibitors in mice do not support clinical implementation of these therapeutic strategies.

Table 2.1 Overview of Targets and Selected Trials in chondrosarcoma

Target	Drug	Mechanism	Clinical results	Clinical trial identifyer or reference
DNA synthesis	gemcitabine	Nucleoside analog	Phase II (n=53) combination with docetaxel. Terminated due to lack of evidence of efficacy	(10).
	permetrexed	Prevents formation of DNA and RNA	Study completed, no results posted	NCT00107419
AKT/PI3K	perifosine	Inhibits AKT membrane recruitment	Phase I (n=10) combination with gemcitabine CS patient showed 17% decrease in tumor size after two cycles	NCT00401388 (Steinert CTOS 2006)
mTOR	sirolimus	mTOR inhibitor	Combination with cyclophosphamide in 10 patients disease control rate of 70%	(53)
SRC	dasatinib	Small molecule kinase inhibitor	Phase II, ongoing, NOR in CS	NCT00464620 (Schuetze CTOS 2006)

PDGF	sunitinib (SU11248)	Multi-targeted receptor tyrosine kinase inhibitor	Phase II, completed, no results posted Case study: Antitumor activity in 2 patients with extraskeletal myxoid CS Case study: Durable response after combination with proton beam radiation in 1 patient with metastatic clear cell CS	NCT00474994 (104) (63)
	imatinib	Competitive tyrosine kinase inhibitor	Phase II (n=26), NOR	(62)
	pazopanib	Blocks autophosphosphorylation of PDGF receptors, VEGF receptors, FGF receptors 1 and 3; inhibits Kit and Lck	Recruiting	NCT01330966
Hedgehog	saridegib (IPI-926)	Smoothened inhibitor	Study terminated due to lack of evidence of efficacy Ongoing	NCT01609179 NCT01310816
	vismodegib (GDC-0449)	Smoothened inhibitor	Ongoing	NCT01267955

Apoptosis	Dulanermin rhAPO2L/TRAIL (AMG 951)	induces apoptosis through binding to DR4 and DR5	Phase I study n=71 2 CS patients durable PR Case study: near CR over 78 months in one patient with metastatic disease	(81;105)
	apomab	Mono-clonal IgG1 anti-antibody that triggers extrinsic apoptotic pathway through DR5	Phase I study n=50, terminated due to lack of evidence of efficacy CS patient 20% reduction in measurable disease	(82)
Rb pathway	alvespimycin	HSP90 inhibitor	Phase I study n=25 CS patient CR with reduction in CDK4 levels	(9)

CS: chondrosarcoma, NOR: no objective response, CR: complete response, PR: partial response.

References

(1) Fletcher C.D.M., Bridge JA, Hogendoorn PCW, Mertens F. WHO Classification of Tumours of Soft Tissue and Bone. 4 ed. 2013.

(2) Hogendoorn PCW, Bovée JVMG, Nielsen GP. Chondrosarcoma (grades I-III), including primary and secondary variants and periosteal chondrosarcoma. In: Fletcher C.D.M., Bridge JA, Hogendoorn PCW, Mertens F, editors. World Health Classification of Tumours. Pathology and Genetics of Tumours of Soft Tissue and Bone. 4 ed. 2013. p. 264-8.

(3) Gelderblom H, Hogendoorn PCW, Dijkstra SD, van Rijswijk CS, Krol AD, Taminiau AH, Bovee JV. The clinical approach towards chondrosarcoma. Oncologist 2008;13(3):320-9.

(4) Evans HL, Ayala AG, Romsdahl MM. Prognostic factors in chondrosarcoma of bone. A clinicopathologic analysis with emphasis on histologic grading. Cancer 1977;40:818-31.

(5) Inwards CY, Hogendoorn PCW. Dedifferentiated Chondrosarcoma. In: Fletcher C.D.M., Bridge JA, Hogendoorn PCW, Mertens F, editors. World Health Organization Classification of Tumours. Pathology and Genetics of Tumours of Soft Tissue and Bone. 4 ed. 2013. p. 269-70.

(6) Nakashima Y, de Pinieux G, Ladanyi M. Mesenchymal Chondrosarcoma. In: Fletcher C.D.M., Bridge JA, Hogendoorn PCW, Mertens F, editors. World Health Organization Classification of Tumours. Pathology and Genetics of Tumours of Soft Tissue and Bone. 2013. p. 271-2.

(7) McCarthy EF, Hogendoorn PCW. Clear Cell Chondrosarcoma. In: Fletcher C.D.M., Bridge JA, Hogendoorn PCW, Mertens F, editors. World Health Organization Classification of Tumours. Pathology and Genetics of Tumours of Soft Tissue and Bone. 4 ed. 2013. p. 273-4.

(8) Verdegaal SH, Brouwers HF, van Zwet EW, Hogendoorn PC, Taminiau AH. Low-grade chondrosarcoma of long bones treated with intralesional curettage followed by application of phenol, ethanol, and bone-grafting. J Bone Joint Surg Am 2012;94(13):1201-7.

(9) Bone sarcomas: ESMO Clinical Practice Guidelines for diagnosis, treatment and follow-up. Ann Oncol 2012;23 Suppl 7:vii100-vii109.

(10) Fox E, Patel S, Wathen JK, Schuetze S, Chawla S, Harmon D, Reinke D, Chugh R, Benjamin RS, Helman LJ. Phase II Study of Sequential Gemcitabine Followed by Docetaxel for Recurrent Ewing Sarcoma, Osteosarcoma, or Unresectable or Locally Recurrent Chondrosarcoma: Results of Sarcoma Alliance for Research Through Collaboration Study 003.

Oncologist 2012;17(3):321-e329.

(11) Yokota K, Sakamoto A, Matsumoto Y, Matsuda S, Harimaya K, Oda Y, Iwamoto Y. Clinical outcome for patients with dedifferentiated chondrosarcoma: a report of 9 cases at a single institute. J Orthop Surg Res 2012;7(1):38.

(12) Bovée JVMG, Hogendoorn PCW, Wunder JS, Alman BA. Cartilage tumours and bone development: molecular pathology and possible therapeutic targets. Nat Rev Cancer 2010;10(7):481-8.

(13) David E, Blanchard F, Heymann MF, De PG, Gouin F, Redini F, Heymann D. The Bone Niche of Chondrosarcoma: A Sanctuary for Drug Resistance, Tumour Growth and also a Source of New Therapeutic Targets. Sarcoma 2011;2011:-932451.

(14) van Oosterwijk JG, Herpers B, Meijer D, Briaire-de Bruijn IH, Cleton-Jansen AM, Gelderblom H, van de Water B, Bovée JVMG. Restoration of chemosensitivity for doxorubicin and cisplatin in chondrosarcoma in vitro: BCL-2 family members cause chemoresistance. Ann Oncol 2012;23(6):1617-26.

(15) Schaap FG, French PJ, Bovee JVMG. Mutations in the Isocitrate Dehydrogenase Genes IDH1 and IDH2 in Tumors. Adv Anat Pathol 2013;20(1):32-8.

(16) Meijer D, de JD, Pansuriya TC, van den Akker BE, Picci P, Szuhai K, Bovee JV. Genetic characterization of mesenchymal, clear cell, and dedifferentiated chondrosarcoma. Genes Chromosomes Cancer 2012;51(10):899-909.

(17) Pansuriya TC, van ER, d'Adamo P, van Ruler MA, Kuijjer ML, Oosting J, Cleton-Jansen AM, van Oosterwijk JG, Verbeke SL, Meijer D, van WT, Nord KH, Sangiorgi L, Toker B, Liegl-Atzwanger B, San-Julian M, Sciot R, Limaye N, Kindblom LG, Daugaard S, Godfraind C, Boon LM, Vikkula M, Kurek KC, Szuhai K et al. Somatic mosaic IDH1 and IDH2 mutations are associated with enchondroma and spindle cell hemangioma in Ollier disease and Maffucci syndrome. Nat Genet 2011;43(12):1256-61.

(18) Amary MF, Bacsi K, Maggiani F, Damato S, Halai D, Berisha F, Pollock R, O'Donnell P, Grigoriadis A, Diss T, Eskandarpour M, Presneau N, Hogendoorn PC, Futreal A, Tirabosco R, Flanagan AM. IDH1 and IDH2 mutations are frequent events in central chondrosarcoma and central and periosteal chondromas but not in other mesenchymal tumours. J Pathol 2011;224(3):334-43.

(19) Amary MF, Damato S, Halai D, Eskandarpour M, Berisha F, Bonar F, McCarthy S, Fantin VR, Straley KS, Lobo S, Aston W, Green CL, Gale RE, Tirabosco R, Futreal A, Campbell P, Presneau N, Flanagan AM. Ollier disease and Maffucci syndrome are caused by somatic mosaic

mutations of IDH1 and IDH2. Nat Genet 2011.

(20) Damato S, Alorjani M, Bonar F, McCarthy SW, Cannon SR, O'Donnell P, Tirabosco R, Amary MF, Flanagan AM. IDH1 mutations are not found in cartilaginous tumours other than central and periosteal chondrosarcomas and enchondromas. Histopathology 2011.

(21) Leonardi R, Subramanian C, Jackowski S, Rock CO. Cancer-associated isocitrate dehydrogenase mutations inactivate NADPH-dependent reductive carboxylation. J Biol Chem 2012;287(18):14615-20.

(22) Zhao S, Lin Y, Xu W, Jiang W, Zha Z, Wang P, Yu W, Li Z, Gong L, Peng Y, Ding J, Lei Q, Guan KL, Xiong Y. Glioma-derived mutations in IDH1 dominantly inhibit IDH1 catalytic activity and induce HIF-1alpha. Science 2009;324(5924):261-5.

(23) Dang L, White DW, Gross S, Bennett BD, Bittinger MA, Driggers EM, Fantin VR, Jang HG, Jin S, Keenan MC, Marks KM, Prins RM, Ward PS, Yen KE, Liau LM, Rabinowitz JD, Cantley LC, Thompson CB, Vander Heiden MG, Su SM. Cancer-associated IDH1 mutations produce 2-hydroxyglutarate. Nature 2009;462(7274):739-44.

(24) Luchman HA, Stechishin OD, Dang NH, Blough MD, Chesnelong C, Kelly JJ, Nguyen SA, Chan JA, Weljie AM, Cairncross JG, Weiss S. An in vivo patient-derived model of endogenous IDH1-mutant glioma. Neuro Oncol 2012;14(2):184-91.

(25) Ward PS, Patel J, Wise DR, Abdel-Wahab O, Bennett BD, Coller HA, Cross JR, Fantin VR, Hedvat CV, Perl AE, Rabinowitz JD, Carroll M, Su SM, Sharp KA, Levine RL, Thompson CB. The common feature of leukemia-associated IDH1 and IDH2 mutations is a neomorphic enzyme activity converting alpha-ketoglutarate to 2-hydroxyglutarate. Cancer Cell 2010;17(3):225-34.

(26) Dang L, Jin S, Su SM. IDH mutations in glioma and acute myeloid leukemia. Trends Mol Med 2010;16(9):387-97.

(27) Figueroa ME, Abdel-Wahab O, Lu C, Ward PS, Patel J, Shih A, Li Y, Bhagwat N, Vasanthakumar A, Fernandez HF, Tallman MS, Sun Z, Wolniak K, Peeters JK, Liu W, Choe SE, Fantin VR, Paietta E, Lowenberg B, Licht JD, Godley LA, Delwel R, Valk PJ, Thompson CB, Levine RL et al. Leukemic IDH1 and IDH2 mutations result in a hypermethylation phenotype, disrupt TET2 function, and impair hematopoietic differentiation. Cancer Cell 2010;18(6):553-67.

(28) Hartmann C, Meyer J, Balss J, Capper D, Mueller W, Christians A, Felsberg J, Wolter M, Mawrin C, Wick W, Weller M, Herold-Mende C, Unterberg A, Jeuken JW, Wesseling P, Reifenberger G, von DA. Type and frequency of IDH1 and IDH2 mutations are related to astrocytic and oligodendroglial differentiation and age: a study

of 1,010 diffuse gliomas. Acta Neuropathol 2009;118(4):469-74.

(29) Kang MR, Kim MS, Oh JE, Kim YR, Song SY, Seo SI, Lee JY, Yoo NJ, Lee SH. Mutational analysis of IDH1 codon 132 in glioblastomas and other common cancers. Int J Cancer 2009;125(2):353-5.

(30) Murugan AK, Bojdani E, Xing M. Identification and functional characterization of isocitrate dehydrogenase 1 (IDH1) mutations in thyroid cancer. Biochem Biophys Res Commun 2010;393(3):555-9.

(31) Yan H, Parsons DW, Jin G, McLendon R, Rasheed BA, Yuan W, Kos I, Batinic-Haberle I, Jones S, Riggins GJ, Friedman H, Friedman A, Reardon D, Herndon J, Kinzler KW, Velculescu VE, Vogelstein B, Bigner DD. IDH1 and IDH2 mutations in gliomas. N Engl J Med 2009;360(8):765-73.

(32) Noushmehr H, Weisenberger DJ, Diefes K, Phillips HS, Pujara K, Berman BP, Pan F, Pelloski CE, Sulman EP, Bhat KP, Verhaak RG, Hoadley KA, Hayes DN, Perou CM, Schmidt HK, Ding L, Wilson RK, Van Den Berg D, Shen H, Bengtsson H, Neuvial P, Cope LM, Buckley J, Herman JG, Baylin SB et al. Identification of a CpG island methylator phenotype that defines a distinct subgroup of glioma. Cancer Cell 2010;17(5):510-22.

(33) Lu C, Ward PS, Kapoor GS, Rohle D, Turcan S, Abdel-Wahab O, Edwards CR, Khanin R, Figueroa ME, Melnick A, Wellen KE, O'Rourke DM, Berger SL, Chan TA, Levine RL, Mellinghoff IK, Thompson CB. IDH mutation impairs histone demethylation and results in a block to cell differentiation. Nature 2012;483(7390):474-8.

(34) Sasaki M, Knobbe CB, Itsumi M, Elia AJ, Harris IS, Chio II, Cairns RA, McCracken S, Wakeham A, Haight J, Ten AY, Snow B, Ueda T, Inoue S, Yamamoto K, Ko M, Rao A, Yen KE, Su SM, Mak TW. D-2-hydroxyglutarate produced by mutant IDH1 perturbs collagen maturation and basement membrane function. Genes Dev 2012;26(18):2038-49.

(35) Koivunen P, Lee S, Duncan CG, Lopez G, Lu G, Ramkissoon S, Losman JA, Joensuu P, Bergmann U, Gross S, Travins J, Weiss S, Looper R, Ligon KL, Verhaak RG, Yan H, Kaelin WG, Jr. Transformation by the (R)-enantiomer of 2-hydroxyglutarate linked to EGLN activation. Nature 2012;483(7390):484-8.

(36) Greer SN, Metcalf JL, Wang Y, Ohh M. The updated biology of hypoxia-inducible factor. EMBO J 2012;31(11):2448-60.

(37) Robey IF, Lien AD, Welsh SJ, Baggett BK, Gillies RJ. Hypoxia-inducible factor-1alpha and the glycolytic phenotype in tumors. Neoplasia 2005;7(4):324-30.

(38) O'Donnell JL, Joyce MR, Shannon AM, Harmey J, Geraghty J, Bouchier-Hayes D. Oncological implications of hypoxia inducible factor-1alpha (HIF-1alpha) expression.

Cancer Treat Rev 2006;32(6):407-16.

(39) Fang J, Yan L, Shing Y, Moses MA. HIF-1alpha-mediated up-regulation of vascular endothelial growth factor, independent of basic fibroblast growth factor, is important in the switch to the angiogenic phenotype during early tumorigenesis. Cancer Res 2001;61(15):5731-5.

(40) Lin C, McGough R, Aswad B, Block JA, Terek R. Hypoxia induces HIF-1alpha and VEGF expression in chondrosarcoma cells and chondrocytes. J Orthop Res 2004;22(6):1175-81.

(41) Boeuf S, Bovee JVMG, Lehner B, Hogendoorn PCW, Richter W. Correlation of hypoxic signalling to histological grade and outcome in cartilage tumours. Histopathology 2009.

(42) Agani F, Jiang BH. Oxygen-independent regulation of HIF-1: novel involvement of PI3K/AKT/mTOR pathway in cancer. Curr Cancer Drug Targets 2013.

(43) Maddika S, Ande SR, Panigrahi S, Paranjothy T, Weglarczyk K, Zuse A, Eshraghi M, Manda KD, Wiechec E, Los M. Cell survival, cell death and cell cycle pathways are interconnected: implications for cancer therapy. Drug Resist Updat 2007;10(1-2):13-29.

(44) Schrage YM, Briaire-de Bruijn IH, de Miranda NFCC, van Oosterwijk JG, Taminiau AHM, van Wezel T, Hogendoorn PCW, Bovée JVMG. Kinome profiling of chondrosarcoma reveals Src-pathway activity and dasatinib as option for treatment. Cancer Res 2009;69(15):6216-22.

(45) Akiyama H, Furukawa S, Wakisaka S, Maeda T. Cartducin stimulates mesenchymal chondroprogenitor cell proliferation through both extracellular signal-regulated kinase and phosphatidylinositol 3-kinase/Akt pathways. FEBS J 2006;273(10):2257-63.

(46) Ikegami D, Akiyama H, Suzuki A, Nakamura T, Nakano T, Yoshikawa H, Tsumaki N. Sox9 sustains chondrocyte survival and hypertrophy in part through Pik3ca-Akt pathways. Development 2011;138(8):1507-19.

(47) Cajaiba MM, Jianhua L, Goodman MA, Fuhrer KA, Rao UN. Sox9 expression is not limited to chondroid neoplasms: variable occurrence in other soft tissue and bone tumors with frequent expression by synovial sarcomas. Int J Surg Pathol 2010;18(5):319-23.

(48) Wehrli BM, Huang W, De CB, Ayala AG, Czerniak B. Sox9, a master regulator of chondrogenesis, distinguishes mesenchymal chondrosarcoma from other small blue round cell tumors. Hum Pathol 2003;34(3):263-9.

(49) Lin C, Meitner PA, Terek RM. PTEN Mutation Is Rare in Chondrosarcoma. Diagn Mol Pathol 2002;11(1):22-6.

(50) Brown RE, Boyle JL. Mesenchymal chondrosarcoma: molecular characterization by a proteomic approach, with morphogenic and therapeutic

implications. Ann Clin Lab Sci 2003;33(2):131-41.

(51) Perez J, Decouvelaere AV, Pointecouteau T, Pissaloux D, Michot JP, Besse A, Blay JY, Dutour A. Inhibition of chondrosarcoma growth by mTOR inhibitor in an in vivo syngeneic rat model. PLoS ONE 2012;7(6):e32458.

(52) Yang S, Xiao X, Meng X, Leslie KK. A mechanism for synergy with combined mTOR and PI3 kinase inhibitors. PLoS ONE 2011;6(10):e26343.

(53) Bernstein-Molho R, Kollender Y, Issakov J, Bickels J, Dadia S, Flusser G, Meller I, Sagi-Eisenberg R, Merimsky O. Clinical activity of mTOR inhibition in combination with cyclophosphamide in the treatment of recurrent unresectable chondrosarcomas. Cancer Chemother Pharmacol 2012;70(6):855-60.

(54) Aligayer H, Boyd DD, Heiss MM, Abdalla EK, Curley SA, Gallick GE. Activation of Src kinase in primary colorectal carcinoma: an indicator of poor clinical prognosis. Cancer 2002;94(2):344-51.

(55) Fizazi K. The role of Src in prostate cancer. Ann Oncol 2007;18(11):1765-73.

(56) Matsumura T, Whelan MC, Li XQ, Trippel SB. Regulation by IGF-I and TGF-beta1 of Swarm-rat chondrosarcoma chondrocytes. J Orthop Res 2000;18(3):351-5.

(57) Wu CM, Li TM, Hsu SF, Su YC, Kao ST, Fong YC, Tang CH. IGF-I enhances alpha5beta1 integrin expression and cell motility in human chondrosarcoma cells. J Cell Physiol 2011;226(12):3270-7.

(58) Ho L, Stojanovski A, Whetstone H, Wei QX, Mau E, Wunder JS, Alman B. Gli2 and p53 cooperate to regulate IGFBP-3- mediated chondrocyte apoptosis in the progression from benign to malignant cartilage tumors. Cancer Cell 2009;16(2):126-36.

(59) Masui F, Ushigome S, Fujii K. Clear cell chondrosarcoma: a pathological and immunohistochemical study. Histopathology 1999;34(5):447-52.

(60) Sulzbacher I, Birner P, Trieb K, Muhlbauer M, Lang S, Chott A. Platelet-derived growth factor-alpha receptor expression supports the growth of conventional chondrosarcoma and is associated with adverse outcome. Am J Surg Pathol 2001;25(12):1520-7.

(61) Franchi A, Baroni G, Sardi I, Giunti L, Capanna R, Campanacci D. Dedifferentiated peripheral chondrosarcoma: a clinicopathologic, immunohistochemical, and molecular analysis of four cases. Virchows Arch 2012;460(3):335-42.

(62) Grignani G, Palmerini E, Stacchiotti S, Boglione A, Ferraresi V, Frustaci S, Comandone A, Casali PG, Ferrari S, Aglietta M. A phase 2 trial of imatinib mesylate in patients with recurrent nonresectable chondrosarcomas expressing platelet-derived growth factor receptor-alpha or -beta: An Italian Sarcoma

Group study. Cancer 2011;117(4):826-31.

(63) Dallas J, Imanirad I, Rajani R, Dagan R, Subbiah S, Gaa R, Dwarica WA, Ivey AM, Zlotecki RA, Malyapa R, Indelicato DJ, Scarborough MT, Reith JD, Gibbs CP, Dang LH. Response to sunitinib in combination with proton beam radiation in a patient with chondrosarcoma: a case report. J Med Case Rep 2012;6:41.

(64) Jennes I, Pedrini E, Zuntini M, Mordenti M, Balkassmi S, Asteggiano CG, Casey B, Bakker B, Sangiorgi L, Wuyts W. Multiple osteochondromas: mutation update and description of the multiple osteochondromas mutation database (MOdb). Hum Mutat 2009;30(12):1620-7.

(65) Stickens D, Brown D, Evans GA. EXT genes are differentially expressed in bone and cartilage during mouse embryogenesis. Dev Dyn 2000;218(3):452-64.

(66) de Andrea CE, Reijnders CM, Kroon HM, de JD, Hogendoorn PC, Szuhai K, Bovee JV. Secondary peripheral chondrosarcoma evolving from osteochondroma as a result of outgrowth of cells with functional EXT. Oncogene 2011.

(67) Chung U-I, Lanske B, Lee K, Li E, Kronenberg HM. The parathyroid hormone/parathyroid hormone-related peptide receptor coordinates endochondral bone development by directly controlling chondrocyte differentiation. Proc Natl Acad Sci USA 1998;95:13030-5.

(68) Chung UI, Schipani E, McMahon AP, Kronenberg HM. Indian hedgehog couples chondrogenesis to osteogenesis in endochondral bone development. J Clin Invest 2001;107(3):295-304.

(69) Schrage YM, Hameetman L, Szuhai K, Cleton-Jansen AM, Taminiau AHM, Hogendoorn PCW, Bovée JVMG. Aberrant heparan sulfate proteoglycan localization, despite normal exostosin, in central chondrosarcoma. Am J Pathol 2009;174(3):979-88.

(70) Tiet TD, Hopyan S, Nadesan P, Gokgoz N, Poon R, Lin AC, Yan T, Andrulis IL, Alman BA, Wunder JS. Constitutive hedgehog signaling in chondrosarcoma up-regulates tumor cell proliferation. Am J Pathol 2006;168(1):321-30.

(71) Oji GS, Gomez P, Kurriger G, Stevens J, Morcuende JA. Indian hedgehog signaling pathway differences between swarm rat chondrosarcoma and native rat chondrocytes. Iowa Orthop J 2007;27:9-16.

(72) Tremblay MR, Lescarbeau A, Grogan MJ, Tan E, Lin G, Austad BC, Yu LC, Behnke ML, Nair SJ, Hagel M, White K, Conley J, Manna JD, Alvarez-Diez TM, Hoyt J, Woodward CN, Sydor JR, Pink M, MacDougall J, Campbell MJ, Cushing J, Ferguson J, Curtis MS, McGovern K, Read MA et al. Discovery of a potent and orally active hedgehog pathway antagonist (IPI-926). J

Med Chem 2009;52(14):4400-18.

(73) de Andrea CE, Wiweger M, Prins F, Bovee JVMG, Romeo S, Hogendoorn PCW. Primary cilia organization reflects polarity in the growth plate and implies loss of polarity and mosaicism in osteochondroma. Lab Invest 2010;90(7):1091-101.

(74) Ho L, Ali SA, Al-Jazrawe M, Kandel R, Wunder JS, Alman BA. Primary cilia attenuate hedgehog signalling in neoplastic chondrocytes. Oncogene 2012.

(75) Rozeman LB, Hameetman L, Cleton-Jansen AM, Taminiau AHM, Hogendoorn PCW, Bovée JVMG. Absence of IHH and retention of PTHrP signalling in enchondromas and central chondrosarcomas. J Pathol 2005;205(4):476-82.

(76) Shen ZN, Nishida K, Doi H, Oohashi T, Hirohata S, Ozaki T, Yoshida A, Ninomiya Y, Inoue H. Suppression of chondrosarcoma cells by 15-deoxy-Delta 12,14-prostaglandin J2 is associated with altered expression of Bax/Bcl-xL and p21. Biochem Biophys Res Commun 2005;328(2):375-82.

(77) Kim DW, Kim KO, Shin MJ, Ha JH, Seo SW, Yang J, Lee FY. siRNA-based targeting of antiapoptotic genes can reverse chemoresistance in P-glycoprotein expressing chondrosarcoma cells. Mol Cancer 2009;8:28.

(78) Kim DW, Seo SW, Cho SK, Chang SS, Lee HW, Lee SE, Block JA, Hei TK, Lee FY. Targeting of cell survival genes using small interfering RNAs (siRNAs) enhances radiosensitivity of Grade II chondrosarcoma cells. J Orthop Res 2007;25(6):820-8.

(79) Lechler P, Renkawitz T, Campean V, Balakrishnan S, Tingart M, Grifka J, Schaumburger J. The antiapoptotic gene survivin is highly expressed in human chondrosarcoma and promotes drug resistance in chondrosarcoma cells in vitro. BMC Cancer 2011;11:-120.

(80) Machado I, Giner F, Mayordomo E, Carda C, Navarro S, Llombart-Bosch A. Tissue microarrays analysis in chondrosarcomas: light microscopy, immunohistochemistry and xenograft study. Diagn Pathol 2008;3 Suppl 1:S25.

(81) Subbiah V, Brown RE, Buryanek J, Trent J, Ashkenazi A, Herbst R, Kurzrock R. Targeting the Apoptotic Pathway in Chondrosarcoma Using Recombinant Human Apo2L/TRAIL (Dulanermin), a Dual Proapoptotic Receptor (DR4/DR5) Agonist. Mol Cancer Ther 2012;11(11):2541-6.

(82) Camidge DR. Apomab: an agonist monoclonal antibody directed against Death Receptor 5/TRAIL-Receptor 2 for use in the treatment of solid tumors. Expert Opin Biol Ther 2008;8(8):1167-76.

(83) Witkiewicz AK, Knudsen KE, Dicker AP, Knudsen ES. The meaning of p16(ink4a) expression in tumors: functional

significance, clinical associations and future developments. Cell Cycle 2011;10(15):2497-503.

(84) Landman AS, Danielian PS, Lees JA. Loss of pRB and p107 disrupts cartilage development and promotes enchondroma formation. Oncogene 2012.

(85) Schrage YM, Lam S, Jochemsen AG, Cleton-Jansen AM, Taminiau AHM, Hogendoorn PCW, Bovee JVMG. Central chondrosarcoma progression is associated with pRb pathway alterations; CDK4 downregulation and p16 overexpression inhibit cell growth in vitro. J Cell Mol Med 2008;13(9A):2843-52.

(86) Hallor KH, Staaf J, Bovée JVMG, Hogendoorn PCW, Cleton-Jansen AM, Knuutila S, Savola S, Niini T, Brosjo O, Bauer HCF, Vult von Steyern F., Jonsson K, Skorpil M, Mandahl N, Mertens F. Genomic Profiling of Chondrosarcoma: Chromosomal Patterns in Central and Peripheral Tumors. Clin Cancer Res 2009;15(8):2685-94.

(87) van Beerendonk HM, Rozeman LB, Taminiau AHM, Sciot R, Bovée JVMG, Cleton-Jansen AM, Hogendoorn PCW. Molecular analysis of the INK4A/INK4A-ARF gene locus in conventional (central) chondrosarcomas and enchondromas: indication of an important gene for tumour progression. J Pathol 2004;202(3):359-66.

(88) Asp J, Inerot S, Block JA, Lindahl A. Alterations in the regulatory pathway involving p16, pRb and cdk4 in human chondrosarcoma. J Orthop Res 2001;19(1):149-54.

(89) Niini T, Scheinin I, Lahti L, Savola S, Mertens F, Hollmen J, Bohling T, Kivioja A, Nord KH, Knuutila S. Homozygous deletions of cadherin genes in chondrosarcoma-an array comparative genomic hybridization study. Cancer Genet 2012;205(11):588-93.

(90) Ropke M, Boltze C, Neumann HW, Roessner A, Schneider-Stock R. Genetic and epigenetic alterations in tumor progression in a dedifferentiated chondrosarcoma. Path Res Pract 2003;199(6):437-44.

(91) Pacey S, Wilson RH, Walton M, Eatock MM, Hardcastle A, Zetterlund A, Arkenau HT, Moreno-Farre J, Banerji U, Roels B, Peachey H, Aherne W, de Bono JS, Raynaud F, Workman P, Judson I. A phase I study of the heat shock protein 90 inhibitor alvespimycin (17-DMAG) given intravenously to patients with advanced solid tumors. Clin Cancer Res 2011;17(6):1561-70.

(92) Jagasia AA, Block JA, Qureshi A, Diaz MO, Nobori T, Gitelis S, Iyer AP. Chromosome 9 related aberrations and deletions of the CDKN2 and MTS2 putative tumor suppressor genes in human chondrosarcomas. Cancer Lett 1996;105:91-103.

(93) Jagasia AA, Block JA, Diaz MO, Nobori T, Gitelis S, Inerot SE, Iyer AP. Partial deletions of the CDKN2 and MTS2 putative tumor suppressor genes in a

myxoid chondrosarcoma. Cancer Lett 1996;105:77-90.

(94) Chow WA, Bedell V, Gaytan P, Borden E, Goldblum J, Hicks D, Slovak ML. Methylthioadenosine phosphorylase gene deletions are frequently detected by fluorescence in situ hybridization in conventional chondrosarcomas. Cancer Genet Cytogenet 2006;166(2):95-100.

(95) Bertino JR, Waud WR, Parker WB, Lubin M. Targeting tumors that lack methylthioadenosine phosphorylase (MTAP) activity: current strategies. Cancer Biol Ther 2011;11(7):627-32.

(96) Cleton-Jansen AM, van Beerendonk HM, Baelde HJ, Bovée JVMG, Karperien M, Hogendoorn PCW. Estrogen signaling is active in cartilaginous tumors: implications for antiestrogen therapy as treatment option of metastasized or irresectable chondrosarcoma. Clin Cancer Res 2005;11(22):8028-35.

(97) Grifone TJ, Haupt HM, Podolski V, Brooks JJ. Immunohistochemical expression of estrogen receptors in chondrosarcomas and enchondromas. Int J Surg Pathol 2008;16(1):31-7.

(98) Meijer D, Gelderblom H, Karperien M, Cleton-Jansen A-M, Hogendoorn PCW, Bovee JVMG. Expression of aromatase and estrogen receptor alpha in chondrosarcoma, but no beneficial effect of inhibiting estrogen signaling both *in vitro* and *in vivo*. Clinical Sarcoma Research 2011.

(99) Fong YC, Yang WH, Hsu SF, Hsu HC, Tseng KF, Hsu CJ, Lee CY, Scully SP. 2-methoxyestradiol induces apoptosis and cell cycle arrest in human chondrosarcoma cells. J Orthop Res 2007;25(8):1106-14.

(100) Rizzo MT. Cyclooxygenase-2 in oncogenesis. Clin Chim Acta 2011 April 11;412(9-10):671-87.

(101) Sutton KM, Wright M, Fondren G, Towle CA, Mankin HJ. Cyclooxygenase-2 expression in chondrosarcoma. Oncology 2004;66(4):275-80.

(102) Schrage YM, Machado I, Meijer D, Briaire-de Bruijn I, van den Akker B, Taminiau AHM, Kalinski T, Llombart-Bosch A, Bovée JVMG. COX-2 expression in chondrosarcoma: a role for celecoxib treatment? Eur J Cancer 2010;46:616-24.

(103) Endo M, Matsumura T, Yamaguchi T, Yamaguchi U, Morimoto Y, Nakatani F, Kawai A, Chuman H, Beppu Y, Shimoda T, Hasegawa T. Cyclooxygenase-2 overexpression associated with a poor prognosis in chondrosarcomas. Hum Pathol 2006;37(4):471-6.

(104) Stacchiotti S, Dagrada GP, Morosi C, Negri T, Romanini A, Pilotti S, Gronchi A, Casali PG. Extraskeletal myxoid chondrosarcoma: tumor response to sunitinib. Clin Sarcoma Res 2012;2(1):22.

(105) Herbst RS, Eckhardt SG, Kurzrock R, Ebbinghaus S, O'Dwyer PJ, Gordon MS, Novotny W, Goldwasser MA, Tohnya TM, Lum BL,

Ashkenazi A, Jubb AM, Mendelson DS. Phase I dose-escalation study of recombinant human Apo2L/TRAIL, a dual proapoptotic receptor agonist, in patients with advanced cancer. J Clin Oncol 2010;28(17):2839-46.

Chapter 3

Three new chondrosarcoma cell lines: one grade III conventional central chondrosarcoma and two dedifferentiated chondrosarcomas of bone

This chapter is based on the manuscript: van Oosterwijk JG, de Jong D, van Ruler MAJH, Hogendoorn PCW, Dijkstra PDS, van Rijswijk CSP, Machado I, Llombart-Bosch A, Szuhai K, Bovée JVMG. *BMC Cancer 2012 Aug 28;12:375*

Abstract

Chondrosarcoma is the second most common primary sarcoma of bone. High-grade conventional chondrosarcoma and dedifferentiated chondrosarcoma have a poor outcome. In pre-clinical research aiming at the identification of novel treatment targets, the need for representative cell lines and model systems is high, but availability is scarce.
We developed and characterized three cell lines, derived from conventional grade III chondrosarcoma (L835), and dedifferentiated chondrosarcoma (L2975 and L3252) of bone. Proliferation and migration were studied and we used COBRA-FISH and array-CGH for karyotyping and genotyping. Immunohistochemistry for p16 and p53 was performed as well as TP53 and IDH mutation analysis. Cells were injected into nude mice to establish their tumorigenic potential.
We show that the three cell lines have distinct migrative properties, L2975 had the highest migration rate and showed tumorigenic potential in mice. All cell lines showed chromosomal rearrangements with complex karyotypes and genotypic aberrations were conserved throughout late passaging of the cell lines. All cell lines showed loss of CDKN2A, while TP53 was wild type for exons 5-8. L835 has an IDH1 R132C mutation, L2975 an IDH2 R172W mutation and L3252 is IDH wild type.
Based on the stable culturing properties of these cell lines and their genotypic profile resembling the original tumors, these cell lines should provide useful functional models to further characterize chondrosarcoma and to evaluate new treatment strategies.

Background

Chondrosarcoma is a malignant bone neoplasm characterized by the deposition of a hyaline cartilaginous extracellular matrix. With an incidence of 1:50,000 it typically occurs in adults in their 3rd to 6th decade of life. Chondrosarcoma represents a heterogeneous group of tumors. Primary central chondrosarcoma is defined by the formation of hyaline cartilage with decreasing matrix production in higher grades and constitutes about 80% of all chondrosarcomas (1). Dedifferentiated chondrosarcoma is characterized by a low-, or intermediate grade chondrosarcoma juxtaposed to a high grade anaplastic sarcoma and constitutes about 10% of all chondrosarcomas (2).
Both high grade conventional and dedifferentiated chondrosarcoma respond poorly to conventional chemo- and/or radiotherapy, have a high metastatic rate, and consequently have a very poor prognosis (3). It is because of these features that there is an urgent need for model systems in pre-clinical research aimed at evaluating new targeted treatment strategies for chondrosarcoma (4).
Recently IDH1 and IDH2 mutations were found in conventional central and dedifferentiated chondrosarcomas (5). IDH1 and IDH2 mutations are well known

in gliomas (6), but are notoriously difficult to grow in culture (7). This is a feature shared by, in particular, grade I chondrosarcomas. Recently, a new cell line derived from a grade II chondrosarcoma was published, CH-3573 (8). Over the last years, cell lines derived from dedifferentiated chondrosarcomas have been developed (9;10). In the pursuit of expanding the panel of cell lines we have succeeded in creating three new chondrosarcoma cell lines. L835 is derived from a grade III conventional chondrosarcoma, while L2975 and L3252 originate from dedifferentiated chondrosarcomas of bone. These three new cell lines provide a valuable addition to the current panel of chondrosarcoma cell lines.

Methods

Culture of human chondrosarcoma cells
Tumor-tissue derived from three resected specimens derived from one conventional and two dedifferentiated chondrosarcomas were used for culture. Samples were coded and all procedures were performed according to the ethical guidelines "Code for Proper Secondary Use of Human Tissue in The Netherlands 2002" (Dutch Federation of Medical Scientific Societies http://www.federa.org/sites/default/files/bijlagen/coreon/codepropersecondaryuseofhumantissue1_0.pdf). Specimens were washed 3x with RPMI1640 (Gibco, Invitrogen Life-Technologies, Scotland, UK) containing 1% penicillin/streptomycin (100U/mL), minced with razor blades and immersed in collagenase dispase overnight. After washing, the cells were transferred into small collagen-coated culture flasks and cultured in RPMI1640 supplemented with 20% heat inactivated Fetal Calf Serum (Gibco, Invitrogen Life-Technologies, Scotland, UK), 1% L-glutamax, and 1% penicillin/streptomycin (100U/mL). Cells were grown in a humidified incubator with 95% air and 5% CO_2 and cultured until stably multiplying.

COBRA-Fluoresence in-situ hybridization
COBRA-FISH on metaphase slides was performed as described previously (11). For each cell line several cell culture passages were studied (L835: passage 17 and 35, L2975 passage 20 and 30, L3252 passage 7, 8, and 20) and karyotypes were described for each cell line according to the International System of Human Cytogenetic Nomenclature (ISCN) 2009.

Expression of cartilaginous genes
RNA was isolated from L835 (passage 40), L2975 (passage 58), and L3252 (passage 21). Chondrogenic phenotype was assessed using RT-PCR for collagen I, IIB, III, and X, aggrecan, and SOX9 as described previously (12).

Assessment of cell line identity
DNA isolation from cell pellets was performed using the wizard genomic DNA purification kit (Promega, Madison, WI) according to manufacturer's instructions. DNA concentrations were measured using a Nanodrop ND-1000 spectrophotometer and quality was checked on a 1% agarose gel stained with ethidium bromide. Identity of cell lines was confirmed using the PowerPlex® 1.2 system (Promega Benelux BV, Leiden, The Netherlands). For L835 passage 36 was compared to primary tumor tissue, for L2975 passage 37 was used, and for L3252 passage 20 was compared to primary tumor tissue.

Doubling time and migration assays
The RTCA xCelligence system (Roche Applied Sciences, Almere, the Netherlands), based on cell-electrode substract impedance detection technology (13), was used for doubling time and migration assays. Prior to starting experiments cell number curves were run to determine optimal growth curves and for doubling time experiments cell lines were plated at a density of 1,000 cells per well for L2975 and L3252 and 10,000 cells per well for L835 in growth medium (10% FCS in RPMI1640). For migration experiments, 100,000 cells were optimal.
For doubling time assays, 30 minutes after plating, view-plates were loaded into the RTCA station in the cell culture incubator. Cell index (CI) was acquired every hour.
Proliferation was monitored for 400hrs. Every day plates were taken from the machine and most representative areas were photographed using a Zeiss axiovert 40C light microscope (Rijswijk, the Netherlands).
For migration assays, lower wells of the SIM plates (migration plates) were filled with growth medium (20% FCS in RPMI1640) as a chemoattractant, and cells were plated in the top wells in empty buffer (RPMI1640 only). CIM plates with 8µm pores were loaded into the RTCA station in the cell culture incubator immediately after plating and cell index (CI) was acquired every 5 minutes. Migration was monitored for 24hrs. Experiments were performed in triplicate.

Mutation analysis
Mutation analysis was performed for TP53 (exons 5-8) (14), and IDH1 and -2 exons 4 (15) using direct sequencing of DNA as described (14;15). Mutation analysis for PIK3CA, KRAS, BRAF, EGFR was performed using hydrolysis probes assay (16) at L835 (passage 36), L2975 (passage 37), and L3252 (passage 20). Mutation analysis for TP53 was performed at those same passage numbers and IDH mutation analysis was performed at L835 passage 38 and 47, L2975 passage 31 and 46, and L3252 passage 20, as well as on DNA obtained from CH-3573 (8). To determine expression of the IDH mutated allele cDNA was generated using 1µg total RNA as described (12) for L835 (passage 38), L2975 (passage 31), and L3252 (passage 20). Primers were designed with primer3 software (http://frodo.wi.mit.edu/primer3/) and ordered from ISOGEN Bioscience BV

(Maarssen, the Netherlands). PCR was done with the quantitative PCR core kit for SYBR green I supplemented with fluorescin (Eurogentec, Seraing, Belgium) on 0.2µL cDNA per reaction in an iCycler iQ Real-time Detection system (Bio-Rad Laboratories, Hercules, CA). PCR was done for 40 cycles. PCR products were purified using QIAquick PCR purification Kit (Qiagen, Hilden, Germany) according to manufacturer's instructions. Purified products were sequenced by Macrogen (Amstelveen, the Netherlands) and resulting sequences were analyzed using MutationSurveyor DNA Variant Analysis software (Softgenetics, UK). Primer sequences and annealing temperatures are listed in table 3.1.

Table 3.1. IDH primers

Primer			**Tm**	**Product**
IDH1	Forward	CGGTCTTCAGAGAAGCCATT	59.4	113
IDH1	Reverse	GCCAACATGACTTACTTGATCC	58.6	
IDH2	Forward	AACATCCACGCCTAGTCC	56.3	90
IDH2	Reverse	CAGTGGATCCCCTCTCCAC	60.5	
IDH1	Forward	CGGTCTTCAGAGAAGCCATT	59.4	131
IDH1	Reverse	AGGCCCAGGAACAACAAAAT	56.4	
IDH2	Forward	AGTGTGGCTGCAAGTGTGC	60.0	365
IDH2	Reverse	GAGATGGACTCGTCGGTGTT	60.1	

Table 3.2. Antibodies

Antibody	**Clone**	**Dilution**	**Antigen Retrieval**	**Blocking**	**Source**
p16	g175-405	1:800	Citrate	-	BD Pharmingen (550834)
p53	DO-7	1:800	Citrate	-	Dako (M7001)
Ki67	MIB-1	1:800	Citrate	-	Dako (M7240)

Array-CGH analysis

Array-CGH was performed on DNA derived from the primary tumor as well as from cultured cells of all three cases as described (17). DNA of L835 passage 36, L2975 passage 37, and L3252 passage 20 was used. In brief, labeling of 1µg DNA was performed using the BioPrime Total Genomic Labeling System (***Invitrogen Corporation***, ***Carlsbad***, ***CA***) following the manufacturer's protocol. As reference, DNA from a commercial source (Promega Corporation, Madison, WI) was used. Labeled test and reference samples were mixed and hybridized as a gender mismatch. Hybridization was performed on an Agilent 105k oligonucleotide array according to manufacturer's instructions. Slides were scanned using the Agilent Scanner with 5µm scan resolution. Scan images were processed with the Feature Extraction Software and the generated raw data files were analyzed using Genomic Workbench (Agilent Technologies, Santa Clara, CA). In short, the mean of the background corrected and Lowess normalized log2 ratios of identical features was calculated. Normalization of ratios was done using the overall values as well as the values of the control reporter probes on the array. Aberrations were calculated using the ADM-2 algorithm with a threshold of 8.6 and displayed with a moving average of 1Mb.

Tumorigenicity in mice

All the experimentation involving laboratory animals was approved by the Institutional Animal Care of Valencia University and the Local Government and was performed in accordance with the national legislation of Spain. Male nude mice were purchased from IFFA-CREDO (Lyon, France), and kept under specific pathogen-free conditions throughout the experiments. For each cell line, 2,000,000 cells were subcutaneously injected in a total of 3 mice (2 months old) under sterile conditions. Tumor was removed when size reached 4mm in diameter and a fragment of non-necrotic tumor, about 3 to 5 mm^3 in size, was used for xenografting into two new male nude mice. The second neoplasm was removed when the size reached 20mm in diameter. From each tumor a part was snap-frozen in liquid nitrogen, a part fixed in formalin and embedded in paraffin, a part was used for xenografting into 2 new mice, and a part for further culturing of post-xenograft cell lines.

(Immuno)histochemical analysis
L835 (passage 35), L2975 (passage 55), and L3252 (passage 17) cells were fixed in formalin and prepared using the Shandon Cytoblock cell block preparation system (Thermo Scientific, Etten-Leur, the Netherlands). Cells were embedded in paraffin according to standard laboratory procedures for tissue fixation. Sections (4-µm thick) of these paraffin blocks as well as from formalin fixed paraffin embedded original tumor tissue and xenograft passages, were used for H&E, toluidine blue, and immunohistochemistry for ki67, p53, and p16 according to standard procedures (18). Details of the antibodies can be found in table 3.2.

Results
Clinicopathological data
The tissue specimen of L835 was retrieved from the resection specimen of the local recurrence of a chondrosarcoma occurring in the left distal radius (figure 3.1A) of a 54 year-old male. The primary tumor had been resected seven months earlier. Histological examination revealed a highly cellular cartilaginous neoplasm, with myxoid matrix changes and the presence of mitoses, and spindle cell changes at the edge of the lobuli, consistent with a primary central chondrosarcoma of bone, grade III according to Evans (19) (figure 3.1D).
L2975 was derived from the resection of a metastasis of a dedifferentiated chondrosarcoma located at the spine of a 57 year-old male. The primary tumor was located at the right distal femur, and was originally resected eight months earlier (figure 3.1B, 3.B'). The primary tumor was 13.6 cm in size and histological examination revealed two components with a sharp interface indicative of dedifferentiated chondrosarcoma; a grade II chondrosarcoma was juxtaposed to a high grade anaplastic sarcoma (figure 3.1F) with focal deposition of osteoid, indicating differentiation towards osteosarcoma (figure 3.1G). Histological examination of the spine metastasis revealed exclusively the high-grade anaplastic sarcoma, in which osteoid deposition was absent.
L3252 is derived from the local recurrence of a chondrosarcoma located at the chest wall (costa) (Fig 3.1C, D) that had already metastasized to the spine and the lung at the time of first presentation. The primary tumor of this 52 year-old female demonstrated a cellular, partly myxoid and necrotic cartilaginous tumor, with mitoses, indicative of a grade III chondrosarcoma (figure 3.1H). However, at local recurrence eight months later, areas of a cartilaginous tumor were intermingled with an anaplastic sarcoma lacking differentiation, indicating dedifferentiated chondrosarcoma. The tissue used for cell culture was derived from an area in which dedifferentiated areas were absent (figure 3.1I).

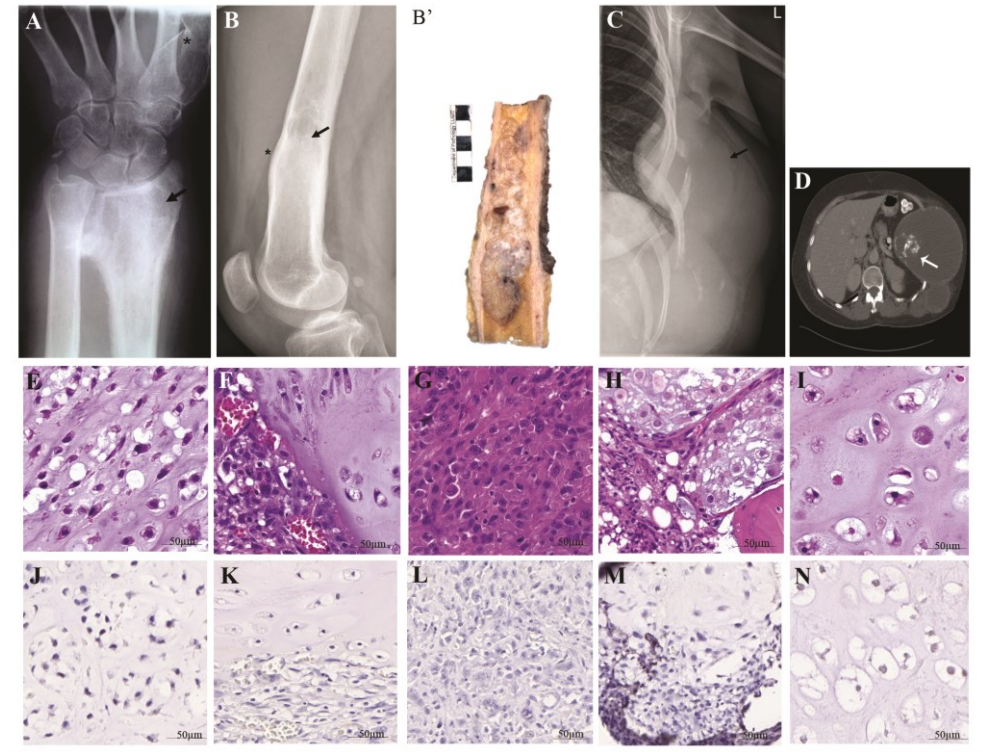

Figure 3.1 - Radiologic and histologic examination of original tumors.
A: L835 conventional radiography demonstrates a mildly expansile mixed lytic and sclerotic lesion in the distal radius with spiculated borders (arrow) and an irregular periosteal reaction. Note the presence of an enchondroma in the first metatarsal bone (asterisk). B: L2975 conventional radiography shows an ill-defined expansile mixed lytic and sclerotic lesion (arrow) originating from the distal femur diaphysis with endosteal scalloping of the anterior cortex (asterisk). The sclerotic areas within the lesion suggest osteoid matrix formation. B': L2975 gross specimen shows intramedullar localization of dedifferentiated chondrosarcoma with chondrocytic and lobulated dedifferentiated compartments. C: L3252 conventional chest radiography shows a large lobulated mass originating from the left chest wall with extensive rib destruction. Subtle chondroid mineralization can be observed in the lesion. Radiological features are suggestive for a chondrosarcoma with a higher grade of malignancy. D: Axial CT image demonstrates chondroid mineralization (arrow) within the intra-abdominal component consistent with the diagnosis of chondrosarcoma. E: H&E staining of high grade L835 original tumor. H&E staining of L2975 original tumor shows anaplastic and cartilaginous component (F) and metastasis of the anaplastic component (G). H&E staining of L3252 original tumor shows anaplastic and cartilaginous component (H) and recurrence of the cartilaginous component (I). J-N: absence of p16 staining is observed in L835 original tumor, L2975 original tumor and metastasis, and L3252 original tumor and recurrence, respectively.

Establishment of cell lines and transmission light microscopy

L835 was passaged routinely *in vitro* for 50 generations, L2975 for 60 generations, and L3252 for 30 generations. The cell lines derived from dedifferentiated chondrosarcoma (L2975 and L3252) were noticeably easier to culture than the L835 cells. This was also reflected by Ki-67 staining on embedded cells, with proliferation rates of ~60% (L835) versus ~100% and ~80% for L2975 and L3252, respectively. The dedifferentiated chondrosarcoma cells were less susceptible to changes in culture conditions reflecting their more aggressive nature. Transmission light microscopy revealed L2975 cells to retain their elongated morphology when in confluence and L3252 cells to detach when reaching confluence (figure 3.2A). Identity of cell lines was confirmed using the PowerPlex® 1.2 system (Promega Benelux BV, Leiden, The Netherlands). L835 passage 36, L2975 passage 37, and L3252 passage 20 showed identical STR loci when compared to their matching original tumors. Data are available on request. qPCR for expression of cartilage markers revealed expression of ColI, ColIII, aggrecan, and SOX9 in L835 cell line. L2975 cell line expressed ColI, ColIII, ColX, and SOX9. L3252B cell line expressed ColI, ColII, ColIII, ColX, aggrecan, and SOX9.

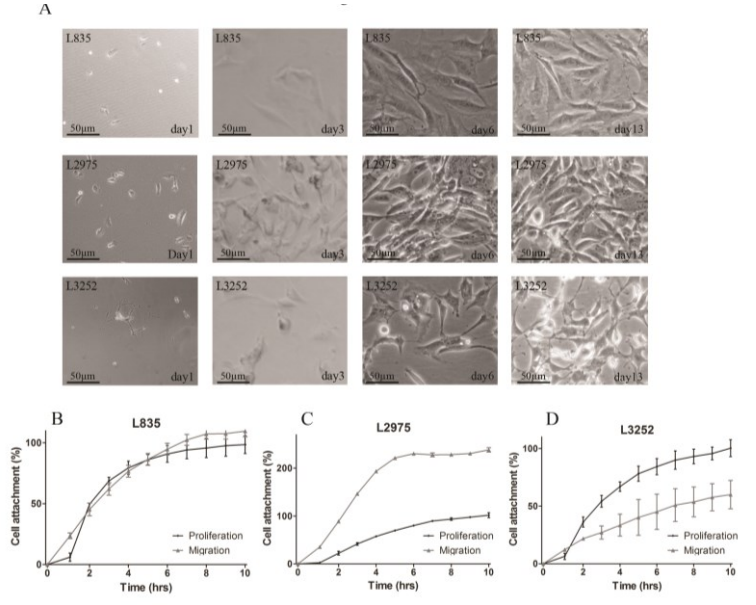

Figure 3.2 - Cell morphology and migration. A: Light microscopy at 40x magnification. Top panel shows L835 cells with round nuclei do not fully populate the flask; day 13 is representative of a full flask for this cell line. Middle panel shows L2975 showing a full flask at day 6 already, multinucleated cells can be observed. Bottom panel shows L3252 still actively dividing, and dividing cells tend to detach and re-attach to the bottom of the flask. B-D Migration plotted against proliferation for the first 10 hours after plating. 1,000 – 10,000 cells were used in the proliferation assay and 100,000 cells in the migration assay. Though all cell lines show migrative capacity, L2975 cells are most successful and high migrative activity during the first 4 hours after which the slope flattens.

Migration
All cell lines were able to migrate. Migration for L835 was at the same rate as cell attachment in the proliferation assay (figure 3.2B). For L2975, cell migration occurred much more rapidly than cell attachment (figure 3.2C). Moreover, due to high migration efficiency, and the fact that more cells were applied in the migration assay, the cell attachment percentage exceeds that of which is achieved in the proliferation assay. For L3252 cells, migration was observed but only for a small percentage of cells (figure 3.2D).

Transplantation into nude mice
L2975 cells were subcutaneously transplanted into nude mice and a tumor of 4mm in diameter was observed in 1 out of 3 mice after 3 months. A fragment of the resulting tumor was subsequently subcutaneously transplanted into 2 nude mice and a tumor of 20mm in diameter was observed in 2 out of 2 mice. Morphologically, tumor cells of both the first and second xenograft showed a more epithelioid morphology (figure 3.3A, B) while no deposition of cartilaginous matrix was observed at H&E or Toluidine Blue staining (results not shown). Immunohistochemistry showed that 90% of cells of both xenografts were positive for Ki-67 and were thus actively proliferating (results not shown). Cells obtained from both xenografts were successfully passaged. Xenografting of L835 and L3252 did not result in tumors in 8 months.

COBRA-Fluorescence in-situ hybridization
The cell line L835 showed a stable karyotype (figure 3.4A'). There were many numerical changes with some translocations. The resulting karyotype at passage 35 was: 63-67<3n>,XY,-X,+Y,+der(1;19)t(1;19)(p11;p13.3)trp(19)(p13.3p13.2), der(1;19)t(1;19)(p11;p13.3)trp(19)(p13.3p13.2),-3,-4,+5,-6,+7,-8,-9,-10,-11,+13,t(14;15)(q22;q24),+der(15)t(14;15)(q22;q24)del(15)(q21q24),+16,-17,i(17)(q10),-18,-19,+20,+21,-22.
L2975 also revealed a stable karyotype at passage 30 with many numerical changes and complex rearrangements (figure 3.4B'). The resulting karyotype was: 61-65<3n>der(X;4)(p10;p10),der(X;8)(q10;q10),-Y,+der(Y;9)(p10;p10)x2,+der(1;15)(q10;q10),der(1;1)(q10;q10)t(1;6)(q21;q24)t(1;8)(q31;p11),der(1;8)(p10;p10),del(2)(q22q32),-4,-5,+der(7;15)(q10;q10),t(9;16)(q10;q10)x2,der(10;18)(q10;q10),-13,der(13;13)(q10;q10),der(14;15)(q10;q10)t(8;15)(q11;q21),-15,-15,-16,-17,i(17)(q10),-18,der(18)t(1;18)(p31;q22),der(20)t(X;20)(q23,p12),-21,+mar3x
L3252 was stable at passage 20 with many numerical changes and complex rearrangements (figure 3.4C'): 51<2n+>,X,-X,+der(3;11)t(3;11)(p10;q10)t(11;17) (q14;q22), der(4;8)t(4;8)(q10;p10),der(4),+der(5),der(6;15)t(6;15)(p10;q10), der(7)t(7;18),der(7),+der(8)x2,der(8),der(9),der (10),+12,der(13;13)(q10;q10),-13,der(17),i(17)(p10;p10)der(18)t(7;18),+der(20), der(21),+mar

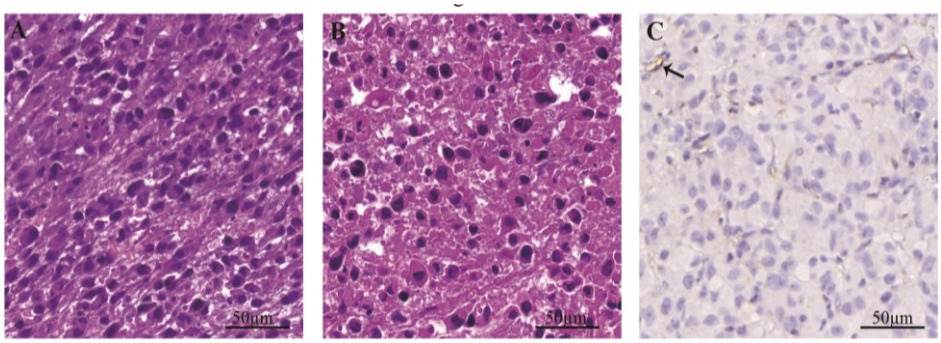

Figure 3.3 - Histologic examination of xenografted L2975.
A, B: H&E stainings of first and second passage of L2975 in nude mice showed L2975 cells had adapted a more rounded morphology. C: p16 staining of first passage confirmed absence of p16 expression; note positive vessel walls (arrow).

Array-CGH and mutation analyses
In L835 and L2975, all aberrations present in the tumor were retained in the cell lines. L835 showed a homozygous CDKN2A deletion in both the original tumor and the cell line (figure 3.4A"). L2975 and L3252 both showed a homozygous deletion in the cell line (figure 3.4B" and 3.4C"), the deletion status of the primary tumor was difficult to assess due to low tumor content and consequently resulting suppressed ratio profiles. For both L835 and L2975 clear DNA copy number alterations could be observed in the original tumor samples that were enhanced in the cell lines. For L3252 tumor DNA this was less pronounced. On close examination of the profile, however, one can observe small copy number changes consistent with those observed in the cell line. We previously demonstrated L835 (passage 38) to harbor an IDH1 R132C mutation and L2975 (passage 31) an IDH2 R172W mutation (15). We here show that L3252 (passage 20) is wild type and that also later passages of L835 (passage 47) and L2975 (passage 46) retain the IDH mutation. Using cDNA we found the mutated IDH alleles to be expressed (results not shown). No hotspot mutations were detected for TP53, PIK3CA, BRAF, KRAS, and EGFR in any of the cell lines.

Immunohistochemical characterization
Since p16 is frequently silenced in human chondrosarcoma (18) we evaluated p16 in the original tumors, the cell lines and the L2975 xenografts using immunohistochemistry. All primary tumors (figure 1J, L, M) and recurrences (figure 1L, N) were negative for p16. Consistent with the tumor tissue, all derived cell lines lacked p16 protein expression (table 3.3), as did xenografts created from L2975 (figure 3.3C). We proceeded to test embedded cells from all cell lines shown in table 3.3 for p16 expression and found all to be negative. Immunohistochemistry showed nuclear expression of p53 in 10-20% of the tumor

cells in L835 and L3252 primary tumor and cell line, while L2975 tumor, cell line, or xenograft was completely negative (results not shown).

Figure 4

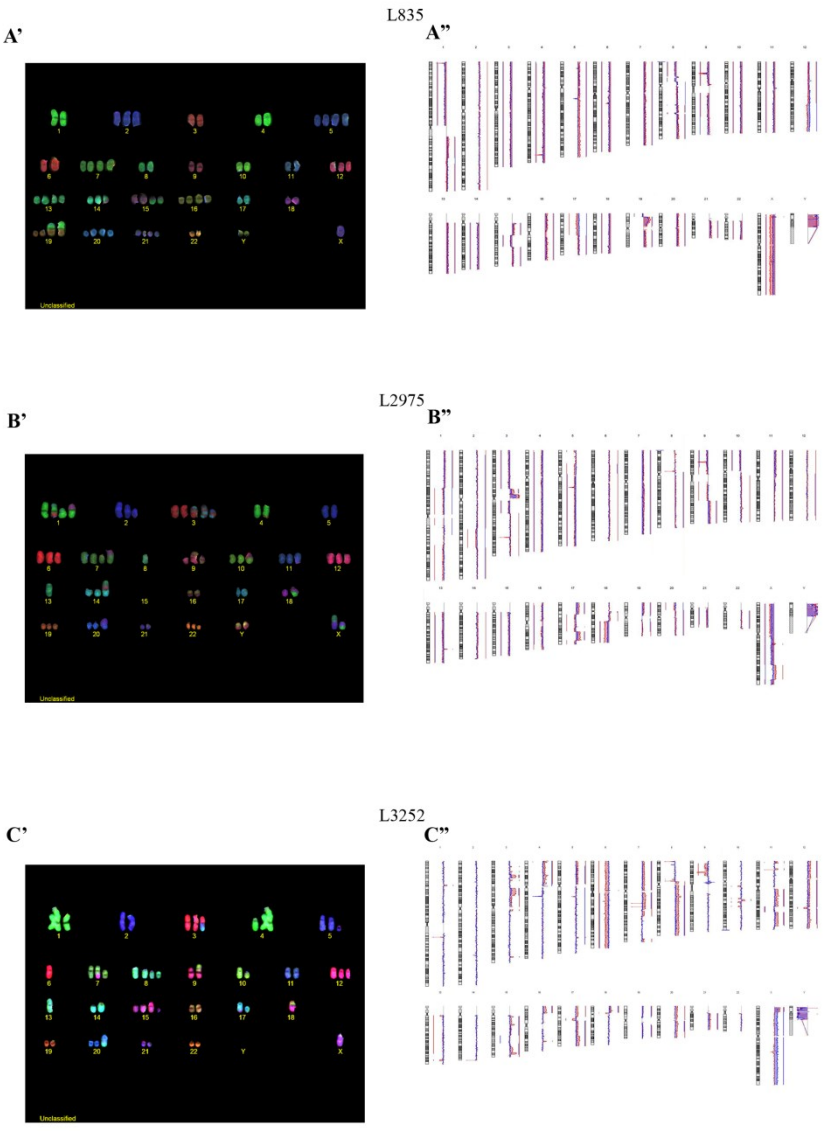

Figure 3.4 - COBRA-FISH and Array-CGH.
A: chromosomal analysis of L835 tumor and cell line showed numerical changes. B, C: chromosomal analysis of L2975, L3252 showed complex rearrangements consistent with the aggressive nature of dedifferentiated chondrosarcoma.

Discussion

Chondrosarcoma is the second most common primary sarcoma of bone and to date unresectable chondrosarcomas have a poor outcome (3). Grade III and dedifferentiated chondrosarcomas are extremely aggressive in nature and there is an urgent need for model systems facilitating research in order to develop novel therapeutic strategies. Growing chondrosarcoma cells in culture, however, is a challenge and well growing chondrosarcoma cell lines are sparse. We present here the establishment and characterization of three new chondrosarcoma cell lines originating from grade III and dedifferentiated chondrosarcoma.

Recently chondrosarcoma has been found to harbor IDH1 and IDH2 mutations (5;15) and we published that the mutation is retained in a subset of chondrosarcoma cell lines (15). In glioma IDH mutations seem to be the earliest event in gliomagenesis even before TP53 mutations occur (20). In conventional chondrosarcoma we observe a similar phenomenon, where IDH mutations are present already in a high percentage of low-grade tumors and TP53 mutations are observed to increase with grade (4;5;15). Cell lines created from IDH mutant gliomas have been reported to eliminate their IDH mutation under standard culture conditions (7). Recently, however, a glioma cell line carrying an endogenous IDH1 R132H mutation was published, but this cell line showed a slow growth rate in culture (21). We here present three chondrosarcoma cell lines, one carrying an IDH1 R132C mutation, one carrying an IDH2 R172W mutation, and one wild type for IDH mutations with stable karyotypes and steady growth patterns. These cell lines show numerical changes and additional mutations. We speculate that in IDH mutant chondrosarcoma the acquisition of additional mutations as we have shown here have facilitated their growth in culture.

The inactivation of tumor suppressor genes is a well-known phenomenon in cancer and p16 mutations have been reported in 20-41% of human chondrosarcomas (22-25). Interestingly, all studies observed loss of p16 to be correlated with increasing histological grade in conventional chondrosarcoma. Recently, we showed inactivation of p16 in 30/38 (79%) dedifferentiated chondrosarcoma cases (26). We previously published three chondrosarcoma cell lines to be negative for p16 using western blot (18) and upon overexpression of p16 using lentiviral vectors the metabolic activity and cell viability of these cell lines was decreased, indicating loss of p16 to play a role in the proliferative capacity of chondrosarcoma cells. Introduction of p16 in the endogenously TP53 mutant HT-1080 fibrosarcoma cell line, which was recently reported to carry an IDH1 R132C mutation (5), also led to cell cycle arrest and growth inhibition (27-29). We report here three new chondrosarcoma cell lines lacking p16 expression based on a homozygous deletion of the CDKN2A locus as shown by aCGH analysis, and confirmed loss of p16 expression using immunohistochemistry. Moreover, aCGH analysis showed a copy number loss around the 17p13.1 locus in L835, whereas a copy number gain was observed in L2975 and L3252. However, mutation analysis for TP53 showed no

Table 3.2 - Overview of chondrosarcoma cell lines and their characteristics

Cell line	Tumor subtype	Histological Grade	Passage	IDH1[1]	IDH2[1]	p53[2]	p16[3]	Reference
Conventional Chondrosarcoma								
SW1353	Solitary Central	II	p50	wt	R172S	V203L	-	ATCC
JJ012	Solitary Central	II	P26	R132G	wt	G199V	-	(30)
CH3573	Solitary Central	II	P60	wt	wt	T201-	na	(8)
CH2879	Solitary Central	III	P31	G105G	wt	wt	-	(31)
OUMS27	Solitary Central	III	P29	wt	wt	wt	-	(32)
L835	Solitary Central	III	p51	R132C	wt	wt	-	Present Study
Dedifferentiated Chondrosarcoma								
L2975	Dedifferentiated		p59	wt	R172W	wt	-	Present Study
NDCS1	Dedifferentiated		P22	wt	wt	C242S	-	(9)
L3252	Dedifferentiated		P26	wt	wt	wt	-	Present Study

[1]IDH mutations for existing cell lines were described in (15)
[2]p53 mutations for existing cell lines were described in (33)
[3]p16 mutations for existing cell lines were described in (18)
na: not available

activating mutations in exons 5-8, and immunohistochemistry showed no p53 overexpression. Together, our data suggest that while IDH mutations are important as early events in a subset of chondrosarcomas, additional inactivation of p16 may be crucial for acquiring a more aggressive phenotype.

The literature presents us with 5 conventional chondrosarcoma cell lines that have been well characterized using pathological, immunohistochemical, and molecular genetic methods (8;30-32), and we here present L835 as an additional cell line. We previously published L835 to be able to form 3D pellets (33) and we now show it to be highly stable in culture. L835 cell line showed a slower growth rate compared to the dedifferentiated chondrosarcoma cell lines. In all cases complex genome alterations were observed. Dedifferentiated chondrosarcoma is comprised of two separate components, a high grade anaplastic component and a low to intermediate grade cartilaginous component (2). The histogenesis has been under debate but evidence points to a single precursor cell with early separation of the two components as a small number of genetic changes is identical in both components, with additional genetic alterations in the anaplastic component (26;34). Indeed, 3 out of 3 dedifferentiated chondrosarcomas with IDH1 mutations carried the mutation in both components (26). Moreover, 79% of the anaplastic and 82% of the cartilaginous components show loss of p16 expression (26). L2975 and L3252 were both derived from the recurrence of a dedifferentiated chondrosarcoma; both cell lines exhibited a higher growth rate in vitro, than the L835 cell line, but the cells in culture expressed chondrogenic markers. L2975 proved to be the most aggressive cell line both in culture and in our *in vitro* migration assay, which may explain why this was the only cell line to be successfully xenografted. We show here the use of L2975 dedifferentiated chondrosarcoma cells with an IDH2 R172W mutation in mouse models, which can be an important asset in the research for new treatment strategies.

We report the establishment and molecular, genetic and functional characterization of one grade III (L835) and two dedifferentiated chondrosarcoma (L2975 and L3252) cell lines. This represents a substantial addition to the already existing panel of chondrosarcoma cell lines, which together may reflect their heterogeneity. In addition to the existing cell lines these cell lines present the field with an extensive model system as heterogeneous in IDH1 and IDH2 and TP53 mutations as the tumors they are derived from. This panel can be implemented in studies ascertaining human chondrosarcoma tumorigenesis, should provide useful tools in the ongoing search for new targeted therapies, and aid in expanding our knowledge on the role of IDH1 and IDH2 mutations in chondrosarcoma formation.

References

1. Bertoni F, Bacchini P, Hogendoorn PCW. Chondrosarcoma. In World Health Organisation classification of tumours. Pathology and genetics of tumours of soft tissue and bone.Edited by: Fletcher CDM, Unni KK, Mertens F. Lyon: IARC Press; 2002:247-51.

2. Milchgrub S, Hogendoorn PCW. Dedifferentiated chondrosarcoma. In: World Health Organisation classification of tumours. Pathology and genetics of tumours of soft tissue and bone.Edited by: Fletcher CDM, Unni KK, Mertens F. Lyon: IARC Press; 2002:252-4.

3. Gelderblom H, Hogendoorn PCW, Dijkstra SD, van Rijswijk CS, Krol AD, Taminiau AHM, Bovée JVMG: The clinical approach towards chondrosarcoma. Oncologist 2008, 13(3):320-9.

4. Bovee JVMG, Hogendoorn PCW, Wunder JS, Alman BA. Cartilage tumours and bone development: molecular pathology and possible therapeutic targets. Nat Rev Cancer 2010, 10(7):481-8.

5. Amary MF, Bacsi K, Maggiani F, Damato S, Halai D, Berisha F, Pollock R, O'Donnell P, Grigoriadis A, Diss T, Eskandarpour M, Presneau N, Hogendoorn PCW, Futreal A, Tirabosco R, Flanagan AM. IDH1 and IDH2 mutations are frequent events in central chondrosarcoma and central and periosteal chondromas but not in other mesenchymal tumours. J Pathol 2011, 224(3):334-43.

6. Yan H, Parsons DW, Jin G, McLendon R, Rasheed BA, Yuan W, Kos I, Batinic-Haberle I, Jones S, Riggins GJ, Friedman H, Friedman A, Reardon D, Herndon J, Kinzler KW, Velculescu VE, Vogelstein B, Bigner DD. IDH1 and IDH2 mutations in gliomas. N Engl J Med 2009, 360(8):765-73.

7. Piaskowski S, Bienkowski M, Stoczynska-Fidelus E, Stawski R, Sieruta M, Szybka M, Papierz W, Wolanczyk M, Jaskolski DJ, Liberski PP, Rieske P. Glioma cells showing IDH1 mutation cannot be propagated in standard cell culture conditions. Br J Cancer 2011, 104(6):968-70.

8. Calabuig-Farinas S, Benso RG, Szuhai K, Machado I, Lopez-Guerrero JA, de JD, Peydro A, Miguel TS, Navarro L, Pellin A, Llombart-Bosch A. Characterization of a New Human Cell Line (CH-3573) Derived from a Grade II Chondrosarcoma with Matrix Production. Pathol Oncol Res, in press.

9. Kudo N, Ogose A, Hotta T, Kawashima H, Gu W, Umezu H, Toyama T, Endo N. Establishment of novel human dedifferentiated chondrosarcoma cell line with osteoblastic differentiation. Virchows Arch 2007 451(3):691-9.

10. Yang L, Chen Q, Zhang S, Wang X, Li W, Wen J, Huang X, Zheng J, Huang G, Huang T, Ju G. A novel mutated cell line with characteristics of dedifferentiated chondrosarcoma. Int J Mol Med 2009, 24(4):427-35.

11. Tanke HJ, Wiegant J, Van Gijlswijk RPM, Bezrookove V, Pattenier H, Heetebrij RJ, Talman EG, Raap AK, Vrolijk J. New strategy for multi-colour fluorescence in situ hybrydisation: COBRA: COmbined Binary RAtio labelling. Eur J Hum Genet 1999, 7(1):2-11.

12 Cleton-Jansen AM, van Beerendonk HM, Baelde HJ, Bovée JVMG, Karperien M, Hogendoorn PCW. Estrogen signaling is active in cartilaginous tumors: implications for antiestrogen therapy as treatment option of metastasized or irresectable chondrosarcoma. Clin Cancer Res 2005, 11(22):8028-35.

13 Atienzar FA, Tilmant K, Gerets HH, Toussaint G, Speeckaert S, Hanon E,

Depelchin O, Dhalluin S. The Use of Real-Time Cell Analyzer Technology in Drug Discovery: Defining Optimal Cell Culture Conditions and Assay Reproducibility with Different Adherent Cellular Models. J Biomol Screen 2011, 16(6):575-87.

14. Ottaviano L, Schaefer KL, Gajewski M, Huckenbeck W, Baldus S, Rogel U, Mackintosh C, de AE, Myklebost O, Kresse SH, Meza-Zepeda LA, Serra M, Cleton-Jansen AM, Hogendoorn PCW, Buerger H, Aigner T, Gabbert HE, Poremba C. Molecular characterization of commonly used cell lines for bone tumor research: a trans-European EuroBoNet effort. Genes Chromosomes Cancer 2010, 49(1):40-51.

15. Pansuriya TC, van Eijk, R, d'Adamo P, van Ruler MA, Kuijjer ML, Oosting J, Cleton-Jansen AM, van Oosterwijk JG, Verbeke SL, Meijer D, van WT, Nord KH, Sangiorgi L, Toker B, Liegl-Atzwanger B, San-Julian M, Sciot R, Limaye N, Kindblom LG, Daugaard S, Godfraind C, Boon LM, Vikkula M, Kurek KC, Szuhai K, French, PJ, Bovée, JVMG. Somatic mosaic IDH1 and IDH2 mutations are associated with enchondroma and spindle cell hemangioma in Ollier disease and Maffucci syndrome. Nat Genet 2011, 43(12):1256-61.

16. van Eijk R, Licht J, Schrumpf M, Talebian YM, Ruano D, Forte GI, Nederlof PM, Veselic M, Rabe KF, Annema JT, Smit V, Morreau H, van Wezel T. Rapid KRAS, EGFR, BRAF and PIK3CA mutation analysis of fine needle aspirates from non-small-cell lung cancer using allele-specific qPCR. PLoS ONE 2011, 6(3):e17791.

17. De Jong D, Verbeke SL, Meijer D, Hogendoorn PCW, Bovee JVMG, Szuhai K. Opening the archives for state of the art tumour genetic research: sample processing for array-CGH using decalcified, formalin-fixed, paraffin-embedded tissue-derived DNA samples. BMC Res Notes 2011, 4:1.

18. Schrage YM, Lam S, Jochemsen AG, Cleton-Jansen AM, Taminiau AHM, Hogendoorn PCW, Bovee JVMG. Central chondrosarcoma progression is associated with pRb pathway alterations; CDK4 downregulation and p16 overexpression inhibit cell growth in vitro. J Cell Mol Med 2008, 13(9A):2843-52.

19. Evans HL, Ayala AG, Romsdahl MM. Prognostic factors in chondrosarcoma of bone. A clinicopathologic analysis with emphasis on histologic grading. Cancer 1977, 40:818-31.

20. Watanabe T, Nobusawa S, Kleihues P, Ohgaki H. IDH1 mutations are early events in the development of astrocytomas and oligodendrogliomas. Am J Pathol 2009, 174(4):1149-53.

21. Luchman HA, Stechishin OD, Dang NH, Blough MD, Chesnelong C, Kelly JJ, Nguyen SA, Chan JA, Weljie AM, Cairncross JG, Weiss S. An in vivo patient-derived model of endogenous IDH1-mutant glioma. Neuro Oncol 2012, 14(2):184-91.

22. Asp J, Sangiorgi L, Inerot SE, Lindahl A, Molendini L, Benassi MS, Picci P. Changes of the p16 gene but not the p53 gene in human chondrosarcoma tissues. Int J Cancer 2000, 85(6):782-6.

23. Asp J, Brantsing C, Lovstedt K, Benassi MS, Inerot S, Gamberi G, Picci P, Lindahl A. Evaluation of p16 and Id1 status and endogenous reference genes in human chondrosarcoma by real-time PCR. Int J Oncol 2005, 27(6):1577-82.

24. Ropke M, Boltze C, Neumann HW, Roessner A, Schneider-Stock R. Genetic and epigenetic alterations in tumor progression in a dedifferentiated chondrosarcoma. Pathol Res Pract 2003, 199(6):437-44.

25. van Beerendonk HM, Rozeman LB, Taminiau AHM, Sciot R, Bovée JVMG, Cleton-Jansen AM, Hogendoorn PCW. Molecular analysis of the INK4A/INK4A-ARF gene locus in conventional (central) chondrosarcomas and enchondromas: indication of an important gene for tumour progression. J Pathol 2004, 202(3):359-66.

26. Meijer D, de Jong D, Pansuriya TC, van den Akker BE, Picci P, Szuhai K, Bovee JVMG. Genetic characterization of mesenchymal, clear cell, and dedifferentiated chondrosarcoma. Genes Chromosomes Cancer, in press.

27. Fahham N, Sardari S, Ostad SN, Vaziri B, Ghahremani MH. C-terminal domain of p16(INK4a) is adequate in inducing cell cycle arrest, growth inhibition and CDK4/6 interaction similar to the full length protein in HT-1080 fibrosarcoma cells. J Cell Biochem 2010, 111(6):1598-606.

28. Li WW, Takahashi N, Jhanwar S, Cordon-Cardo C, Elisseyeff Y, Jimeno J, Faircloth G, Bertino JR. Sensitivity of soft tissue sarcoma cell lines to chemotherapeutic agents: identification of ecteinascidin-743 as a potent cytotoxic agent. Clin Cancer Res 2001, 7(9):2908-11.

29. Rasheed S, Nelson-Rees WA, Toth EM, Arnstein P, Gardner MB. Characterization of a newly derived human sarcoma cell line (HT-1080). Cancer 1974, 33(4):1027-33.

30. Scully SP, Berend KR, Toth A, Qi WN, Qi Z, Block JA. Marshall Urist Award. Interstitial collagenase gene expression correlates with in vitro invasion in human chondrosarcoma. Clin Orthop Relat Res 2000, 376:291-303.

31. Gil-Benso R, Lopez-Gines C, Lopez-Guerrero JA, Carda C, Callaghan RC, Navarro S, Ferrer J, Pellin A, Llombart-Bosch A. Establishment and characterization of a continuous human chondrosarcoma cell line, ch-2879: comparative histologic and genetic studies with its tumor of origin. Lab Invest 2003, 83(6):877-87.

32. Kunisada T, Miyazaki M, Mihara K, Gao C, Kawai A, Inoue H, Namba M. A new human chondrosarcoma cell line (OUMS-27) that maintains chondrocytic differentiation. Int J Cancer 1998, 77(6):854-9.

33. van Oosterwijk JG, Herpers B, Meijer D, Briaire-de Bruijn IH, Cleton-Jansen AM, Gelderblom H, van de Water B, Bovée JVMG. Restoration of chemosensitivity for doxorubicin and cisplatin in chondrosarcoma in vitro: BCL-2 family members cause chemoresistance. Ann Oncol in press.

34. Bovée JVMG, Cleton-Jansen AM, Rosenberg C, Taminiau AHM, Cornelisse CJ, Hogendoorn PCW. Molecular genetic characterization of both components of a dedifferentiated chondrosarcoma, with implications for its histogenesis. J Pathol 1999, 189:454-62.

Chapter 4

Orthotopic mouse model for chondrosarcoma of bone: an *in vivo* tool for drug testing

This chapter is based on the manuscript: van Oosterwijk JG, Plass JRM, Meijer D, Que I, Karperien M, Bovée JVMG. Orthotopic mouse model for chondrosarcoma of bone: an *in vivo* tool for drug testing. *Submitted*

Abstract

Chondrosarcoma is a malignant cartilaginous tumor of bone. Recently, mutations in isocitrate dehydrogenase-1 (IDH1) and -2 (IDH2) were identified in central chondrosarcomas. Notoriously resistant to conventional treatment modalities the need for model systems to screen new treatment options is high.
We used two cell lines, CH2879 (wildtype for IDH and TP53 mutations) and SW1353 (harboring IDH2 R172S and TP53 V203L mutations) to generate new chondrosarcoma mouse models. Cell lines were stably transduced with a lentiviral luciferase expression vector and after clonal selection luciferase expressing clones were subcutaneously and orthotopically implanted in nude mice. Mice injected with CH2879 cells were treated with doxorubicin over a period of 6 weeks.
Both cell lines resulted in tumor growth. CH2879 tumors were consistently larger than SW1353 tumors. No difference in size could be observed between subcutaneous and orthotopic tumors. Tumor growth could be monitored over time through assessment of luciferase activity, without harming the mice. Using this model we show that doxorubicin does not have a significant effect on *in vivo* tumor growth.
We here show an orthotopic chondrosarcoma mouse model that can be used to test new treatment strategies evolving from *in vitro* research.

Introduction

Chondrosarcoma is a malignant cartilaginous tumor, predominantly affecting adults. Several subtypes with different clinicopathological features are recognized, of which conventional central chondrosarcoma is most common (~90%). Chondrosarcoma is characterized by the deposition of cartilaginous matrix, which is abundant in low grade tumors, and becomes more myxoid in high grade chondrosarcomas. Grade I chondrosarcoma has recently been reclassified as atypical cartilaginous tumor, due to its locally aggressive, but non-metastatic behavior (1). Grade II and grade III chondrosarcomas, showing a decrease in deposition of hyaline cartilaginous matrix along with increased cellularity, show an increased metastatic behavior (2). The current therapeutic strategy for chondrosarcoma is surgical resection, however due to the intrinsic resistance to conventional chemo- and radiotherapy there is nothing to offer patients with inoperable tumors and metastatic disease (3). The past decade has brought major advances in the field of chondrosarcoma genetics and therapeutic targets. Early on, EXT mutations have been identified in osteochondromas (4;5), and recently IDH mutations were identified in enchondroma, conventional central chondrosarcoma as well as dedifferentiated chondrosarcoma (6-8). The advances in the field also include an expansion in the number of cell lines. At the moment of writing there is a total of 7 conventional chondrosarcoma cell lines (9-13), and 3 dedifferentiated

chondrosarcoma cell lines (9;14). 5 of these cell lines show mutations in IDH1 (n=3) or IDH2 (n=2) (8;9). However, for advancing chondrosarcoma research and to rapidly translate results from basic research to clinical practice, reliable and representative animal models are necessary.
Most current models are based on the subcutaneous xenografting of chondrosarcoma cell lines or human tumor tissue, misrepresenting the natural niche of the tumor in the bone (15). Currently, a swarm rat chondrosarcoma model exists, derived from a tumor tissue line originally isolated from a spontaneously arising tumor in a Sprague-Dawley rat. Though a working model, the original tissue has given rise to several different lines of differentiation, each showing unique cytogenetic profiles and tumorigenic properties *in vivo* (16). In 2010, an orthotopic chondrosarcoma mouse model derived from the grade II cell line JJ012 was published. Cells were injected in matrigel, and 2/4 intratibial tumors showed spontaneous metastasis formation (17). Transgenic models for chondrosarcoma have not been developed yet. Mouse models with EXT mutations show formation of exostoses, but no progression to chondrosarcoma (18-20). Similarly, transgenic mice carrying IDH mutations in neural progenitor cells show a defect in collagen maturation, but no chondrosarcoma formation (21).
We here present 2 models, derived from the grade II SW1353 (IDH2 R172S p53 V203L) cell line and from the grade III CH2879 (IDH wt p53 wt) cell line. Using CH2879 we were able to confirm the resistance to doxorubicin, and show that this model can be used for pre-clinical therapeutic testing.

Methods

Cell lines
The chondrosarcoma cell lines CH2879 and SW1353 were cultured in RPMI 1640 medium (Invitrogen) supplemented with 10% heat-inactivated fetal bovine serum (Lonza, Breda, the Netherlands), 1% glutaMAX (Invitrogen, Bleiswijk, the Netherlands), and 50 U/mL penicillin with 50 µg/mL streptomycin (MP Biomedicals, Eindhoven, the Netherlands). Hek293t cells were cultured in DMEM (Invitrogen, Bleiswijk, the Netherlands) supplemented with 10% heat-inactivated fetal bovine serum (Lonza) and 100 U/mL penicillin with 100 µg/mL streptomycin.

Production of lentiviral particles in Hek293t cells
The self-inactivating lentiviral vector, pLV.CMV.luc.bc.PURO, and "helper" vectors, pMD 2\VSV-G, pMD L\pRRE, and pRSV-rev, were kindly provided by dr. Eric Kaijzel (LUMC). Briefly, the lentiviral vector together with the three "helper" vectors were cotransfected overnight into Hek293t cells using Lipofectamine 2000 (Invitrogen, Bleiswijk, the Netherlands) in OptiMem (Invitrogen, Bleiswijk, the Netherlands) after which medium was replaced by fresh culture medium. Viral supernatants were harvested 48hrs after transfection, filtered

through a 0.45 μm filter, and stored at -80°C until transduction in chondrosarcoma cell lines.

Generation of clonal luciferase expressing chondrosarcoma cell lines
The chondrosarcoma cells were transduced with the lentiviral supernatant in the presence of 1 μg/mL dextran (Sigma-Aldrich, Zwijndrecht, the Netherlands) for 4 hours. After transduction, cells were selected using 2 μg/mL puromycin (Sigma-Aldrich, Zwijndrecht, the Netherlands). Following antibiotic selection, single cell-derived cultures were obtained using limited dilution and screened for luciferase activity. As estrogen signaling was shown to be active in cartilaginous tumors (22), clones were selected using TaqMan gene expression arrays for ESR1, CYP19A1, and AR according to manufacturer's protocol (Applied Biosystems, Bleiswijk, the Netherlands). All cultures selected for *in vivo* implantation were tested for the presence of HIV p24.

Animals
All procedures were approved by the Leiden University animal experimental committee and Local Government (Animal protocols 08158 and 10019), performed in accordance with the national legislation of the Netherlands and in compliance with the 'Code of Practice Use of Laboratory Animals in Cancer Research' (Inspectie W&V, July 1999). Athymic mice (BALB/c *nu/nu* 6 weeks old) were acquired from Charles River (Charles River, L'Arbresle, France), housed in individually ventilated cages, and food and water was provided *ad libitum*. For all *in vivo* experiments, a total of 46 mice were used.

CH2879 and SW1353 tumor cell injection in mice
For both CH2879 and SW1353 cell lines, three single-cell derived luciferase expressing clones were used for both subcutaneous and orthotopic implantation into mice. 12 mice were subcutaneously injected. A total of 4 mice were injected with the different CH2879 clones, 4 mice with the different SW1353 clones and 4 with non-transduced cell lines to control for interference with tumorigenicity by luciferase construct.
Orthotopic injection was performed using two separate methods. In total 33 mice were orthotopically injected with either SW1353 or CH2879. Mice were anesthetized by isoflurane prior to subcutaneous or orthotopic injection in the tibia with luciferase expressing cells ($1*10^6$ cells in 40 μL PBS or $2.5*10^5$ cells in 10 μL PBS respectively). Eighteen mice were injected using the first method; 9 with SW1353 LUC clones and 9 with CH2879 clones; 3 mice per clone. Orthotopical injection was performed with an injection of a single-cell suspension of luc+ cells into the right tibiae as described previously (23). In brief, two small holes (~0.35mm each) 4-5 mm apart were created in the bone cortex of the upper right tibiae using a dental drill, and reservoir for the cells was created by flushing out the bone marrow from the proximal end of the shaft. After inoculation with a 30-gauge

needle through the lower hole, the cutaneous wound was sutured. In the second method, 15 mice were injected with CH2879 LUC 10. Orthotopical injection was performed with an injection of a single cell suspension directly into the tibia without the prior creation of a reservoir.
The progression of cancer cell growth was monitored weekly by optical imaging. After the experimental period, or 7 weeks after start of signal detection for mice not on treatment regime, the animals were sacrificed and tumors were collected for histological assessment.

In vivo treatment of CH2879 orthotopic tumors
The 15 mice injected using the second method (immediate injection without prior creation of a reservoir), were divided into two groups after signal detection for investigating the effect of doxorubicin on tumor growth. Seven mice were treated with 12 mg/kg doxorubicin over a course of 6 weeks in which they were administered a single dose once every 2 weeks through i.p. injection. Control group consisted of eight mice monitored over 6 weeks. Doxorubicin was obtained from the in-house hospital pharmacy in a 0.9% NaCl solution. Treatment was started when tumors could be detected using the IVIS 100 (Caliper LifeSciences, Hopkinton, MA), ie bioluminescent (BLI) signals of 10^5 P/s/cm^2 (~0.6cm^3). In case mice would show a bioluminescent signal $\geq 10^9$ P/s/cm^2 (~1cm^3) they were to be considered to have too severe a tumor burden and were sacrificed. After treatment course was completed, or mice showed severe clinical signs as a result of tumor burden or treatment, mice were sacrificed and tibiae were collected for histological assessment. Lungs were harvested to investigate possible metastases.

In vivo imaging
To monitor luciferase activity, mice were anesthetized using isoflurane. Images were acquired 5 minutes after i.p. injection of D-luciferin (150 mg/kg) using 30 sec exposure time. Tumor take was monitored using the IVIS 100 (Caliper LifeSciences, Hopkinton, MA) and bioluminescent signals were quantified using Living Image 3.0 (Caliper LifeSciences, Hopkinton, MA).

Tissue embedding and staining
Lungs were fixed in 4% paraformaldehyde and embedded in paraffin. Tibiae were decalcified in 0.4M EDTA/PBS after fixing in 4% paraformaldehyde. After decalcification with EDTA, tibiae were embedded in paraffin and 5µm sections were stained with hematoxylin and eosin (H&E) for morphology or 0.08% toluidine blue (Brocacef Holding, Maarssen, The Netherlands) to assess matrix formation.

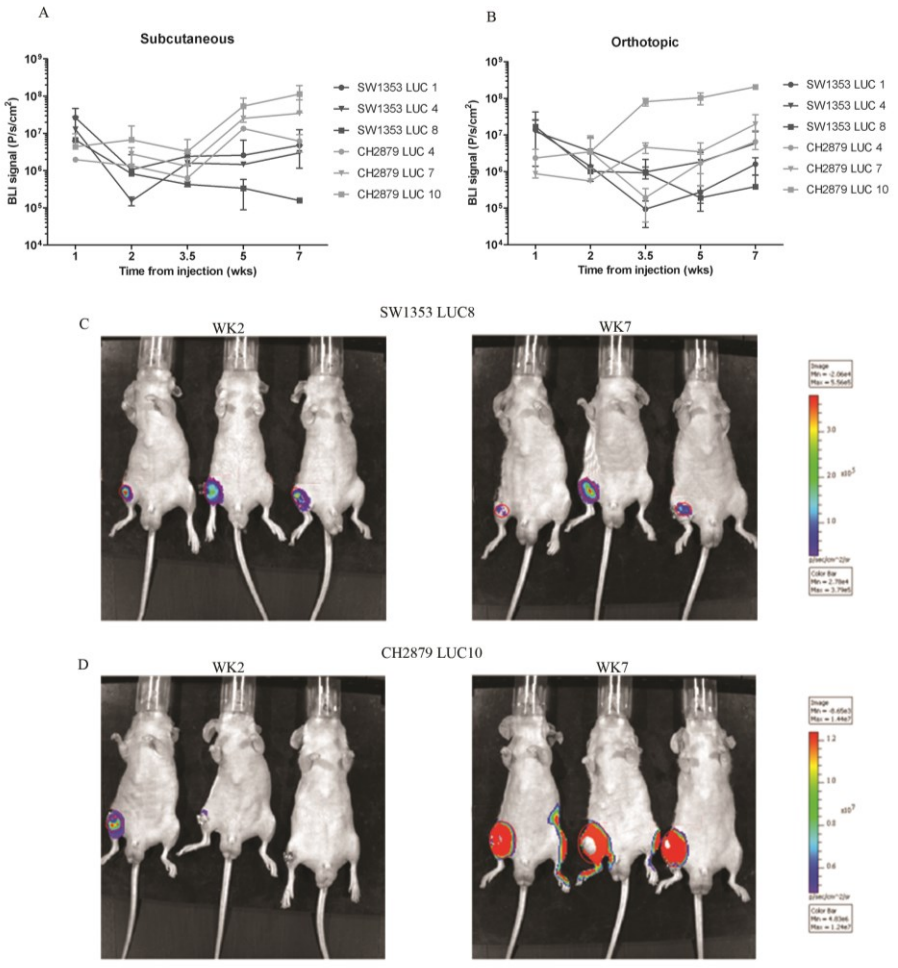

Figure 4.1: Generation of chondrosarcoma mouse model. A: Subcutaneous injection of SW1353 and CH2879 cells led to tumor growth in 4/4 mice. Standard deviation indicates variation in measurements between the 4 injected mice. B: Orthotopic injection of SW1353 and CH2879 cells led to tumor growth in 3/3 mice, CH2879 clone luc 10 resulted in larger tumors than other clones. Standard deviation indicates variation in measurements between the 4 injected mice. C: Each SW1353 clone was injected orthotopically in the left tibia of 3 mice. SW1353 clone 8 is shown with BLI signals at week 2 (left panel) and week 7 (central panel) with luminescence scale (right panel). Luciferase signals for this clone did not show an increase during the 7 week observation time. Standard deviation indicates variation in measurements between the 9 injected mice. D: Each CH2879 clone was injected orthotopically in the left tibia of 3 mice. CH2879 clone LUC 10 is shown with BLI signals at week 2 (left panel) and week 7 (central panel) with luminescence scale (right panel). This clone showed the strongest increase in luciferase signals during the 7 week observation time, as evidenced by the strong red signal. Standard deviation indicates variation in measurements between the 9 injected mice.

Results

Transduction of CH2879 and SW1353 cell lines

Based upon expression of estrogen signaling markers (results not shown), three representative clones were selected for each cell line. For SW1353, clones 1, 4, and 8 most closely resembled the nontransduced cell line, for CH2879, clones 4, 7, and 10 were most similar. All clones showed luciferase expression and were negative for HIV p24.

Tumor growth after injection of luciferase transduced SW1353 and CH2879 chondrosarcoma cell lines

Six week old Balb/C nude mice were injected with either SW1353 or CH2879. Tumor growth was observed within 1 week, evidenced by emission of bioluminescent signal at the first measurement (week 1) after both subcutaneous (fig 4.1A) and orthotopic (fig 4.1B, C, D) injection. Subcutaneous injection of SW1353 clone 1 and 4 led to tumors in 4/4 mice, whereas clone 8 led to tumors in 1/4 mice, orthotopic injection of SW1353 clones led to tumor growth in all cases (9/9 mice). CH2879 clone 4 and 7 led to tumor growth in 3/4 mice, clone 4 led to tumor growth in 4/4 mice, orthotopic injection of CH2879 clones led to tumor growth in all 9 mice. No bioluminescent signals were observed in the lungs and histological examination also indicated no evidence of metastases.

Luciferase activity of CH2879 tumors continued to increase during the course of 7 weeks, indicative of progressive tumor growth, whereas SW1353 derived tumors showed a stagnated signal strength, suggestive of halted growth. The size of the CH2879 derived tumors were consistently larger than the SW1353 derived tumor, as evidenced by stronger BLI signals (fig 4.1A, B). In both SW1353 and CH2879, orthotopic and subcutaneous injection resulted in comparable BLI signal. The clone showing the strongest luciferase signal, CH2879 LUC 10, (fig 4.1B, D), was selected for further experiments. Orthotopic injection of luciferase transfected cells using prior creation of a reservoir for the cells led to tumor growth within one to two weeks. Using the second method using immediate injection of the cells, it took up to 4 weeks until tumors were detectable by bioluminescent imaging. However, as immediate orthotopic injection was considered less painful for the mice and did result in successful tumor growth, in subsequent experiments mice were directly injected with tumor cells.

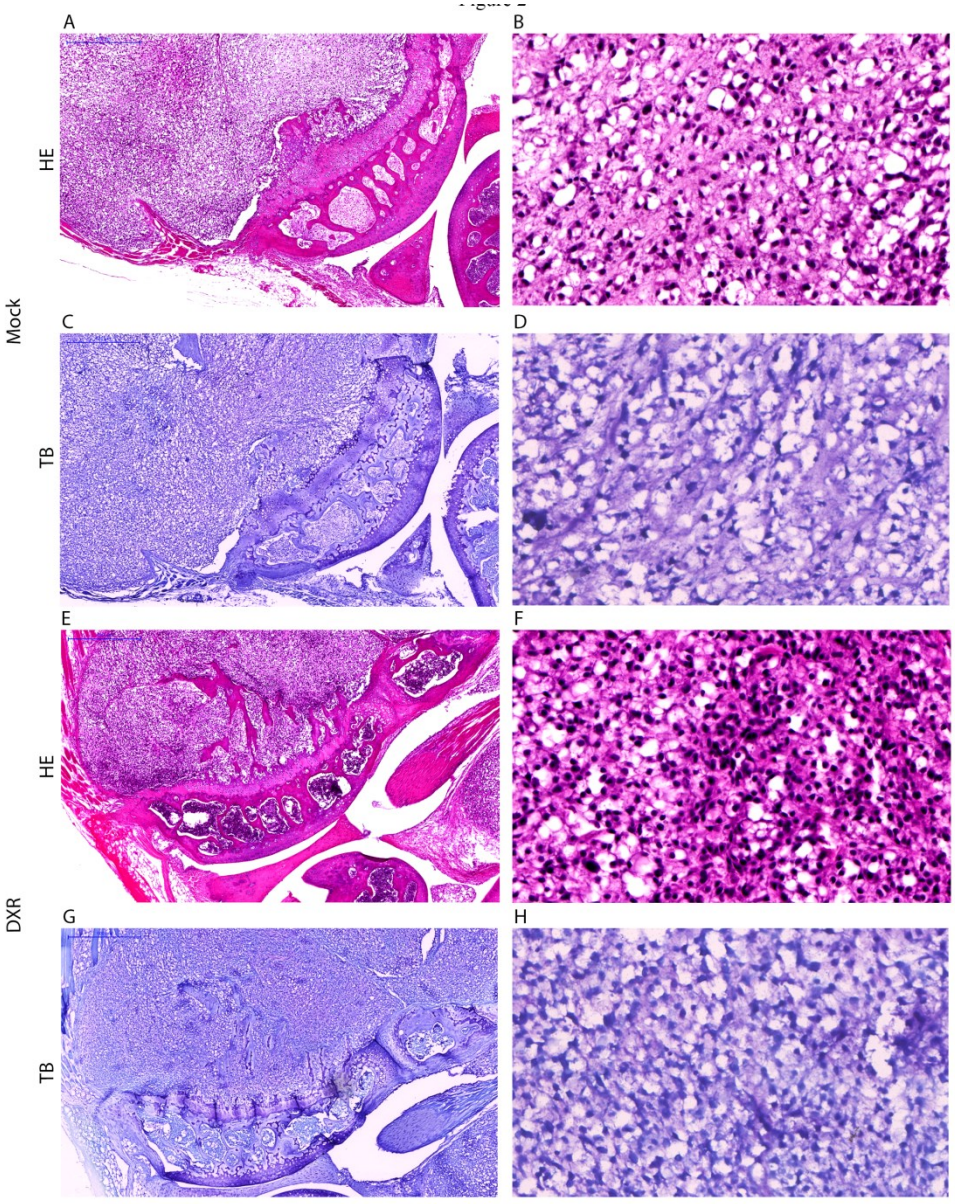

Figure 4.2: Orthotopic CH2879 tumor resemble chondrosarcoma morphology with matrix deposition. Control mouse (Mock A-D) and mouse treated with doxorubicin (DXR, E-H) using H&E staining (A,B; E,F) and toluidine blue staining (C,D; G,H) showing purple coloration where cartilaginous matrix is produced.

CH2879 tumors resemble high grade chondrosarcoma
Orthotopic injection of CH2879 LUC 10 cells shows diaphyseal localization of tumor cells, with tumor cells growing circumferentially and expanding through the cortex (fig 4.2 A, E). The histological analysis of the tumor cells shows that they strongly resemble that of a high grade chondrosarcoma (fig 4.2 B, D, F, H). The tumor is located close to the growth plate, but does not infiltrate the growth plate (fig 4.2 A, C, E, G). Toluidine blue staining shows matrix formation (fig 4.2 C, D, G, H).

Doxorubicin treatment does not influence chondrosarcoma tumor growth
Mice orthotopically injected with CH2879 LUC 10 cells were treated with doxorubicin 12mg/kg for 6 weeks. Treatment started when luciferase measurements were at BLI 10^5. Mean BLI starting values for mice on doxorubicin (n=7) were $8.4x10^6$ P/s/cm^2 ($\pm 3.5\ x10^6$) with end BLI values $1.9x10^8$ P/s/cm^2 ($\pm 1.5\ x10^8$). For the control group (n=8) starting BLI values were $4.1x10^6$ P/s/cm^2 ($\pm 5.3\ x10^6$) with end BLI values $5.9x10^7$ P/s/cm^2 ($\pm 2.1\ x10^7$). Fold change of tumor growth at the start of treatment was set at 1 to allow for comparison of the different groups. After start of treatment, mice receiving doxorubicin showed a delay in tumor progression when compared to control mice (fig 4.3A). However, during the last cycle of doxorubicin, a strong increase in tumor growth was observed (fig 4.3A), suggesting resistance to doxorubicin. Figure 4.3 B-E shows bioluminescent imaging of 3 control mice at start of treatment (fig 4.3B) and end of treatment (fig 3C) as well as 3 mice treated with doxorubicin at start of treatment (fig 4.3D) and end of treatment cycle (fig 3E) along with the luminescence scale (fig 4.3F). As tumors in the doxorubicin treated group show stronger BLI signals both at start and end of treatment, the total tumor growth over the course of 6 weeks, as calculated by fold change (fig 4.3A), amounts to a similar signal increase. Statistical analysis of both the BLI signals and the fold change showed that doxorubicin treatment was not found to significantly influence the tumor growth (two tailed independent t-test for fold change $p=0.143$; for BLI signals $p=0.2$). Mouse weight was stable during the entire experiment.

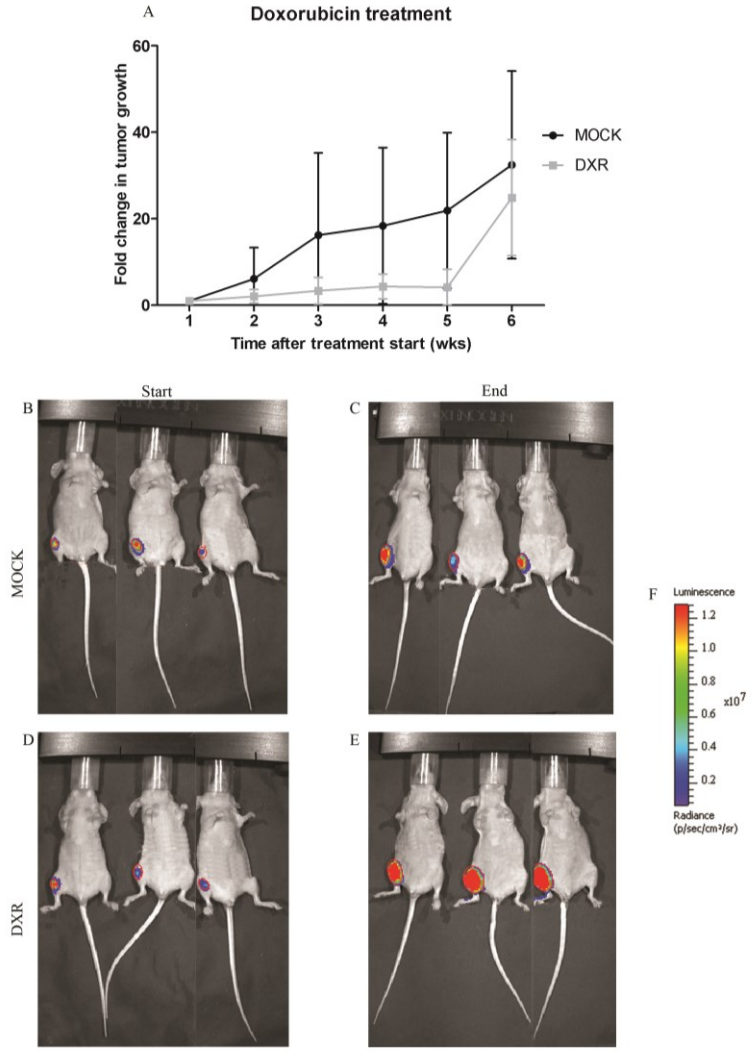

Figure 4.3: Orthotopic CH2879 tumors are resistant to doxorubicin. A: Mice were followed for bioluminescent signal indicating tumor presence from injection of tumor cells. At treatment start fold change of tumor growth was set at 1 and change in tumor growth monitored per week. Treated mice (DXR) showed a short lapse in tumor growth but start to catch up with untreated (MOCK) mice in tumor size at week 6. Standard deviation indicated variation in measurements of 8 untreated mice, and 7 doxorubicin treated mice. B,C: Bioluminescent signals for 3 untreated mice at start of signal detection (B) and after 6 weeks (C). D, E: Bioluminescent signals for 3 mice treated with doxorubicin at start of signal detection and doxorubicin treatment (D) and after 6 weeks at completion of treatment cycle (E). F: Luminescence scale indicating the strength of BLI signals in p/sec/cm^2/sr, based on the premise that a larger tumor will emit more luciferase and therefore a stronger signal will be detected, represented in the red spectrum on the scale. The increase is tumor size from B-C and D-E in control and doxorubicin treated mice is observed by the increase in red signal.

Discussion

Chondrosarcoma is notoriously resistant to conventional chemotherapy. The mouse model developed here supports this resistance as it is observed in the clinic. Indeed, no significant difference between untreated tumors and tumors treated with doxorubicin is observed. In this era of targeted therapeutics, identification of targets is crucial, and over the past years new therapeutic targets have been identified using the growing number of chondrosarcoma cell lines. Apoptotic pathways have been shown to be upregulated in chondrosarcoma, and inhibition of survivin (24) and the anti-apoptotic Bcl-2 family members (25-27) were shown to result in increased sensitivity to chemotherapeutics and radiotherapy (28). Moreover, survival pathways involving HIF1α (29-31), Src (32;33), PI3K (32;34), and the mTOR (35;36) pathways have been shown to play crucial roles in chondrosarcoma survival. The development of new targeted therapeutics targeting the apoptosis and survival pathways provides unlimited opportunities for combination treatments. Recently, synergy between PI3K and Bcl-2/Bcl-xl inhibition was shown in renal cell carcinoma cell lines (37), and both were shown to potentiate MEK inhibition in lung and pancreatic tumor models (38). Preclinical results in chondrosarcoma strongly advocate similar combinations in chondrosarcoma. However, due to the rarity of chondrosarcoma, the execution of large clinical trials is a major hurdle. The presence of good animal models, such as the one presented here, to test therapeutic candidates before proceeding to the clinic is therefore invaluable.

Most existing chondrosarcoma mouse models are subcutaneous (15), whereas human chondrosarcoma typically occurs either in the medulla of the bone or on the surface of the bone (1). A mouse model mimicking the human situation is preferable when studying chondrosarcoma characteristics and new therapeutic strategies, especially since matrix deposition around the tumor cells and tumor blood supply have been hypothesized to play a role in chemoresistance (33). The models presented here utilize a luciferase construct enabling the live imaging of tumor growth, an especially useful tool when studying drug response. Interestingly, during the development of our model, we observed that direct deposition of tumor cells in the bone resulted in better grafting than subcutaneous injection. Possibly through creating a niche which better resembles the natural environment of the tumor. We compared two injection methods, in the first method cells were injected after drilling a hole in the tibia, and in the second method cells were immediately injected in the tibia. Even though a short delay in tumor onset was observed, tumors succeeded to grow without prior creation of a reservoir, a method also considered to be less painful for the mice.

However, subcutaneous xenograft chondrosarcoma mouse models have advanced our understanding of EXT mutations and the hedgehog signaling in cartilage tumors (39). Recently, an orthotopic xenograft mouse model with spontaneous metastases, derived from the chondrosarcoma cell line JJ012, was developed. We

were unable to grow tumors using the JJ012 cell line (results not shown). This discrepancy could be explained by the fact that we did not use matrigel to facilitate injection and homing of the chondrosarcoma cells. However, the CH2879 and SW1353 cell lines did not need matrigel to form tumors.

We here show the development of orthotopic chondrosarcoma mouse models, using a luciferase construct for live imaging of tumor growth. Strongly resembling human chondrosarcoma, these models provide a new tool for *in vivo* studying of targeted therapeutics. Especially in chondrosarcoma, a rare malignancy making large randomized trials difficult to conduct, the development of such a mouse model can aid in bridging the gap between pre-clinical research and clinical implementation of new therapeutic strategies.

Reference List

(1) Hogendoorn PCW, Bovée JVMG, Nielsen GP. Chondrosarcoma (grades I-III), including primary and secondary variants and periosteal chondrosarcoma. In: Fletcher C.D.M., Bridge JA, Hogendoorn PCW, Mertens F, editors. World Health Classification of Tumours. Pathology and Genetics of Tumours of Soft Tissue and Bone. 4 ed. 2013. p. 264-8.

(2) Evans HL, Ayala AG, Romsdahl MM. Prognostic factors in chondrosarcoma of bone. A clinicopathologic analysis with emphasis on histologic grading. Cancer 1977;40:818-31.

(3) Gelderblom H, Hogendoorn PCW, Dijkstra SD, van Rijswijk CS, Krol AD, Taminiau AH, Bovee JVMG. The clinical approach towards chondrosarcoma. Oncologist 2008;13(3):320-9.

(4) Jennes I, Pedrini E, Zuntini M, Mordenti M, Balkassmi S, Asteggiano CG, Casey B, Bakker B, Sangiorgi L, Wuyts W. Multiple osteochondromas: mutation update and description of the multiple osteochondromas mutation database (MOdb). Hum Mutat 2009;30(12):1620-7.

(5) Hecht JT, Hogue D, Strong LC, Hansen MF, Blanton SH, Wagner M. Hereditary multiple exostosis and chondrosarcoma: linkage to chromosome 11 and loss of heterozygosity for EXT-linked markers on chromosomes 11 and 8. Am J Hum Genet 1995;56:1125-31.

(6) Amary MF, Bacsi K, Maggiani F, Damato S, Halai D, Berisha F, Pollock R, O'Donnell P, Grigoriadis A, Diss T, Eskandarpour M, Presneau N, Hogendoorn PC, Futreal A, Tirabosco R, Flanagan AM. IDH1 and IDH2 mutations are frequent events in central chondrosarcoma and central and periosteal chondromas but not in other mesenchymal tumours. J Pathol 2011;224(3):334-43.

(7) Amary MF, Damato S, Halai D, Eskandarpour M, Berisha F, Bonar F, McCarthy S, Fantin VR, Straley KS, Lobo S, Aston W, Green CL, Gale RE, Tirabosco R, Futreal A, Campbell P, Presneau N, Flanagan AM. Ollier disease and Maffucci syndrome are caused by somatic mosaic mutations of IDH1 and IDH2. Nat Genet 2011.

(8) Pansuriya TC, van ER, d'Adamo P, van Ruler MA, Kuijjer ML, Oosting J, Cleton-Jansen AM, van Oosterwijk JG, Verbeke SL, Meijer D, van WT, Nord KH, Sangiorgi L, Toker B, Liegl-Atzwanger B, San-Julian M, Sciot R, Limaye N, Kindblom LG, Daugaard S, Godfraind C, Boon LM, Vikkula M, Kurek KC, Szuhai K et al. Somatic mosaic IDH1 and IDH2 mutations are associated with enchondroma and spindle cell hemangioma in Ollier disease and Maffucci syndrome. Nat Genet 2011;43(12):1256-61.

(9) van Oosterwijk JG, de JD, van Ruler MA, Hogendoorn PC, Dijkstra PS, van Rijswijk CS, Machado IS, Llombart-Bosch A, Szuhai K, Bovée JVMG. Three new chondrosarcoma cell lines: one grade III conventional central chondrosarcoma and two dedifferentiated chondrosarcomas of bone. BMC Cancer 2012;12(375):-375.

(10) Calabuig-Farinas S, Benso RG, Szuhai K, Machado I, Lopez-Guerrero JA, de JD, Peydro A, Miguel TS, Navarro L, Pellin A, Llombart-Bosch A. Characterization of a New Human Cell Line (CH-3573) Derived from a Grade II Chondrosarcoma with Matrix Production. Pathol Oncol Res 2012.

(11) Gil-Benso R, Lopez-Gines C, Lopez-Guerrero JA, Carda C, Callaghan RC, Navarro S, Ferrer J, Pellin A, Llombart-Bosch A. Establishment and characterization of a continuous human chondrosarcoma cell line, ch-2879:

comparative histologic and genetic studies with its tumor of origin. Lab Invest 2003;83(6):877-87.
(12) Scully SP, Berend KR, Toth A, Qi WN, Qi Z, Block JA. Marshall Urist Award. Interstitial collagenase gene expression correlates with in vitro invasion in human chondrosarcoma. Clin Orthop Relat Res 2000;(376):291-303.
(13) Kunisada T, Miyazaki M, Mihara K, Gao C, Kawai A, Inoue H, Namba M. A new human chondrosarcoma cell line (OUMS-27) that maintains chondrocytic differentiation. Int J Cancer 1998;77(6):854-9.
(14) Kudo N, Ogose A, Hotta T, Kawashima H, Gu W, Umezu H, Toyama T, Endo N. Establishment of novel human dedifferentiated chondrosarcoma cell line with osteoblastic differentiation. Virchows Arch 2007;451(3):691-9.
(15) Clark JC, Dass CR, Choong PF. Development of chondrosarcoma animal models for assessment of adjuvant therapy. ANZ J Surg 2009;79(5):327-36.
(16) Stevens JW, Patil SR, Jordan DK, Kimura JH, Morcuende JA. Cytogenetics of swarm rat chondrosarcoma. Iowa Orthop J 2005;25:135-40.
(17) Clark JC, Akiyama T, Dass CR, Choong PF. New clinically relevant, orthotopic mouse models of human chondrosarcoma with spontaneous metastasis. Cancer Cell Int 2010;10:20.
(18) Stickens D, Zak BM, Rougier N, Esko JD, Werb Z. Mice deficient in Ext2 lack heparan sulfate and develop exostoses. Development 2005 19;132(22):5055-68.
(19) Zak BM, Schuksz M, Koyama E, Mundy C, Wells DE, Yamaguchi Y, Pacifici M, Esko JD. Compound heterozygous loss of Ext1 and Ext2 is sufficient for formation of multiple exostoses in mouse ribs and long bones. Bone 2011 1;48(5):979-87.
(20) Matsumoto K, Irie F, Mackem S, Yamaguchi Y. A mouse model of chondrocyte-specific somatic mutation reveals a role for Ext1 loss of heterozygosity in multiple hereditary exostoses. Proc Natl Acad Sci U S A 2010;107(24):10932-7.
(21) Sasaki M, Knobbe CB, Itsumi M, Elia AJ, Harris IS, Chio II, Cairns RA, McCracken S, Wakeham A, Haight J, Ten AY, Snow B, Ueda T, Inoue S, Yamamoto K, Ko M, Rao A, Yen KE, Su SM, Mak TW. D-2-hydroxyglutarate produced by mutant IDH1 perturbs collagen maturation and basement membrane function. Genes Dev 2012;26(18):2038-49.
(22) Cleton-Jansen AM, van Beerendonk HM, Baelde HJ, Bovée JVMG, Karperien M, Hogendoorn PCW. Estrogen signaling is active in cartilaginous tumors: implications for antiestrogen therapy as treatment option of metastasized or irresectable chondrosarcoma. Clin Cancer Res 2005;11(22):8028-35.
(23) van der Pluijm G, Que I, Sijmons B, Buijs JT, Lowik CW, Wetterwald A, Thalmann GN, Papapoulos SE, Cecchini MG. Interference with the microenvironmental support impairs the de novo formation of bone metastases in vivo. Cancer Res 2005;65(17):7682-90.
(24) Lechler P, Renkawitz T, Campean V, Balakrishnan S, Tingart M, Grifka J, Schaumburger J. The antiapoptotic gene survivin is highly expressed in human chondrosarcoma and promotes drug resistance in chondrosarcoma cells in vitro. BMC Cancer 2011;11:-120.
(25) van Oosterwijk JG, Herpers B, Meijer D, Briaire-de Bruijn IH, Cleton-Jansen AM, Gelderblom H, van de Water B, Bovée JVMG. Restoration of chemosensitivity for doxorubicin and cisplatin in chondrosarcoma in vitro: BCL-2 family members cause

chemoresistance. Ann Oncol 2012;23(6):1617-26.
(26) van Oosterwijk JG, Meijer D, van Ruler MA, van den Akker BE, Oosting J, Krenacs T, Picci P, Flanagan AM, Liegl-Atzwanger B, Leithner A, Athanasou N, Daugaard S, Hogendoorn PCW, Bovee JVMG. Screening for Potential Targets for Therapy in Mesenchymal, Clear Cell, and Dedifferentiated Chondrosarcoma Reveals Bcl-2 Family Members and TGFbeta as Potential Targets. Am J Pathol 2013;182(4):1347-56.
(27) Kim DW, Kim KO, Shin MJ, Ha JH, Seo SW, Yang J, Lee FY. siRNA-based targeting of antiapoptotic genes can reverse chemoresistance in P-glycoprotein expressing chondrosarcoma cells. Mol Cancer 2009;8:28.
(28) Kim DW, Seo SW, Cho SK, Chang SS, Lee HW, Lee SE, Block JA, Hei TK, Lee FY. Targeting of cell survival genes using small interfering RNAs (siRNAs) enhances radiosensitivity of Grade II chondrosarcoma cells. J Orthop Res 2007;25(6):820-8.
(29) Boeuf S, Bovee JVMG, Lehner B, Hogendoorn PCW, Richter W. Correlation of hypoxic signalling to histological grade and outcome in cartilage tumours. Histopathology 2009.
(30) Chen C, Zhou H, Wei F, Jiang L, Liu X, Liu Z, Ma Q. Increased levels of hypoxia-inducible factor-1alpha are associated with Bcl-xL expression, tumor apoptosis, and clinical outcome in chondrosarcoma. J Orthop Res 2010.
(31) Schaap FG, French PJ, Bovee JVMG. Mutations in the Isocitrate Dehydrogenase Genes IDH1 and IDH2 in Tumors. Adv Anat Pathol 2013 January;20(1):32-8.
(32) Schrage YM, Briaire-de Bruijn IH, de Miranda NFCC, van Oosterwijk JG, Taminiau AHM, van Wezel T, Hogendoorn PCW, Bovée JVMG. Kinome profiling of chondrosarcoma reveals Src-pathway activity and dasatinib as option for treatment. Cancer Res 2009;69(15):6216-22.
(33) Bovee JVMG, Cleton-Jansen AM, Taminiau AHM, Hogendoorn PCW. Emerging pathways in the development of chondrosarcoma of bone and implications for targeted treatment. Lancet Oncology 2005 August;6(8):599-607.
(34) Galoian K, Temple HT, Galoyan A. mTORC1 inhibition and ECM-cell adhesion-independent drug resistance via PI3K-AKT and PI3K-RAS-MAPK feedback loops. Tumour Biol 2012 June;33(3):885-90.
(35) Perez J, Decouvelaere AV, Pointecouteau T, Pissaloux D, Michot JP, Besse A, Blay JY, Dutour A. Inhibition of chondrosarcoma growth by mTOR inhibitor in an in vivo syngeneic rat model. PLoS ONE 2012;7(6):e32458.
(36) Bernstein-Molho R, Kollender Y, Issakov J, Bickels J, Dadia S, Flusser G, Meller I, Sagi-Eisenberg R, Merimsky O. Clinical activity of mTOR inhibition in combination with cyclophosphamide in the treatment of recurrent unresectable chondrosarcomas. Cancer Chemother Pharmacol 2012;70(6):855-60.
(37) Zhu S, Cohen MB, Bjorge JD, Mier JW, Cho DC. PI3K inhibition potentiates Bcl-2-dependent apoptosis in renal carcinoma cells. J Cell Mol Med 2013;17(3):377-85.
(38) Tan N, Wong M, Nannini MA, Hong R, Lee LB, Price S, Williams K, Savy PP, Yue P, Sampath D, Settleman J, Fairbrother WJ, Belmont LD. Bcl-2/Bcl-xL Inhibition Increases the Efficacy of Mek Inhibition Alone and in Combination with PI3 Kinase Inhibition in Lung and Pancreatic Tumor Models. Mol Cancer Ther 2013.
(39) Tiet TD, Hopyan S, Nadesan P, Gokgoz N, Poon R, Lin AC, Yan T, Andrulis IL, Alman BA, Wunder JS.

Constitutive hedgehog signaling in chondrosarcoma up-regulates tumor cell proliferation. Am J Pathol 2006;168(1):321-30.

Chapter 5

Restoration of chemosensitivity for doxorubicin and cisplatin in chondrosarcoma *in vitro*: BCL-2 family members cause chemoresistance

This chapter is based on the manuscript: van Oosterwijk JG, Herpers B, Meijer D, Briaire de Bruijn IH, Cleton-Jansen AM, Gelderblom H, van de Water B, Bovée JVMG. *Ann Onc. 2012; 23(6): 1617-26*

Abstract

Chondrosarcomas are malignant cartilage forming tumors notorious for their resistance to conventional chemo- and radiotherapy. Postulated explanations describe the inaccessibility due to abundant hyaline cartilaginous matrix, presence of multi-drug resistance (MDR) pumps, and expression of anti-apoptotic BCL-2 family members.
We studied the sensitivity of chondrosarcoma cell lines (SW1353, CH2879, JJ012, OUMS27) and 2 primary cultures for doxorubicin and cisplatin. We examined the role of extracellular matrix using 3D pellet models and MDR pump activity using FACS analysis. The role of BCL2 family members was investigated using the BH3 mimetic ABT-737.
Chondrosarcoma cells showed highest resistance to cisplatin. 3D cell pellets, morphologically strongly resembling chondrosarcoma *in vivo*, confirmed nuclear incorporation of doxorubicin. MDR pump activity was heterogeneous among cultures. Chondrosarcoma cells responded to ABT-737 and combination with doxorubicin led to complete loss of cell viability and apoptosis with cytochrome C release.
Despite MDR pump activity and abundance of hyaline cartilaginous matrix, doxorubicin is able to accumulate in the cell nuclei. By repairing the apoptotic machinery we were able to sensitize chondrosarcoma cells to doxorubicin and cisplatin, indicating an important role for BCL-2 family members in chemoresistance and a promising new treatment strategy for inoperable chondrosarcoma.

Introduction

Chondrosarcoma is a malignant hyaline cartilaginous tumor of the bone, and is the second most common primary bone malignancy in humans. Several subtypes of chondrosarcoma exist, with conventional chondrosarcoma being the most common (~80%) (1). Conventional chondrosarcomas (CS) can occur either in the medulla of the bone (central chondrosarcoma) or at the surface (peripheral chondrosarcoma). As chondrosarcomas have clinically proven to be resistant to conventional chemo- and radiotherapy, no (systemic) treatment can be offered for high grade, irresectable, or metastatic tumors (2;3). Recent literature focuses on investigating activated pathways and assessing their validity as novel targeted treatment strategies for these inoperable tumors (4).

Several hypotheses explaining primary resistance in conventional chondrosarcoma have been postulated. It is suggested that chemoresistance is caused by a possible impediment of chemotherapeutic agents to penetrate the extracellular matrix (5). In grade I chondrosarcomas, there is a vast amount of hyaline extracellular matrix (3;6-8). Low grade chondrosarcomas are composed of slowly dividing cells while conventional chemo- and radiotherapy target rapidly dividing cells (9). In higher grade chondrosarcomas, the extracellular matrix appears more myxoid and cells divide more rapidly but especially in these tumors

chemoresistance confers an important clinical problem. Alternatively, the activity of multi-drug resistance (MDR) pumps may cause chemoresistance in chondrosarcoma, as has been described in various cancer types. The role of P-glycoprotein in resistance to doxorubicin has been shown in two chondrosarcoma cell lines (10) and retrospective studies (11). Finally, the parathyroid hormone related peptide (PTHrP) pathway was found to be activated in chondrosarcoma with high BCL-2 expression, correlating with increasing histological grade (6;8). Since BCL-2 is an anti-apoptotic protein, its aberrant expression may contribute to chondrosarcoma resistance (12).

In order to determine the cause of chemoresistance in conventional central chondrosarcoma, we tested the different hypotheses described above: 3D pellet models were used to investigate the role of matrix surrounding the tumor cells. We assessed the activity of the multidrug resistance pumps and established the role of BCL-2 family members. Our data indicate that tumor matrix and MDR pumps are not critical to chemoresistance of chondrosarcoma whereas the activity of anti-apoptotic BCL-2 family members controls the onset of cell killing caused by classical anticancer drugs.

Methods

Compounds

Doxorubicin and cisplatin were obtained from the in-house hospital pharmacy in a 0.9% NaCl solution. Therapeutic concentrations of doxorubicin in patients are 5-100μM with an *in vitro* range of 1-10 μM, for cisplatin these are 3-13μM with an *in vitro* range of 1-50μM (13). ABT-737 (Abbott Laboratories Inc, IL, USA) and R-roscovitine (R7772, Sigma Aldrich, Zwijndrecht, The Netherlands) were dissolved in DMSO.

Cell culture

Acute Lymphatic Leukemia cell line HL-60, chondrocyte cell line LBPVA (14), osteosarcoma cell line MNNG, as well as chondrosarcoma cell lines and primary cultures (table 5.1), were cultured in RPMI1640 (Gibco, Invitrogen Life-Technologies, Scotland, UK) supplemented with 1% L-glutamax, 1% penicillin/streptomycin (100U/mL), and 10% (cell lines) or 20% (primary cultures), heat-inactivated Fetal Calf Serum (Gibco, Invitrogen Life-Technologies, Scotland, UK). Normal human mesenchymal stem cells (MSC) L2069 (15) were grown in Dulbecco's Modified Eagle Medium (DMEM) (Invitrogen, Breda, The Netherlands) supplemented with 1 mg/ml glucose, 2% penicillin/streptomycin (P/S), and 10% Fetal Bovine Serum acetyl salicyclic acid (ASA) (FBS ASA; Hyclone, Logan, UT). Cells were grown at 37°C in a humidified incubator with 95% air and 5% CO_2. All primary chondrosarcoma cultures were generated from chondrosarcomas surgically resected in our institute. All samples were coded and all procedures were performed according to the ethical guidelines “Code for Proper

Secondary Use of Human Tissue in The Netherlands" (Dutch Federation of Medical Scientific Societies). Cells were cultured until stably multiplying and chondrogenic phenotype was confirmed using RT-PCR for collagen I, IIB, III, and X, aggrecan, and SOX9 (16). DNA was isolated from the cells for subsequent TP53 mutation analysis (17). Identity of cell lines was confirmed using the PowerPlex® 1.2 system after completion of experiments (Promega Benelux BV, Leiden, The Netherlands).

Cell counting and viability assay

Cell counting for proliferation assay was performed with a Casey ® cell counter (Roche Applied Sciences, Almere, the Netherlands). Chondrosarcoma cell lines and primary cultures were plated in 96 well plates for viability assessment ($2\text{-}5x10^4$ cells/well for cell lines and $2x10^5$ for primary cultures) and allowed to adhere overnight. Cells were incubated with the drugs for 24, 48, or 72 hours, after which a WST-1 assay was performed according to manufacturer's instruction (Cat. No. 11 644 807 001; Roche Diagnostics GmbH, Penzberg, Germany) and analyzed with a light spectrometer (Victor^{3}V, 1420 Multilabel counter, Perkin Elmer, NL). All experiments were performed in triplicate at least three times. Graphs show data from one representative experiment. Error bars indicate standard deviation. Synergy was calculated using the Chou & Talalay method for Combination Index calculations (18).

3D Pellet model

3D cell pellets were generated from cultures CH2879, OUMS27, L835, and MSCs L2069 as described (15). Cell pellets were allowed to differentiate for 4 weeks after which they were treated with either 1μM or 10μM doxorubicin 2x week. After a total of 6 weeks, pellets were harvested, washed in PBS 3x, fixed in formalin, embedded in paraffin. Pellet slides were mounted using 4'-6-diamidino-2phenylindole (DAPI) -containing VECTASHIELD (Vector Laboratories, Burlingame, CA) and examined under a Leica DM500B fluorescent microscope. Doxorubicin incorporation was recorded at 480nm. Pellet morphology and matrix formation were examined using H&E staining and 1% toluidine blue staining (Brocacef Holding, Maarssen, The Netherlands). Immunohistochemistry for Ki-67 (DAKO, Heverlee, Belgium) and cleaved caspase 3 (Cell Signaling, Leiden, The Netherlands) were performed as described (19). Percentage of positive cells was calculated using NuclearQuant software (3DHISTECH, Budapest, Hungary).

Multidrug resistance pump assay

Activities of three multidrug resistance pumps Multidrug Resistance Protein 1 (MDR1), Multidrug Resistance-Associated Protein 1 (MRP1), and Breast Cancer Resistance Protein (BCRP) were measured using the MDQ assay (SOLVO Biotechnology, Budapest, Hungary) according to manufacturer's instructions in all cell lines. Ligand incorporation was analyzed using FACS

Table 5.1. Description of chondrosarcoma cell lines and primary cultures

Cell Line	Bone of origin	Grade	Gender	Age	Passage	Expression cartilage markers (Real-Time PCR)	P53	MDR pump activity	Reference
SW1353	Humerus	II	F	72	21	Col 1, 2B, 3,10,aggr, sox9[a]	V203L	MDR1	ATCC
OUMS27	Humerus	III	M	65	27	Col 1,2B,3,10,aggr [a]	12434-35 del CC	MDR1/ BCRP	(44)
CH2879	Chest wall	III	F	35	>80	Col 1, 2A [a]	wildtype	MRP1/ MDR1/ BCRP	(45)
JJ012	Femur	II	M	39	9	Aggr, sox9 [a]	G199V	MRP1/ MDR1/ BCRP	(46)
L835[b]	Humerus	III	M	55	15	Col 1, 2A, 3, 10, aggr [a]	wildtype	MDR1/ BCRP	
L869[b]	Tibia	II	M	52	27	Col 1,2B,3,10,aggr [a]	wildtype	MRP1/ MDR1/ BCRP	

analysis on a BD™ LSR II flow cytometer. Calcein incorporation was recorded at 488nm, and mitoxantrone at 633nm. Dead cells were labeled with Propidium Iodide (Sigma Aldrich, Zwijndrecht, The Netherlands) (20) and gating was set at 10.000 live cells. Means of Geometric counts were calculated from all events. Experiments were performed in triplicate on one day using the same instrument settings.

BCL-2 and MCL1 expression analysis

A standard quantitative reverse transcriptase PCR (qRT-PCR) with SYBR green (16) was performed for MCL1 and BCL-2. Primers were designed using primer3 software (http://frodo.wi.mit.edu/primer3/) (Table 5.2) and ordered from ISOGEN Bioscience BV (Maarssen, The Netherlands). Relative gene expression levels were normalized for the amount of cDNA input using the genes *CYPa, CPSF, and GPR108, based on their constant expression in chondrosarcoma (21). For immunoblotting, 20µg of each sample was run on SDS-PAGE and proteins were transferred onto polyvinylidene difluoride membranes (Immobilon-P, Millipore, UK) using electrophoresis. Membranes were preincubated with skinned milk in phophate buffered saline-Tween 0.05%. Rabbit monoclonal antibodies against BCLXL (54H6), BCL-2 (50E3), and MCL1 (4572) were obtained from Cell Signaling Technology (Leiden, the Netherlands). Mouse monoclonal antibody against alpha-tubulin (DM1A) was obtained from Sigma-Aldrich (Zwijndrecht, the Netherlands).*

Table 5.2: Primers used in qRT-PCR

Primer		**Sequence**
MCL1	forward	5’ GGT GGC ATC AGG AAT GT 3’
	reverse	5’ ATC AAT GGG GAG CAC T 3’
BCL-2	forward	5’ ACA TCG CCC TGT GGA TGA CT 3’
	reverse	5’ GGG CCG TAC AGT TCC ACA AA 3’

Apoptosis assay

20.000 cells were grown in black 96-well microclear plates (Greiner®, Sigma-Aldrich, Zwijndrecht, The Netherlands) to perform a live cell apoptosis assay based on the binding of AnnexinV-Alexa633 conjugate (prepared as in (22)) to phosphatidyl-serine on the outer membrane of apoptotic cells. Increase of fluorescent apoptotic cells after drug exposure was followed by time-lapse imaging with 30 minute intervals using the BD Pathway® 855 (Becton Dickinson, Breda, The Netherlands) for 24 hours. Time series were quantified using in house developed macros for Image-Pro Plus (Media Cybernetics, Bethesda, USA). Apoptotic cells were expressed as the total pixel area of fluorescent objects in each frame. Drugs were added 0, 0 and 24, or 0, 24 and 48 hours before imaging; last 24 hours of treatment of each culture was measured using AnnexinV labeling

immediately prior to imaging. To establish apoptosis specificity of the assay, all caspase activity was blocked using the pan-caspase inhibitor, z-VAD-fmk (Bachem-Holding AG, Weil am Rhein, Germany) at 50µM, 30 minutes before and continued during treatment and imaging. All experiments were performed in triplicate and at least three times. Error bars show standard deviation from one representative experiment.

Immunofluorescence
Cells were fixed in 4% buffered formaldehyde (Added Pharma, Oss, The Netherlands). Washing steps were performed with 1x PBS and blocking with 0.5% BSA + 0.1% Triton X100 in 1x PBS (TBP) at room temperature. Immunofluorescent staining was performed for cytochrome C (556432, BD PharMingen, CA, USA) and cleaved caspase 3 (9664, Cell Signaling, Leiden, The Netherlands) overnight after which washing steps were performed with TBP. Cells were post-fixed in 4% formaldehyde for 5 minutes. Imaging was performed at a Nikon TiE2000 confocal laser scanning microscope (Nikon, Amstelveen, The Netherlands) at 20x magnification.

Results

Chondrosarcoma cultures are sensitive to doxorubicin while resistant to cisplatin
For doxorubicin an IC_{50} of 6µM was observed in the most responsive cell line (OUMS27) and an IC_{50} of >100µM in the least responsive cell line (SW1353) (figure 5.1A, table 5.3). Cell cultures showed a poor response to cisplatin treatment; total resistance even at 80µM was observed for L869 and SW1353 (figure 5.1B, table 5.3). Live cell imaging with AnnexinV labeling, performed with 10µM doxorubicin and 50µM cisplatin, showed a significant induction of apoptosis ($p<0.05$ one-way ANOVA) for cell lines responsive to doxorubicin, such as OUMS27, but not after cisplatin treatment (figure 5.1C). For non responsive cultures, such as L835, no significant induction of apoptosis could be achieved after either treatment (figure 5.1D). All apoptosis could be inhibited using a general caspase inhibitor zVAD-fmk ($p<0.05$ one-way ANOVA) (figure 5.1C, D). p53 analysis showed three cultures to be negative for p53 mutations with no correlation of mutation status with drug response (table 5.1).

3D pellets show chondrosarcoma morphology and doxorubicin incorporation
3D pellet cultures were created from OUMS27, CH2879, and L835 and 1 MSC culture. Cell pellets had a maximal diameter of about 1mm. 3D pellets made from the MSC culture showed ample matrix surrounding the cells, resembling the cellular make-up of a low grade chondrosarcoma (figure 5.2A, Ai). 3D cell pellets from high grade chondrosarcoma cell lines (grade II, III) morphologically resembled high grade chondrosarcoma (figure 5.2B, Bi) showing high cellularity.

Doxorubicin incorporation showed nuclear accumulation at both 1µM and 10µM, even in L835 which shows resistance to doxorubicin at 10µM (figure 5.2D-Dii), and in MSC cell pellets with ample matrix formation (results not shown). Ki-67 staining showed decreased proliferation in all pellets after treatment although this was not significant (figure 5.2Ci, E-Eii). Cleaved caspase 3 staining on pellets showed 10% of cells had undergone apoptosis in non-treated pellets, whereas pellets treated with doxorubicin showed caspase activation in almost all cells ($p<0.05$, one-way ANOVA, figure 5.2C, F-Fii). Activation of caspase in cell pellets as opposed to the resistance we showed in figure 5.1 in the 2D cultures is due to differences in exposure to doxorubicin: 3D pellets were treated 4x and 2D cultures only once.

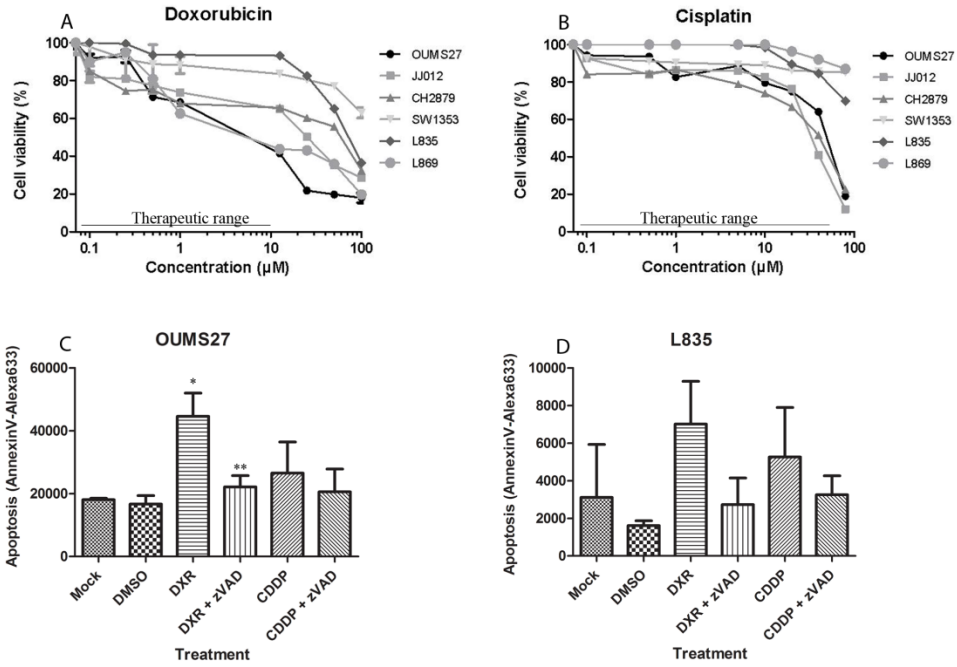

Figure 5.1. Cell viability of chondrosarcoma cells is inhibited and apoptosis induced by high dose doxorubicin but not cisplatin. Dose response curves for chondrosarcoma cell lines show sensitivity to doxorubicin at high concentrations (A) and resistance to cisplatin (B) after 72 hours incubation. OUMS27 cells show a significant increase of apoptosis (AnnexinV) after addition of doxorubicin 1µM (DXR), but not after addition of cisplatin 5µM (CDDP) (C). Addition of zVAD-fmk (zVAD) before doxorubicin allowed for significant inhibition of apoptosis (fluorescence intensity shown by AnnexinV binding, measured over 24hrs). L835 shows no significant induction of apoptosis after either treatment (D). Error bars in graphs show standard deviations from 3 measurements.
*significant increase of apoptosis compared to mock (medium only treatment) and DMSO treatment (one-way ANOVA, $p<0.05$) ** significant decrease of apoptosis compared to treatment without zVAD (one-way ANOVA, $p<0.05$)

Table 5.3. IC50 concentrations and Combination Indices per cell line

	DXR (µM)[a]	CDDP (µM) [a]	ABT-737 (µM) [a]	Combination DXR (µM) [b]	Combination ABT-737 (µM) [b]	Combination index (CI) [d e]	Combination CDDP (µM) [c]	Combination ABT-737 (µM) [c]	Combination index (CI) [d f]
OUMS27	6	50	25	0,1	5	0,22	0,1	5	0,20
CH2879	60	40	20	0,1	0,25	0,01	1	0,1	0,03
JJ012	25	35	100 [g]	0,1	0,5	0,01	0,1	5	0,05
SW1353	150[g]	400 [g]	135 [g]	1	1	0,01	0,5	5	0,04
L835	70	200 [g]	60 [g]	0,25	0,5	0,01	5	5	0,11

[a] Concentrations needed to achieve 50% reduction in cell viability
[b] Concentrations needed to achieve 50% reduction in cell viability during combination assay with Doxorubicin and ABT-737
[c] Concentrations needed to achieve 50% reduction in cell viability during combination assay with Cisplatin and ABT-737
[d] Combination index as calculated according to the Chou & Talalay method for synergistic relationships. A combination index <1 indicates synergy between drugs.
[e] Combination index for the combination Doxorubicin and ABT-737
[f] Combination index for the combination Cisplatin and ABT-737
[g] Values are approximations as IC50 values were not achieved in experiments

Figure 5.2. 3D pellet models show similar cellular organization as chondrosarcoma tissues and doxorubicin incorporation. Low grade chondrosarcoma (A) strongly resembles 3D pellet created from MSC cell culture (L2069) (A'). B: high grade chondrosarcoma strongly resembles 3D pellet created from L835, a grade III chondrosarcoma cell culture (B'). D-D": Fluorescence microscopy of L835 pellet at 120x: dapi staining (D) shows nuclear organization, doxorubicin incorporation is strong at 10µM (D'), overlay (D") shows doxorubicin has successfully entered the nuclei. Pooled data of pellets (L2069, OUMS27, CH2879, and L835) with error bars indicating lowest and highest counts, shows that cleaved caspase 3 staining is present in 100% of cells after 10µM doxorubicin (C) and Ki67 staining in about 5% of cells (C'). Staining for Ki67 (E-E") and cleaved caspase 3 (F-F") in L835 pellets treated with 0, 1, and 10 µM doxorubicin show decrease in number of cells proliferating and an increase in apoptosis. After treatment with 10µM, cellularity decreases, pictures were obtained at 40x magnification

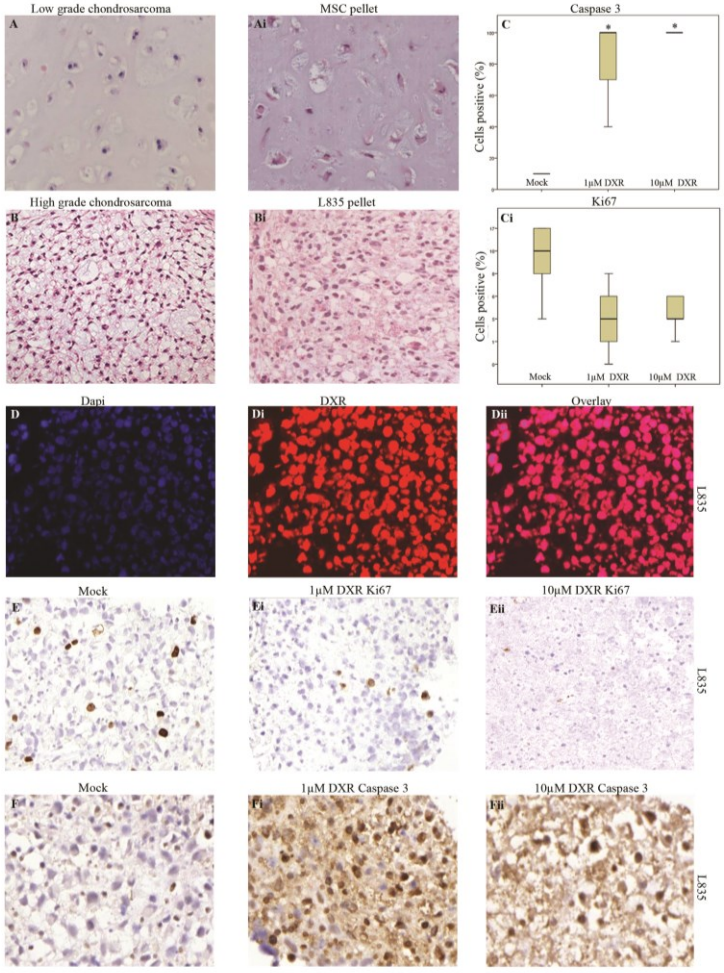

* Significant difference between treated and untreated (one-way ANOVA $p < 0.05$)

MDR pump activity is found in chondrosarcoma cultures

We determined MDR pump activity in chondrosarcoma cell lines and primary cultures, and in a chondrocyte cell line LBPVA (14). Pump activity was compared to HL-60, described to have high MDR1 activity, and to osteosarcoma cell line MNNG which has been described to express MDR1 and MRP1, with higher MDR1 activity (23). This was confirmed using our MDQ assay. Considerable heterogeneity was observed in the activity of MDR pumps throughout the cell lines, with MDR1 (p-glycoprotein) demonstrating activity in all cell lines except OUMS27 and LBPVA. MRP1 activity was observed in LBPVA, 2 cell lines (JJ012, CH2879) and primary cultures. L869, JJ012, and CH2879 showed activity of all three pumps, with highest activity observed in L869 (figure 5.3, table 5.1).

Inhibition of BCL-2 family members but not MCL-1 reduces cell viability and increases apoptosis

RT-PCR confirmed mRNA expression of BCL-2 and BCL-X_L, with expression levels similar to that of HL-60 (figure 5.4A) in which these expression levels have been linked to chemoresistance (24). Western blot analysis showed high expression of BCL-X_L in all cell lines (figure 5.4B) while BCL-2 expression was less uniform. Using ABT-737, HL-60 showed complete loss in cell viability at 0.5μM, as reported (25). In chondrosarcoma cell lines, CH2879 and OUMS27 showed the best response, with IC_{50}s of 20μM and 25μM, respectively. Cell counting showed cell proliferation at 10μM to correspond with cell viability (figure 5.5). L835 showed intermediate response to ABT-737 (IC_{50} 60μM), for other cell lines, the IC_{50} values exceeded 100μM (figure 5.4C, table 5.3). Live cell imaging during 24 hours of ABT-737 (25μM) treatment showed a significant increase of apoptotic cells compared to DMSO treatment, all of which could be inhibited using the caspase inhibitor zVAD-fmk (figure 5.4E,F). It has been described that in tumors resistant to BCL-2 inhibition, MCL1 upregulation might play a role (26). Indeed RT-PCR demonstrated 2-fold increases of MCL1 mRNA expression in chondrosarcoma cell lines compared to household genes (fig 5.4A). Also, MCL1 expression was confirmed at the protein level using western blot (fig 5.4B) although lower than BCL-2 or BCL-X_L. We used R-roscovitine, a non-specific CDK inhibitor described to downregulate MCL-1 (27) to assess the role of MCL-1 in the response to ABT-737. High concentrations of R-roscovitine (5μM and 10μM) failed to induce reduction in cell viability (figure 5.4D) or apoptosis on its own or in combination with ABT-737 (results not shown).

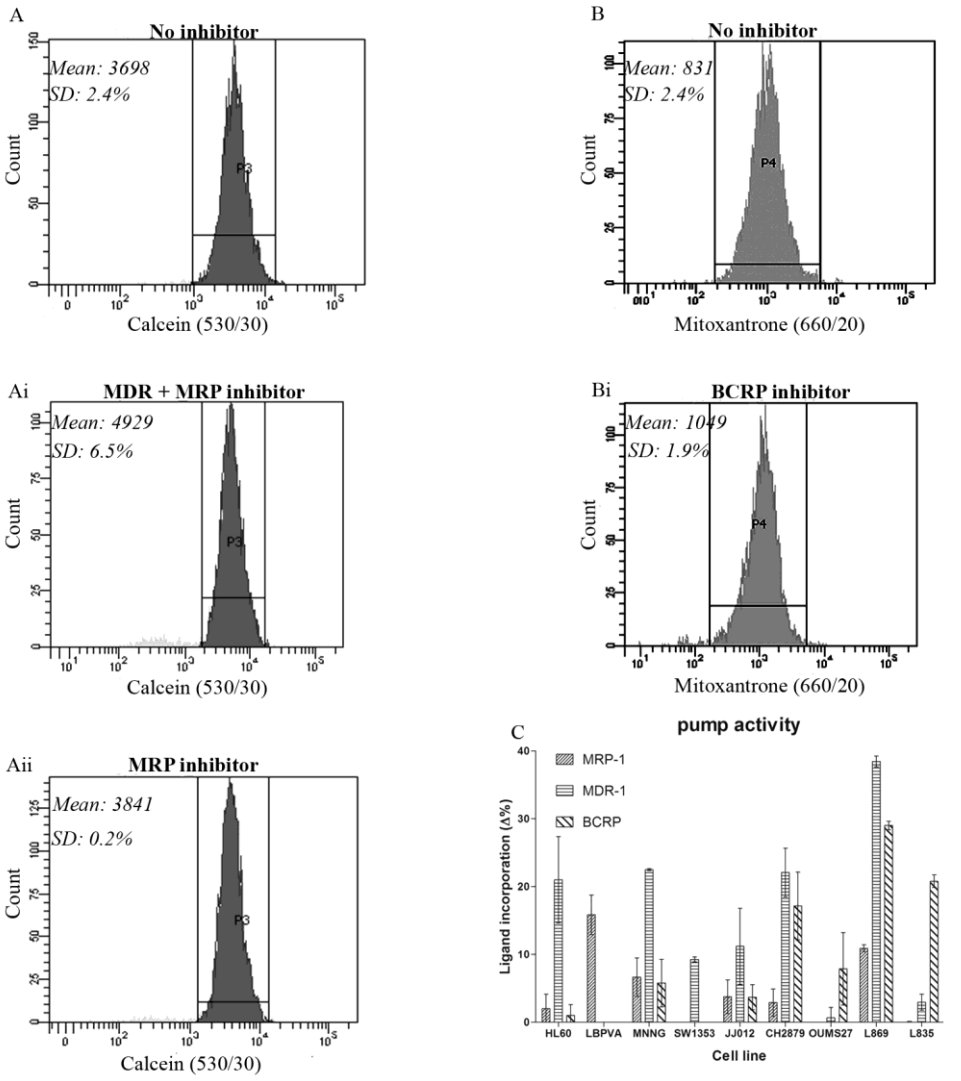

Figure 5.3. Activity of Multi-Drug-Resistance pumps in chondrosarcoma cultures.
Ligand incorporation with and without the presence of pump inhibitors was measured using FACS analysis. A, B:FACS analysis of L835; insets show mean GEO counts with the standard deviation. C: graphical representation of pump activity per cell line. Ligand incorporation (Δ%) represents the difference of total GEO counts with inhibitor to total GEO counts without inhibitor. Activity was compared to HL-60 cell line and to an osteosarcoma cell line (MNNG). MRP1 activity was higher than in HL-60 in the chondrocytic cell line and in L869, but equal in JJ012 and CH2879. Activity of the MDR1 pump (p-glycoprotein) was observed in nearly all cultures. BCRP activity varied highly among cultures.

BCL-2 inhibition can reverse chemoresistance of chondrosarcoma

Simultaneous addition of ABT-737 and doxorubicin or cisplatin to cell cultures did not show additive effects. Combination treatments proved most effective with respect to cell viability when at least 24 hours were left in between drug administration, with ABT-737 treatment before and after doxorubicin or cisplatin addition (results not shown). The combination of doxorubicin or cisplatin with ABT-737 allowed for the reduction of both treatments to sublethal concentrations (table 5.3). Combination Index (CI) calculations for synergy analysis revealed high synergy between ABT-737 and both doxorubicin and cisplatin; a mean CI of 0.05 for the combination with doxorubicin and a mean CI of 0.09 for the combination with Cisplatin (table 5.3). The combination of doxorubicin with ABT-737 was most effective also with respect to apoptosis (figure 5.6). Live cell imaging to evaluate apoptosis was performed using 5μM ABT-737 and 1μM doxorubicin or 5μM cisplatin. For most cell lines a clear advantage was observed when ABT-737 treatment was performed 24 hours before doxorubicin or cisplatin treatment; with doxorubicin being the most effective combination (figure 5.6A, C; OUMS27 and CH2879 shown as representatives for these four cell lines). For L835, ABT-737 treatment showed the largest increase in apoptosis when administered after doxorubicin or cisplatin (figure 5.6B). Immunofluorescence for cytochrome C combined with Hoechst staining 24hrs after addition of each drug showed increase in cytochrome C release after addition of each drug; after the third cycle of drug addition almost all cells had undergone apoptosis and few nuclei could be identified (figure 5.6D).

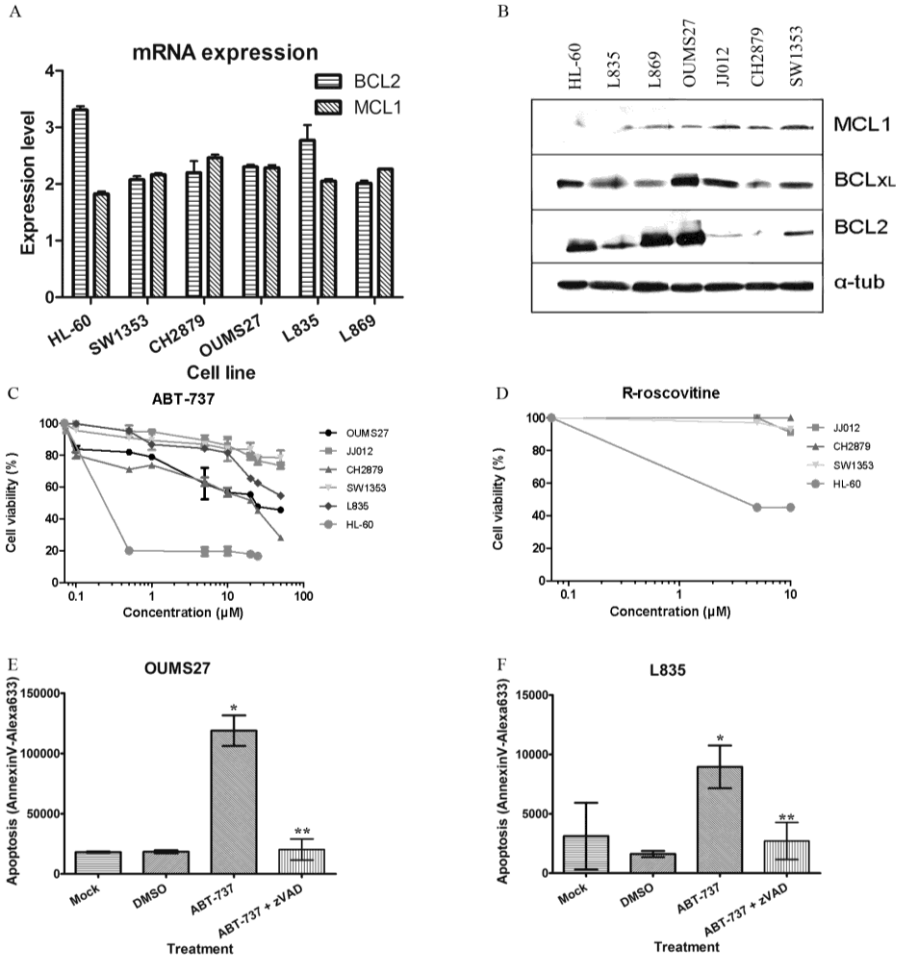

Figure 5.4. BCL-2 but not MCL1 overexpression protects chondrosarcoma cell lines from apoptosis. A: normalized mRNA expression levels of BCL-2 and MCL1 in chondrosarcoma cell lines showing constant expression in chondrosarcoma. B: Western Blot analysis of MCL1, BCL-XL, and BCL-2 expression in chondrosarcoma cell lines. BCL-2 and BCL-XL are present in all cell lines, and markedly higher than MCL1. C,D: Cell lines were treated with ABT-737 (C) or R-roscovitine (D) for 72 hrs. Dose response curves show sensitivity to ABT-737 at high concentrations and resistance to R-roscovitine for mitochondrial activity. E,F: OUMS27 and L835 cells show apoptosis (fluorescence intensity shown by AnnexinV binding) after 72hrs of 25μM ABT-737 treatment. Addition of zVAD before ABT-737 allowed for significant inhibition of apoptosis (AnnexinV binding). Error bars in graphs show standard deviations from 3 measurements.
*significant increase of apoptosis compared to mock (medium only treatment) and DMSO treatment (one-way ANOVA, $p<0.05$) ** significant decrease of apoptosis compared to treatment without zVAD (one-way ANOVA, $p<0.05$)

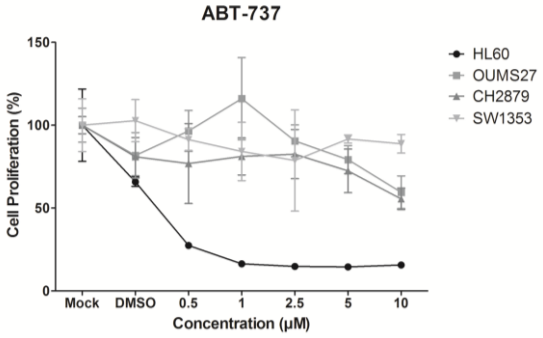

Figure 5.5 ABT-737 successfully inhibits cell proliferation of chondrosarcoma cells. Chondrosarcoma and HL-60 cells were treated with medium (mock), DMSO, or ABT-737 for 72hrs. Cell count for mock treatment was put at 100% proliferation. HL-60 cells showed some sensitivity to DMSO treatment. For all cell lines, sensitivities reduction in cell proliferation (cell number) were comparable to those observed in cell viability.

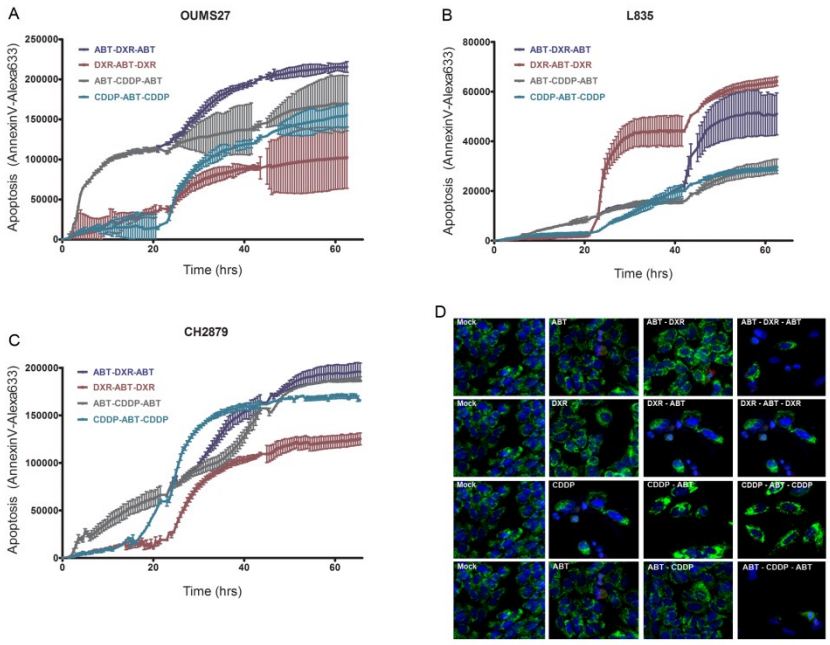

Figure 5.6. Combination therapy of ABT-737 with doxorubicin and cisplatin induces apoptosis in chondrosarcoma cells. Cells were treated with respective drugs for 24hrs time periods, apoptosis was monitored with AnnexinV staining. Y axes show total pixel area of AnnexinV positive cells. Combination therapy of ABT-737 with doxorubicin was most effective in inducing apoptosis in all cell lines. OUMS27 and CH2879 (A,C) were most responsive to treatment with ABT-737 before and after doxorubicin (DXR) treatment, whereas L835 (B) seemed slightly more sensitive to doxorubicin treatment before and after ABT-737. Error bars show standard deviation from 3 measurements. D: Increase in cytochrome C release (green) is observed during treatment, with loss of cells at the end of treatment (Hoechst, blue), caspase 3 release (red) could be observed after ABT-737 addition (20x magnification).

Discussion

Chondrosarcomas are resistant to conventional chemotherapy and radiotherapy. In the ongoing pursuit to find new, targeted, treatment strategies we set out to define the reasons for chemoresistance. Postulated hypotheses regarding the mechanisms underlying chemoresistance include the high abundance of cartilaginous matrix, the expression of MDR pumps, and the expression of anti-apoptotic proteins (5).

We first assessed the sensitivity of our cell lines and primary cultures to single treatments of doxorubicin and cisplatin, the most commonly used chemotherapeutic agents in sarcomas, using 2D cell culture. All cultures responded poorly, especially to cisplatin. As 2D cultures lack matrix formation, we used 3D pellet cultures, shown to be good models for cartilage formation (28;29), to study the effect of the chondroid matrix on diffusion of therapeutic agents *in vitro*. We here demonstrate 3D pellets of MSC and chondrosarcoma cell lines to strongly resemble low grade and high grade chondrosarcoma, respectively. Previously, doxorubicin was reported to remain in chondrosarcoma cells during washout experiments in 2D cell cultures (30;30;31). Using 3D pellets we now show that the chondroid matrix does not hinder doxorubicin from entering the nuclei of the cells.

Numerous reports on the role of MDR pumps in chemoresistance exist. MRP1 (encoded by ABCC1) expression has been described to play a role in resistance to cisplatin (32). P-glycoprotein (ABCB1) activity (33) and BCRP (ABCG2) activity are described to play a role in doxorubicin efflux (34). P-glycoprotein expression has previously been found on the surface of the chondrosarcoma cell lines JJ012 and SW1353 (30;31;35) and endogenous P-glycoprotein expression has been described in human growth plate, suggesting a physiological role (10). Recently, ABT-737 has been shown to be a substrate for P-glycoprotein (36). We show strong variation in the activity of MDR pumps over a wide panel of cell cultures and pump activity could not be correlated with the *in vitro* response to doxorubicin, cisplatin or ABT-737.

Thus, we demonstrate that despite high matrix production (MSCs) and P-glycoprotein activity (CH2879, L835), doxorubicin is able to enter the nuclei of the cells. This suggests a different, more specific mechanism possibly including a defective apoptotic pathway. It has been described that mutations in p53 can influence the response to DNA damaging agents such as doxorubicin (37). However, we found no correlation between p53 status and response.

We previously demonstrated BCL-2 expression in 63-71% of high grade conventional chondrosarcoma (6;8). We investigated the role of anti-apoptotic BCL-2 family members using the BH3 mimetic ABT-737. ABT-737 is a small-molecule inhibitor of the BCL-2 family and has been reported to be effective in, among others, myeloma and ovarian cancer cell lines (38-40). The apoptotic machinery in chondrosarcoma cultures was activated through inhibition of BCL-2 family members with ABT-737 and cells were sensitized to doxorubicin and cisplatin. Using the BH3 mimetic ABT-737 proved more effective than the

previously reported use of small interfering RNA (siRNA) against BCL-2 which was unable to induce apoptosis on its own (30), supporting a role for other BCL-2 family members. Moreover, recently, a small IAP (inhibitor of apoptosis) member, survivin was shown to be highly expressed in chondrosarcoma, indicating that also other factors contribute to a defective apoptotic machinery in chondrosarcoma (41). We show high synergy between ABT-737 and doxorubicin or cisplatin with combination indices for both combinations far below 1. Synergistic effects were observed only when combination treatments were administered with a 24 hour time gap and not when administered simultaneously, this is in concordance with the findings published on ABT-263 which accelerates apoptosis during drug-induced mitotic arrest (42). These data support that aberrant expression of BCL-2 family members, but not MCL-1, in chondrosarcoma debilitates the apoptotic pathway as it should be activated in response to conventional chemotherapy, and that combination strategies are successful in overcoming this resistance mechanism.

In conclusion, using a 3D pellet model we have shown that doxorubicin is able to diffuse across at least 1mm chondroid matrix surrounding chondrosarcoma cells and that it is able to enter and accumulate in the nuclei despite MDR pump activity. We showed *in vitro* that complete apoptosis can be achieved in chondrosarcoma cells at low concentrations of doxorubicin and cisplatin if combined with ABT-737, pointing towards an important role for BCL-2 and BCL-X_L in chemoresistance. The orally available homologue of ABT-737; ABT-263, is used in clinical trials with low side effects (43). Our results strongly support the combination treatment of chondrosarcoma patients with ABT-263, with our data supporting a stronger synergistic effect in combination with doxorubicin.

Reference List

(1) Bertoni F, Bacchini P, Hogendoorn PCW. Chondrosarcoma. In: Fletcher CDM, Unni KK, Mertens F, editors. World Health Organisation classification of tumours. Pathology and genetics of tumours of soft tissue and bone.Lyon: IARC Press; 2002. p. 247-51.

(2) Fiorenza F, Abudu A, Grimer RJ, et al. Risk factors for survival and local control in chondrosarcoma of bone. J Bone Joint Surg [Br] 2002;84(1):93-9.

(3) Gelderblom H, Hogendoorn PCW, Dijkstra SD, et al. The clinical approach towards chondrosarcoma. Oncologist 2008;13(3):320-9.

(4) Bovee JVMG, Cleton-Jansen AM, Taminiau AHM, et al. Emerging pathways in the development of chondrosarcoma of bone and implications for targeted treatment. Lancet Oncology 2005;6(8):599-607.

(5) Bovee JVMG, Hogendoorn PCW, Wunder JS, et al. Cartilage tumours and bone development: molecular pathology and possible therapeutic targets. Nat Rev Cancer 2010;10(7):481-8.

(6) Bovee JVMG, Van den Broek LJCM, Cleton-Jansen AM, et al. Up-regulation of PTHrP and Bcl-2 expression characterizes the progression of osteochondroma towards peripheral chondrosarcoma and is a late event in central chondrosarcoma. Lab Invest 2000;80:1925-33.

(7) Healey JH, Lane JM. Chondrosarcoma. Clinical Orthopaedics and Related Research 1986;(204):119-29.

(8) Rozeman LB, Hameetman L, Cleton-Jansen AM, et al. Absence of IHH and retention of PTHrP signalling in enchondromas and central chondrosarcomas. J Pathol 2005;205(4):476-82.

(9) Rozeman LB, Hogendoorn PCW, Bovée JVMG. Diagnosis and prognosis of chondrosarcoma of bone. Expert Rev Mol Diagn 2002 September;2(5):461-72.

(10) Wyman JJ, Hornstein AM, Meitner PA, et al. Multidrug resistance-1 and p-glycoprotein in human chondrosarcoma cell lines: expression correlates with decreased intracellular doxorubicin and in vitro chemoresistance. J Orthop Res 1999;17(6):935-40.

(11) Terek RM, Schwartz GK, Devaney K, et al. Chemotherapy and P-glycoprotein expression in chondrosarcoma. J Orthop Res 1998;16(5):585-90.

(12) Reed JC. Dysregulation of Apoptosis in Cancer. Journal of Clinical Oncology 1999;17(9):2941-53.

(13) Shrivastav S, Bonar RA, Stone KR, et al. An Invitro Assay Procedure to Test Chemotherapeutic Drugs on Cells from Human Solid Tumors. Cancer Res 1980;40(12):4438-42.

(14) Grigolo B, Roseti L, Neri S, et al. Human articular chondrocytes immortalized by HPV-16 E6 and E7 genes: Maintenance of differentiated phenotype under defined culture conditions. Osteoarthritis and Cartilage 2002;10(11):879-89.

(15) Reijnders CM, Waaijer CJ, Hamilton A, et al. No haploinsufficiency but loss of heterozygosity for EXT in multiple osteochondromas. Am J Pathol 2010;177(4):1946-57.

(16) Cleton-Jansen AM, van Beerendonk HM, Baelde HJ, et al. Estrogen signaling is active in cartilaginous tumors: implications for antiestrogen therapy as treatment option of metastasized or irresectable chondrosarcoma. Clin Cancer Res 2005 15;11(22):8028-35.

(17) Ottaviano L, Schaefer KL, Gajewski M, et al. Molecular characterization of commonly used cell lines for bone tumor research: a trans-European EuroBoNet

effort. Genes Chromosomes Cancer 2010;49(1):40-51.
(18) Chou TC, Talalay P. Quantitative-Analysis of Dose-Effect Relationships - the Combined Effects of Multiple-Drugs Or Enzyme-Inhibitors. Advances in Enzyme Regulation 1984;22:27-55.
(19) Bovée JVMG, Van den Broek LJCM, De Boer WI, et al. Expression of growth factors and their receptors in adamantinoma of long bones and the implications for its histogenesis. J Pathol 1998;184:24-30.
(20) Sasaki DT, Dumas SE, Engleman EG. Discrimination of viable and non-viable cells using propidium iodide in two color immunofluorescence. Cytometry 1987 July;8(4):413-20.
(21) Hameetman L, Rozeman LB, Lombaerts M, et al. Peripheral chondrosarcoma progression is accompanied by decreased Indian Hedgehog (IHH) signalling. J Pathol 2006;209(4):501-11.
(22) Puigvert JC, de Bont H, van de Water B, et al. High-throughput live cell imaging of apoptosis. Curr Protoc Cell Biol 2010;Chapter 18:Unit-13.
(23) Gomes CM, van Paassen H, Romeo S, et al. Multidrug resistance mediated by ABC transporters in osteosarcoma cell lines: mRNA analysis and functional radiotracer studies. Nucl Med Biol 2006;33(7):831-40.
(24) High LM, Szymanska B, Wilczynska-Kalak U, et al. The Bcl-2 homology domain 3 mimetic ABT-737 targets the apoptotic machinery in acute lymphoblastic leukemia resulting in synergistic in vitro and in vivo interactions with established drugs. Mol Pharmacol 2010;77(3):483-94.
(25) Dai Y, Grant S. Targeting multiple arms of the apoptotic regulatory machinery. Cancer Res 2007;67(7):2908-11.
(26) Chen S, Dai Y, Harada H, et al. Mcl-1 down-regulation potentiates ABT-737 lethality by cooperatively inducing Bak activation and Bax translocation. Cancer Res 2007;67(2):782-91.
(27) de Azevedo WF, Leclerc S, Meijer L, et al. Inhibition of cyclin-dependent kinases by purine analogues: crystal structure of human cdk2 complexed with roscovitine. Eur J Biochem 1997;243(1-2):518-26.
(28) Boeuf S, Kunz P, Hennig T, et al. A chondrogenic gene expression signature in mesenchymal stem cells is a classifier of conventional central chondrosarcoma. J Pathol 2008;216(2):158-66.
(29) Stewart MC, Saunders KM, Burton-Wurster N, et al. Phenotypic Stability of Articular Chondrocytes In Vitro: The Effects of Cell Culture Methods, Bone Morphogenetic Protein 2, and Serum Supplementation. Journal of Bone and Mineral Research 2000;15(1):166-74.
(30) Kim DW, Kim KO, Shin MJ, et al. siRNA-based targeting of antiapoptotic genes can reverse chemoresistance in P-glycoprotein expressing chondrosarcoma cells. Mol Cancer 2009;8:28.
(31) Kim R, Emi M, Tanabe K, et al. Therapeutic potential of antisense Bcl-2 as a chemosensitizer for cancer therapy. Cancer 2004;101(11):2491-502.
(32) Hour TC, Chen J, Huang CY, et al. Characterization of chemoresistance mechanisms in a series of cisplatin-resistant transitional carcinoma cell lines. Anticancer Res 2000;20(5A):3221-5.
(33) Shen F, Chu S, Bence AK, et al. Quantitation of doxorubicin uptake, efflux, and modulation of multidrug resistance (MDR) in MDR human cancer cells. J Pharmacol Exp Ther 2008;324(1):95-102.
(34) Doyle LA, Yang W, Abruzzo LV, et al. A multidrug resistance transporter from human MCF-7 breast cancer cells.

Proc Natl Acad Sci U S A 1998;95(26):15665-70.
(35) Kim DW, Seo SW, Cho SK, et al. Targeting of cell survival genes using small interfering RNAs (siRNAs) enhances radiosensitivity of Grade II chondrosarcoma cells. J Orthop Res 2007;25(6):820-8.
(36) Vogler M, Dickens D, Dyer MJ, et al. The B-cell lymphoma 2 (BCL2)-inhibitors, ABT-737 and ABT-263, are substrates for P-glycoprotein. Biochem Biophys Res Commun 2011;408(2):344-9.
(37) Brown JM, Wilson G. Apoptosis genes and resistance to cancer therapy: what does the experimental and clinical data tell us? Cancer Biol Ther 2003;2(5):477-90.
(38) Oltersdorf T, Elmore SW, Shoemaker AR, et al. An inhibitor of Bcl-2 family proteins induces regression of solid tumours. Nature 2005 2;435(7042):677-81.
(39) Shoemaker AR, Oleksijew A, Bauch J, et al. A small-molecule inhibitor of Bcl-XL potentiates the activity of cytotoxic drugs in vitro and in vivo. Cancer Res 2006 1;66(17):8731-9.
(40) Trudel S, Stewart AK, Li Z, et al. The Bcl-2 family protein inhibitor, ABT-737, has substantial antimyeloma activity and shows synergistic effect with dexamethasone and melphalan. Clin Cancer Res 2007;13(2 Pt 1):621-9.
(41) Lechler P, Renkawitz T, Campean V, et al. The antiapoptotic gene survivin is highly expressed in human chondrosarcoma and promotes drug resistance in chondrosarcoma cells in vitro. BMC Cancer 2011;11:120.
(42) Shi J, Zhou Y, Huang H, et al. Navitoclax (ABT-263) accelerates apoptosis during drug-induced mitotic arrest by antagonizing Bcl-cL. Cancer Research 2011.
(43) Richardson A, Kaye SB. Pharmacological inhibition of the Bcl-2 family of apoptosis regulators as cancer therapy. Curr Mol Pharmacol 2008;1(3):244-54.

Chapter 6

Screening for potential targets for therapy in mesenchymal, clear-cell and dedifferentiated chondrosarcoma reveals Bcl-2 family members and TGFbeta as potential targets

.

.

This chapter is based on the manuscript: van Oosterwijk JG, Meijer D, van Ruler MAJH, van den Akker BEWM, Oosting J, Krenács T, Picci P, Flanagan AM, Liegl-Atzwanger B, Leithner A, Athanasou N, Daugaard S, Hogendoorn PCW, Bovée JVMG. *Am J Path. 2013; 182(4): 1347-56*

Abstract

Mesenchymal - , clear cell - , and dedifferentiated chondrosarcoma are extremely rare and together constitute 10-15% of all chondrosarcomas. Their poor prognosis and lack of efficacious treatment emphasizes the need to elucidate the pathways playing a pivotal role in these tumors.
We constructed tissue microarrays containing 42 dedifferentiated - , 23 clear cell - , and 23 mesenchymal chondrosarcomas and performed immunohistochemistry to study the expression of growth plate-signaling molecules, and molecules shown to be involved in conventional chondrosarcoma. We observed high expression of SOX9 and FGFR3, as well as aberrant cellular localization of heparan sulfate proteoglycans, in all subtypes. We found TGFbeta signaling through pSMAD2 and PAI1 to be highly active in all chondrosarcoma subtypes suggesting TGFbeta inhibitors to be a possible therapeutic strategy in rare chondrosarcoma subtypes. Like in conventional chondrosarcoma, antiapoptotic proteins (Bcl-2, and / or Bcl-xl) were highly expressed in all subtypes. Inhibition with the BH-3 mimetic ABT-737 rendered dedifferentiated chondrosarcoma cell lines sensitive to doxorubicin or cisplatin. We here show that antiapoptotic proteins may play an important role in chemoresistance, suggesting a promising role for targeting Bcl-2 family members in chondrosarcoma treatment irrespective of subtype.

Introduction

Chondrosarcoma of bone is a malignant tumor characterized by the formation of cartilage. It mainly affects adults in the third to sixth decades of life. In addition to conventional chondrosarcoma, several rare subtypes are recognized with distinct histological and clinical features. These subtypes include clear cell chondrosarcoma, mesenchymal chondrosarcoma, and dedifferentiated chondrosarcoma. Together they constitute 10-15% of all chondrosarcomas. Previously, it was suggested that the distinct chondrosarcoma subtypes show striking histological similarities with cartilaginous cells of the growth plate in various states of differentiation (1). This model is supported by results from expression analysis of extracellular matrix genes (2).

Clear cell chondrosarcoma (2%) is a low-grade malignant tumor, which rarely metastasizes, but commonly recurs after curettage. About 15% of the patients die as a result of the disease. The disease is characterized by tumor cells with clear, empty cytoplasm, resembling the hypertrophic cells of the growth plate (1). In addition, expression of collagen type X and osteonectin further supports the resemblance to chondrocytes in the hypertrophic state (3).

Mesenchymal chondrosarcoma (2% of all CS) is a highly malignant lesion which occurs in bone as well as in soft tissue of relatively young patients. The tumor consists of differentiated cartilage mixed with undifferentiated small round cells and usually follows an aggressive course with a high rate of distant metastases

and a 5-year overall survival of 55% (4). Histologically the undifferentiated cells resemble the resting cells of the growth plate (1) and Aigner et al confirmed the premesenchymal chondroprogenitor origin of these cells by studying cell differentiation and matrix gene expression (2;5).

Dedifferentiated chondrosarcoma (10%) is a tumor containing two clearly defined components: a high-grade non-cartilaginous anaplastic sarcoma juxtaposed to a usually low-grade well-differentiated cartilage tumor, with a sharply defined junction between the two components (6). It has a poor prognosis and no targets for therapy have been reported to date (7).

Nearly all chondrosarcomas arise in bones formed by endochondral ossification. Endochondral ossification occurs in the growth plate, in which four zones can be distinguished: the resting zone, the proliferating zone, the transition zone, and the hypertrophic zone (8). With the elucidation of the *EXT* genes being involved in the development of multiple as well as solitary osteochondromas (benign cartilaginous tumors at the surface of the bone), parallels between the normal growth plate and cartilage tumors became obvious since they shared a strong morphological resemblance (for review see: (9)). The exostosins are involved in heparan sulfate chain elongation on heparan sulfate proteoglycans (HSPGs). HSPGs include syndecan, perlecan and the splice variant of CD44 including variable exon 3 (CD44v3) and are crucial for facilitating signaling of FGF, Wnt, BMP, TGFbeta and indian hedgehog (IHH), all of which are important for chondrocyte proliferation and differentiation in the normal growth plate (reviewed in 10). The process of chondrocyte proliferation and differentiation is tightly regulated by a paracrine feedback loop involving both IHH/ parathyroid hormone like hormone (PTHLH) and fibroblast growth factor (FGF) signaling (11). Wnt signaling promotes chondrocyte differentiation in a SOX9 dependent manner (12). TGFbeta signaling can regulate PTHLH expression independently of IHH (13). Multiple studies have confirmed the importance of these pathways in conventional central and peripheral chondrosarcoma (14;15). In contrast, because of the rarity of clear cell, dedifferentiated and mesenchymal CS, little information is available on the role of these pathways in rare chondrosarcoma subtypes.

In this study, we therefore investigated the expression of the master transcription regulator for chondrogenic differentiation (SOX9), HS and HSPGs (10E4, syndecan 2, 3 and 4, CD44 variable exon 3 and NDST2), and proteins involved in PTHLH (PTHLH, PTHR1 and BCL-2), FGF (FGF18 and FGFR3), WNT (beta catenin), BMP (pSMAD1) and TGFbeta (pSMAD2 and PAI1) pathways as well as the expression of COX2 and KIT based on possible therapeutic consequences, in 42 dedifferentiated chondrosarcomas, 23 clear cell chondrosarcomas, and 23 mesenchymal chondrosarcomas. Based on the results we further investigated the role of Bcl-2 in chemoresistance of two dedifferentiated chondrosarcoma cell lines.

Materials and Methods

Tumor tissue

For this study, 42 dedifferentiated chondrosarcomas, 23 mesenchymal chondrosarcomas, and 23 clear cell chondrosarcomas were collected within the EuroBoNeT consortium, a European Commission granted Network of Excellence for studying the pathology and genetics of bone tumors. In total, formalin-fixed paraffin-embedded (FFPE) specimens from 88 patients were collected from the archives of the Department of Pathology, LUMC, The Netherlands (n=13), Nuffield Department of Orthopaedic Surgery, University of Oxford, UK (n= 6), The Royal National Orthopaedic Hospital, Middlesex, UK (n=22), Laboratory of Oncologic Research, ROI, Italy (n=30), Department of Pathology, RH, Denmark (n=10), and Department of Pathology, Medizinische Universität Graz, Austria (n=7). All specimens in this study were handled according to the ethical guidelines described in "Code for Proper Secondary Use of Human Tissue in The Netherlands" of the Dutch Federation of Medical Scientific Societies. Tumors were selected based on accepted clinicopathological and radiological criteria (16). All were primary tumors except for three clear cell chondrosarcomas and six mesenchymal chondrosarcomas, from which only material derived from the recurrent tumor was available. Histology was reviewed by two experienced bone tumor pathologists (JVMGB and PCWH). Clinicopathological data are shown in Table 6.1. Histological grading of the cartilaginous component of dedifferentiated CS was performed according to Evans (17).

Tissue microarray (TMA) construction

TMAs containing 2mm cores of all samples in triplicate were prepared using a TMA Master (3DHISTECH Ltd, Budapest, Hungary). From the dedifferentiated chondrosarcomas we included both the cartilaginous and the anaplastic components. From the mesenchymal chondrosarcomas we selected areas with the undifferentiated small cells as well as areas with cartilaginous differentiation. Normal non-decalcified liver, kidney, and tonsil samples were included on the TMAs for orientation purposes and as internal positive controls.

Immunohistochemistry (IHC)

Immunohistochemical reactions were performed according to standard laboratory methods (18) and visualized using DAB+ Substrate Chromogen System (Dako, Heverlee, Belgium). Details of the primary antibodies used for immunohistochemistry are described in Table 6.2. The negative controls were tissue sections incubated in PBS/BSA 1% without primary specific antibodies. All TMAs were scored by two observers independently (DM and JVMGB) both of whom were unaware of the clinicopathological data. Discrepancies were discussed to reach consensus. Staining intensity (0 = absent, 1 = weak, 2 = moderate, 3 = strong) and extent of the staining (0 = 0%, 1 = 1-24%, 2 = 25-49%, 3 = 50-74% and 4 = 75%-100%) were assessed. These two measures were added to the sum

score, which was used in all the analyses. For dedifferentiated chondrosarcoma, the well-differentiated and the dedifferentiated component were scored separately. Likewise, for mesenchymal chondrosarcoma both the cartilaginous areas and the small cell component were evaluated separately. Tumors were divided into two groups, having low (mean sum score of <2.5) or high (mean sum score of ≥2.5) protein expression.

Table 6.1 Clinicopathological data of 88 formalin-fixed paraffin-embedded rare chondrosarcomas

	DDCS	MCS	CCS
Total number of tumors	42	23	23
Male	21	8	17
Female	21	15	6
Median age yrs (range)	66 (26-85)	29.5 (15-70)	43 (20-79)
Median follow up (range)*	11 (1-216)	40 (7-204)	57 (1-408)

*follow-up available for 34 dedifferentiated chondrosarcoma, 18 mesenchymal, and 20 clear cell, chondrosarcoma patients
DDCS: dedifferentiated chondrosarcoma, MCS: mesenchymal chondrosarcoma, CCS: clear cell chondrosarcoma

Statistical analysis

Kaplan Meyer analyses were performed using Breslow Generalized Wilcoxon for statistical significance. Survival analyses were performed for metastasis-free survival per subtype. Cox regression analysis was carried out with clinical outcome (metastasis-free survival) as the independent variable. Correlation between expression and grade and individual stainings were evaluated using Pearson chi-squared test for independent variables. Values of $p \leq 0.05$ for asymptomatic 2 sided testing were considered significant. Spearman rank correlation coefficients were calculated for correlations between protein expression patterns. Due to low patient number, loss of cores, and incomplete information on some cases, it was not possible to calculate Kaplan Meyer curves for each staining. The data was analyzed using SPSS version 17.0 software (Chicago, IL, USA).

Inhibition assay

Dedifferentiated chondrosarcoma cell lines L2975 (19) en NDCS-1 (20) were cultured in RPMI1640 (Gibco, Invitrogen Life-Technologies, Scotland, UK) supplemented with 1% penicillin/streptomycin (100U/mL) and 10% heat-inactivated Fetal Calf Serum (Gibco, Invitrogen Life-Technologies, Scotland, UK). Cells were grown at 37°C in a humidified incubator with 95% air and 5% CO_2. Identity of cell lines was confirmed using the PowerPlex® 1.2 system after completion of experiments (Promega Benelux BV, Leiden, The Netherlands). ABT-737 (Abbott Laboratories Inc, IL, USA) was dissolved in DMSO, and doxorubicin and cisplatin were obtained from the in-house hospital pharmacy in a 0.9% NaCl solution. For inhibition assays, the cell lines were plated in 96 well plates for viability assessment ($2x10^5$ cells/well) and allowed to grow and adhere overnight after which the respective drugs were added in their corresponding concentrations. Combination assays were performed as described (21). In short, over the course of 96hrs, cells were treated twice with ABT-737 with an intermittent treatment of cisplatin or doxorubicin. Dose response curves were established for each cell line using dosages ranging from 100nM to 1µM for doxorubicin and cisplatin and 100nM to 5µM for ABT-737, after which combination assays were performed using combinations of all dosages. Combination indices could not be calculated as IC50s were not reached for single treatments. All experiments were performed in triplicate and at least three times. Graphs show data from one representative experiment. Error bars indicate the standard deviation.

Immunoblotting

Immunoblotting using Bcl-2 (clone C 21 Santa Cruz, Heerhugowaard, the Netherlands) and Bcl-xl (clone 54H6, cell signaling, Leiden, the Netherlands) antibodies was performed as previously described (22), using 20µg of each sample.

Table 6.2. Procedures and details of the primary antibodies used for immunohistochemistry

antibody	Manufacturer	dilution	antigen retrieval	Blocking	localisation	pos. control
PTHLH	Oncogene	1:200	trypsin 30 min	-	cytoplasmic	skin
PTHR1	Upstate	1:400	citrate	-	cytoplasmic	skin
Bcl-2	Dako	1:1000	citrate	-	cytoplasmic	Tonsil
Bcl-xl	Cell Signaling	1:400	citrate	-	cytoplasmic	Prostate
FGFR3	Sigma	1:4000	citrate	-	cytoplasmic	umbilical cord
FGF18	Sigma (Atlas)	1:4000	citrate	-	cytoplasmic	tonsil
SOX9	Atlas	1:100	citrate	Milk	nuclear	testis
pSMAD1	Cell signaling	1:100	citrate	Milk	nuclear	colon
pSMAD2	Cell signaling	1:50	citrate	NGS	nuclear	Kidney
CTNB1	Transduction Biosciences	1:2000	citrate	-	cytoplasmic	Skin
SDC2	Lifespan biosciences	1:200	-	-	cytoplasmic	growth plate
SDC3	Proteintech.Group Inc.	1:200	citrate	NGS	cytoplasmic	colon carcinoma
SDC4	Atlas	1:1000	citrate	-	cytoplasmic	placenta
NDST1	Abcam	1:800	Tris-EDTA	-	cytoplasmic	Ileum
PAI-1	American Diagnostics	1:200	-	-	cytoplasmic	cervix carcinoma
CD44v3	Novocastra	1:200	citrate	-	cytoplasmic	tonsil
10 E4	Seikagaku corporation	1:400	Heparitinase buffer	NGS	cytoplasmic	skin
PTGS2	Nuclilab	1:100	citrate	NGS	cytoplasmic	colon carcinoma
KIT	Dako	1:2000	-	-	cytoplasmic	GIST

Results

Histological analysis of dedifferentiated chondrosarcoma
For the 42 dedifferentiated chondrosarcomas, the anaplastic component demonstrated an undifferentiated sarcoma in 30 cases, of which 23 showed spindle-cell morphology. Nine cases showed osteosarcomatous differentiation in the dedifferentiated component. From three tumors the dedifferentiated part was not available. The cartilaginous component demonstrated grade I morphology in 19 cases, grade II in eight and grade III in four cases. From 11 tumors no cartilaginous component was available.

Wnt and SOX9
Nuclear CTNB1 expression as a read-out for canonical Wnt-signaling was absent in all tumors. Variable intensity of cytoplasmic staining was, however, observed in all tumor subtypes (table 6.3). The master transcriptional regulator for chondrogenic differentiation SOX9 (23) was expressed in a large portion of all three subtypes. A trend of slightly higher expression in the cartilaginous parts of the tumors was observed (fig 6.1A, B, table 6.3). In the cartilaginous cells of dedifferentiated chondrosarcoma Spearman's rank correlation revealed an association ($p < 0.05$) between protein expression of SOX9 and SDC2 ($r_s = 0.70$), SDC3 ($r_s = 0.71$), and SDC4 ($r_s = 0.44$).

Heparan sulfate proteoglycan expression
Heparan sulfate as demonstrated by immunoreactivity for 10E4 was variable. The anaplastic component of dedifferentiated chondrosarcoma as well as the small cell component of mesenchymal chondrosarcoma demonstrated more extensive and more intense expression as compared to their cartilaginous components. The expression in clear cell chondrosarcoma was limited (fig 6.1C). NDST1 (N-deacetylase/N-sulfotransferase), an enzyme that can interact with EXT1 and EXT2 during heparan sulfate chain formation (24), was highly expressed in dedifferentiated chondrosarcoma, and in the small cell component of mesenchymal chondrosarcoma. In the cartilaginous components of mesenchymal chondrosarcoma and in clear cell chondrosarcomas high NDST1 expression was observed in approximately half of the tumors (fig 6.1D, table 6.3). The expression of the heparan sulfate proteoglycans syndecan 2, -3, and -4 and of CD44 variable exon 3 was also variable in all 3 tumor subtypes (fig 6.1E, F, G, H). Expression of syndecans 2, -3, and -4 was higher in the dedifferentiated parts of dedifferentiated chondrosarcomas than in the cartilaginous parts and the other tumor types.

FGF signaling
The expression of FGFR3 was strong and extensive in most tumors of all three subtypes (fig 6.2A, B). The expression of FGF18, the ligand for FGFR3 in the normal growth plate, was more variable (fig 6.1I).

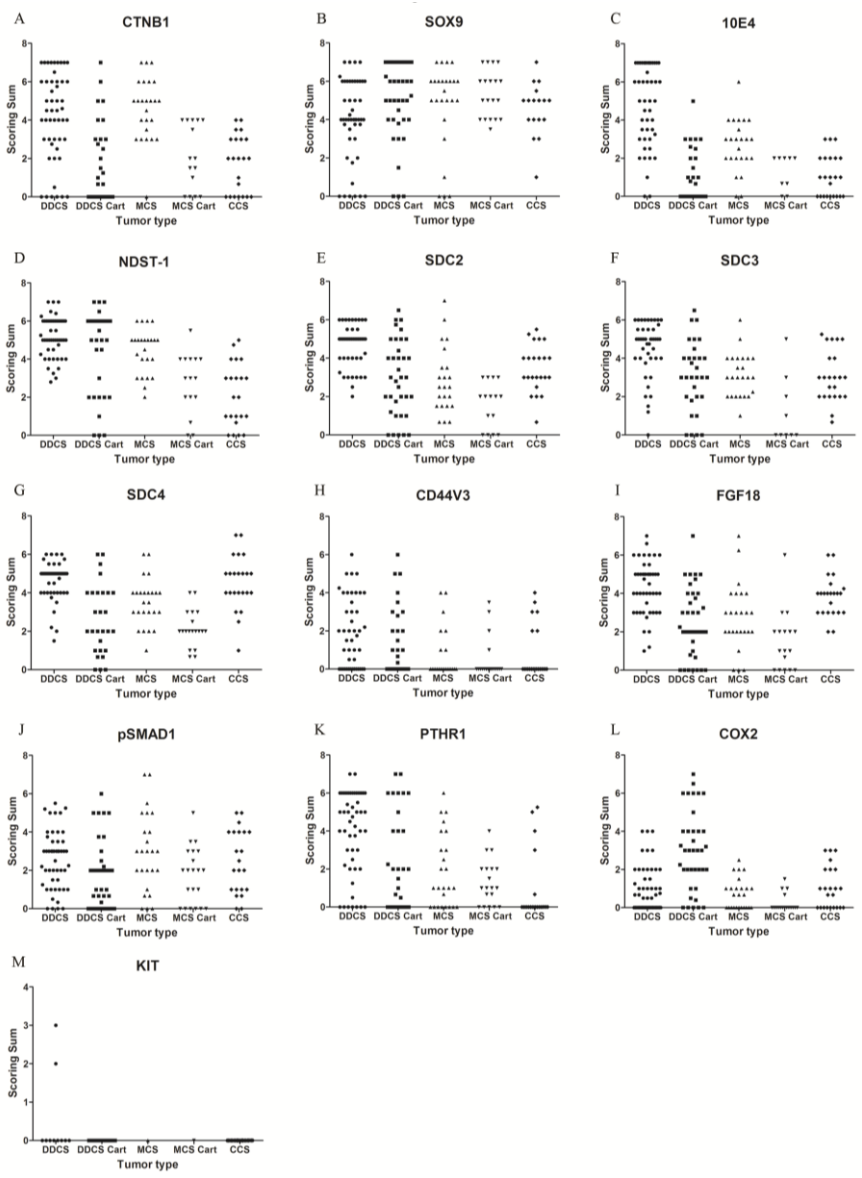

Figure 6.1: Dot plots representing sum scores for all immuno stainings in all tumor tissues included on the TMA, grouped by tumor type.
A: CTNB1. **B**: SOX9. **C**: 10e4. **D**: NDST-1. **E**: Syndecan 2 (SDC2). **F**: Syndecan 3 (SDC3). **G**: Syndecan 4 (SDC4). **H**: CD44v3. **I**: FGF-18. **J**: p-SMAD1. **K**: PTHR1. **L**: COX-2. and **M**: KIT. DDCS, anaplastic component of dedifferentiated chondrosarcoma; DDCS cart, the cartilaginous component of dedifferentiated chondrosarcoma; MCS, the small cell component of mesenchymal chondrosarcoma, MCS cart, the cartilaginous component of mesenchymal chondrosarcoma; CCS, clear cell chondrosarcoma.

TGFbeta/BMP signaling
Nuclear pSMAD1 expression, which indicates active BMP signaling, was moderate in all three subtypes (fig 6.1J). TGFbeta signaling, as evidenced by PAI-1 and nuclear pSMAD2 staining, was rather high in all three subtypes (fig 6.2C-E, table 6.3). Expression of pSMAD2 showed some variation, ranging from high expression in half of the mesenchymal chondrosarcomas in the small-cell component, to almost all clear cell chondrosarcomas. In clear cell chondrosarcoma, PAI-1 expression was positively correlated with both pSMAD2 ($r_s = 0.71$; $p < 0.001$) and pSMAD1 ($r_s = 0.60$; $p = 0.009$). We also demonstrated a positive correlation between PAI-1 and pSMAD2 expression in dedifferentiated chondrosarcoma ($r_s = 0.45$; $p = 0.01$), and high pSMAD2 protein expression was significantly associated with longer metastasis-free survival (HR = 0.38, p=0.048) (fig 6.2F).

PTHLH signaling
Parathyroid-hormone signaling was assessed using PTHLH and PTHR1 (25). PTHLH was high in dedifferentiated chondrosarcoma and clear cell chondrosarcoma (fig 6.3A, B), whereas, PTHR1 expression was found to be low in most of the clear cell chondrosarcomas and mesenchymal chondrosarcomas. In dedifferentiated chondrosarcoma PTHR1 expression was low in the cartilaginous component with higher expression in the anaplastic component (fig 6.1K).

Bcl-2 and Bcl-xl signaling and chemoresistance
Bcl-2 was assessed as the downstream signaling molecule of PTHLH in the growth plate (26). A positive correlation between PTHR1 expression and Bcl-2 was observed in clear cell chondrosarcoma ($r_s = 0.47$; $p = 0.04$). Since anti-apoptotic proteins were shown to play an important role in chemoresistance of conventional chondrosarcoma (21), we additionally evaluated the expression of the Bcl-2 family member Bcl-xl. Both clear cell and mesenchymal chondrosarcoma showed high expression of both Bcl-2 (fig 6.4C, D) and Bcl-xl (fig 6.4F). In contrast, in dedifferentiated chondrosarcoma, high expression of mainly Bcl-xl was found (fig 6.3E, F). L2975 and NDCS-1 are dedifferentiated chondrosarcoma cell lines showing strong expression of Bcl-xl and Bcl-2 (fig 6.4G). As L2975 showed only 40% reduction in cell viability after 1µM doxorubicin and 10% reduction in cell viability after 1µM cisplatin and no reduction in cell viability could be achieved in NDCS-1 after treatment with either doxorubicin or cisplatin (fig 6.3A, B), we continued to investigate the effect of inhibition of Bcl-2 family members using the BH-3 mimetic ABT-737. Cells were treated with ABT-737 prior to and after doxorubicin or cisplatin addition as we previously showed that this was the most effective course of combination treatment (21). Interestingly, even though single treatment with 5µM ABT-737 did not result in a reduction of cell viability in either cell line (fig 6.3C), at concentrations as low as 100nM, inhibition of Bcl-2 family members was sensitizing the cells to both doxorubicin and cisplatin (fig 6.4H).

Table 6.3 Percentage of tumors showing high expression (mean sum score of ≥2.5) of proteins per subtype as determined by immunohistochemistry

	Dedifferentiated CS		**Clear cell CS**	**Mesenchymal CS**	
	dedifferentiated areas	cartilaginous areas		Small cells	Cartilaginous areas
Bcl-2	10/38 (26%)	1/25 (4%)	19/22 (86%)	22/23 (96%)	10/17 (59%)
Bcl-xl	36/39 (92%)	10/32 (31%)	13/17 (76%)	8/12 (67%)	3/8 (38%)
PTHLH	30/37 (81%)	25/27 (93%)	11/12 (92%)	4/7 (57%)	1/5 (20%)
PTHR1	28/38 (74%)	8/25 (32%)	4/22 (18%)	9/23 (39%)	3/17 (18%)
SOX9	31/39 (79%)	26/30 (87%)	16/17 (94%)	19/23 (83%)	18/18 (100%)
NDST1	38/38 (100%)	22/31 (71%)	9/21 (43%)	21/22 (95%)	8/14 (57%)
10 E 4	32/38 (84%)	7/32 (22%)	3/22 (14%)	1/17 (6%)	13/23 (58%)
CD44V3	14/36 (39%)	6/23 (26%)	4/21 (19%)	7/23 30%)	4/18 (22%)
SDC2	36/37 (97%)	18/31 (58%)	19/22 (86%)	13/22 (59%)	4/14 (29%)
SDC3	31/36 (86%)	19/28 (68%)	14/22 (64%)	15/23 (65%)	2/9 (22%)
SDC4	35/38 (92%)	10/23 (43%)	21/22 (95%)	18/23 (78%)	6/17 (35%)
pSMAD1	19/39 (49%)	8/31 (26%)	10/21 (48%)	13/23 (57%)	7/20 (35%)
pSMAD2	29/39 (74%)	22/33 (67%)	21/22 (95%)	9/17 (53%)	15/23 (65%)
PAI1	38/38 (100%)	26/28 (93%)	20/21 (95%)	21/21 (100%)	13/14 (93%)
CTNB1	31/37 (84%)	9/30 (30%)	7/21 (33%)	22/23 (96%)	6/15 (40%)
FGF18	34/38 (89%)	18/30 (60%)	20/22 (91%)	12/23 (52%)	3/16 (19%)
FGFR3	40/40 (100%)	26/31 (84%)	21/21 (100%)	21/23 (91%)	17/18 (94%)
PTGS2	2/39 (5%)	17/32 (53%)	4/22 (18%)	1/23 (4%)	0/17 (0%)
KIT	2/37 (5%)	0/26 (0%)	0/21 (0%)	2/23 (9%)	0/19 (0%)

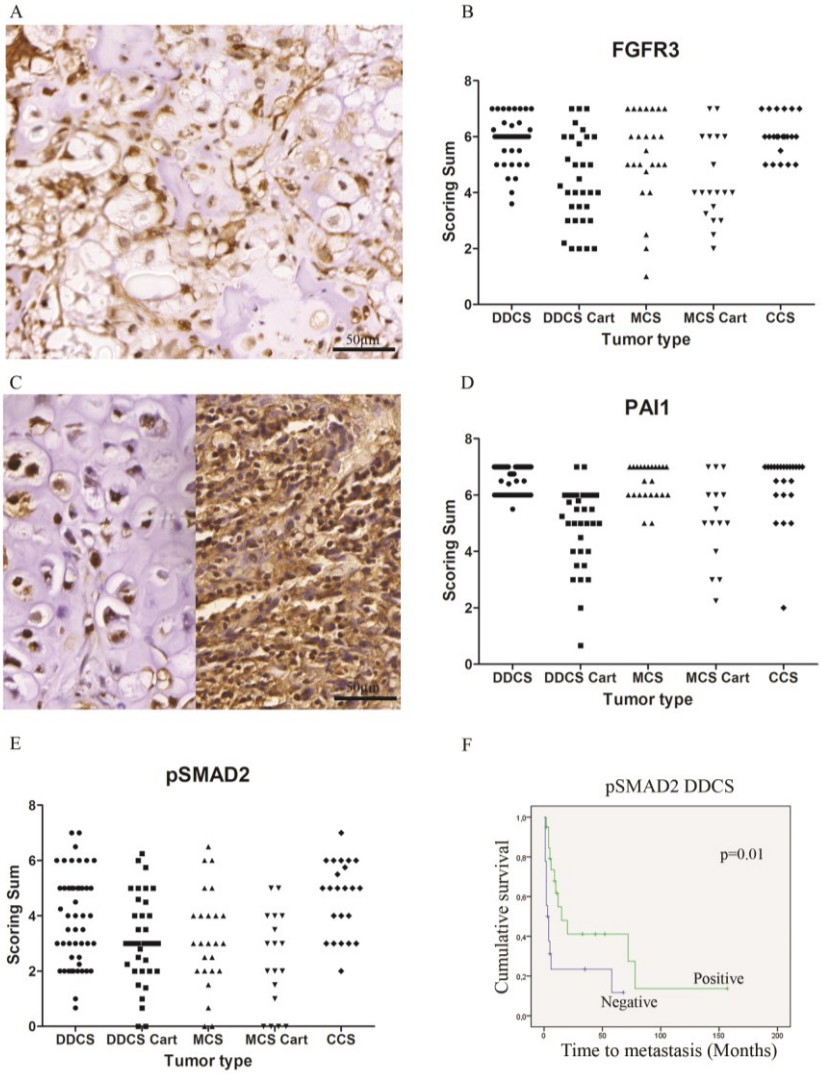

Figure 6.2: Active FGF signaling and TGFbeta signaling through pSMAD2 and PAI1 in all rare subtypes of chondrosarcoma.

A: High FGFR3 expression in CCS. **B**: Sum scores of FGFR3 in all tumor tissues included on TMA, by tumor type. **C**: High level of PAI1 expression in cartiilaginous component (left panel) and anaplastic component (right panel) of dedifferentiated chondrosarcoma. **D,E**: Sum scores of PAI1 (**D**) and pSMAD2 (**E**) in all tumor tissues included on TMA, by tumor type. **F**: Kaplan Meier of pSMAD2 staining in dedifferentiated chondrosarcoma (DDCS) shows positive association between pSMAD2 expression and metastasis free survival (p=0.01).

Possible therapeutic targets PTGS2 and KIT
In contrast to central chondrosarcomas (27), PTGS2 (COX-2) expression was rather low in the rare chondrosarcoma subtypes. Only in the dedifferentiated component of dedifferentiated chondrosarcoma was high expression observed in approximately half of the tumors. Expression of the tyrosine kinase receptor KIT was low to absent in all tumor subtypes (fig 6.1L, M, table 6.3).

Discussion
To identify possible therapeutic targets in rare chondrosarcoma subtypes, we investigated expression of signaling pathways that play pivotal roles in the normal growth plate and in conventional chondrosarcoma. The chondrosarcoma subtypes that are the subject of our study are rare and an extensive study of possible therapeutic targets in these tumors has not previously been carried out. Through the EuroBoNeT consortium we were able to collect paraffin blocks of a relatively large series enabling us to systematically analyze the activity of growth plate signaling pathways. Not only did we observe differences between the subtypes, but also between the cartilaginous cells and anaplastic or small cells in dedifferentiated and mesenchymal chondrosarcoma, respectively. Heparan sulfate proteoglycan and PTHLH expression were noted to vary between tumor types and cell types (fig 6.1). All heparan sulfate proteoglycans studied, including SDC2-4 and CD44v3, as well as 10E4 and NDST1, were expressed in the cytoplasm of the cells and sometimes to a lesser extent on the membrane. Aberrant cellular localization of these proteins is a known phenomenon in osteochondromas and chondrosarcomas (15;28;29).
SOX9, TGFbeta, and FGFR3 signaling was highly active in all chondrosarcoma subtypes. Whereas activating FGFR3 mutations stimulate proliferation in certain types of cancer, they cause several forms of dwarfism-associated chondrodysplasias in humans and mice, demonstrating an inhibitory effect in bone (30). In this study, we demonstrated high FGFR3 expression in central dedifferentiated -, mesenchymal - , and clear cell chondrosarcoma. Previously, we demonstrated high FGFR3 in peripheral dedifferentiated chondrosarcomas, but rather low expression in secondary peripheral chondrosarcomas (31). In 2007, Oji et al demonstrated high FGFR3 mRNA and protein in rat chondrosarcoma cells *in vitro*. Stimulation of the FGFR3 receptor with an FGFR3 agonist reduced the proliferative rate of the cells. However, the addition of a polyclonal antibody for FGFR3 did not reverse this effect, suggesting a deregulation in the FGFR3 signaling pathway (32). Based on the literature, overexpression of FGFR3 in chondrosarcoma would be expected to inhibit IHH and thereby PTHLH (25). However, our study showed PTHLH to be highly expressed in most of the tumors, indicating pathway activity independent of FGFR3, as was also found for conventional chondrosarcoma (14;18).

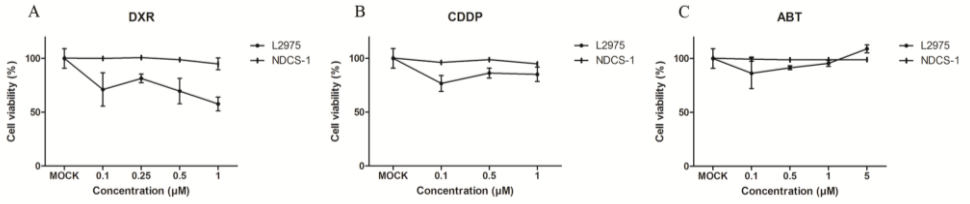

Figure 6.3: Dose response curves for doxorubicin (A) cisplatin (B) and ABT-737 (C). A, B: L2975 shows 40% reduction in cell viability after 1µM doxorubicin (DXR) and 10% reduction in cell viability after 1µM cisplatin (CDDP), whereas NDCS-1 shows no reduction in cell viability after either doxorubicin or cisplatin. **C:** Neither cell line shows a response to ABT-737 treatment alone.

In accordance with previous findings in central chondrosarcoma (18) we found PTHR1 expression to be higher in the anaplastic cells of dedifferentiated and mesenchymal chondrosarcomas as compared to the cartilaginous cells in these tumors and in clear cell chondrosarcomas, suggesting a role for PTHLH signaling in the fast proliferation of these tumors. Despite the low PTHR1 expression in clear cell and mesenchymal chondrosarcoma, we observed high expression of Bcl-2, indicating that this might be induced via a different signaling pathway, such as an apoptosis directed pathway. We previously found absence of Bcl-2 in peripheral dedifferentiated chondrosarcomas (31). We here show that Bcl-2 expression was generally high in mesenchymal and clear cell chondrosarcoma, whereas dedifferentiated chondrosarcoma rather shows high expression of Bcl-xl. In conventional central chondrosarcoma, we previously showed high Bcl-2 expression (18) and recently showed that conventional central chondrosarcoma cells with high expression of Bcl-2 family members could be sensitized to doxorubicin and cisplatin by inhibition of Bcl-2 family members using the BH-3 mimetic ABT-737 indicating an important role for Bcl-2 family members in chemoresistance of conventional chondrosarcoma (21). We now also show high Bcl-2 and Bcl-xl expression in the two dedifferentiated chondrosarcoma cell lines and a reversal of chemoresistance during combination treatment with ABT-737 and conventional chemotherapeutics. As a BH-3 mimetic ABT-737 has also been shown to inhibit Bcl-xl (33). Our results indicate an important role for Bcl-2 and Bcl-xl in the chemoresistance of dedifferentiated chondrosarcoma cells. The high Bcl-2 and Bcl-xl expression in mesenchymal and clear cell chondrosarcoma suggests that also in these subtypes Bcl-2 family members contribute to chemoresistance and that patients might benefit from a treatment combining Bcl-2 family inhibitors and chemotherapy. At the time of preparing this manuscript, no cell lines of these subtypes are available to further test this.

Figure 6.4: Bcl-2 as a possible target in rare chondrosarcoma subtypes. **A**: PTHLH expression in dedifferentiated chondrosarcoma. **C**: High Bcl-2 expression in mesenchymal chondrosarcoma. **E**: Bcl-xl expression in dedifferentiated chondrosarcoma, showing high expression in dedifferentiated component, with few positive cells in cartilage component. **B**, **D**, **F**: Sum scores of PTHLH (**B**), Bcl-2 (**D**), and Bcl-xl (**F**) in all tumor tissues included on the TMA, by tumor type. **G**: Western blotting shows strong expression of Bcl-2 and Bcl-xl in dedifferentiated chondrosarcoma cell lines L2975 and NDCS-1. **H**: Reversal of chemoresistance using the BH3 mimetic ABT-737 in dedifferentiated chondrosarcoma cell lines L2975 and NDCS1. Both cell lines show resistance to doxorubicin (DXR) and cisplatin (CDDP) alone, and were not responsive to ABT-737 as a single agent. Combination of ABT-737 with doxorubicin or cisplatin, however, showed strong inhibition of cell viability suggesting a role for Bcl-2 family members in chemoresistance of dedifferentiated chondrosarcoma (concentrations are in µM).

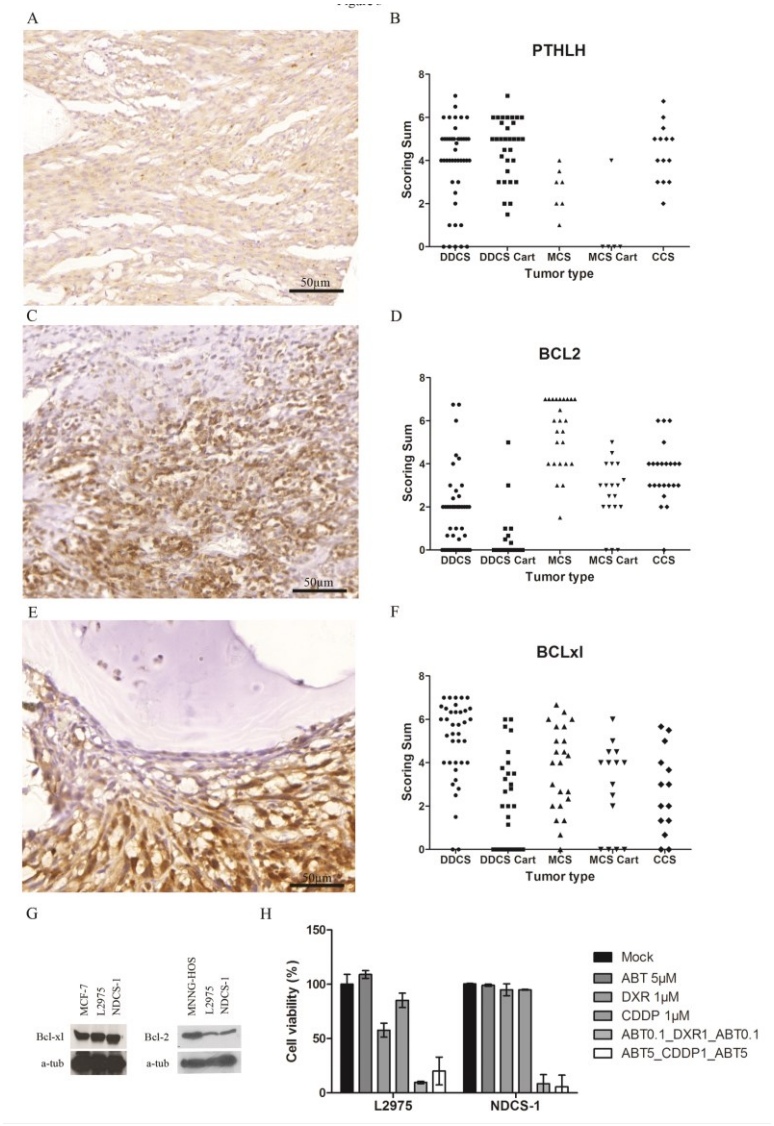

To investigate BMP and TGFbeta signaling, we evaluated the expression of pSMAD1, and pSMAD2 and PAI-1, respectively. BMP signaling, as indicated by pSMAD1 expression, was variable in all three subtypes. pSMAD1 expression was slightly higher in the dedifferentiated and small cell components of dedifferentiated and mesenchymal chondrosarcoma, respectively. In the growth plate, pSMAD1 plays a role in early condensation, correlating with the phenotypic characteristics of these components. TGFbeta signaling, as indicated by expression of pSMAD2 and PAI-1, was highly active in all chondrosarcoma subtypes investigated. High expression of PAI-1 was observed previously in the anaplastic components of conventional and peripheral dedifferentiated chondrosarcomas (31;34). In the cartilaginous components of peripheral dedifferentiated chondrosarcomas a prognostic value has been described for PAI-1 expression (31). In our study, high pSMAD2 in the anaplastic component of dedifferentiated chondrosarcoma was related to longer metastasis-free survival.

TGFbeta is known to have a dual role in cancer. Not only does it promote tumor growth, invasion and metastasis, it is also described to prevent malignant progression in the surrounding environment of an oncogenic process (35). Since TGFbeta signaling was active in a subset of dedifferentiated - and mesenchymal chondrosarcomas, and in almost all clear cell chondrosarcomas, TGFbeta might be a promising therapeutic target. The most useful agents in blocking TGFbeta signaling are likely TGFbeta-targeting monoclonal antibodies like fresolimumab and tyrosine kinase inhibitors (36). In dedifferentiated and mesenchymal chondrosarcomas, PAI-1 expression was higher than pSMAD2 expression indicating that PAI-1 may also be under the influence of other signaling pathways, like the EGFR signaling pathway (37). Further studies will be needed to determine the involvement of the EGFR pathway and the value of EGFR-targeting treatment in these subtypes.

As in conventional chondrosarcoma (38), KIT expression was absent in rare chondrosarcoma subtypes. In addition, the absence of nuclear CTNB1 indicated that canonical Wnt signaling is not important in these tumor types. Recently our group demonstrated beneficial effects of celecoxib treatment in central chondrosarcomas (27). However, whereas 65% of the conventional chondrosarcomas express PTGS2, expression was absent in most of the rare chondrosarcoma subtypes making beneficial effects of celecoxib unlikely.

In summary, we observed both common and distinct protein expression patterns in three rare chondrosarcoma subtypes. High pSMAD2 and PAI-1 expression emphasize the importance of TGFbeta signaling and suggest that TGFbeta inhibitors might be a promising therapeutic option for patients with rare chondrosarcoma subtypes. In addition, our results suggest an important role for the Bcl-2 family members Bcl-2 and Bcl-xl in chemoresistance of the rare chondrosarcoma subtypes. Similar to conventional chondrosarcoma, the chemoresistance of dedifferentiated chondrosarcoma *in vitro* could be overcome

using inhibition of Bcl-2 family members, repairing the apoptotic machinery rendering the cells sensitive to chemotherapy. This suggests that the combination of BH-3 mimetics with conventional chemotherapeutic agents is a promising therapeutic strategy for metastatic or inoperable chondrosarcoma, irrespective of the histological subtype.

Reference List

1. Bovée JVMG, Cleton-Jansen AM, Taminiau AHM, and Hogendoorn PCW: Emerging pathways in the development of chondrosarcoma of bone and implications for targeted treatment. Lancet Oncology 2005, 6:599-607

2. Aigner T: Towards a new understanding and classification of chondrogenic neoplasias of the skeleton--biochemistry and cell biology of chondrosarcoma and its variants. Virchows Arch 2002, 441:219-230

3. Aigner T, Dertinger S, Belke J, and Kirchner T: Chondrocytic cell differentiation in clear cell chondrosarcoma. Hum Pathol 1996, 27:1301-1305

4. Nakashima Y, Park YK, and Sugano O: Mesenchymal chondrosarcoma. World health organization classification of tumours. Pathology and genetics. Tumours of soft tissue and bone. Edited by Fletcher C.D.M., Unni KK, and Mertens F. 2002, pp. 255-256

5. Aigner T, Loos S, Muller S, Sandell LJ, Unni KK, and Kirchner T: Cell differentiation and matrix gene expression in mesenchymal chondrosarcomas. Am J Pathol 2000, 156:1327-1335

6. Milchgrub S and Hogendoorn PCW: Dedifferentiated chondrosarcoma. World health organization classification of tumours. Pathology and genetics. Tumours of soft tissue and bone. Edited by Fletcher C.D.M., Unni KK, and Mertens F. 2002, pp. 252-254

7. Grimer RJ, Gosheger G, Taminiau A, Biau D, Matejovsky Z, Kollender Y, San Julian M, Gherlinzoni F, and Ferrari C: Dedifferentiated chondrosarcoma: Prognostic factors and outcome from a European group. Eur J Cancer 2007, 43:2060-2065

8. Hogendoorn PCW, Bovée JVMG, Karperien M, and Cleton-Jansen AM: Skeletogenesis: Genetics. Nature Encyclopedia of the Human Genome. Edited by Cooper DN. London, Nature Publishing Group, 2003, pp. 306-313

9. Bovée JVMG, Hogendoorn PCW, Wunder JS, and Alman BA: Cartilage tumours and bone development: molecular pathology and possible therapeutic targets. Nat Rev Cancer 2010, 10:481-488

10. Kronenberg HM: Developmental regulation of the growth plate. Nature 2003, 423:332-336

11. Van der Eerden BCJ, Karperien M, Gevers EF, Lowik CWGM, and Wit JM: Expression of Indian Hedgehog, PTHrP and their receptors in the postnatal growth plate of the rat: evidence for a locally acting growth restraining feedback loop after birth. J Bone Miner Res 2000, 15:1045-1055

12. Yano F, Kugimiya F, Ohba S, Ikeda T, Chikuda H, Ogasawara T, Ogata N, Takato T, Nakamura K, Kawaguchi H, and Chung UI: The canonical Wnt signaling pathway promotes chondrocyte differentiation in a Sox9-dependent manner. Biochem Biophys Res Commun 2005, 333:1300-1308

13. Ferguson CM, Schwarz EM, Puzas JE, Zuscik MJ, Drissi H, and O'Keefe RJ: Transforming growth factor-beta1 induced alteration of skeletal morphogenesis in vivo. J Orthop Res 2004, 22:687-696

14. Hameetman L, Rozeman LB, Lombaerts M, Oosting J, Taminiau AHM, Cleton-Jansen AM, Bovée JVMG, and Hogendoorn PCW: Peripheral chondrosarcoma progression is accompanied by decreased Indian

Hedgehog (IHH) signalling. J Pathol 2006, 209:501-511

15. Schrage YM, Hameetman L, Szuhai K, Cleton-Jansen AM, Taminiau AHM, Hogendoorn PCW, and Bovée JVMG: Aberrant heparan sulfate proteoglycan localization, despite normal exostosin, in central chondrosarcoma. Am J Pathol 2009, 174:979-988

16. Bertoni F, Bacchini P, and Hogendoorn PCW: Chondrosarcoma. World Health Organisation classification of tumours. Pathology and genetics of tumours of soft tissue and bone. Edited by Fletcher CDM, Unni KK, and Mertens F. Lyon, IARC Press, 2002, pp. 247-251

17. Evans HL, Ayala AG, and Romsdahl MM: Prognostic factors in chondrosarcoma of bone. A clinicopathologic analysis with emphasis on histologic grading. Cancer 1977, 40:818-831

18. Bovée JVMG, Van den Broek LJCM, Cleton-Jansen AM, and Hogendoorn PCW: Up-regulation of PTHrP and Bcl-2 expression characterizes the progression of osteochondroma towards peripheral chondrosarcoma and is a late event in central chondrosarcoma. Lab Invest 2000, 80:1925-1933

19. van Oosterwijk JG, de JD, van Ruler MA, Hogendoorn PC, Dijkstra PS, van Rijswijk CS, Machado IS, Llombart-Bosch A, Szuhai K, and Bovée JV: Three new chondrosarcoma cell lines: one grade III conventional central chondrosarcoma and two dedifferentiated chondrosarcomas of bone. BMC Cancer 2012, 12:375

20. Kudo N, Ogose A, Hotta T, Kawashima H, Gu W, Umezu H, Toyama T, and Endo N: Establishment of novel human dedifferentiated chondrosarcoma cell line with osteoblastic differentiation. Virchows Arch 2007, 451:691-699

21. van Oosterwijk JG, Herpers B, Meijer D, Briaire-de Bruijn IH, Cleton-Jansen AM, Gelderblom H, van de Water B, and Bovée JV: Restoration of chemosensitivity for doxorubicin and cisplatin in chondrosarcoma in vitro: BCL-2 family members cause chemoresistance. Ann Oncol 2012, 23:1617-1626

22. Schrage YM, Briaire-de Bruijn IH, de Miranda NFCC, van Oosterwijk J, Taminiau AHM, van Wezel T, Hogendoorn PCW, and Bovée JVMG: Kinome profiling of chondrosarcoma reveals Src-pathway activity and dasatinib as option for treatment. Cancer Res 2009, 69:6216-6222

23. Akiyama H and Lefebvre V: Unraveling the transcriptional regulatory machinery in chondrogenesis. J Bone Miner Metab 2011, 29:390-395

24. Presto J, Thuveson M, Carlsson P, Busse M, Wilen M, Eriksson I, Kusche-Gullberg M, and Kjellen L: Heparan sulfate biosynthesis enzymes EXT1 and EXT2 affect NDST1 expression and heparan sulfate sulfation. Proc Natl Acad Sci U S A 2008,

25. Amling M, Posl M, Hentz MW, Priemel M, and Delling G: PTHrP and Bcl-2: essential regulatory molecules in chondrocyte differentiation and chondrogenic tumors. Verh Dtsch Ges Path 1998, 82:160-169

26. Amling M, Neff L, Tanaka S, Inoue D, Kuida K, Weir E, Philbrick WM, Broadus AE, and Baron R: Bcl-2 lies downstream of parathyroid hormone related peptide in a signalling pathway that regulates chondrocyte maturation during skeletal development. J Cell Biol 1997, 136:205-213

27. Schrage YM, Machado I, Meijer D, Briaire-de B, I, van den Akker BE, Taminiau AH, Kalinski T, Llombart-Bosch A, and Bovée JV: COX-2 expression in chondrosarcoma: a role for celecoxib treatment? Eur J Cancer 2010, 46:616-624

28. Hameetman L, David G, Yavas A, White SJ, Taminiau AHM, Cleton-Jansen AM, Hogendoorn PCW, and Bovée JVMG: Decreased EXT expression and intracellular accumulation of heparan sulphate proteoglycan in osteochondromas and peripheral chondrosarcomas. J Pathol 2007, 211:399-409

29. Reijnders CM, Waaijer CJ, Hamilton A, Buddingh EP, Dijkstra SP, Ham J, Bakker E, Szuhai K, Karperien M, Hogendoorn PC, Stringer SE, and Bovée JV: No haploinsufficiency but loss of heterozygosity for EXT in multiple osteochondromas. Am J Pathol 2010, 177:1946-1957

30. Foldynova-Trantirkova S, Wilcox WR, and Krejci P: Sixteen years and counting: the current understanding of fibroblast growth factor receptor 3 (FGFR3) signaling in skeletal dysplasias. Hum Mutat 2012, 33:29-41

31. Rozeman LB, de Bruijn IH, Bacchini P, Staals EL, Bertoni F, Bovée JVMG, and Hogendoorn PCW: Dedifferentiated peripheral chondrosarcomas: regulation of EXT-downstream molecules and differentiation-related genes. Mod Pathol 2009, 22:1489-1498

32. Oji GS, Gomez P, Kurriger G, Stevens J, and Morcuende JA: Indian hedgehog signaling pathway differences between swarm rat chondrosarcoma and native rat chondrocytes. Iowa Orthop J 2007, 27:9-16

33. Lee SJ, Park HJ, Kim YH, Kim BY, Jin HS, Kim HJ, Han JH, Yim H, and Jeong SY: Inhibition of Bcl-xL by ABT-737 enhances chemotherapy sensitivity in neurofibromatosis type 1-associated malignant peripheral nerve sheath tumor cells. Int J Mol Med 2012, 30:443-450

34. Hackel C, Czerniak B, Ayala AG, Radig K, and Roessner A: Expression of plasminogen activators and plasminogen activator inhibitor 1 in dedifferentiated chondrosarcoma. Cancer 1997, 79:53-58

35. Massague J: TGFbeta in Cancer. Cell 2008, 134:215-230

36. Lonning S, Mannick J, and McPherson JM: Antibody targeting of TGF-beta in cancer patients. Curr Pharm Biotechnol 2011, 12:2176-2189

37. Samarakoon R, Higgins CE, Higgins SP, and Higgins PJ: TGF-beta1-Induced Expression of the Poor Prognosis SERPINE1/PAI-1 Gene Requires EGFR Signaling: A New Target for Anti-EGFR Therapy. J Oncol 2009, 2009:342391

38. Lagonigro MS, Tamborini E, Negri T, Staurengo S, Dagrada GP, Miselli F, Gabanti E, Greco A, Casali PG, Carbone A, Pierotti MA, and Pilotti S: PDGFRalpha, PDGFRbeta and KIT expression/activation in conventional chondrosarcoma. J Pathol 2006, 208:615-623

Chapter 7

Src Kinases in Chondrosarcoma Chemoresistance and Migration: Dasatinib Sensitizes to Doxorubicin in TP53 Mutant Cells

This chapter is based on the manuscript: van Oosterwijk JG, van Ruler MAJH, Briaire- de Bruijn IH, Herpers B, Gelderblom H, van de Water B, Bovée JVMG *Br J Cancer. 2013;109(5):1214-22*

Abstract

Chondrosarcomas are malignant cartilage-forming tumors of bone. Due to their resistance to conventional chemotherapy and radiotherapy currently no treatment strategies exist for unresectable and metastatic chondrosarcoma. Previously, PI3K/AKT/GSK3β and Src kinase pathways were shown to be activated in chondrosarcoma cell lines. Our aim was to investigate the role of these kinases in chemoresistance and migration in chondrosarcoma in relation to TP53 mutation status.
We used 5 conventional and 3 dedifferentiated chondrosarcoma cell lines and investigated the effect of PI3K/AKT/GSK3β pathway inhibition (enzastaurin) and Src pathway inhibition (dasatinib) in chemoresistance using WST assay and Live cell imaging with AnnexinV staining. Immunohistochemistry on tissue microarrays (TMAs) containing 157 cartilaginous tumors was performed for Src family members. Migration assays were performed with the RTCA xCelligence System.
Src inhibition was found to overcome chemoresistance, to induce apoptosisand to inhibit migration. Cell lines with TP53 mutations responded better to combination therapy than wildtype cell lines (*p=0.002*). TMA immunohistochemistry confirmed active Src (pSrc) signaling, with Fyn being most abundantly expressed (76.1%).
These results strongly indicate Src family kinases, in particular Fyn, as a potential target for the treatment of inoperable and metastatic chondrosarcomas, and to sensitize for doxorubicin especially in the presence of TP53 mutations.

Introduction

Chondrosarcoma is a malignant cartilage-forming neoplasm of bone and the second most common bone sarcoma in humans (1). Conventional chondrosarcoma does not respond to existing chemo- and radiotherapy modalities (2). Metastasis formation eventually occurs in 71% of grade III chondrosarcoma cases, andwith a 10 year survival rate of 29% this poses a serious treatment problem (3).
Chemoresistance in chondrosarcoma has long been ascribed to poor vascularization, hyaline extracellular matrix production and slowly dividing cells (4;5). Though this is true for low grade chondrosarcomas, high grade chondrosarcomas typically are composed of rapidly dividing cells with more myxoid matrix production (2;6). In the search for molecular targets, negative regulators of the apoptotic pathway, such as BCL-2 (7-10), and survivin (11), were identified to be upregulated in chondrosarcoma, and shown to play a role in chemoresistance (11;12).
Apart from defective apoptotic pathways, deregulated kinase pathways are of growing interest in the field of cancer and have been suggested to play a role in chondrosarcoma (6). We have previously shown activating hyperphosphorylation

of AKT, and Src family kinases and inactivating hyperphosphorylation of GSK3β using kinome profiling of chondrosarcoma cell lines and primary cultures (13).
Both PI3K/AKT/GSK3β and Src signaling pathways are described in a variety of different cancer types as well as in progression to malignancy (14-17) and can be activated by receptor tyrosine kinases (RTKs) (18-20). Activation of the Src pathway promotes cell survival, proliferation, and migration, but can also activate the PI3K/AKT/GSK3β pathway through phosphorylation of PI3K, thereby leading to increased AKT phosphorylation (21). Activation of Protein Kinase C (PKC) by RTKs can also activate the PI3K/AKT pathway, either through phosphorylation of PI3K or through direct phosphorylation of AKT (22;23) (figure 7.1A). Moreover, PKC and AKT can both phosphorylate GSK3β at Ser9 (19;24).
Due to the intricate interplay of PI3K/AKT/GSK3β and Src signaling pathways in cancer and the observation that both pathways are activated in chondrosarcoma we hypothesized that the activation of these pathways in chondrosarcoma contributes to chemoresistance
We therefore investigated the role of both pathways in cell proliferation and chemoresistance. Our data indicate that Src family kinases, Fyn in particular, play a role in chemoresistance and cell migration, and that TP53 mutated cells are especially sensitive to combination therapy with doxorubicin and the Src inhibitor dasatinib.

Methods

Compounds
Doxorubicin and cisplatin were obtained from the in-house hospital pharmacy in a 0.9% NaCl solution. Therapeutic concentrations of doxorubicin in patients are 5-50μM with an *in vitro* range of 1-10 μM, for cisplatin these are 3-13μM with an *in vitro* range of 1-50μM (25). The PKC inhibitor enzastaurin (26) (Eli Lilly, IN, USA) and the Src inhibitordasatinib (27) (Bristol-Meyers Squibb, Princeton, NJ, USA) were dissolved in DMSO.

Cell culture
Chondrosarcoma cell lines (table 7.1), as well as MCF-7 and HeLa cell lines were cultured in RPMI1640 (Gibco, Invitrogen Life-Technologies, Scotland, UK) supplemented with 1% L-glutamax, 1% penicillin/streptomycin (100U/mL), and 10% heat-inactivated Fetal Calf Serum (Gibco, Invitrogen Life-Technologies, Scotland, UK). Cells were grown at 37°C in a humidified incubator with 95% air and 5% CO_2. Cells were cultured until stably multiplying.Chondrogenic phenotype was confirmed using RT-PCR for collagen I, IIB, III, and X, aggrecan, and SOX9(28). Identity of cell lines was confirmed using the Cell ID^{TM} System after completion of experiments (Promega Benelux BV, Leiden, The Netherlands).

Table 7.3. Cell lines

Cell Line	Tumor Type	Grade	Gender	Age	Passage	TP53[1]	IDH1[2]	IDH2[2]	Reference
SW1353	Solitary Central	II	F	72	21	V203L	wt	R172S	ATCC
OUMS27	Solitary Central	III	M	65	27	wt	wt	wt	(58)
CH2879	Solitary Central	III	F	35	>80	wt	wt	wt	(59)
JJ012	Solitary Central	II	M	39	9	G199V	R132G	wt	(60)
L835	Solitary Central	III	M	55	50	wt	R132C	wt	(12)
L2975	Dedifferentiated CS		M	57	60	wt	R172W	wt	(12)
NDCS1	Dedifferentiated CS		M	38	60	C242S	wt	wt	(61)
L3252	Dedifferentiated CS		F	52	30	wt	wt	wt	(12)

[1]IDH mutations for used cell lines were described in (12;30)
[2]TP53 mutations for used cell lines were described in (12;29)

Cell viability assay
Chondrosarcoma cell lines were plated in 96 well plates for viability assessment ($2x10^4$-$2x10^5$ cells/well depending on growth rate) and allowed to grow and adhere overnight after which the respective drugs were added in their corresponding concentrations. Combination assays were performed as described (29) with alternating treatments combining enzastaurin, dasatinib, and/ or doxorubicin. All experiments were performed in triplicate and at least three times. Graphs show data from one representative experiment. Error bars indicate the standard deviation.

Immunoblotting
Immunoblotting using AKT, pAKT, Fyn (Cell Signaling, Leiden, the Netherlands) and pSrc antibody (pSrc pY418, Invitrogen Life Technologies, Bleiswijk, the Netherlands) to investigate the Src and PI3K/AKT signaling pathway and p53 (Do7, Dako, Heverlee, Belgium), MDM2 (IF2, Zymed, Bleiswijk, the Netherlands) and p21 (Santa Cruz, Heidelberg, Germany) was performed as previously described (13), using 20μg of each sample.

Mutation analysis
To identify mutations in AKT1, direct sequencing was performed as described (30), using DNA derived from 57 tumors, 8 cell lines, and 1 primary culture (L3310) using forward primer 3'-TAGAGTGTGCGTGGCCTCTCA-5' and reverse primer 3'-CTGAATCCCGAGAGGCCAA-5' to screen for hotspot mutations in the AKT1-E17K pleckstrin homology domain.

Apoptosis assay and Immunofluorescence
Apoptosis assay and immunofluorescence for caspase 3 and cytochrome C were performed as described (29;31). In short, 20.000 chondrosarcoma cells were grown in black 96-well microclear plates (Greiner®, Sigma-Aldrich, Zwijndrecht, The Netherlands) to perform a live cell apoptosis assay (31), with AnnexinV-Alexa633 conjugate using the BD Pathway® 855 (Becton Dickinson, Breda, The Netherlands). Time series were quantified using in house developed macros for Image-Pro Plus (Media Cybernetics, Bethesda, USA). Drugs were added 0, 24, and 48 hours before imaging and Annexin V-Alexa633 conjugate was added immediately prior to imaging. For all treatments, a pan-caspase inhibitor, z-VAD-fmk (Bachem-Holding AG, Weil am Rhein, Germany), was added 30 minutes before drug addition and imaging in order to establish apoptosis specificity of the assay. Prior to imaging, live nuclei were stained with HOECHST-33342 at 100ng/ml. All experiments were performed in triplicate and at least three times. Error bars show standard deviation from one representative experiment.

Migration assays
The RTCA xCelligence system (Roche Applied Sciences, Almere, the Netherlands), based on cell-electrode substract impedance detection technology, was used for migration assays. For migration assays, lower wells of the SIM plates (migration plates) were filled with growth medium (20% FCS in RPMI).Cell lines were plated at a density of 80.000 cells per well in the top wells in empty buffer (RPMI only) containing0, 0.2, 0.4, 0.6, 0.8, or 1.0 μM dasatinib.SIM plates were loaded into the RTCA station in the cell culture incubator immediately after plating and cell index was acquired every 5 minutes. Cell index as acquired by the software was set to 100% migration after flattening of the slope. Experiments were performed in triplicate.

TMA construction and clinicopathological data
Tissue microarrays (TMAs) were constructed from formalin-fixed, paraffin-embedded tissue using standard procedures (32) using a 2.0 mm diameter punch automated tissue arrayer (3DHistech Ltd, Budapest, Hungary). Each array contained three cores per tumor wherever possible including 7 control tissues (skin, colon, tonsil, prostate, mamma carcinoma, spleen and liver). Using a tape-transfer system (Instrumedics, Hackensack, NJ, USA), 4-μm sections were transferred to glass slides.All specimens in this study were handled according to the ethical guidelines described in "Code for Proper Secondary Use of Human Tissue in The Netherlands" of the Dutch Federation of Medical Scientific Societies. 157 patients with cartilaginous tumors were selected from the archives of the Leiden University Medical Centre. Selected cases included 137 conventional chondrosarcomas (central chondrosarcoma, n=92; peripheral chondrosarcoma, n=45) and 20 benign cartilage tumors (osteochondroma, n=9; enchondroma, n=11). Only primary tumors were selected. Histology was reviewed by an experienced bone tumor pathologist (J.V.M.G.B.). Clinicopathological data are shown in table 7.2.Total follow up was available for 136 of 157 patients, with 14 patients showing metastasis at completion of this study. Histological grading of chondrosarcoma was performed according to Evans (3). Rare chondrosarcoma subtypes were excluded.

Table 7.4 Clinicopathological data

	Peripheral (n =45)	Central (n =92)
Male vs female	27 vs 18	39 vs. 53
Median age at diagnosis	37 (14-82)	50 (20-84)
Histology		
Grade I	31	42
Grade II	11	36
Grade III	3	14
Metastasis	4/45	10/92
Median follow-up (months)	121 (15-299)	103 (7-292)

Immunohistochemistry

Immunohistochemistry was performed on the TMAs. Slides were incubated with antibodies against Src, Lck, Fyn, Yes, and phosphorylated Src (pSrc, recognizes active Src family members phosphorylated at Y419). Details of antibodies and procedures are provided in table 7.3. Immunohistochemical reactions were performed according to standard laboratory methods (7) and visualized using DAB+ Substrate Chromogen System (Dako, Heverlee, Belgium). TMA slides were scanned using a high resolution Mirax Desk Intrument (Zeiss, Mirax 3D Histech, Hungary) and scored independently by two observers (JVMGB and JGvO) and discrepancies were discussed. Staining intensity (0 = absent, 1 = weak, 2 = moderate, 3 = strong) and extent of the staining (0 = 0%, 1 = 1-24%, 2 = 25-49%, 3 = 50-74% and 4 = 75%-100%) were assessed. Staining was considered high (score ≥4) or low (score <4). As external positive and negative control for all the antibodies specimens of normal tonsil were used. Cores with a negative internal control or loss of tissue were excluded from the analysis.

Statistical analysis
Survival was evaluated by Kaplan–Meier analysis and the log-rank test. Values of $p \leq 0.05$ were considered statistically significant. Variables that achieved significance ($p \leq 0.05$) were entered subsequently into a multivariate analysis using the Cox regression model. Cox regression analysis was carried out with clinical outcome (overall survival) as the independent variable. Correlation between expression and grade and individual stainings were evaluated using Pearson chi-squared test for independent variables. Values of $p \leq 0.05$ for asymptomatic 2 sided testing were considered significant. The data were analyzed using SPSS version 17.0 software (Chicago, IL, USA).
For combination assays the combination index according to the method of Chou and Talalay (33) was calculated. A combination index (CI) of below 1 indicates synergy, and CI of above 1 indicates additive effect. Correlation between combination indices was evaluated using independent 2 sided t-test using Graphpad Prism 5 software (La Jolla, CA, USA). Values of $p \leq 0.05$ were considered significant.

Table 7.3. Antibodies used for immunohistochemistry

Antibody	Clone	Dilution	Antigen Retrieval	Blocking	Source
Src	*327554*	*1:200*	*Citrate*	*NGS*	*R&D Systems Europe Ltd, Oxon, UK*
Yes	*339827*	*1:4000*	*Citrate*	*Milk*	*R&D Systems Europe Ltd, Oxon, UK*
Lck	*Y123*	*1:250*	*Citrate*	-	*Abcam, Cambridge, UK*
Fyn	*Y303*	*1:30000*	*Citrate*	*Milk*	*Abcam, Cambridge, UK*
pSrc	*AF2685*	*1:200*	*Citrate*	*Milk*	*R&D Systems Europe Ltd, Oxon, UK*

Results

PI3K/AKT/GSK3β pathway is not involved in chemoresistance of chondrosarcoma cell lines
To investigate the PI3K/AKT/GSK3β pathway, chondrosarcoma cells were treated with 1μM and 10μM enzastaurin (26), a PKCβ inhibitor shown to inhibit AKT signaling and GSK3β phosphorylation (34). Whereas the cervical cancer cell line HeLa shows 70% reduction in cell viability after treatment with 10μM enzastaurin (fig 7.1B), chondrosarcoma cell lines were less sensitive to enzastaurin treatment. Two chondrosarcoma cell lines showed complete resistance (NDCS-1 and L2975) while in the two most responsive cell lines (SW1353 and L3252) a maximum reduction in cell viability of ~40% was achieved (fig 7.1B). As the PI3K/AKT/GSK3β pathway is involved in cell survival, we set out to examine its role in chemoresistance. Enzastaurin was combined with doxorubicin over the course of 72hrs, alternating treatments every 24hrs, as we previously showed that drug

administration on separate days was most effective (29). While there was no difference in response between IDH mutated and IDH wildtype cell lines, cell lines with TP53 mutations responded better to combination treatment than TP53 wildtype cell lines (*p=0.002*) (fig 7.1B) . However, a lack of synergy between the two drugs was observed (combination indices >2), as reduction in cell viability was attributed to the effect of doxorubicin alone (NDCS-1) or the additive effect of enzastaurin and doxorubicin. Activation of AKT1 can be through mutations in the pleckstrin homology domain, found mostly in solid tumors (35), leading to activated downstream signaling and decreased sensitivity to kinase inhibitors (36). Hotspot mutations in the pleckstrin homology domain of AKT1 were absent in the primary chondrosarcoma tumor tissues or cell lines.

Inhibition of Src family kinases with dasatinib does not potentiate the effect of enzastaurin in chondrosarcoma cell lines

To exclude active Src signaling causing the limited response we observed to enzastaurin we combined enzastaurin with the Src inhibitor dasatinib. In five cell lines (CH2879, OUMS27, SW1353, NDCS-1, and L3252) cell viability after combination treatment dropped below 50% (fig 7.1C). However, the reduction in cell viability could not be ascribed to a synergistic effect in any of the cell lines. Rather it was found to be due to the effect of dasatinib (L835, NDCS-1 and L3252) or the additive effect of dasatinib and enzastaurin (combination indices >2, fig 7.1C). TP53 mutation status was not correlated to response (*p=0.38*, fig 7.1C). Interestingly, treatment with 1μM dasatinib for 24hrs was found to decrease phosphorylation of AKT in OUMS27, L835, L3252 and NDCS-1 cell lines (fig 7.2A).

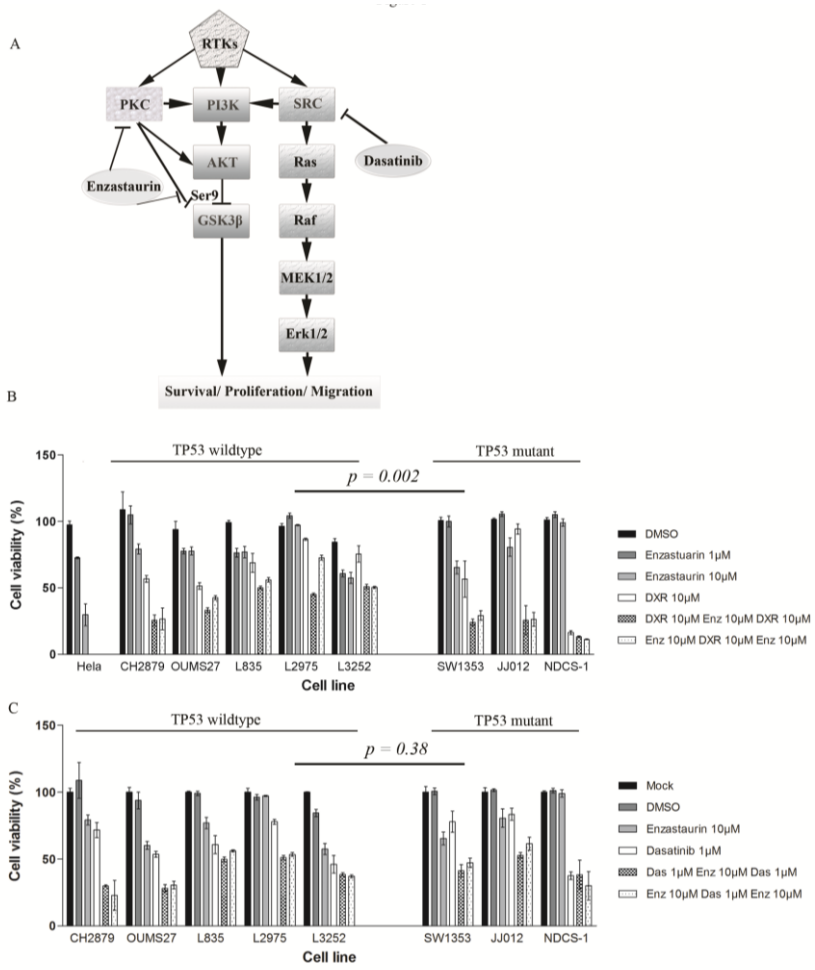

Figure 7.1. Chondrosarcoma cell lines are not sensitive to PKC inhibition. A: Schematic representation of activation of PI3K and Src pathway by receptor tyrosine kinases (RTKs). RTKs can activate protein kinase C (PKC), phosphatidylinositol 3-kinase (PI3K), and Src. PKC and Src can also activate the PI3K/AKT/GSK3β pathway, promoting survival, proliferation, and migration. The Src pathway activates the Ras/Raf pathway. Enzastaurin is a selective PKC inhibitor also reported to inhibitinactivating phosphorylation of GSK3β. Dasatinib is a Src inhibitor. Adapted from Fizazi (62).B: HeLa cell line showing 70% decrease in cell viability after treatment with enzastaurin. Chondrosarcoma cell lines poorly respond to enzastaurin alone, and an additive effect is observed when alternating 10μM doxorubicin (DXR) and 10μM enzastaurin (Enz) for 24hrs each for 72hrs in total. No difference is observed when order of administration is reversed. Significant difference between TP53 mutant and wildtype cell lines (*p=0.002*).C: Combination of enzastaurin with Src inhibitor dasatinib (Das) showing additive effect in chondrosarcoma cell lines. No significant difference is observed between TP53 mutant and wildtype cell lines (*p=0.38*).

Src signaling contributes to chemoresistance of chondrosarcoma cells
We have previously shown Src signaling to be involved in chondrosarcoma cell proliferation (13). Immunoblotting confirmed the presence of phosphorylated Src (Y418) in the chondrosarcoma cell lines, with lowest expression in L835 cells, and 24hrs with 1µM dasatinib resulted in decreased pSrc levels (Fig 7.2A). To examine the role of Src signaling in chemoresistance, dasatinib was combined with doxorubicin. A synergistic effect was observed in cell lines CH2879, OUMS27, SW1353, JJ012, NDCS-1, and L2975 (combination indices ranging from 0.09 to 0.88 fig 7.2C), and the order of drug administration did not influence efficacy. Interestingly, a significant difference between both the cell viability (*p=0.002*) and the combination indices (*p=0.043*) was observed between cell lines with and without TP53 mutations, and both cell lines that were resistant to combination treatment (L835 and L3252) were wildtype for TP53 mutations. We continued to investigate p53 accumulation as well as MDM2 and p21 expression in cells treated with and without treatment with dasatinib (fig 7.2B). As expected, high p53 protein expression with low to absent p21was seen in the three TP53 mutant cell lines. All TP53 wildtype cell lines demonstrated low p53 and p21 protein expression with the exception of CH2879, demonstrating high levels of p53 and p21. Protein levels were not affected by dasatinib treatment. All cell lines showed low MDM2 protein expression. No correlation with IDH mutations was found.

Src inhibition combined with doxorubicin induces apoptosis
Using annexinV binding live cell imaging we confirmed our previous findings (13) that dasatinib monotreatment does not induce apoptosis (fig 7.2D first 24 hours). However, when combined with doxorubicin, up to 50% of cells had entered apoptosis after completion of the third cycle of combination treatment; (JJ012 cell line shown as representative cell line, fig 7.2D). Due to the effect of doxorubicin during the first 24 hours, 10% more cells had entered apoptosis during combination treatment starting doxorubicin, than during combination treatment starting with dasatinib. Apoptosis could be inhibited using the pan-caspase inhibitor zVADfmk (results not shown).

Dasatinib inhibits migration of chondrosarcoma cell lines
As Src family members also play a role in motility and adhesion (37), we continued to investigate the migratory capacity of the chondrosarcoma cell lines. Using a transwell system, all chondrosarcoma cell lines showed migratory properties, and started migrating approximately 30 minutes after plating, except for JJ012 cells, which started migrating only 4 hours after plating (results not shown). In the presence of dasatinib, however, a complete inhibition of cell migration was achieved for all cell lines at concentrations as low as 200nM (fig 7.2E, F). No difference between cell lines harboring TP53 mutations and wildtype cell lines was observed.

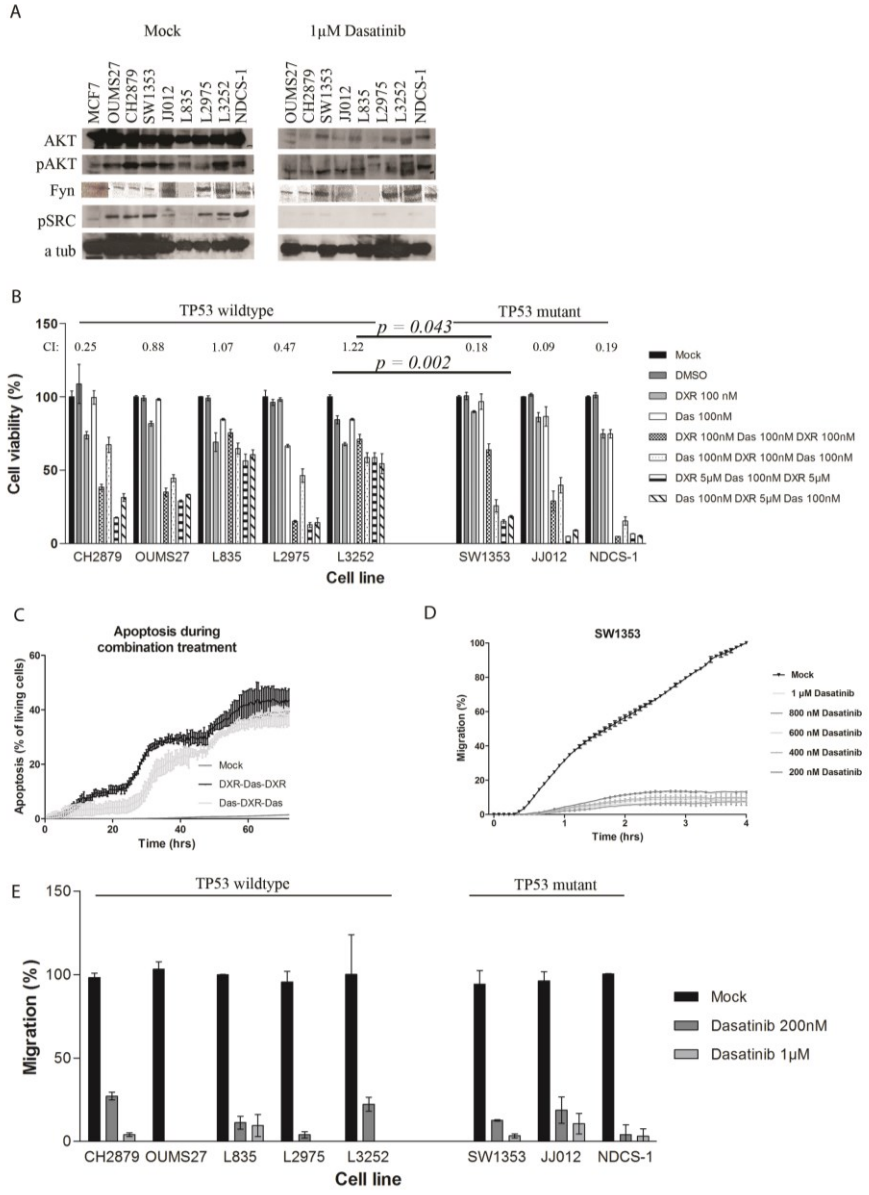

Figure 7.2. The Src pathway is involved in chondrosarcoma chemoresistance.
A: Immunoblotting showing AKT, pAKT, Fyn, pSrc and loading control α-tubulin (a tub) for untreated chondrosarcoma cell lines and after 24 hrs 1µM dasatinib (Das). MCF-7: breast cancer cell line, shown as positive control. Presence of all kinases in all cell lines. phophorylated Src in all cell lines, although levels are very low in L835. After 24hrs 1µM

dasatinib treatment, levels of pSrc (at Y418) are decreased in all cell lines, and of pAKT in OUMS27, L835, L3252, JJ012, and NDCS-1. B: Immunoblotting showing p53, MDM2, and p21 in untreated chondrosarcoma cell lines (Mock) and after 24hrs 1µM dasatinib (Das). U2OS (osteosarcoma) cell line is shown as positive control. MDM2 expression is low in all cell lines. TP53 wildtype cell lines are negative for p53 protein expression, with low p21 protein expression, except for CH2879. TP53 mutant cell lines show high TP53 protein expression with low p21 protein expression. No change in protein levels is observed after 24hrs 1µM dasatinib treatment. C: Combination of dasatinib (Das) with doxorubicin (DXR) leads to synergistic loss of cell viability at concentrations which are ineffective on their own in most cell lines. Combination treatment was more effective in TP53 mutant cell lines than in TP53 wildtype cell lines (*p=0.002* for cell viability, *p=0.043* for combination indices). D: Apoptosis assay in JJ012 cell line alternating 1µM dasatinib (Das)and 1µM doxorubicin (DXR)demonstrates the occurrence of apoptosis during combination. Apoptosis is calculated as percentage of AnnexinV-Alexxa633 stained cells per total number of HOECHST stained cells. D, E: Dasatinib successfully inhibits migration in chondrosarcoma cell lines in concentrations as low as 200nM. E: SW1353 cell line shown as representative over the course of 4 hrs, F: bar chart showing migration for all cell lines.

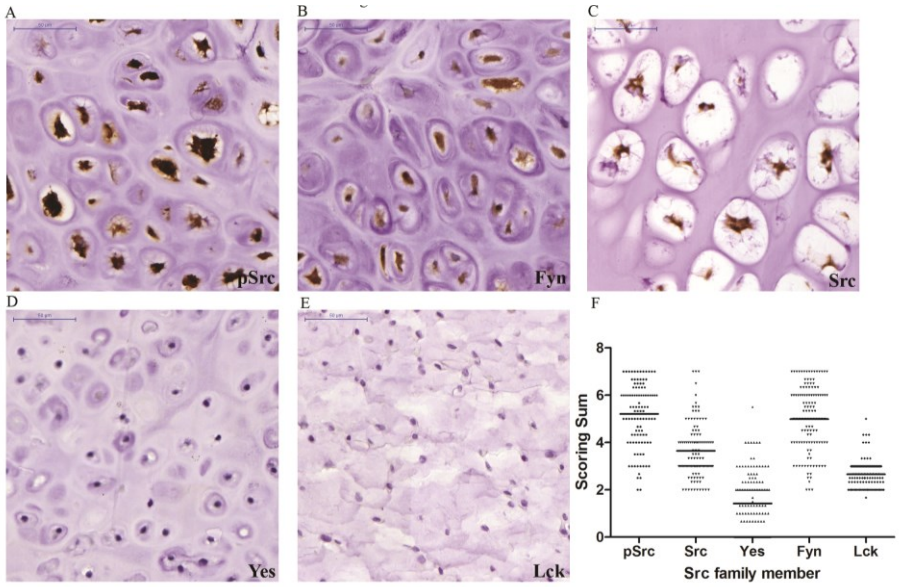

Figure 7.3. Immunohistochemistry demonstrating expression of Src family members in conventional chondrosarcoma tissue.
A: High pSrc expression in grade I chondrosarcoma. B: High intensity nuclear FYN expression in grade I chondrosarcoma. C: High intensity cytoplasmic and nuclear Srcexpression in grade I chondrosarcoma. D: Absence of Yes expression in grade II chondrosarcoma. E: Absence of Lck in grade II chondrosarcoma. Scale bars: 50µm. F: Scatterplot showing distribution of staining scores among chondrosarcoma tissue samples.

Fyn is the most important Src family member in chondrosarcoma tissues
To identify the most important Src family member in chondrosarcoma, we evaluated the expression of the 4 family members Src, Yes, Fyn and Lck, as well as pSrc in primary tumor samples. Active Src signaling as evidenced by positive staining for pSrc was found in 88-100% of the tumors (table 7.4, fig 7.3A, F).Of the 4 Src family members we found Fyn (76.1% high expression (89/117)) and Src (46.6% high expression (48/103)) to be most abundantly expressed in chondrosarcoma (table 7.4, figure 7.3B, C, F). In contrast, high expression of Yes and Lck was observed in only 5% of all chondrosarcoma cases (6/116 and 6/120 respectively) (table 7.4, figure 7.3D, E, F). During the staining procedures some cores were lost due to inherent structural instability of the tissue. A significant increase in Src expression was seen between grade I and grade II peripheral CS (p=0.005 Pearson chi squared test). Though not significant, Src expression in tumors was found to be inversely correlated with overall survival (p=0.3 log rank). Fyn expression was found to significantly increase with increasing histological grade in both peripheral chondrosarcoma (p= 0.05 Pearson chi squared test) and central chondrosarcoma (p= 0.000 Pearson chi squared test). No significant correlations to metastasis were found. Using western blot we confirmed expression of FYN in all cell lines, with low expression in L835 (fig 7.2A)

Discussion

Chondrosarcomas are resistant to conventional chemotherapy. Despite ongoing research, there is still nothing to offer patients with unresectable or metastatic disease and the need for new, targeted therapies is high. We here explored the effects of increased PI3K/AKT/GSK3β and Src signaling on chondrosarcoma chemoresistance and cell migration using enzastaurin and dasatinib, respectively. We show that dasatinib is more effective in overcoming chondrosarcoma chemoresistance than enzastaurin, and acts synergistically with doxorubicin to inhibit cell viability and induce apoptosis. Most importantly, we show that in cell lines with TP53 mutations, the combination of tyrosine kinase inhibitors with doxorubicin is more beneficial than in wildtype TP53 cell lines.
Chondrosarcoma is a heterogeneous disease, and this heterogeneity is represented in the cell lines. Recently, IDH1 and IDH2 mutations were found in chondrosarcoma (38), and we published that these mutations are retained in chondrosarcoma cell lines (12;30). Of the two cell lines that were nonresponsive to combination treatment of doxorubicin with dasatinib, one central chondrosarcoma cell line (L835) carried an IDH1 mutation, whereas the other (dedifferentiated chondrosarcoma cell line (L3252)) was wildtype for IDH. Thus, no correlation between IDH mutation status and response to dasatinib monotreatment or combination treatment with doxorubicin was observed. More likely, the lack of

sensitivity to dasatinib in the L835 cell line is caused by the low pSrc activity in this cell line.

Src inhibition with dasatinib resulted in successful sensitization for doxorubicin treatment, especially in TP53 mutant chondrosarcoma cell lines. Approximately 30% of chondrosarcomas carry TP53 mutations, and these mutations are found especially in high grade chondrosarcomas (39;40). Three of the eight cell lines carry a TP53 mutation (SW1353, JJ012, and NDCS-1), and these cell lines also showed a better response to combination treatment with low combination indices when compared to TP53 wildtype cell lines. This is an interesting result as mutant TP53 is described to actively inhibit apoptosis through activation of p21 (41) or to confer chemoresistance through engaging in oncogenic transcription complexes (42). Previously, dasatinib was found to interfere with the p53 transcriptional activity induced by the MDM2 inhibitor nutlin-3(43). We show that dasatinib does not affect p53 nor p21 protein expression in chondrosarcoma cells. Dasatinib as a single agent proved ineffective in chondrosarcoma patients (Schuetze, CTOS 2010). However, recent clinical studies with dasatinib in other malignancies have shown its efficacy not only irrespective of TP53 status as a single agent (44), but also to overcome TP53 mutation status related chemoresistance (45). The results of these clinical studies in combination with the data we show here strongly suggest clinical evaluation of the efficacy of dasatinib in combination with doxorubicin in chondrosarcoma patients harboring TP53 mutations.

Since we demonstrate Src signaling to play a role in chemoresistance, we further explored the expression of the different Src family kinases (SFKs) in human chondrosarcoma tissues. Fyn was most widely expressed (89/117) and was found to increase with increasing histological grade, suggesting a role in chondrosarcoma progression. Fyn is reported to be upregulated in multiple cancers, and to be associated with malignant progression and metastasis formation (37;46;47). We confirmed that indeed the Src pathway is important in chondrosarcoma cell motility, since dasatinib completely inhibited migratory capacity of all chondrosarcoma cell lines even at low dose.

Clinical trials with dasatinib have shown the efficacy and low toxicity of dasatinib in combination with conventional chemotherapeutic agents in solid tumors (48). In a phase II study of dasatinib with hyper-CVAD in patients with Philadelphia chromosome positive lymphoblastic leukemia, long term remission was achieved in newly diagnosed patients (49), and in a phase I-II study of dasatinib with doxetaxel in castration resistant prostate cancer, disappearance of bone lesions was obtained (50). The results obtained with dasatinib in combination with chemotherapy strongly encourage the exploration of dasatinib in combination with doxorubicin in patients with chondrosarcoma.

Table 7.4 Protein expression in tumors using immunohistochemistry

	Osteochondroma	**Peripheral Chondrosarcoma**			**Enchondroma**	**Central Chondrosarcoma**		
		Grade I	**Grade II**	**Grade III**		**Grade I**	**Grade II**	**Grade III**
pSrc	3/3 (100%)	12/13 (92%)	6/6 (**100**%)	3/3 (**100**%)	4/5 (80%)	21/24 (88%)	21/22 (96%)	10/10 (**100**%)
Src	1/7 (14%)	7/17 (41%)	8/8 (**100**%)	2/3 (67%)	4/7 (57%)	12/31 (39%)	12/31 (39%)	7/13 (54%)
Yes	0/7 (0%)	3/23 (13%)	0/10 (0%)	0/3 (0%)	0/7 (0%)	0/36 (0%)	3/30 (10%)	0/14 (0%)
Fyn	7/8 (88%)	16/20 (80%)	9/10 (90%)	3/3 (**100**%)	5/5 (**100%**)	17/35 (49%)	31/35 (89%)	13/14 (93%)
Lck	0/3 (0%)	1/23 (4%)	2/10 (20%)	0/3 (0%)	0/7 (0%)	1/38 (3%)	0/33 (0%)	2/13 (15%)

Both the PI3K/AKT/GSK3β and Src kinase pathways are activated by receptor tyrosine kinases (RTKs) (18;19), and play diverse roles in promoting growth, survival, and metastasis (16-18;20;51). We show here that constitutive activation of AKT due to mutations does not play a role in chondrosarcoma, and further research should elucidate which RTK is responsible for the high AKT, GSK3β, and Src phosphorylation (13). A possible candidate is IGF-1, which can activate the PI3K/AKT and Src pathway through the RTK IGF-1R (52), and has been shown to induce PI3K/AKT signaling and migration in chondrosarcoma cell lines (53). Src family kinases can induce phosphorylation of the RTK domains of IGF-1 as well as the PDGF receptors through SHP-2 leading to receptor internalization. This increases binding efficacy with PI3K, leading to increased proliferative capacity of cancer cells (54;55). Moreover, AKT functions as a gatekeeper of apoptosis through phosphorylation of BAD. AKT mediated phosphorylation of BAD inhibits its binding capacity to antiapoptotic BCL-2 family members, which will prevent a cell from entering apoptosis (56;57). We recently published that the antiapoptotic BCL-2 family members also play a role in chondrosarcoma chemoresistance (29). Combined with the results of the present study, this is suggestive of a common mechanism. However, more studies are needed to explore whether the activation of the IGF pathway by Src leading to the inhibition of BH3 proteins and apoptosis through AKT may be involved in chondrosarcoma chemoresistance.

In conclusion, we found that inhibition of the Src pathway was successful in overcoming chemoresistance and inhibited migration. A synergistic response to combination treatment was observed which was significantly stronger ($p=0.002$) in cell lines harboring TP53 mutations. Moreover, as we observed the Src family member Fyn to be the most prevalent in chondrosarcoma tissues, we hypothesize Fyn to play a major role in the chemoresistance and malignant progression of chondrosarcoma. These results aid in the understanding of signaling pathways in chondrosarcoma and may lead to the development of effective therapeutic strategies for currently untreatable metastatic chondrosarcoma.

Reference List

(1) Hogendoorn PCW, Bovée JVMG, Nielsen GP. Chondrosarcoma (grades I-III), including primary and secondary variants and periosteal chondrosarcoma. In: Fletcher C.D.M., Bridge JA, Hogendoorn PCW, Mertens F, editors. World Health Classification of Tumours. Pathology and Genetics of Tumours of Soft Tissue and Bone. 4 ed. 2013. p. 264-8.

(2) Gelderblom H, Hogendoorn PCW, Dijkstra SD, van Rijswijk CS, Krol AD, Taminiau AH, Bovee JV. The clinical approach towards chondrosarcoma. Oncologist 2008;13(3):320-9.

(3) Evans HL, Ayala AG, Romsdahl MM. Prognostic factors in chondrosarcoma of bone. A clinicopathologic analysis with emphasis on histologic grading. Cancer 1977;40:818-31.

(4) David E, Blanchard F, Heymann MF, De PG, Gouin F, Redini F, Heymann D. The Bone Niche of Chondrosarcoma: A Sanctuary for Drug Resistance, Tumour Growth and also a Source of New Therapeutic Targets. Sarcoma 2011;2011:-932451.

(5) Staals EL, Bacchini P, Bertoni F. Dedifferentiated central chondrosarcoma. Cancer 2006 June 15;106(12):2682-91.

(6) Bovée JVMG, Hogendoorn PCW, Wunder JS, Alman BA. Cartilage tumours and bone development: molecular pathology and possible therapeutic targets. Nat Rev Cancer 2010;10(7):481-8.

(7) Bovée JVMG, Van den Broek LJCM, Cleton-Jansen AM, Hogendoorn PCW. Up-regulation of PTHrP and Bcl-2 expression characterizes the progression of osteochondroma towards peripheral chondrosarcoma and is a late event in central chondrosarcoma. Lab Invest 2000;80:1925-33.

(8) Hameetman L, Kok P, Eilers PHC, Cleton-Jansen AM, Hogendoorn PCW, Bovée JVMG. The use of Bcl-2 and PTHLH immunohistochemistry in the diagnosis of peripheral chondrosarcoma in a clinicopathological setting. Virchows Arch 2005;446:430-7.

(9) Rozeman LB, Hameetman L, Cleton-Jansen AM, Taminiau AHM, Hogendoorn PCW, Bovée JVMG. Absence of IHH and retention of PTHrP signalling in enchondromas and central chondrosarcomas. J Pathol 2005;205(4):476-82.

(10) Soderstrom M, Palokangas T, Vahlberg T, Bohling T, Aro H, Carpen O. Expression of ezrin, Bcl-2, and Ki-67 in chondrosarcomas. APMIS 2010;118(10):769-76.

(11) Lechler P, Renkawitz T, Campean V, Balakrishnan S, Tingart M, Grifka J, Schaumburger J. The antiapoptotic gene survivin is highly expressed in human chondrosarcoma and promotes drug resistance in chondrosarcoma cells in vitro. BMC Cancer 2011;11:-120.

(12) van Oosterwijk JG, de JD, van Ruler MA, Hogendoorn PC, Dijkstra PS, van Rijswijk CS, Machado IS, Llombart-Bosch A, Szuhai K, Bovée JVMG. Three new chondrosarcoma cell lines: one grade III conventional central chondrosarcoma and two dedifferentiated chondrosarcomas of bone. BMC Cancer 2012 August 28;12(375):-375.

(13) Schrage YM, Briaire-de Bruijn IH, de Miranda NFCC, van Oosterwijk JG, Taminiau AHM, van Wezel T, Hogendoorn PCW, Bovée JVMG. Kinome profiling of chondrosarcoma reveals Src-pathway activity and dasatinib as option for treatment. Cancer Res 2009;69(15):6216-22.

(14) Verbeek BS, Vroom TM, Adriaansen-Slot SS, Ottenhoff-Kalff AE, Geertzema JG, Hennipman A, Rijksen G. c-Src protein expression is increased in human breast cancer. An immunohistochemical and biochemical analysis. J Pathol 1996;180(4):383-8.

(15) Gelman IH. Src-family tyrosine kinases as therapeutic targets in advanced cancer. Front Biosci (Elite Ed) 2011;3:801-7.

(16) McNamara CR, Degterev A. Small-molecule inhibitors of the PI3K signaling network. Future Med Chem 2011;3(5):549-65.

(17) Aligayer H, Boyd DD, Heiss MM, Abdalla EK, Curley SA, Gallick GE. Activation of Src kinase in primary colorectal carcinoma: an indicator of poor clinical prognosis. Cancer 2002;94(2):344-51.

(18) Wheeler DL, Iida M, Dunn EF. The role of Src in solid tumors. Oncologist 2009;14(7):667-78.

(19) Goode N, Hughes K, Woodgett JR, Parker PJ. Differential regulation of glycogen synthase kinase-3 beta by protein kinase C isotypes. J Biol Chem 1992;267(24):16878-82.

(20) Saini S, Arora S, Majid S, Shahryari V, Chen Y, Deng G, Yamamura S, Ueno K, Dahiya R. Curcumin modulates microRNA-203-mediated regulation of the Src-Akt axis in bladder cancer. Cancer Prev Res (Phila) 2011;4(10):1698-709.

(21) Johnson D, Agochiya M, Samejima K, Earnshaw W, Frame M, Wyke J. Regulation of both apoptosis and cell survival by the v-Src oncoprotein. Cell Death Differ 2000;7(8):685-96.

(22) Aeder SE, Martin PM, Soh JW, Hussaini IM. PKC-eta mediates glioblastoma cell proliferation through the Akt and mTOR signaling pathways. Oncogene 2004 December 2;23(56):9062-9.

(23) Kawakami Y, Nishimoto H, Kitaura J, Maeda-Yamamoto M, Kato RM, Littman DR, Leitges M, Rawlings DJ, Kawakami T. Protein kinase C betaII regulates Akt phosphorylation on Ser-473 in a cell type- and stimulus-specific fashion. J Biol Chem 2004;279(46):47720-5.

(24) Fang X, Yu S, Tanyi JL, Lu Y, Woodgett JR, Mills GB. Convergence of multiple signaling cascades at glycogen synthase kinase 3: Edg receptor-mediated phosphorylation and inactivation by lysophosphatidic acid through a protein kinase C-dependent intracellular pathway. Mol Cell Biol 2002;22(7):2099-110.

(25) Shrivastav S, Bonar RA, Stone KR, Paulson DF. An Invitro Assay Procedure to Test Chemotherapeutic Drugs on Cells from Human Solid Tumors. Cancer Res 1980;40(12):4438-42.

(26) Faul MM, Gillig JR, Jirousek MR, Ballas LM, Schotten T, Kahl A, Mohr M. Acyclic N-(azacycloalkyl)bisindolylmaleimides: isozyme selective inhibitors of PKCbeta. Bioorg Med Chem Lett 2003;13(11):1857-9.

(27) Lombardo LJ, Lee FY, Chen P, Norris D, Barrish JC, Behnia K, Castaneda S, Cornelius LA, Das J, Doweyko AM, Fairchild C, Hunt JT, Inigo I, Johnston K, Kamath A, Kan D, Klei H, Marathe P, Pang S, Peterson R, Pitt S, Schieven GL, Schmidt RJ, Tokarski J, Wen ML et al. Discovery of N-(2-chloro-6-methyl- phenyl)-2-(6-(4-(2-hydroxyethyl)- piperazin-1-yl)-2-methylpyrimidin-4- ylamino)thiazole-5-carboxamide (BMS-354825), a dual Src/Abl kinase inhibitor with potent antitumor activity in preclinical assays. J Med Chem 2004;47(27):6658-61.

(28) Cleton-Jansen AM, van Beerendonk HM, Baelde HJ, Bovée JVMG, Karperien M, Hogendoorn PCW. Estrogen signaling is active in cartilaginous tumors: implications for antiestrogen therapy as treatment option of metastasized or irresectable chondrosarcoma. Clin Cancer Res 2005;11(22):8028-35.

(29) van Oosterwijk JG, Herpers B, Meijer D, Briaire-de Bruijn IH, Cleton-Jansen AM, Gelderblom H, van de Water B, Bovée JVMG. Restoration of chemosensitivity for doxorubicin and cisplatin in chondrosarcoma in vitro: BCL-2 family members cause chemoresistance. Ann Oncol 2012;23(6):1617-26.

(30) Pansuriya TC, van ER, d'Adamo P, van Ruler MA, Kuijjer ML, Oosting J, Cleton-Jansen AM, van Oosterwijk JG, Verbeke SL, Meijer D, van WT, Nord KH, Sangiorgi L, Toker B, Liegl-Atzwanger B, San-Julian M, Sciot R, Limaye N, Kindblom LG, Daugaard S, Godfraind C, Boon LM, Vikkula M, Kurek KC, Szuhai K et al. Somatic mosaic IDH1 and IDH2 mutations are associated with enchondroma and spindle cell hemangioma in Ollier disease and Maffucci syndrome. Nat Genet 2011;43(12):1256-61.

(31) Puigvert JC, de BH, van de Water B, Danen EH. High-throughput live cell imaging of apoptosis. Curr Protoc Cell Biol 2010 June;Chapter 18:Unit-13.

(32) Kononen J, Bubendorf L, Kallioniemi A, Barlund M, Schraml P, Leighton S, Torhorst J, Mihatsch MJ, Sauter G, Kallioniemi OP. Tissue microarrays for high-throughput molecular profiling of tumor specimens. Nat Med 1998 \;4(7):844-7.

(33) Chou TC, Talalay P. Quantitative analysis of dose-effect relationships: the combined effects of multiple drugs or enzyme inhibitors. Adv Enzyme Regul 1984;22:27-55.

(34) Graff JR, McNulty AM, Hanna KR, Konicek BW, Lynch RL, Bailey SN, Banks C, Capen A, Goode R, Lewis JE, Sams L, Huss KL, Campbell RM, Iversen PW, Neubauer BL, Brown TJ, Musib L, Geeganage S, Thornton D. The protein kinase Cbeta-selective inhibitor, Enzastaurin (LY317615.HCl), suppresses signaling through the AKT pathway, induces apoptosis, and suppresses growth of human colon cancer and glioblastoma xenografts. Cancer Res 2005 \ 15;65(16):7462-9.

(35) Mahajan K, Mahajan NP. PI3K-independent AKT activation in cancers: a treasure trove for novel therapeutics. J Cell Physiol 2012 \;227(9):3178-84.

(36) Carpten JD, Faber AL, Horn C, Donoho GP, Briggs SL, Robbins CM, Hostetter G, Boguslawski S, Moses TY, Savage S, Uhlik M, Lin A, Du J, Qian YW, Zeckner DJ, Tucker-Kellogg G, Touchman J, Patel K, Mousses S, Bittner M, Schevitz R, Lai MH, Blanchard KL, Thomas JE. A transforming mutation in the pleckstrin homology domain of AKT1 in cancer. Nature 2007 26;448(7152):439-44.

(37) Saito YD, Jensen AR, Salgia R, Posadas EM. Fyn: a novel molecular target in cancer. Cancer 2010 April 1;116(7):1629-37.

(38) Amary MF, Bacsi K, Maggiani F, Damato S, Halai D, Berisha F, Pollock R, O'Donnell P, Grigoriadis A, Diss T, Eskandarpour M, Presneau N, Hogendoorn PC, Futreal A, Tirabosco R, Flanagan AM. IDH1 and IDH2 mutations are frequent events in central chondrosarcoma and central and periosteal chondromas but not in other mesenchymal tumours. J Pathol 2011;224(3):334-43.

(39) Terek RM, Healey JH, Garin-Chesa P, Mak S, Huvos A, Albino AP. p53

mutations in chondrosarcoma. Diagn Mol Pathol 1998;7(1):51-6.

(40) Oshiro Y, Chaturvedi V, Hayden D, Nazeer T, Johnson M, Johnston DA, Ordonez NG, Ayala AG, Czerniak B. Altered p53 is associated with aggressive behavior in chondrosarcoma; a long term follow-up study. Cancer 1998;83:2324-34.

(41) Donzelli S, Fontemaggi G, Fazi F, Di AS, Padula F, Biagioni F, Muti P, Strano S, Blandino G. MicroRNA-128-2 targets the transcriptional repressor E2F5 enhancing mutant p53 gain of function. Cell Death Differ 2012;19(6):1038-48.

(42) Huang Y, Jeong JS, Okamura J, Sook-Kim M, Zhu H, Guerrero-Preston R, Ratovitski EA. Global tumor protein p53/p63 interactome: making a case for cisplatin chemoresistance. Cell Cycle 2012;11(12):2367-79.

(43) Zauli G, Voltan R, Bosco R, Melloni E, Marmiroli S, Rigolin GM, Cuneo A, Secchiero P. Dasatinib plus Nutlin-3 shows synergistic antileukemic activity in both p53 wild-type and p53 mutated B chronic lymphocytic leukemias by inhibiting the Akt pathway. Clin Cancer Res 2011;17(4):762-70.

(44) Bosco R, Rabusin M, Voltan R, Celeghini C, Corallini F, Capitani S, Secchiero P. Anti-leukemic activity of dasatinib in both p53(wild-type) and p53(mutated) B malignant cells. Invest New Drugs 2012;30(1):417-22.

(45) Amrein L, Hernandez TA, Ferrario C, Johnston J, Gibson SB, Panasci L, Aloyz R. Dasatinib sensitizes primary chronic lymphocytic leukaemia lymphocytes to chlorambucil and fludarabine in vitro. Br J Haematol 2008;143(5):698-706.

(46) Posadas EM, Al-Ahmadie H, Robinson VL, Jagadeeswaran R, Otto K, Kasza KE, Tretiakov M, Siddiqui J, Pienta KJ, Stadler WM, Rinker-Schaeffer C, Salgia R. FYN is overexpressed in human prostate cancer. BJU Int 2009;103(2):171-7.

(47) Chen ZY, Cai L, Bie P, Wang SG, Jiang Y, Dong JH, Li XW. Roles of Fyn in pancreatic cancer metastasis. J Gastroenterol Hepatol 2010;25(2):293-301.

(48) Montero JC, Seoane S, Ocana A, Pandiella A. Inhibition of SRC family kinases and receptor tyrosine kinases by dasatinib: possible combinations in solid tumors. Clin Cancer Res 2011 1;17(17):5546-52.

(49) Ravandi F, O'Brien S, Thomas D, Faderl S, Jones D, Garris R, Dara S, Jorgensen J, Kebriaei P, Champlin R, Borthakur G, Burger J, Ferrajoli A, Garcia-Manero G, Wierda W, Cortes J, Kantarjian H. First report of phase 2 study of dasatinib with hyper-CVAD for the frontline treatment of patients with Philadelphia chromosome-positive (Ph+) acute lymphoblastic leukemia. Blood 2010;116(12):2070-7.

(50) Araujo JC, Mathew P, Armstrong AJ, Braud EL, Posadas E, Lonberg M, Gallick GE, Trudel GC, Paliwal P, Agrawal S, Logothetis CJ. Dasatinib combined with docetaxel for castration-resistant prostate cancer: results from a phase 1-2 study. Cancer 2012;118(1):63-71.

(51) Yang J, Takahashi Y, Cheng E, Liu J, Terranova PF, Zhao B, Thrasher JB, Wang HG, Li B. GSK-3beta promotes cell survival by modulating Bif-1-dependent autophagy and cell death. J Cell Sci 2010;123(Pt 6):861-70.

(52) Grimberg A. Mechanisms by which IGF-I may promote cancer. Cancer Biol Ther 2003;2(6):630-5.

(53) Wu CM, Li TM, Hsu SF, Su YC, Kao ST, Fong YC, Tang CH. IGF-I enhances alpha5beta1 integrin expression and cell motility in human

chondrosarcoma cells. J Cell Physiol 2011;226(12):3270-7.

(54) Carver KC, Piazza TM, Schuler LA. Prolactin enhances insulin-like growth factor I receptor phosphorylation by decreasing its association with the tyrosine phosphatase SHP-2 in MCF-7 breast cancer cells. J Biol Chem 2010;285(11):8003-12.

(55) Wu CJ, O'Rourke DM, Feng GS, Johnson GR, Wang Q, Greene MI. The tyrosine phosphatase SHP-2 is required for mediating phosphatidylinositol 3-kinase/Akt activation by growth factors. Oncogene 2001;20(42):6018-25.

(56) Gilmore AP, Valentijn AJ, Wang P, Ranger AM, Bundred N, O'Hare MJ, Wakeling A, Korsmeyer SJ, Streuli CH. Activation of BAD by therapeutic inhibition of epidermal growth factor receptor and transactivation by insulin-like growth factor receptor. J Biol Chem 2002;277(31):27643-50.

(57) Maddika S, Ande SR, Panigrahi S, Paranjothy T, Weglarczyk K, Zuse A, Eshraghi M, Manda KD, Wiechec E, Los M. Cell survival, cell death and cell cycle pathways are interconnected: implications for cancer therapy. Drug Resist Updat 2007;10(1-2):13-29.

(58) Kunisada T, Miyazaki M, Mihara K, Gao C, Kawai A, Inoue H, Namba M. A new human chondrosarcoma cell line (OUMS-27) that maintains chondrocytic differentiation. Int J Cancer 1998;77(6):854-9.

(59) Gil-Benso R, Lopez-Gines C, Lopez-Guerrero JA, Carda C, Callaghan RC, Navarro S, Ferrer J, Pellin A, Llombart-Bosch A. Establishment and characterization of a continuous human chondrosarcoma cell line, ch-2879: comparative histologic and genetic studies with its tumor of origin. Lab Invest 2003;83(6):877-87.

(60) Scully SP, Berend KR, Toth A, Qi WN, Qi Z, Block JA. Marshall Urist Award. Interstitial collagenase gene expression correlates with in vitro invasion in human chondrosarcoma. Clin Orthop Relat Res 2000;(376):291-303.

(61) Kudo N, Ogose A, Hotta T, Kawashima H, Gu W, Umezu H, Toyama T, Endo N. Establishment of novel human dedifferentiated chondrosarcoma cell line with osteoblastic differentiation. Virchows Arch 2007;451(3):691-9.

(62) Fizazi K. The role of Src in prostate cancer. Ann Oncol 2007;18(11):1765-73.

Chapter 8

Functional profiling of receptor tyrosine kinases and downstream signaling in human chondrosarcomas identifies pathways for rational targeted therapy

This chapter is based on the manuscript: Zhang Y-X, van Oosterwijk JG, Sicinska E, Moss S, Remillard SP, Wezel T, Bühnemann C, Hassan AB, Demetri GD, Bovée JVMG, Wagner AJ. *Clin Cancer Res. 2013;19(14):3796-807*

Translational Relevance

Chondrosarcomas are notoriously resistant to conventional chemotherapy. There is an urgent need to identify therapeutic targets and to develop novel treatment strategies for this disease.
We found multiple RTKs to be activated in chondrosarcoma cells and to have critical roles in mediating cell growth. Strong phosphorylation of S6 was detected in 69% of conventional chondrosarcoma and 44% of dedifferentiated chondrosarcoma clinical samples and is likely due to RTK activation. Inhibition of PI3K and mTOR, signaling proteins downstream of RTKs and upstream of S6, potently blocked the growth of chondrosarcoma cells *in vitro* and *in vivo*.
NRAS mutations were identified in 12% of conventional central chondrosarcoma tumor tissues. An *NRAS* mutation-harboring chondrosarcoma cell line was sensitive to treatment with a MEK inhibitor.
Our findings provide new insights into the genetics and the heterogeneity of chondrosarcomas, and have implications for the clinical development of PI3K/mTOR or MEK inhibitors in this disease.

Abstract

Chondrosarcomas are notoriously resistant to cytotoxic chemotherapeutic agents. We sought to identify critical signaling pathways that contribute to their survival and proliferation, and which may provide potential targets for rational therapeutic interventions.
Activation of receptor tyrosine kinases (RTKs) was surveyed using phospho-RTK arrays. S6 phosphorylation and *NRAS* mutational status were examined in chondrosarcoma primary tumor tissues. Small interfering RNA or small molecule inhibitors against RTKs or downstream signaling proteins were applied to chondrosarcoma cells and changes in biochemical signaling, cell cycle, and cell viability were determined. *In vivo* anti-tumor activity of BEZ235, a phosphoinositide-3-kinase (PI3K)/mammalian target of rapamycin (mTOR) inhibitor, was evaluated in a chondrosarcoma xenograft model.
Several RTKs were identified as critical mediators of cell growth, but the RTK dependencies varied among cell lines. In exploration of downstream signaling pathways, strong S6 phosphorylation was found in 69% of conventional chondrosarcomas and 44% of dedifferentiated chondrosarcomas. Treatment with BEZ235 resulted in dramatic reduction in the growth of all chondrosarcoma cell lines. Tumor growth was similarly inhibited in a xenograft model of chondrosarcoma. In addition, chondrosarcoma cells with an *NRAS* mutation were sensitive to treatment with a MEK inhibitor. Functional *NRAS* mutations were found in 12% of conventional central chondrosarcomas.
RTKs are commonly activated in chondrosarcoma, but because of their considerable heterogeneity, targeted inhibition of the PI3K/mTOR pathway

represents a rational therapeutic strategy. Chondrosarcomas with *NRAS* mutations may benefit from treatment with MEK inhibitors.

Introduction

Chondrosarcomas, mesenchymal tumors with cartilaginous differentiation, are biologically and clinically heterogeneous. Complete surgical resection of localized disease remains the only known curative treatment. No systemic treatments have been proven to be effective in the metastatic or unresectable setting. Therefore, there is an urgent need to identify therapeutic targets and to develop novel treatment strategies for patients with this disease (1-4).

Deregulated expression and/or function of receptor tyrosine kinases (RTKs) by gene amplification, mutation, or translocation has been found to be important for cancer cell proliferation, survival, motility and invasion, as well as tumor angiogenesis and resistance to chemotherapy (5, 6). Given their pivotal role in tumor initiation and progression, RTKs have become one of the most prominent target families for drug development, and more than ten inhibitors or antagonistic antibodies have been approved for the treatment of cancer (7, 8).

In this study, we used phospho-RTK arrays to simultaneously assess the phosphorylation status of 40+ RTKs in chondrosarcoma cells under conditions of serum depletion. We found that although several RTKs are constitutively activated, this occurs in differing patterns among different human tumor-derived cell lines. Several RTKs were identified as critical mediators of cell growth through the use of small interfering RNAs (siRNAs) and small molecular inhibitors. To seek a therapeutic strategy for chondrosarcoma, we explored the effects of targeting a common downstream signaling pathway of RTKs on cell growth, and found that the dual pan-class I phosphoinositide-3-kinase (PI3K)/mammalian target of rapamycin (mTOR) inhibitor BEZ235 significantly inhibited growth of chondrosarcomas both *in vitro* and *in vivo*. A chondrosarcoma cell line with an *NRAS* mutation was exclusively sensitive to MEK inhibition.

Materials and Methods

Cell lines and Culture Conditions

Human chondrosarcoma cell lines included SW1353 **(**American Type Culture Collection), CS-1 (gift of Dr. Francis J. Hornicek, Massachusetts General Hospital, Boston, MA), JJ012 (gift of Dr. Joel A. Block, Rush University, Chicago, IL), CH-2879 (kindly provided by Prof. Antonio Llombart-Bosch, Valencia University, Spain) and OUMS-27 (kindly provided by Dr. M. Namba, Okayama University Medical School, Japan) (9-12). Cells were cultured in RPMI 1640 supplemented with 10% fetal bovine serum and 1x Penicillin-Streptomycin-Glutamine (10378-016, Invitrogen, Carlsbad, CA) at 37ºC in a humidified incubator with 95% air and

5% CO2. Cell line identity was verified by high-resolution short tandem repeat (STR) profiling with Promega PowerPlex ®1.2 system.

Phospho-RTK Array

First-generation phospho-RTK arrays (#ARY001, R&D Systems, Minneapolis, MN) were used for assessing the phosphorylation status of 42 RTKs in chondrosarcoma cells under serum-depleted condition. Phospho-RTK analyses were performed as recommended by the manufacturer. Subconfluent cells were washed once with serum-free media, and incubated in serum-depleted medium for 24 hr before harvest. A total of 450 μg of protein was used for the assay.

For qualitative assessment of signal, pixel densities on developed X-ray film were analyzed using a transmission mode scanner and the Adobe Photoshop software. The pixel densities of the areas (49 x 26 pixels, width x height) surrounding the pair of duplicate dots were determined. The pixel density of the PBS negative control was used as a background value and subtracted from each read. RTKs with a signal greater than the positive controls were scored as "+++"; RTKs with a signal level similar to positive controls were scored as "++"; and RTKs with a signal less than positive controls, but 5-fold higher than antibody isotype negative controls were scored as "+". RTKs with signal less than 5-fold higher than the antibody isotype negative control were labeled as "-".

We used second-generation phospho-RTK arrays (#ARY001B, R&D Systems, Minneapolis, MN) to analyze the effects of long-term treatment of BEZ235 on the phosphorylation of RTKs because the first-generation RTK arrays were no longer available. The new arrays include 49 RTK capture antibodies but no longer contain antibody isotype negative controls. The pixel density was measured as described above. The changes in the phosphorylation level of RTKs were determined by comparing the intensity of RTK signals in BEZ235-treated samples to the 0.1% DMSO-treated control samples.

Immunoprecipitation and Immunoblots

Cells were lysed on ice in buffer containing 50 mM HEPES (pH 7.5), 150 mM NaCl, 1 mM EGTA, 10% glycerol, 1% Triton X-100, 100 mM NaF, 10 mM $Na_4P_2O_7 \cdot 10\ H_2O$, 1 mM Na_3VO_4, and 1x Protease Inhibitor Cocktail (Roche Diagnostics, Germany). The following antibodies were used for immunoprecipitation from clarified cell lysates: EGFR (Calbiochem #GR01, San Diego, CA), ERBB2 (Calbiochem #OP15), Insulin Rβ (Santa Cruz #sc-711, Santa Cruz, CA), IGF1Rβ (Santa Cruz #sc-713), EphA2 (Upstate, #05-480), AXL (Santa Cruz #SC-1096), and PDGFRα (Santa Cruz #SC-338). The immunoprecipitants were separated by SDS/PAGE and transferred to nitrocellulose membranes (Bio-Rad, Hercules, CA). Antibodies for immunoblotting were purchased from Calbiochem (ERBB2 #OP15), Lab Vision, Fremont, CA (ERBB3 #MS-201-P), Upstate Biotechnology, Lake Placid, NY (anti-phosphotyrosine antibody 4G10 #05-1050), Sigma, St. Louis, MO (α-tubulin T9026), Santa Cruz (AXL #SC-1096,

PDGFRα #SC-338) and Cell Signaling, Danvers, MA (EGFR #2232, p-EGFR #2234, p-ERBB2 #2243, p-ERBB3 #4791, MET #3127, p-MET #3129, p-PDGFRα #2992, Insulin Rβ #3025, IGF1Rβ #3027, AKT #9272, p-AKT (Ser^{473}) #9271, p-AKT (Thr^{308}) #9275, MAPK #9107, p-MAPK #9101, S6 #2217 and p-S6 ($Ser^{235/236}$) #2211, 4EBP1 #9644, p-4EBP1($Thr^{37/46}$) #2855, p-4EBP1(Ser^{65}) #9451, p-4EBP1 (Thr^{70}) #9455).

Inhibitors
MET inhibitor PHA665752 was purchased from Tocris Biosciences (Ellisville, MO). EGFR/ERBB2 inhibitor BIBW-2992 and MEK inhibitor ARRY-142886 (AZD6244) were purchased from Medicilon (Shanghai, China) and OTAVA (Toronto, Canada), respectively. Insulin-like Growth Factor 1 Receptor (IGF1R)/Insulin Receptor (INSR) inhibitor PQIP was a kind gift from OSI Pharmaceuticals (Melville, NY). PI3K/mTOR inhibitor BEZ235 was purchased from AXON Medchem (Groningen, The Netherlands). PI3K inhibitor GDC-0941 and mTOR inhibitor rapamycin were purchased from Chemdea (Ridgewood, NJ) and Calbiochem, respectively.

siRNA
ON-TARGETplus SMARTpools siRNA against EGFR, ERBB2, ERBB3, MET and a scrambled control were purchased from Dharmacon (Layfayette, CO). Cells were transfected with siRNA at a final concentration of 12.5 or 25 nM with RNAiMAX (Invitrogen) according to the manufacturer's protocol. Cells were incubated with siRNA for 72 or 96 hr prior to analysis of cell viability.

Cell Viability Assays
Cells were plated in 96-well plates at 1000-2000 cells/well in 100 µl of medium containing 10% FBS. After 24 hr, cells were exposed to increasing concentrations of compounds. Each treatment was tested in triplicate. Cell viability was determined after 72 hr using the CellTiter-Glo Luminescent Cell Viability Assay Kit (Promega, Madison, WI) with a modification in the protocol in that the CellTiter-Glo reagent was diluted 1:3 with PBS. The relative luminescence units (RLU) were measured using the FLUOstar Optima plate reader (BMG Labtech GmbH, Germany) and relative cell number was calculated by normalization to the RLU of the control treated cells.

Cell Cycle Analysis
Cells were exposed to inhibitors or 0.1% DMSO for 24 hr and harvested. After washing with ice-cold PBS, cells were fixed in 70% ethanol at 4 ºC for at least 2 hr. Fixed cells were stained in PBS containing 10 µg/mL RNase A and 20 µg/mL propidium iodide (Sigma, St. Louis, MO) in the dark. DNA content analysis was performed by flow cytometry (FACSCalibur; Becton Dickinson, Mountain View, CA) with CellQuest and ModFIT LT software (Becton Dickinson).

Mutation analysis
Genomic DNA was extracted from chondrosarcoma cell lines using DNeasy Blood & Tissue Kit (Qiagen, Valencia, CA) according to the manufacturer's protocol. The coding sequences of selected genes in the PI3K/mTOR and RAS/MAPK pathways were amplified from genomic DNA by PCR with primers listed in the Table 8.1. PCR was performed in 50 µl reactions containing Platinum PCR SuperMix (Invitrogen), 200 ng DNA, 0.3 µM forward and reverse primers using GeneAmp® PCR System 9700 (Applied Biosystems, Carlsbad, CA). The PCR product was purified using Qiaquick PCR purification Kit (Qiagen), and sequenced using Big Dye Terminator V3.1 chemistry in combination with an Applied Biosystems 3730xl Sequencer.
For chondrosarcoma primary tumor tissues, mutation analysis for *PIK3CA* (13) and *NRAS* was performed using DNA available from 89 chondrosarcomas. Hydrolysis probes assay was used to specifically screen for the *PIK3CA* c.1624G>A (p.E542K), c.1633G>A (p.E545K), and c.3140A>G (p.H1047R) and the *NRAS* c.35G>A (p.G12D), c.183A>T (p.Q61H), c.181C>A (p.Q61K), c.182A>T (p.Q61L), and c.182A>G (p.Q61R) hotspot mutations as described (13). Primer and probe sequences for *NRAS* mutation analysis are provided in Table 8.2.

Tumor Xenografts in Nude Mice
JJ012 cells (1 x 10^6) were suspended in PBS, mixed 1:1 with Matrigel (BD Biosciences), and subcutaneously injected into nude female mice (Nu/Nu, Charles River) in a final volume of 100 µl. Treatment began when tumors reached an average size of approximately 50 mm^3. Mice were randomized into statistically identical cohorts (≥ 6 mice/group). BEZ235 was freshly prepared in 10:90 (v/v) N-methyl pyrrolidone: polyethylene glycol 300 (Fluka #69118 and #81160), as described (14), and was administered daily at 35 mg/kg by oral gavage. Tumor xenografts were measured twice a week by ultrasound imaging (VisualSonic Vevo 770, Toronto, Canada), and animal weight was recorded every 3-4 days. Following drug administration, tumors were harvested and fixed for histologic and immunohistochemical analysis or snap-frozen for immunoblot analysis. All procedures were performed according to protocols approved by the Institutional Animal Care and Use Committee of the Dana-Farber Cancer Institute.

Tumor Xenograft Histology and Immunohistochemistry
Haematoxylin and eosin staining as well as immunohistochemistry were performed on five-micron sections of formalin-fixed paraffin-embedded (FFPE) samples from tumors resected from mice. Tissue sections were deparaffinized, rehydrated, and microwaved in 10 mM citrate buffer (pH 6.0) in a 750 W microwave oven for 15 min. Anti-phospho-S6 ribosomal protein (Ser 240/244) primary antibody (Cell Signaling, #2215) was added at a dilution of 1:100 and incubated overnight at 4 ℃. Sections were further processed with horseradish peroxidase-conjugated secondary

antibody. The reaction was detected by 3,3-diaminobenzidine and hematoxylin staining. Images were taken by using Olympus CX41 microscope with QCapture software (QImaging, Surrey, Canada).

Tissue microarray immunohistochemistry

Tissue microarrays (TMAs) containing 157 conventional chondrosarcomas and 25 dedifferentiated chondrosarcomas were described previously (15, 16). All specimens were handled according to the ethical guidelines described in "Code for Proper Secondary Use of Human Tissue in The Netherlands" of the Dutch Federation of Medical Scientific Societies. TMAs contained 2 mm cores of all samples in triplicate. After de-waxing and rehydrating, TMAs were permeabilized with Tris-buffered saline (TBS)/0.5% Tween20 for 30 min at room temperature (RT) and washed several times in distilled water. For antigen de-masking, slides were immersed in citrate buffer (pH 6.0) and antigen retrieval was performed in a pressure cooker (Biocare Medical, UK) for 2 min at 125 °C followed by 10 min at 85 °C. Non-specific binding was blocked in TBS/Tween20 (0.5%) and 10% goat serum for 1 hour at RT. Primary rabbit anti-pS6 antibodies (1:100, New England Biolabs, UK #4857) were incubated with the slides in a humidified chamber at 4 °C over night. After washing 3 times, a secondary goat anti-rabbit Alexa 594 antibody (1:300, Invitrogen, UK) was added. Nuclei were labeled with DAPI and slides were mounted with Prolong Gold Antifade (Invitrogen, UK). Images were acquired with an Olympus Fluoview FV1000 confocal microscope and a 60x oil objective (NA: 1.35). Each image had a size of 2048 x 2048 pixels, a horizontal and vertical dimension of 211 µm x 211 µm and a thickness of 1.292 µm.

Statistical Analysis

Drug concentrations required to inhibit cell growth by 50% (IC_{50}) were calculated by dose-response curve fitting with Prism version 5.0 (GraphPad Software). Comparisons between groups were made using the unpaired *t*-test. Differences in means ± SEM with $p < 0.05$ were considered statistically significant.

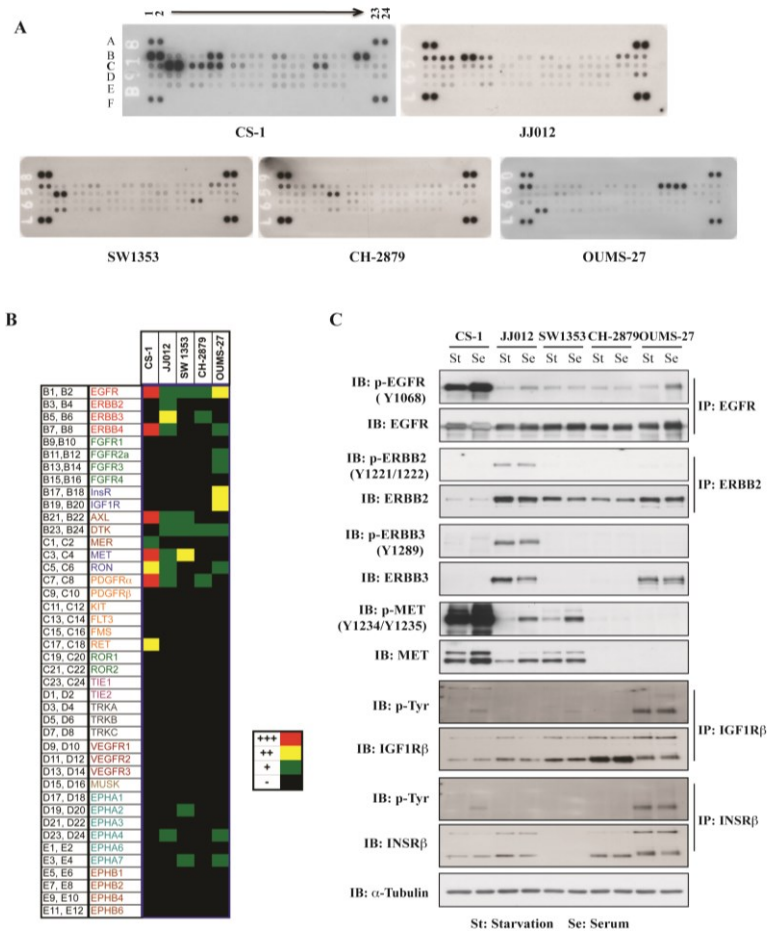

Figure 8.1. Activation of multiple RTKs in chondrosarcoma cells.
A. The phosphorylation status of 42 RTKs in chondrosarcoma cells under serum-depleted conditions was assessed by phospho-RTK arrays. Anti-RTK antibodies spotted on nitrocellulose membrane in duplicate were incubated with cell lysates followed by secondary anti-phosphotyrosine antibody detection. Positive controls are represented in the 4 corners of each blot; negative antibody isotype controls and PBS control are represented in E13-20 and E21-22, respectively. The location and names of capture antibodies are listed in the first and second column of B. **B**. Qualitative heat-blot map of RTK array data. "+++": RTK signal is higher than postive controls; "++": signal is similar to positive controls; "+": signal is lower than postive control but 5-fold higher than antibody isotype negative controls; "-": low signal. **C**. Validation of phospho-RTK array data by immunoblot (IB) or immunoprecipitation (IP)/IB analysis.

Table 8.1. Oligos for gene mutation detection

Gene Symbol	Coding Exon Number	Hotspot Mutation at This Exon§		Primer for Amplification§§ (5'-3')	References	Sequencing Primer 1§§ (5'-3')	Sequencing Primer 2§§ (5'-3')	References
PIK3CA	9	E542, E545	**F**	GATTGGTTCTTTCCTGTCTCTG	1	TTGCTTTTTCTGTAAATCATCTGTG		6
			R	CCACAAATATCAATTTACAACCATTG				
PIK3CA	20	H1047	**F**	TGGGGTAAAGGGAATCAAAAG	1	TGACATTTGAGCAAAGACCTG		6
			R	CCTATGCAATCGGTCTTTGC				
AKT1	2	E17	**F**	M13-CCTAAGAAACAGCTCCCGTACC	2	M13		2
			R	AGCCAGTGCTTGTTGCTTG				
PTEN	5	A130	**F**	TGCAACATTTCTAAAGTTACCTACTTG	2	M13		2
			R	M13-TTTACTTGTCAATTACACCTCAATAAA				
HRAS	2	G12, G13	**F**	CAGGAGACCCTGTAGGAGGA	3	CGCCAGGCTCACCTCTAT	GCGATGACGGAATATAAGCTG	6
			R	CCTATCCTGGCTGTGTCCTG				
HRAS	3	Q61	**F**	AGAGGCTGGCTGTGTGAACT	3	ATGGCAAACACACACAGGAA	GTCCCTGAGCCCTGTCCT	6
			R	TCACGGGGTTCACCTGTACT				
KRAS	2	G12, G13	**F**	TACTGGTGGAGTATTTGATAGT	4	GGTGGAGTATTTGATAGTGTATTAACC	AGAATGGTCCTGCACCAGTAA	6
			R	CATGAAAATGGTCAGAGAAACC				
KRAS	3	Q61	**F**	TTGAAGTAAAAGGTGCACTGT	5	TGCACTGTAATAATCCAGACTGTG	GCATGGCATTAGCAAAGACTC	6,5
			R	GCATGGCATTAGCAAAGACTC				
NRAS	2	G12, G13	**F**	GAACCAAATGGAAGGTCACA	3	GAACCAAATGGAAGGTCACA		3
			R	TGGGTAAAGATGATCCGACA				
NRAS	3	Q61	**F**	TGCCCCCTTACCCTCCACA	4	CACCCCCAGGATTCTTACAG	CCTCATTTCCCCATAAAGATTCAGA	6,4
			R	CCTCATTTCCCCATAAAGATTCA				

				GA			
BRAF	15	V600	**F**	TCATAATGCTTGCTCTGATAGGA	3	TGCTTGCTCTGATAGGAAAATG	6
			R	GGCCAAAAATTTAATCAGTGGA			

[§§]M13 denotes the universal sequencing primer 5'-GTAAAACGACGGCCAGT-3'.

References

1. Samuels Y, et al, Science. 2004. 304(5670):554
2. Parsons DW, et al; Science. 2008 Sep 26;321(5897):1807-12
3. Davies H, et al, Nature. 2002. 417(6892): 949-954
4. Case M, et al, Cancer Research, 2008. 68(16):6803-09
5. Bezieau S, et al.Hum Mutat. 2001.18(3):212-24.
6. Primer3 Plus software at http://www.primer3plus.com

Table 8.2. Primers and reporters for NRAS mutation analysis

Forward Primer Name	Forward Primer Seq.	Reverse Primer Name	Reverse Primer Seq.
NRAS35GA_F	ATGACTGAGTACAAACTGGTGGTG	NRAS35GA_R	GGATTGTCAGTGCGCTTTTCC
NRAS181CA_F	GGTGAAACCTGTTTGTTGGACATAC	NRAS181CA_R	CCTGTCCTCATGTATTGGTCTCTCA
NRAS182AT_F	GGTGAAACCTGTTTGTTGGACATAC	NRAS182AT_R	GTATTGGTCTCTCATGGCACTGTAC
NRAS182AG_F	GGTGAAACCTGTTTGTTGGACATAC	NRAS182AG_R	TGGTCTCTCATGGCACTGTACT
NRAS183AT_F	GGTGAAACCTGTTTGTTGGACATAC	NRAS183AT_R	CCTGTCCTCATGTATTGGTCTCTCA

Reporter 1 Name	Reporter 1 Dye	Reporter 1 Sequence	Reporter 1 Conc.
NRAS35GA_V	VIC	TTGGAGCAGGTGGTGTT	8
NRAS181CA_V	VIC	CTGTACTCTTCTTGTCCAGC	8
NRAS182AT_V	VIC	CAGCTGGACAAGAAGA	8
NRAS182AG_V	VIC	ACAGCTGGACAAGAAG	8
NRAS183AT_V	VIC	CACTGTACTCTTCTTGTCCAG	8

Reporter 2 Name	Reporter 2 Dye	Reporter 2 Sequence	Reporter 2 Conc.
NRAS35GA_M	FAM	TTGGAGCAGATGGTGTT	8
NRAS181CA_M	FAM	CTGTACTCTTCTTTTCCAGC	8
NRAS182AT_M	FAM	ATACAGCTGGACTAGAAGA	8
NRAS182AG_M	FAM	ACAGCTGGACGAGAAG	8
NRAS183AT_M	FAM	ACTGTACTCTTCATGTCCAG	8

Results

Coactivation of RTKs in Chondrosarcoma Cells

We employed phospho-RTK arrays to detect the phosphorylation status of 42 RTKs in five human tumor-derived chondrosarcoma cell lines, and we observed that multiple RTKs were phosphorylated in cells under serum depletion conditions (Fig. 8.1A and B). For example, EGFR, MET, ERBB4, AXL, PDGFRα, RON, and RET were phosphorylated in CS-1 cells. All four EGFR family members were phosphorylated in JJ012 cells. IGF1R, INSR, EGFR and EphA7 were phosphorylated in OUMS-27 cells.

To further validate the phospho-RTK array data, we analyzed by immunoblot the expression and phosphorylation status of the 9 RTKs which were most strongly phosphorylated in the respective chondrosarcoma cell lines. As shown in Fig. 8.1C and Fig. 8.2A, the phospho-RTK array data were confirmed: EGFR (site Tyr^{1068}) was highly phosphorylated in CS-1 cells and less so in the four other cell lines; ERBB2 (site $Tyr^{1221/1222}$) and ERBB3 (site Tyr^{1289}) were highly phosphorylated in JJ012 cells; phosphorylation of MET was detected in CS-1, JJ012, and SW1353 cells, with the highest level in CS-1 cells; INSR β and IGF1Rβ were highly phosphorylated in OUMS-27 cells; the highest phosphorylation level of AXL and EphA2 was observed in CS-1 and SW1353 cells, respectively; and phosphorylation of PDGFRα was detected in CS-1 and CH-2879 cells.

Moreover, most kinases remained constitutively phosphorylated under conditions of serum depletion at levels similar to that seen in the serum-containing media (Fig. 8.1C). While the precise mechanism(s) of kinase activation remains unknown, it appears to be cell-autonomous and independent of exogenous growth factors.

Taken together, the immunoblot data confirmed that RTKs are constitutively activated in chondrosarcoma cells, and that the patterns of activation vary among cell lines.

Effects of RTK inhibition on the Growth of Chondrosarcoma Cells

To explore the involvement of the above-noted highly activated RTKs on the growth and survival of chondrosarcoma cells, we applied small molecule inhibitors and/or siRNAs targeting corresponding RTKs to cells (Fig. 8.3). We examined the effects of the MET inhibitor PHA665752 (17) on MET signaling pathways and cell growth in the CS-1 cell line because of its high level of constitutive phosphorylation. MET phosphorylation at key residues in the kinase domain ($Tyr^{1234/1235}$) was greatly suppressed by treatment with 200 nM PHA665752 in the presence of serum (Fig. 8.3A, left panel). Correspondingly, PHA665752 induced a dramatic reduction in cell number with 43% inhibition at 125 nM (Fig. 8.3B, left panel). We also applied MET siRNAs to exclude the possibility of off-target effects of the small molecule inhibitor. As shown in 8.2B, the expression of MET was dramatically decreased by MET siRNA. Cells transfected with MET siRNA had an obvious decrease (approximately 30%) in cell viability in comparison to control siRNA transfected cells after 72 hr (Fig. 8.2C). These results demonstrate

that MET is involved in the regulation of CS-1 chondrosarcoma cell growth. There was no significant effect of MET pathway inhibition in cell lines JJ012 and SW1353 that have low basal phospho-MET levels (Fig. 3B, left panel). In addition, we determined the effects of the EGFR inhibitor gefitinib and the anti-EGFR antibody cetuximab on the viability of CS-1 cells because of the high phosphorylation level of EGFR, but no significant changes were observed (data not shown).

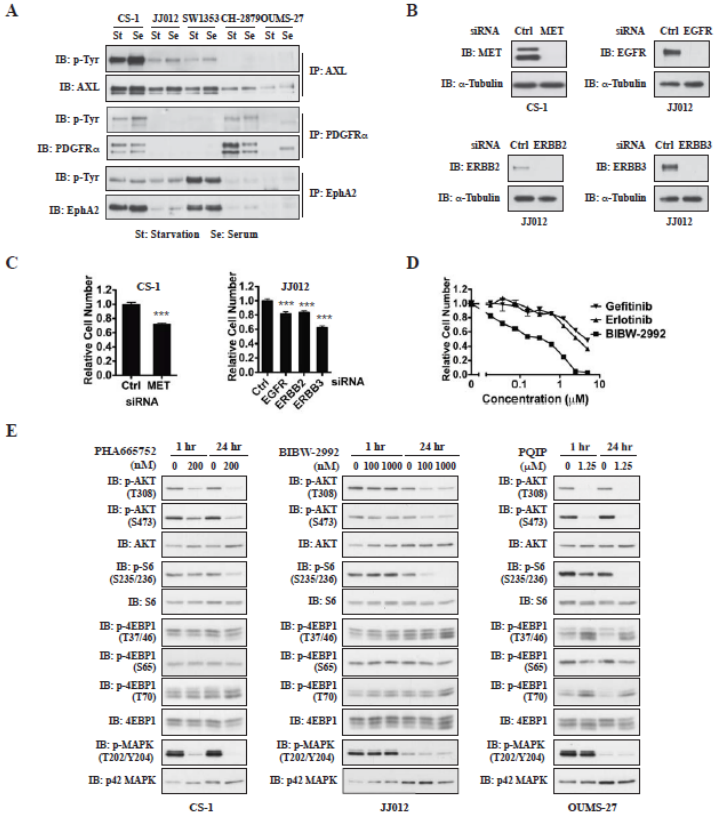

Figure 8.2. Effects of RTK inhibition in chondrosarcoma cells.

A. Validation of phospho-RTK array data by immunoblot (IB) or immunoprecipitation (IP)/IB analysis. B. siRNA-mediated knockdown of RTK expression at 48 hr. C. siRNA-mediated knockdown of RTKs on growth of CS-1 (at 72 hr) and JJ012 (at 96 hr) cells evaluated by CellTiter-Glo viability assay. Values represent mean ± SEM (n>3). ***, $P<0.001$, compared with scrambled siRNA-transfected cells. D. Effects of EGFR kinase family inhibitors on cell viability of JJ012 cells were evaluated by CellTiter-Glo viability assay at 72 hr. E. Effects of RTK inhibition on the signaling of PI3K/mTOR and MAPK pathways were evaluated by immunoblots.

In JJ012 cells, four members of the EGFR kinase family were phosphorylated. The irreversible EGFR/ERBB2 inhibitor BIBW-2992 (18) decreased phosphorylation of ERBB2 and ERBB3 (Fig. 8.3A, central panel), and inhibited cell growth in a dose-dependent manner with an IC_{50} of 0.38 ± 0.02 μM (Fig. 8.3B, central panel). siRNA-mediated knockdown of ERBB3 also significantly reduced cell number (37.7% ± 6.1%) compared to control siRNA at 96 hr after transfection (P<0.001; Fig. 8.2B and 8.2C). However, the EGFR-specific inhibitors gefitinib and erlotinib only demonstrated mild effects as did siRNA mediated knockdown of EGFR and ERBB2 (Fig. 8.2C and 8.2D). These findings suggest that EGFR family kinases, and in particular ERBB3, are important regulators of the growth of JJ012 cells.
In OUMS-27 cells, IGF1R and INSR are highly phosphorylated. Treatment with the IGF1R/INSR inhibitor PQIP (19, 20) decreased phosphorylation of IGF1Rβ and INSRβ (Fig. 8.3A, right panel), and inhibited growth in a dose-dependent manner with an IC_{50} of 1.42 ± 0.08 μM (Fig. 8.3B, right panel). These data suggest that the insulin receptor kinase family is involved in the growth of OUMS-27 cells.

Effects of RTK Inhibition on the Activity of PI3K/mTOR and MAPK Pathways in Chondrosarcoma cells

We further examined the effects of RTK inhibition on the PI3K/mTOR and MAPK pathways. In MET-dependent CS-1 cells, treatment with the MET inhibitor PHA665752 for 2 hr led to a dose-dependent decrease in the phosphorylation of AKT at Thr^{308} and Ser^{473}, S6 at $Ser^{235/236}$ and p44/42 MAPK at Thr^{202}/Tyr^{204} (Fig. 8.3A, left panel). In JJ012 cells, phosphorylation of AKT and S6 was partially reduced by BIBW-2992 treatment, but no effect on MAPK phosphorylation was observed (Fig. 8.3A, central panel). In OUMS-27 cells, IGF1R/INSR inhibitor PQIP treatment decreased AKT and S6 phosphorylation in a dose-dependent manner, with complete inhibition at 1.25 μM, but had no effect on MAPK phosphorylation (Fig. 8.3A, right panel). The inhibition of phosphorylation in the presence of the above inhibitors was continued for at least 24 hr, with the level of phosphorylation at 24 hr even somewhat lower (Fig. 8.2E). No significant inhibition on the phosphorylation of 4EBP1 was observed following the treatment of RTK inhibitors for 1 or 24 hr (Fig. 8.2E).

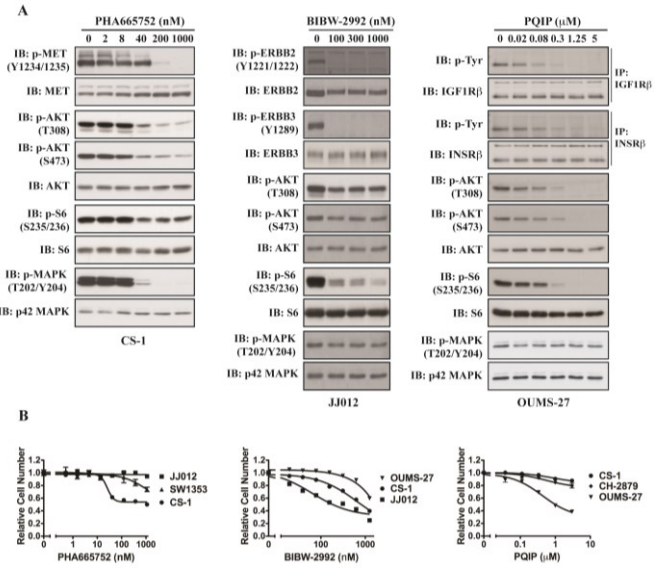

Figure 8.3. Effects of RTK inhibition in chondrosarcoma cells. **A.** Effects of MET inhibitor PHA665752 (left panel, at 2 hr), EGFR/ERBB2 inhibitor BIBW-2992 (central panel, at 2 h) and IGF1R/INSR inhibitor PQIP (right panel, at 6 h) on the phosphrylation of RTKs and their downstream effectors were evaluated by immunoblot. **B.** Effects of RTK inhibitors on cell viability were evaluated by CellTiter-Glo assay at 72 hr.

Chondrosarcomas have PI3K/mTOR Activation and are Sensitive to Inhibitors in vitro

The above data suggest that RTKs are important mediators of chondrosarcoma cell growth. However, the heterogeneity of implicated pathways poses a considerable challenge to the clinical evaluation of any single tyrosine kinase inhibitor for the treatment of this disease. Targeting common pathways downstream of RTKs may instead be a method to inhibit cell growth irrespective of the particular upstream signaling molecule.

We hypothesized that the PI3K/mTOR pathway might commonly mediate signaling from heterogeneous RTK activation and thus we examined the activity of this pathway in human primary chondrosarcoma tissue specimens. As an established surrogate of PI3K/mTOR pathway activity, we analyzed the S6 phosphorylation status in chondrosarcoma tissue microarray samples by immunohistochemical staining. In total, 73 out of 106 (69%) conventional chondrosarcomas and 11 out of 25 (44%) dedifferentiated chondrosarcomas were positive (Table 8.3, Fig. 8.4).

In order to determine whether PI3K/mTOR signaling and S6 phosphorylation were relevant to chondrosarcoma growth, we tested the effects of BEZ235, a dual PI3K/mTOR inhibitor (14). Treatment with BEZ235 potently inhibited the growth of all of the chondrosarcoma cell lines, with IC_{50} values below 10 nM (Fig. 8.8A, left panel). Cell cycle analysis showed a substantial increase in the proportion of cells in the G_0/G_1 phase of the cell cycle after treatment with the inhibitor (Fig. 8.5A). No induction of apoptosis was observed (data not shown).

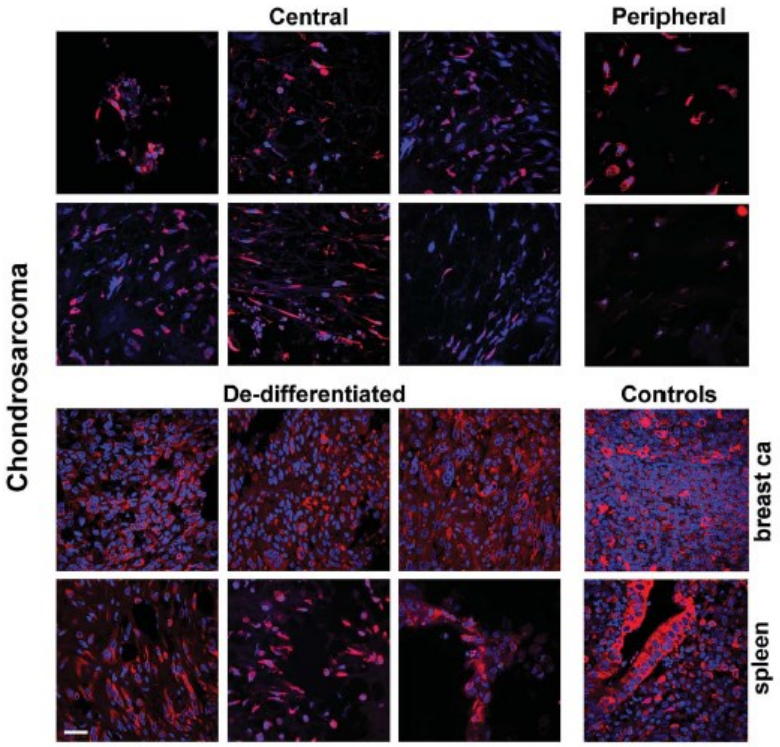

Figure 8.4. S6 phosphorylation in chondrosarcoma clinical tissue microarray samples. Confocal images of immune-labeled sections with DAPI and anti-pS6 antibody in chondrosarcoma samples. Example images from central chondrosarcoma, peripheral chondrosarcoma and high grade areas of dedifferentiated chondrosarcoma display the sometimes sparse distribution and heterogeneity of cellular labeling in tumor regions. Positive controls are of breast carcinoma and normal spleen. Bar 20μm.

We also tested the effects of the PI3K inhibitor GDC-0941 and the mTOR inhibitor rapamycin on cell growth. Each were significantly less potent than BEZ235, with GDC-0941 inhibiting the growth of chondrosarcoma cell lines with IC_{50} values of 0.9-2.5 μM, and rapamycin causing 22-49% growth inhibition at a concentration of 1000 nM (Fig. 8.5B).

Functionally important mutations in the PI3K/mTOR pathway have been reported as potential predictors of sensitivity to the treatment of PI3K/mTOR pathway inhibitors (21, 22). We sequenced selected hotspot sites, including *PIK3CA* (exon 9 and 20), *AKT1* (exon 2), and *PTEN* (exon 5). However, no mutations were detected in these five chondrosarcoma cell lines (data not shown). Moreover, *PIK3CA* hotspot mutations were absent in all 88 chondrosarcomas tested using hydrolysis probe assays (data not shown).

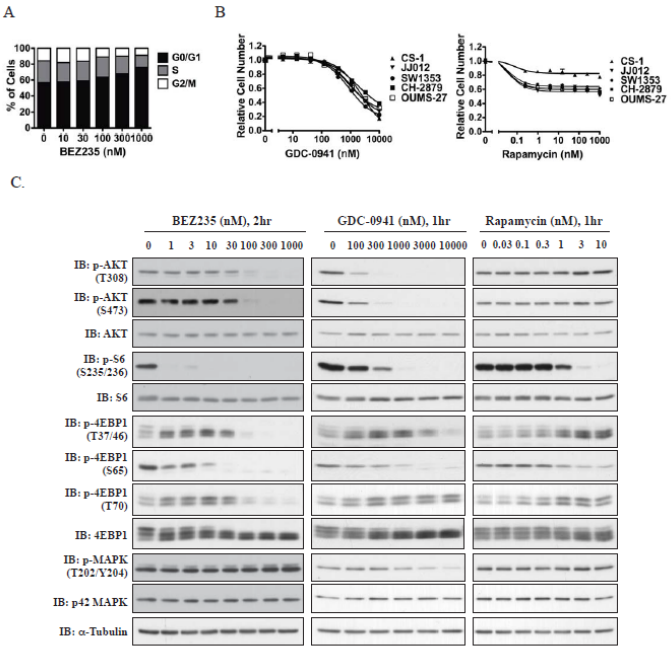

Figure 8.5. Effects of PI3K/mTOR pathway inhibitors in chondrosarcoma cells. A. Cell cycle analysis of JJ012 cells following 24hrs treatment with BEZ235. B. Effects of PI3K inhibitor GDC-0941 and mTOR inhibitor rapamycin on chondrosarcoma cell viability evaluated by CellTiter-Glo assay after 72 hr. Values represent mean ± SEM (n=3). C. Effects of BEZ235, GDC-0941 and rapamycin treatment on the phosphorylation of AKT, S6, 4EBP1, and MAPK in JJ012 cells were evaluated by immunoblot.

Sustained suppression of phosphorylation of S6 and 4EBP1, and feedback induction of AKT phosphorylation after prolonged treatment with BEZ235 in vitro

We used the phosphorylation state of AKT, S6 [a major substrate of p70 S6 kinase 1 (S6K1)], and 4EBP1 as markers to monitor the activity of PI3K/mTOR pathway inhibitors. The Thr^{308} site and Ser^{473} sites of AKT are regulated by PDK1 (a major downstream effector of PI3K kinase) and the mTORC2 complex, respectively. The mTORC1 complex catalyzes the phosphorylation of S6K1 and 4EBP1. (23-25) Following 2 hr treatment of JJ012 with BEZ235, the phosphorylation of S6 and the Ser^{65} site of 4EBP1 were suppressed at 1 nM and 30 nM, respectively, and the phosphorylation of AKT and the $Thr^{37/46}$ and Thr^{70} sites of 4EBP1 was inhibited at 100 nM (Fig. 8.5C). Following 24 hr treatment, the inhibition of S6 and 4EBP1 phosphorylation was well sustained or even strengthened (Fig. 8.8B, left panel), while the initial inhibition on the AKT phosphorylation was dramatically reversed at 24 hr with an increase in phosphorylation level at the Thr^{308} site of AKT at 10 and 100 nM. At 300 nM, BEZ235 treatment still potently inhibited the phosphorylation of Ser^{473} at 24 h, keeping AKT activity in a partially suppressed status, as phosphorylation of both Thr^{308} and Ser^{473} sites is required for full AKT activation (26, 27) (Fig. 8.8B, left panel). We further examined the effects of

BEZ235 treatment on the PI3K/mTOR signaling in the other four chondrosarcoma cell lines, and similar results were observed: the phosphorylation of S6, 4EBP1 and the Ser^{473} site of AKT, but not Thr^{308} site, were effectively inhibited by 300 nM BEZ235 treatment at 24 hr (Fig. 8.6A-8.6D). The effects of BEZ235 on MAPK phosphorylation were also examined, and a slight increase in its phosphorylation level was observed when JJ012 and SW1353 cells were treated with 100-1000 nM BEZ235 (Fig. 8.5B, Fig. 8.6B).

In comparison to BEZ235, GDC-0941 effectively inhibited the phosphorylation of AKT at 300 nM, but required a much higher concentration (1000-10000 nM) to inhibit the phosphorylation of S6 and 4EBP1 (Fig. 8.5C). Following 24 h treatment with GDC-0941, the phosphorylation level of the Thr^{308} site of AKT remained suppressed. A slight induction of the phosphorylation signal of S6 and Ser^{473} site of AKT was observed in OUMS-27 and CS-1 cells, respectively (Fig. 8.6A and 8.6D).

Rapamycin treatment blocked S6 phosphorylation but only slightly decreased the phosphorylation of 4EBP1 at 10 nM (Fig. 8.5C, Fig. 8.8B). It has previously been demonstrated that mTORC1 inhibition can lead to feedback activation of PI3K in cancer cells (25). In SW1353 and OUMS-27 cells, we also observed a dramatic and lasting increase in the phosphorylation level of AKT at Thr^{308} and Ser^{473} following rapamycin treatment (Fig. 8.6B and 8.6D). However, in JJ012 cells rapamycin treatment enhanced the phosphorylation level of AKT only at Thr^{308}, and not at Ser^{473} (Fig. 8.8B). There were no obvious changes observed in CS-1 and CH-2879 cells (Fig. 8.6A and 8.6C).

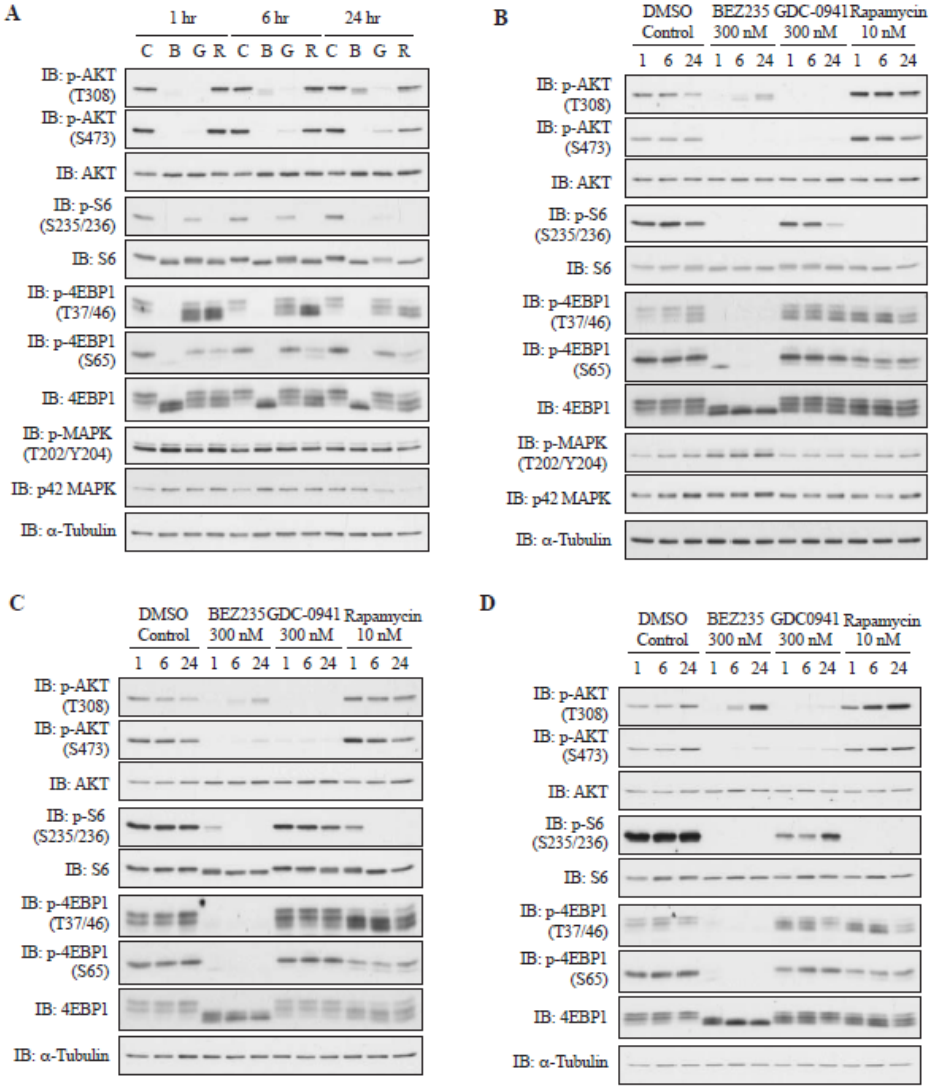

Figure 8.6. Time-dependent effects of PI3K/mTOR pathway inhibitors on the activation of AKT and MAPK signaling pathway in chondrosarcoma cells.
A. Effects of BEZ235 (B), GDC-0941 (G), rapamycin (R), and DMSO control (C) on the phosphorylation of AKT, S6, 4EBP1, and MAPK in CS-1 (panel **A**), SW1353 (panel **B**), CH-2879 (panel **C**), and OUMS27 (panel **D**). Cells were evaluared by immunoblot at 1, 6, and 24 hr.

Table 8.3. Phosphorylated S6 Staining in Chondrosarcoma Clinical Samples

	Total	Number Positive for pS6[§] (%)
Enchondroma	7	5 (71)
Osteochondroma	6	5 (83)
Conventional Chondrosarcoma	106	73 (69)
Central Chondrosarcoma	80	58 (73)
Grade I	37	27 (73)
Grade II	30	20 (67)
Grade III	13	11 (85)
Peripheral Chondrosarcoma	26	15 (58)
Grade I	14	9 (64)
Grade II	9	5 (56)
Grade III	3	1 (33)
Dedifferentiated Chondrosarcoma	25	11 (44)

[§] pS6: phosphorylated S6 staining as performed on tissue microarrays

In vivo effects of PI3K/mTOR inhibitor BEZ235 on chondrosarcoma tumor growth and PI3K/mTOR signaling

The antitumor activity of BEZ235 was studied in a mouse xenograft model of the JJ012 cell line treated for 21 days with drug or vehicle control. As shown in Fig. 8.7A, BEZ235 significantly suppressed tumor growth ($p<0.01$). No significant weight loss of the mice was observed (data not shown). Histologic analysis demonstrated a marked decrease in tumor cell viability as well as in the phosphorylation of S6 protein (Fig. 8.7B). We also explored the effects of short-term (2 hr) and long-term (21 days+2 hr) treatment of BEZ235 on PI3K/mTOR signaling in JJ012 xenografts by immunoblots (Fig. 8.7C). The phosphorylation signal of S6 was diminished in all of the xenografts samples treated with 35 mg/kg BEZ235. The multiple phosphorylation sites of 4EBP1 were differentially dephosphorylated: phosphorylation of Ser^{65} site was suppressed, and phosphorylation of Thr^{70} and $Thr^{37/46}$ sites were partially decreased, which may enable 4EBP1 to partially block the function of the eukaryotic translation initiation factor 4E (eIF4E), since the phosphorylation of Thr^{70} and Ser^{65} sites are critical for the release of 4E-BP1 from eIF4E (28, 29). BEZ235 treatment also decreased the phosphorylation of AKT at the Ser^{473} site, but the inhibition became less profound following the prolonged treatment of BEZ235. A slight increase in phosphorylation of Thr^{308} of AKT was observed.

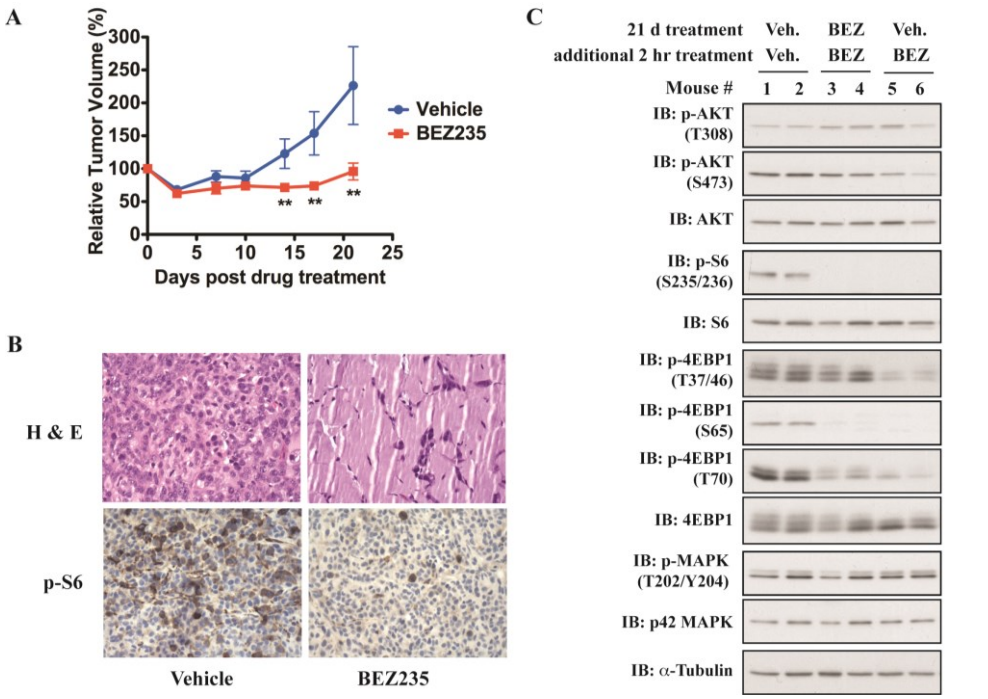

Figure 8.7. BEZ235 inhibits *in vivo* growth of JJ012 chondrosarcoma xenografts and reduced phosphorylation of S6 and 4EBP1

A. JJ012 xenografts were treated with 35 mg/kg BEZ235 daily or with vehicle alone by oral gavage for 21 days. Tumor size was determined by ultrasound every 3-4 days. Values represent mean volume ± SEM (n>5). **, $p<0.01$, compared with respective control group treated with vehicle. **B**. Representative examples of hematoxylin and eosin staining in tumor xenografts 21 days after vehicle or BEZ235 treatment; and representative immunohistochemistry staining for phospho-S6 in tumor xenografts 2 hr after vehicle or BEZ235 treatment. Original magnification: 400×. **C**. After 21 days of BEZ235 (BEZ) or vehicle (Veh.) treatment, 6 mice were given an additional dose of vehicle or 35 mg/kg BEZ235 2 hr before the tumors were harvested. The phosphorylation levels of AKT, S6, 4EBP1, and MAPK in those xenograft tumors were examined by immunoblots.

BEZ235-induced hyperphosphorylation of IGF1R family kinases and feedback activation of AKT in chondrosarcoma cells

Since it has been reported that rapamycin can induce feedback activation of AKT through RTK-dependent mechanisms (25), we used RTK arrays to explore the changes in RTK phosphorylation following 24 hr treatment with BEZ235. A common increase in the phosphorylation levels of IGF-1R and/or INSR was observed (Fig. 8.8C and 8.9A and 8.9B). We further checked the combinational effects of BEZ235 and the IGF1R/INSR inhibitor PQIP on AKT phosphorylation at the Thr^{308} site in OUMS-27 and SW1353 cells, and found that this remained suppressed following combination treatment with BEZ235 and PQIP for 24 hr (Fig.

8.8D). These data suggest that BEZ235 induces feedback activation of IGF1R/INSR, which further induces AKT phosphorylation in chondrosarcoma cells.

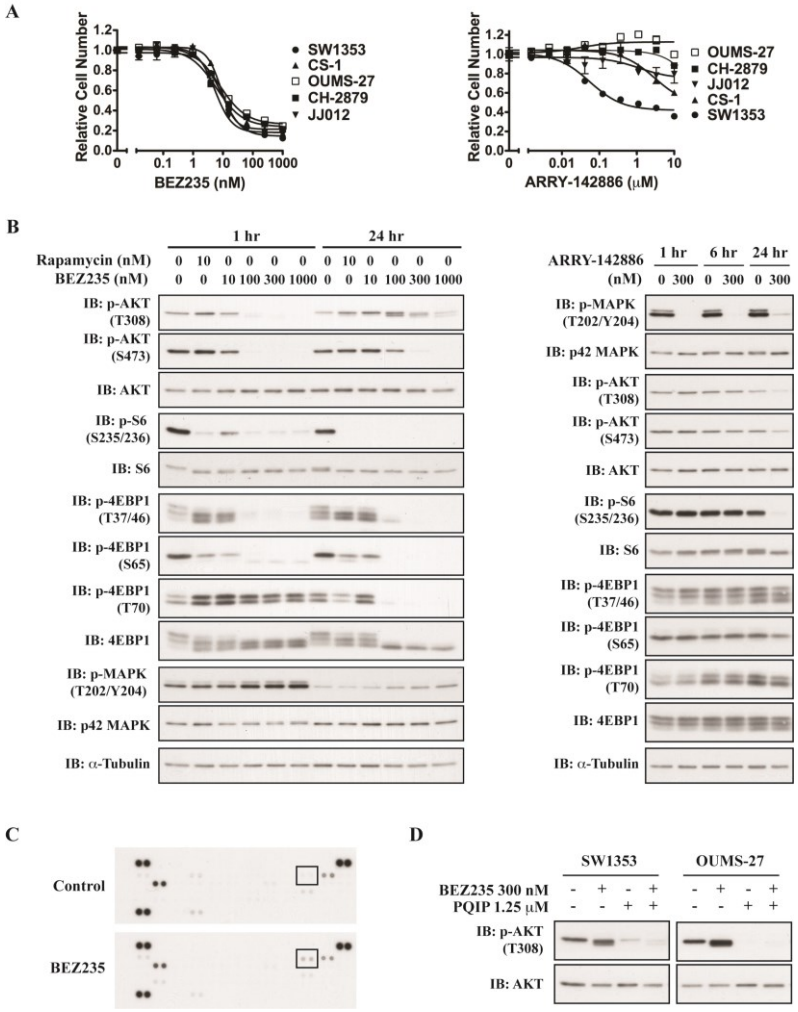

Figure 8.8. Effects of PI3K/mTOR inhibitor BEZ235 and MEK Inhibitor ARRY-142886 on chondrosarcoma cells *in vitro*.

A. Dose-dependent reduction in chondrosarcoma cell number following 72 hr treatment with BEZ235 (left panel) or ARRY-142886 (right panel). Values represent mean ± SEM (n=3). **B.** Effects of rapamycin, BEZ235 (left panel, in JJ012 cells), and ARRY-142886 (right panel, in SW1353 cells) treatment on the activation of AKT, S6, 4EBP1, and MAPK. **C**. The phosphorylation status of 49 RTKs in SW1353 cells was assessed by phospho-RTK arrays after 24 hr treatment with 0.1% DMSO (control) or 300 nM BEZ235. The location and names of capture antibodies are listed in Fig. 8.9B. The IGF1R kinase is highlighted with a rectangle. **C**. Combinational treatment with BEZ235 and IGF1R/INSR inhibitor PQIP prevented AKT from reactivation as evaluated by immunoblot at 24 hr.

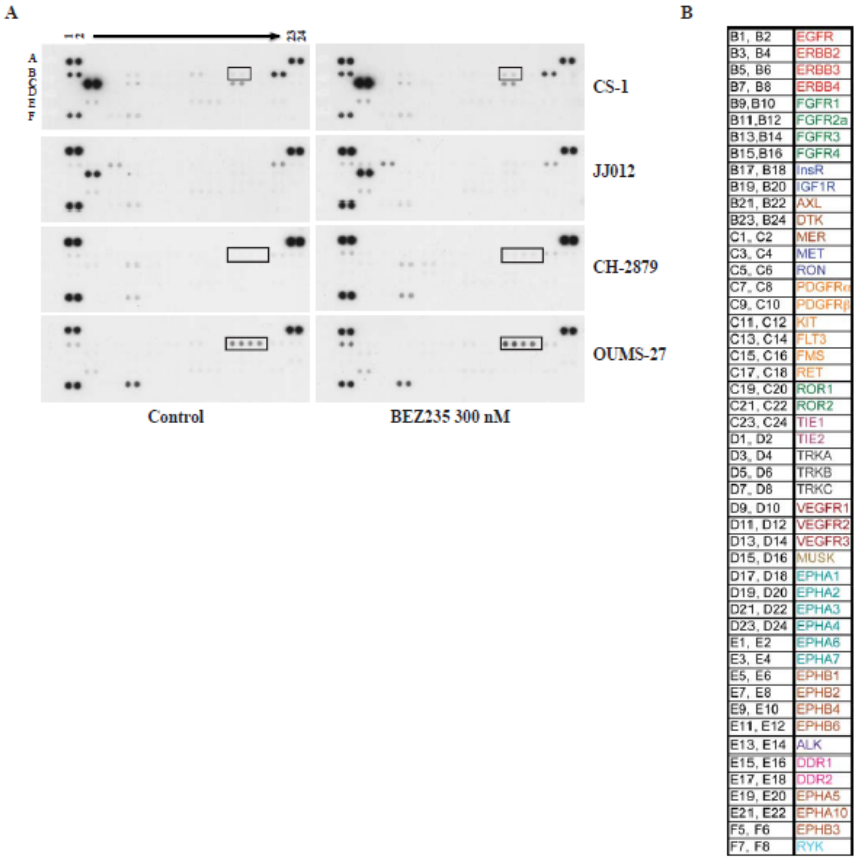

B

B1, B2	EGFR
B3, B4	ERBB2
B5, B6	ERBB3
B7, B8	ERBB4
B9,B10	FGFR1
B11,B12	FGFR2a
B13,B14	FGFR3
B15,B16	FGFR4
B17, B18	InsR
B19, B20	IGF1R
B21, B22	AXL
B23, B24	DTK
C1, C2	MER
C3, C4	MET
C5, C6	RON
C7, C8	PDGFRα
C9, C10	PDGFRβ
C11, C12	KIT
C13, C14	FLT3
C15, C16	FMS
C17, C18	RET
C19, C20	ROR1
C21, C22	ROR2
C23, C24	TIE1
D1, D2	TIE2
D3, D4	TRKA
D5, D6	TRKB
D7, D8	TRKC
D9, D10	VEGFR1
D11, D12	VEGFR2
D13, D14	VEGFR3
D15, D16	MUSK
D17, D18	EPHA1
D19, D20	EPHA2
D21, D22	EPHA3
D23, D24	EPHA4
E1, E2	EPHA6
E3, E4	EPHA7
E5, E6	EPHB1
E7, E8	EPHB2
E9, E10	EPHB4
E11, E12	EPHB6
E13, E14	ALK
E15, E16	DDR1
E17, E18	DDR2
E19, E20	EPHA5
E21, E22	EPHA10
F5, F6	EPHB3
F7, F8	RYK

Figure 8.9. Feedback effects on phosphorylation of RTKs following 24hr treatment of BEZ235 in chondrosarcoma cells.

A. The phosphorylation status of 49 RTKs was assessed by phospho-RTK arrays after 24 hr treatment with 0.1% DMSO (Control) of 300nM BEZ235. The positive controls are represented at A1-2, A23-24, adn F1-2; the PBS negative control is represented at F23-24. The location of capture antibodies for RTKs is listed in panel B. The changes in the phosphorylation level of IGF1R kinase family members were highlighted with a rectangle. **B**. The location of capture antibodies in RTK array.

NRAS-Mutated Chondrosarcoma Cell Line is Sensitive to Inhibition of MAPK pathway

In contrast to BEZ235, the MEK inhibitor ARRY-142886 (30) only inhibited the growth of SW1353, and had minimal effects on the other 4 chondrosarcoma cell lines (Fig. 8.5A, right panel). Sequencing of hotspot mutation-containing exons of *HRAS, KRAS, NRAS* (exon 2 and 3) and *BRAF* (exon 15) genes (31, 32) revealed a heterozygous c.181C>A (Q61K) mutation in *NRAS* in SW1353 cells (Fig. 8.10A). No mutation was found in these exons in the other four cell lines.

We additionally performed hotspot mutation analysis for NRAS exons 2 and 3 in DNA from frozen chondrosarcoma clinical samples. NRAS mutations were found to be specific for a subset of conventional central chondrosarcomas: six samples (12%) harbored NRAS mutations, including 2 c.181C>A (Q61K) mutations, and 4 c.182A>T (Q61H) mutations (Table 8.4). The other chondrosarcoma subtypes were negative.

We examined the effects of ARRY-142886 on the MAPK and PI3K/mTOR pathways in SW1353 cells. Treatment with ARRY-142886 for 1 hr led to a dose-dependent decrease in the phosphorylation of MAPK with complete inhibition at 300 nM, but had no obvious effect on the phosphorylation of AKT, S6, or 4EBP1 (Fig. 8.5B, right panel, Fig. 8.10B). With more prolonged treatment, a dramatic decrease in S6 phosphorylation and a partial inhibition of AKT phosphorylation were observed following 24 hr treatment with ARRY-142886 (Fig. 8.8B, right panel). The mechanism is unclear.

We also examined the combinational effects of BEZ235 and ARRY-142886 on MAPK and AKT signaling pathways in SW1353 cells, and found stronger inhibition in comparison to BEZ235 treatment alone (Fig. 8.10C). Correspondingly, the combination of BEZ235 and ARRY-142886 had additive inhibitory effects on the cell viability in SW1353 cells (Fig. 8.10D). However, apoptosis was not observed following the combination treatment.

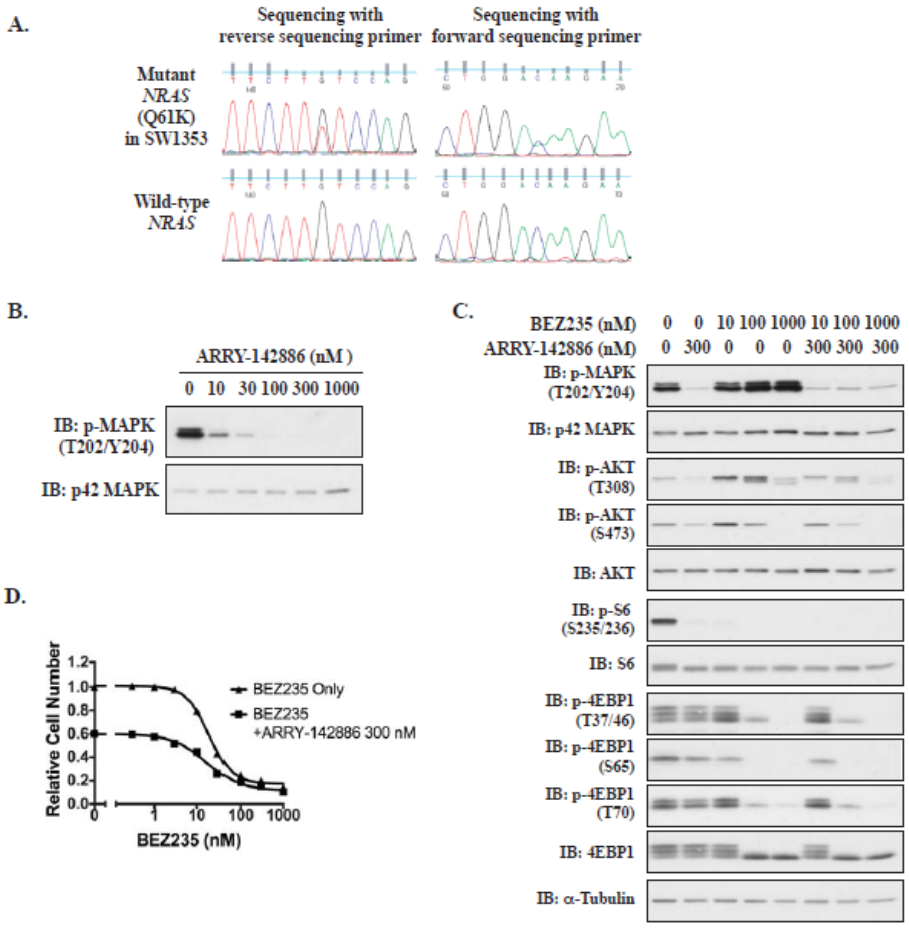

Figure 8.10. Combinational effects of BEZ235 and MEK inhibitor ARRY-142886 in SW1353 cells with *NRAS* mutation.

A. Sequencing was performed with forward or reverse sequencing primer. The top chromatogram is the mutant sequence of *NRAS* in SW1353 cells, and the bottom is a wild-type sequence. **B.** Effects of MEK inhibitor ARRY-142886 on MAPK phosphorylation evaluated by immunoblot at 1hr. **C**. Effects of combination treatment with BEZ235 and ARRY-142886 on the signaling of PI3K/mTOR pathway and MAPK pathway analyzed by immunoblot at 24hr in SW1353 cells. **D**. Effects of combination treatment with BEZ235 and ARRY-142886 on cell viability evaluated by CellTiter-Glo cell viability assay at 72 hr in SW1353 cells.

Discussion

Sarcomas constitute a heterogeneous family of mesenchymal tumors with divergent lineages of differentiation. Some sarcomas have well-defined pathogenic genetic lesions, such as activating kinase mutations in gastrointestinal stromal tumors (GIST) or translocations that yield aberrant chimeric transcription factors in Ewing sarcoma, for example. Many other subtypes of sarcomas have no known dominant molecular pathogenic lesions to explain disease initiation, maintenance, or progression. Chondrosarcomas fall in this latter category (1, 4, 33) although recent reports indicate that approximately half have mutations in *IDH1* or *IDH2* (34), which are considered to be an early event and of which the functional consequences remain to be established. Chondrosarcomas are notoriously resistant to conventional chemotherapeutic agents and currently no effective systemic therapies exist for metastatic or unresectable disease. A better molecular and biochemical understanding of this malignancy may yield novel and effective treatment approaches.

We explored the potential role of receptor tyrosine kinases in driving chondrosarcoma cell survival and proliferation. We identified constitutive, serum-independent activation of the MET, EGFR family, and IGF1R/INSR family kinases in multiple cell lines through as of yet unidentified mechanisms. Inhibition of RTK signaling by treatment with small molecule kinase inhibitors or by suppressing RTK expression with siRNA led to alterations in phosphorylation of downstream pathway members and a concomitant decrease in cellular proliferation. The incomplete block of cell growth suggests that other parallel pathways are also likely to be important.

Consistent with our data demonstrating RTK activation, strong and common phosphorylation of the downstream signaling proteins AKT, MEK, and S6 kinase was previously demonstrated using kinase substrate peptide arrays and extracts from chondrosarcoma cell lines and primary cultures (35). Here, we have linked RTK activation in chondrosarcoma cells to PI3K/AKT/mTOR signaling by demonstrating that RTK inhibitors suppress AKT and S6 phosphorylation. Moreover, high-level phosphorylation of S6 was found in approximately 70% of chondrosarcoma tumors, suggesting that activation of the PI3K/AKT/mTOR pathway in cell lines is clinically relevant. We also identified functional mutations of *NRAS* in a chondrosarcoma cell line and in clinical samples; these may contribute to the activation of the MAPK signaling pathway.

Notably, the heterogeneous pattern of RTK and NRAS activation among the varying human tumor-derived chondrosarcoma cell lines poses a challenge for the potential clinical development of tyrosine kinase inhibitors for this disease. Molecular profiling of signaling pathways in any given individual tumor might suggest a specific kinase inhibitor as a rational agent to test in that specific individual patient. Accordingly, such drugs could be studied in selected groups of patients, but this is a highly personalized and potentially cumbersome approach to

rare tumor subsets. An alternative approach may be to target shared downstream kinases, such as components of the PI3K/mTOR pathway. Indeed, the PI3K/mTOR inhibitor BEZ235 dramatically and potently blocked the growth of all chondrosarcoma cell lines *in vitro* and inhibited tumor growth *in vivo*. These data suggest that PI3K/mTOR pathway inhibitors, many of which are currently in clinical development (36-38), should be studied for their efficacy in the treatment of advanced chondrosarcoma.

In chondrosarcoma cells, BEZ235 exhibited more potent inhibition on cell growth than the mTORC1 inhibitor rapamycin and PI3K inhibitor GDC-0941. A detailed comparison of the effects of these three inhibitors on PI3K/mTOR signaling showed that BEZ235 is a more potent inhibitor of the phosphorylation of S6 and 4EBP1, important regulators of global protein synthesis and cap-dependent protein translation, respectively (39). Increases in the overall rate of protein synthesis as well as enhanced translation of oncogenes are often driven by the hyperactivation of RTKs and their downstream effectors, allowing uncontrolled growth and survival of cancer cells (40). The ability of BEZ235 to inhibit S6 and 4EBP1 phosphorylation both *in vitro* and *in vivo* may account for its potent antitumor activity in chondrosarcoma as well as in other cancer types (41, 42).

In the models presented here, the major effect of BEZ235 treatment was primarily cell cycle inhibition and a delay in tumor growth. A combination of BEZ235 and IGF1R/INSR inhibitor prevented AKT from reactivation, but still failed to induce apoptosis. High expression of BCL2 family members was recently shown to play an important role in chemoresistance of chondrosarcoma, and inhibition of BCL2 was shown to repair the apoptotic machinery, rendering chondrosarcoma cells chemosensitive (43). Inhibition of BCL2 may further supplement the observed outcome of PI3K/mTOR blockade by inducing cell apoptosis.

Recently, growth inhibitory effects of BEZ235 were reported in osteosarcoma, Ewing sarcoma, and rhabdomyosarcoma model systems (44). However, aside from their common mesenchymal origin, these sarcoma subtypes are generally chemosensitive and are unrelated to chemo- and radio-resistant chondrosarcomas, strongly differing in their biology and clinical behavior.

Table 8.4. NRAS Mutation Analysis in Chondrosarcoma Clinical Samples

	Total	Number with NRAS 181 C>A (%)	Number with NRAS 183 A>T (%)	Total number with NRAS mutations (%)
Chondrosarcoma				
Conventional Central	50	2 (4)	4 (8)	6 (12)
Grade I	13	0 (0)	0 (0)	0 (0)
Grade II	28	2 (7.1)	1 (3.6)	3 (10.7)
Grade III	9	0 (0)	3 (33.3)	3 (33.3)
Conventional Peripheral	17	0 (0)	0 (0)	0 (0)
Dedifferentiated Chondrosarcoma	10	0 (0)	0 (0)	0 (0)
Clear Cell Chondrosarcoma	9	0 (0)	0 (0)	0 (0)
Mesenchymal Chondrosarcoma	3	0 (0)	0 (0)	0 (0)

In our study, an activating *NRAS* mutation was identified in 12% of clinical chondrosarcoma samples. Two of these 6 chondrosarcoma samples also contain an *IDH1* R132C mutation (45). Similarly, SW1353 carries *IDH2* (45) and *NRAS* mutations, indicating that these mutations are not mutually exclusive. SW1353 cells were found to be sensitive to MEK inhibitors as well as to a PI3K/mTOR inhibitor. A combination of these two inhibitors had additive suppresion of SW1353 cell viability but did not induce apoptosis, consistent with reported effects of the combination in colorectal carcinomas with RAS mutations (46).

Taken together, our study identifies the heterogeneity of RTK activation present in chondrosarcoma cell lines, and suggests that inhibition of the PI3K/mTOR pathway, a common signaling pathway downstream of RTKs, may be a rational therapeutic strategy for the treatment of advanced chondrosarcoma. Identification of *NRAS* mutations show that a subset may be particularly sensitive to MEK inhibitors, and these should also be tested in selected patients with chondrosarcoma.

References

1.Bovee JV, Cleton-Jansen AM, Taminiau AH, Hogendoorn PC. Emerging pathways in the development of chondrosarcoma of bone and implications for targeted treatment. Lancet Oncol 2005;6: 599-607.

2.Riedel RF, Larrier N, Dodd L, Kirsch D, Martinez S, Brigman BE. The clinical management of chondrosarcoma. Curr Treat Options Oncol 2009;10: 94-106.

3.Skubitz KM, D'Adamo DR. Sarcoma. Mayo Clin Proc 2007;82: 1409-32.

4.Gelderblom H, Hogendoorn PC, Dijkstra SD, van Rijswijk CS, Krol AD, Taminiau AH, et al. The clinical approach towards chondrosarcoma. Oncologist 2008;13: 320-9.

5.Blume-Jensen P, Hunter T. Oncogenic kinase signalling. Nature 2001;411: 355-65.

6.Zwick E, Bange J, Ullrich A. Receptor tyrosine kinases as targets for anticancer drugs. Trends Mol Med 2002;8: 17-23.

7.Giamas G, Stebbing J, Vorgias CE, Knippschild U. Protein kinases as targets for cancer treatment. Pharmacogenomics 2007;8: 1005-16.

8.Sebolt-Leopold JS, English JM. Mechanisms of drug inhibition of signalling molecules. Nature 2006;441: 457-62.

9.Shao L, Kasanov J, Hornicek FJ, Morii T, Fondren G, Weissbach L. Ecteinascidin-743 drug resistance in sarcoma cells: transcriptional and cellular alterations. Biochem Pharmacol 2003;66: 2381-95.

10.Scully SP, Berend KR, Toth A, Qi WN, Qi Z, Block JA. Marshall Urist Award. Interstitial collagenase gene expression correlates with in vitro invasion in human chondrosarcoma. Clin Orthop Relat Res 2000: 291-303.

11.Gil-Benso R, Lopez-Gines C, Lopez-Guerrero JA, Carda C, Callaghan RC, Navarro S, et al. Establishment and characterization of a continuous human chondrosarcoma cell line, ch-2879: comparative histologic and genetic studies with its tumor of origin. Lab Invest 2003;83: 877-87.

12.Kunisada T, Miyazaki M, Mihara K, Gao C, Kawai A, Inoue H, et al. A new human chondrosarcoma cell line (OUMS-27) that maintains chondrocytic differentiation. Int J Cancer 1998;77: 854-9.

13.van Eijk R, Licht J, Schrumpf M, Talebian Yazdi M, Ruano D, Forte GI, et al. Rapid KRAS, EGFR, BRAF and PIK3CA mutation analysis of fine needle aspirates from non-small-cell lung cancer using allele-specific qPCR. PLoS One 2011;6: e17791.

14.Maira SM, Stauffer F, Brueggen J, Furet P, Schnell C, Fritsch C, et al. Identification and characterization of NVP-BEZ235, a new orally available dual phosphatidylinositol 3-kinase/mammalian target of rapamycin inhibitor with potent in vivo antitumor activity. Mol Cancer Ther 2008;7: 1851-63.

15.Waaijer CJ, de Andrea CE, Hamilton A, van Oosterwijk JG, Stringer SE, Bovée JVMG. Cartilage tumour progression is characterized by an increased expression of heparan sulphate 6O-sulphation-modifying enzymes. Virchows Arch 2012;461: 475-81.

16.Meijer D, de Jong D, Pansuriya TC, van den Akker BE, Picci P, Szuhai K, et al. Genetic characterization of mesenchymal, clear cell, and dedifferentiated chondrosarcoma. Genes Chromosomes Cancer 2012;51: 899-909.

17.Christensen JG, Schreck R, Burrows J, Kuruganti P, Chan E, Le P, et al. A selective small molecule inhibitor of c-

Met kinase inhibits c-Met-dependent phenotypes in vitro and exhibits cytoreductive antitumor activity in vivo. Cancer Res 2003;63: 7345-55.

18.Minkovsky N, Berezov A. BIBW-2992, a dual receptor tyrosine kinase inhibitor for the treatment of solid tumors. Curr Opin Investig Drugs 2008;9: 1336-46.

19.Ji QS, Mulvihill MJ, Rosenfeld-Franklin M, Cooke A, Feng L, Mak G, et al. A novel, potent, and selective insulin-like growth factor-I receptor kinase inhibitor blocks insulin-like growth factor-I receptor signaling in vitro and inhibits insulin-like growth factor-I receptor dependent tumor growth in vivo. Mol Cancer Ther 2007;6: 2158-67.

20.Buck E, Eyzaguirre A, Rosenfeld-Franklin M, Thomson S, Mulvihill M, Barr S, et al. Feedback mechanisms promote cooperativity for small molecule inhibitors of epidermal and insulin-like growth factor receptors. Cancer Res 2008;68: 8322-32.

21.Janku F, Wheler JJ, Westin SN, Moulder SL, Naing A, Tsimberidou AM, et al. PI3K/AKT/mTOR inhibitors in patients with breast and gynecologic malignancies harboring PIK3CA mutations. J Clin Oncol 2012;30: 777-82.

22.Meric-Bernstam F, Akcakanat A, Chen H, Do KA, Sangai T, Adkins F, et al. PIK3CA/PTEN mutations and Akt activation as markers of sensitivity to allosteric mTOR inhibitors. Clin Cancer Res 2012;18: 1777-89.

23.Wullschleger S, Loewith R, Hall MN. TOR signaling in growth and metabolism. Cell 2006;124: 471-84.

24.Bhaskar PT, Hay N. The two TORCs and Akt. Dev Cell 2007;12: 487-502.

25.Efeyan A, Sabatini DM. mTOR and cancer: many loops in one pathway. Curr Opin Cell Biol 2010;22: 169-76.

26.Alessi DR, Andjelkovic M, Caudwell B, Cron P, Morrice N, Cohen P, et al. Mechanism of activation of protein kinase B by insulin and IGF-1. EMBO J 1996;15: 6541-51.

27.Yang J, Cron P, Good VM, Thompson V, Hemmings BA, Barford D. Crystal structure of an activated Akt/protein kinase B ternary complex with GSK3-peptide and AMP-PNP. Nat Struct Biol 2002;9: 940-4.

28.Gingras AC, Raught B, Gygi SP, Niedzwiecka A, Miron M, Burley SK, et al. Hierarchical phosphorylation of the translation inhibitor 4E-BP1. Genes Dev 2001;15: 2852-64.

29.Karim MM, Hughes JM, Warwicker J, Scheper GC, Proud CG, McCarthy JE. A quantitative molecular model for modulation of mammalian translation by the eIF4E-binding protein 1. J Biol Chem 2001;276: 20750-7.

30.Yeh TC, Marsh V, Bernat BA, Ballard J, Colwell H, Evans RJ, et al. Biological characterization of ARRY-142886 (AZD6244), a potent, highly selective mitogen-activated protein kinase kinase 1/2 inhibitor. Clin Cancer Res 2007;13: 1576-83.

31.Vogelstein B, Fearon ER, Hamilton SR, Kern SE, Preisinger AC, Leppert M, et al. Genetic alterations during colorectal-tumor development. N Engl J Med 1988;319: 525-32.

32.Davies H, Bignell GR, Cox C, Stephens P, Edkins S, Clegg S, et al. Mutations of the BRAF gene in human cancer. Nature 2002;417: 949-54.

33.Chow WA. Update on chondrosarcomas. Curr Opin Oncol 2007;19: 371-6.

34.Amary MF, Bacsi K, Maggiani F, Damato S, Halai D, Berisha F, et al. IDH1 and IDH2 mutations are frequent

events in central chondrosarcoma and central and periosteal chondromas but not in other mesenchymal tumours. J Pathol 2011;224: 334-43.

35.Schrage YM, Briaire-de Bruijn IH, de Miranda NF, van Oosterwijk J, Taminiau AH, van Wezel T, et al. Kinome profiling of chondrosarcoma reveals SRC-pathway activity and dasatinib as option for treatment. Cancer Res 2009;69: 6216-22.

36.Garcia-Echeverria C, Sellers WR. Drug discovery approaches targeting the PI3K/Akt pathway in cancer. Oncogene 2008;27: 5511-26.

37.Engelman JA. Targeting PI3K signalling in cancer: opportunities, challenges and limitations. Nat Rev Cancer 2009;9: 550-62.

38.Liu P, Cheng H, Roberts TM, Zhao JJ. Targeting the phosphoinositide 3-kinase pathway in cancer. Nat Rev Drug Discov 2009;8: 627-44.

39.Gingras AC, Raught B, Sonenberg N. Regulation of translation initiation by FRAP/mTOR. Genes Dev 2001;15: 807-26.

40.Grzmil M, Hemmings BA. Translation regulation as a therapeutic target in cancer. Cancer Res 2012;72: 3891-900.

41.Chapuis N, Tamburini J, Green AS, Vignon C, Bardet V, Neyret A, et al. Dual inhibition of PI3K and mTORC1/2 signaling by NVP-BEZ235 as a new therapeutic strategy for acute myeloid leukemia. Clin Cancer Res 2010;16: 5424-35.

42.Nawroth R, Stellwagen F, Schulz WA, Stoehr R, Hartmann A, Krause BJ, et al. S6K1 and 4E-BP1 are independent regulated and control cellular growth in bladder cancer. PLoS One 2011;6: e27509.

43.van Oosterwijk JG, Herpers B, Meijer D, Briaire-de Bruijn IH, Cleton-Jansen AM, Gelderblom H, et al. Restoration of chemosensitivity for doxorubicin and cisplatin in chondrosarcoma in vitro: BCL-2 family members cause chemoresistance. Ann Oncol 2012;23: 1617-26.

44.Manara MC, Nicoletti G, Zambelli D, Ventura S, Guerzoni C, Landuzzi L, et al. NVP-BEZ235 as a new therapeutic option for sarcomas. Clin Cancer Res 2010;16: 530-40.

45.Pansuriya TC, van Eijk R, d'Adamo P, van Ruler MA, Kuijjer ML, Oosting J, et al. Somatic mosaic IDH1 and IDH2 mutations are associated with enchondroma and spindle cell hemangioma in Ollier disease and Maffucci syndrome. Nat Genet 2011;43: 1256-61.

46.Migliardi G, Sassi F, Torti D, Galimi F, Zanella ER, Buscarino M, et al. Inhibition of MEK and PI3K/mTOR suppresses tumor growth but does not cause tumor regression in patient-derived xenografts of RAS-mutant colorectal carcinomas. Clin Cancer Res 2012;18: 2515-25.

Chapter 9

Summary and concluding remarks

I. Chondrosarcoma from bench to bedside

Chapter 1 emphasizes the need for translational research in chondrosarcoma. Model systems are needed to establish a bench to bedside pipeline and translate laboratory findings to new therapeutic strategies. The application of model systems and the importance of translational research in chondrosarcoma is illustrated in **chapter 2** which reviews recent advances in pre-clinical chondrosarcoma research unraveling the role of EXT and IDH mutations in tumorigenesis as well as the therapeutic potential of targeting apoptosis and survival pathways. This thesis has shown the development of two model systems, both *in vitro* (cell lines, 2D and 3D culture) and *in vivo* (orthotopic mouse models), to aid in the search for new therapeutic strategies in chondrosarcoma. These model systems were subsequently used to study the role of apoptotic and survival pathways in chemoresistance.
As translational research is focused around the patient (fig 9.1), the collection of tumor material for frozen tissue, paraffin embedded tissue and cell culture is crucial. Frozen tissue can be used for DNA, RNA, and protein analysis, and paraffin embedded tissue is used for immunohistochemical analysis. When tissue microarrays (**chapter 6- 8**) are created, immunohistochemical analysis of multiple tissues simultaneously is facilitated. Collection of cells for cell culture and the use of cell lines (**chapter 3**) are vital in chondrosarcoma translational research, as in vitro tumor cell behavior can be studied in 2D and 3D culture (**chapter 5**) , in response to drug treatment (**chapters 5-8**). Moreover, stable cell lines can be used for injection in mouse models (**chapter 4**), to generate xenografts. These in vivo models enable the evaluation of drug efficacy taking into account the microenvironment. If a drug proves to be safe and effective in the mouse models, the results can guide the design of clinical trials increasing the chance of a successful trial. Conducting large clinical trials is difficult, requiring large multicenter collaboration given the rarity of these tumors, and obtaining funding is challenging. Through combined European efforts, such as EuroBoNet and euroSARC, the study of larger patient groups and design of multicenter clinical trials has been made possible, significantly advancing chondrosarcoma research.

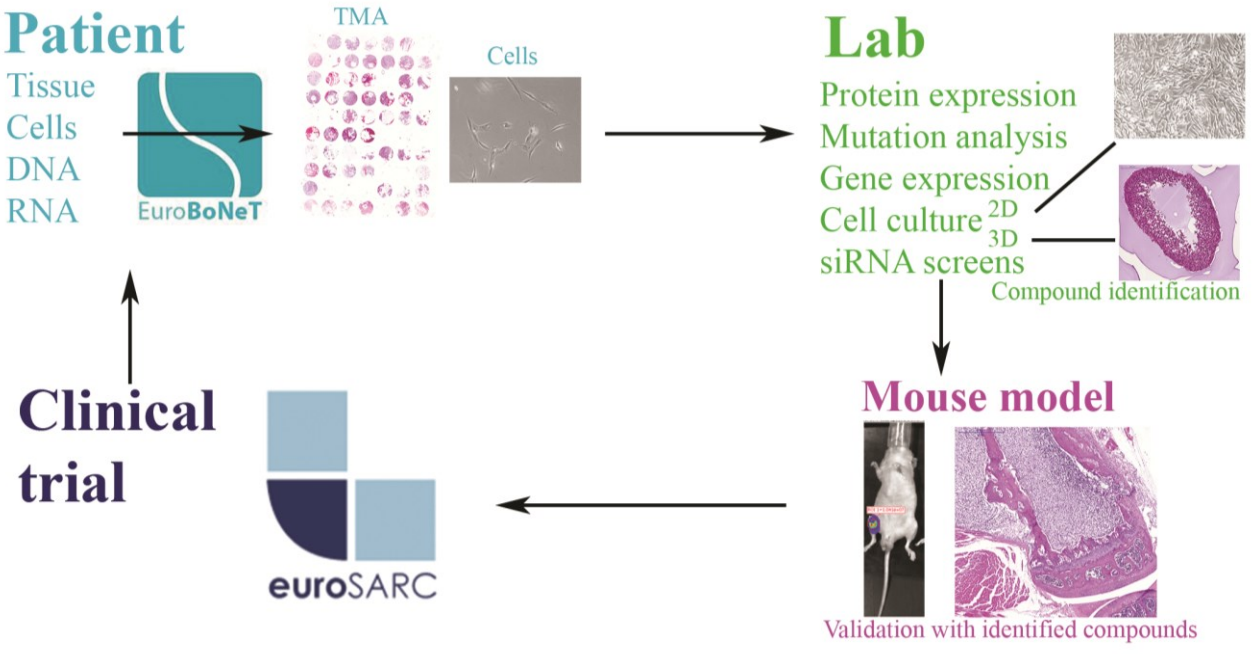

Figure 9.1. Chondrosarcoma from bench to bedside. Tumor material obtained from the patient can be used for several research purposes. Tissue embedded in paraffin can be used for protein expression and tissue microarrays are especially useful for the detection of proteins on multiple tumor tissues at once. Tissue microarrays are increasingly used for the identification of biomarkers. The isolation of fresh cells can be used for 2D and 3D cell culture to study in vitro tumor cell behavior and to possibly generate new cell lines. Frozen tissue can be used for DNA , RNA and protein analyses. Using cell culture models and siRNA screens, targets for treatment can be identified and compound screens can be performed. Compounds proven successful *in vitro,* can then be validated in the orthotopic mouse model, which will also allow for safety testing of combination strategies. Collaborative efforts such as EuroBoNet and euroSARC have enabled the collection of large databases for pre-clinical studies and are now facilitating clinical trials. For a rare malignancy such as chondrosarcoma, large cohort studies such as also performed in this thesis would have been impossible without the existence of such networks.

II. Cell lines as model systems to study chondrosarcoma

In order to establish representative models fully representing chondrosarcoma heterogeneity, in **chapter 3** the existing cell line panel for chondrosarcoma was expanded. Growing chondrosarcoma cells in culture is a challenge, and often overgrowth of fibroblasts is observed. At the start of this thesis, four stable chondrosarcoma cell lines were available, all derived from conventional central chondrosarcoma. One more cell line derived from conventional central chondrosarcoma and two derived from dedifferentiated chondrosarcoma were generated, and over time four additional cell lines were developed by others (1). This panel is representing the genetic heterogeneity of chondrosarcoma as three cell lines harbor IDH1 mutations, two IDH2 mutations, and five TP53 mutations. Moreover, all show loss of p16 expression, not always due to CDKN2A mutations/chromosomal aberrations, emphasizing the role of p16 in progression (table 3 chapter 3). The importance of a cell line panel representing the full heterogeneity of chondrosarcoma is subsequently illustrated in both **chapter 7** and **chapter 8**. In **chapter 7**, TP53 mutant cell lines were more sensitive to tyrosine kinase inhibition in combination with doxorubicin than TP53 wildtype cell lines. In **chapter 8** receptor tyrosine kinase profiling revealed heterogeneity in receptor tyrosine kinase activation among the cell lines. For instance, only SW1353 was particularly sensitive to MEK inhibition, which was based on the presence of an NRAS mutation, which was subsequently found in 12% of conventional central chondrosarcomas. These results strongly emphasize the importance of a broad and extensive cell line panel, representing the full heterogeneity of chondrosarcoma.

III. Orthotopic mouse model to study chondrosarcoma

Cell lines can provide information about tumor cell behavior, however, during the development of new therapeutic strategies, information about the tumor microenvironment should also be taken into account. The natural niche for chondrosarcoma is in the bone, and the communication between healthy bone and tumor cells as well as the influence of blood supply and the immune system on tumor development and chemoresistance cannot be investigated using cell lines. A reliable mouse model, representing human chondrosarcoma, could aid in providing answers about *in vivo* tumor behavior and drug response, and bridge the gap between cell lines and clinical trials.
As the natural niche for chondrosarcoma is in the bone, in **chapter 4**, orthotopicchondrosarcoma mouse models were created. A chondrosarcoma grade II cell line with IDH2 and TP53 mutations, and a chondrosarcoma grade III cell line wild type for IDH and TP53 were used. Rather than subcutaneous xenografting of tumor tissue or cell lines, luciferase transformed cell lines were injected in the tibiae. Therefore, tumor growth could be monitored throughout the duration of the experiment. Using doxorubicin, we show that this model is a valuable tool to

monitor *in vivo* tumor growth over time and will prove useful when testing new therapeutic strategies.

IV. Apoptosis signaling in conventional chondrosarcoma and rare chondrosarcorcoma subtypes

In **chapter 5** 2D and 3D cell culture models were used to explore the underlying causes of chemoresistance in conventional chondrosarcoma. We first established that resistance was not due to the extracellular matrix or multidrug resistance pump activity. As the literature showed high expression of the anti-apoptotic proteins Bcl-2 and Bcl-w in high grade conventional chondrosarcoma, the role of Bcl-2 proteins in chemoresistance was further investigated in the cell lines using the BH-3 mimetic ABT-737 (fig 9.2). Intermittent combination therapy with doxorubicin or cisplatin allowed for a dramatic reduction in concentrations used and induced apoptosis in all cell lines, indicating that Bcl-2 anti-apoptotic proteins are important in chemoresistance and that inhibition of Bcl-2 family members sensitizes chondrosarcoma cells for subsequent treatment with conventional chemotherapeutic agents.
In **chapter 6**, the original hypothesis was to correlate the morphological resemblance of clear cell chondrosarcoma, dedifferentiated chondrosarcoma and mesenchymalchondrosarcoma with the different stages of the growth plate by studying proteins involved in growth plate signaling. To this end a tissue microarray study was performed, however, protein expression patterns in the different subtypes were not correlated to differentiation stages in the growth plate. Interestingly, in both dedifferentiated and mesenchymal chondrosarcoma, differences in protein expression could be observed between the cartilaginous components and the anaplastic components, indicating distinctive pathway activations in the respective malignant components. In all subtypes, strong expression of anti-apoptotic Bcl-2 family members was found, suggesting a specific upregulation of anti-apoptotic proteins in chondrosarcoma irrespective of subtype. For dedifferentiated chondrosarcoma, 2 cell lines were available, and combination treatment of ABT-737 with doxorubicin or cisplatin showed a reduction in cell viability, indicating a similar resistance mechanism in place as in conventional chondrosarcoma. The uniformity of inhibition of chondrosarcoma cell proliferation through the combination of Bcl-2 family inhibitors with chemotherapy indicates that this strategy is a strong therapeutic candidate for chondrosarcoma treatment.

V. Survival pathways in conventional chondrosarcoma

In **chapters 7** and **8** increased kinase signaling was hypothesized to contribute to increased chondrosarcoma survival and as such to chemoresistance. As the Src pathway was previously found to be active in chondrosarcoma (2), its role in

chemoresistance was investigated in **chapter 7** . Moreover, since TP53 mutations are described to play a role in chemoresistance as well (3;4), a possible correlation between response and functional p53 was investigated. Cell lines with mutant TP53 were found to be especially sensitive to the combination of doxorubicin with dasatinib (Src inhibition, fig 9.2). However, dasatinib as a single agent has been shown to overcome chemoresistance in other malignancies despite TP53 mutations (5;6). Thus, also in chondrosarcoma resistance mechanisms could be operable that can be overcome by dasatinib. Interestingly, Src inhibition was additionally found to uniformly inhibit migration across all cell lines, suggesting that chemoresistance and migration act through different pathways.
In **chapter 8,** the chondrosarcoma cell line panel was used toinvestigate activation of receptor tyrosine kinases which further confirmed the heterogeneity of chondrosarcoma cell lines. Moreover, mutation analysis revealed an NRAS mutation in one cell line (SW1353) and in 12% of conventional chondrosarcomas. Downstream pathway analysis showed that despite heterogeneity in RTK activation, all cell lines showed activation of the PI3K/mTOR pathway (fig 9.2). Going back to human chondrosarcoma tissues using tissue microarrays, using pS6 immunohistochemistry, mTOR pathway activation was confirmed in 69% of conventional and 44% of dedifferentiated chondrosarcomas. Using both cell lines and xenograft mouse models, dual PI3K/mTOR inhibitors were found to successfully inhibit chondrosarcoma tumor growth.
In 2D cell culture, a combined strategy of dual PI3K/mTOR inhibitors with MEK inhibitors was found to be most successful, especially in NRAS mutated cells. However, in this study as well as in the literature, in RAS mutated cells such an approach does not lead to the induction of apoptosis.

VI. Leads for new therapeutic strategies to overcome chemoresistance in chondrosarcoma

Chemoresistance mechanisms in chondrosarcoma prove to be complicated. This thesis shows the activation of apoptosis pathways as well as survival pathways. In all cell lines inhibition of Bcl-2 family members with BH3 mimetics in combination with conventional chemotherapeutic agents leads to a dramatic reduction in cell viability. Src inhibition with dasatinib was found to be especially successful in TP53 mutant cell lines when combined with doxorubicin. In addition, circumventing the heterogeneity of upstream RTK activation, PI3K/mTOR activation was found to be a common downstream activation mechanism across cell lines. Moreover, preliminary data show that mTOR inhibition in combination with doxorubicin overcomes chemoresistance (van Oosterwijk et al, unpublished results), providing a third option for treatment in chondrosarcoma. Thus, using the bench to bedside pipeline, the importance of Bcl-2 family members, Src family kinases, and the PI3K/mTOR pathway in chemoresistance was demonstrated. Moreover, in vitro studies suggest a role for combination strategies, in which

inhibition of one of these three pathways renders the tumor cells sensitive to conventional chemotherapeutic agents, overcoming chemoresistance.

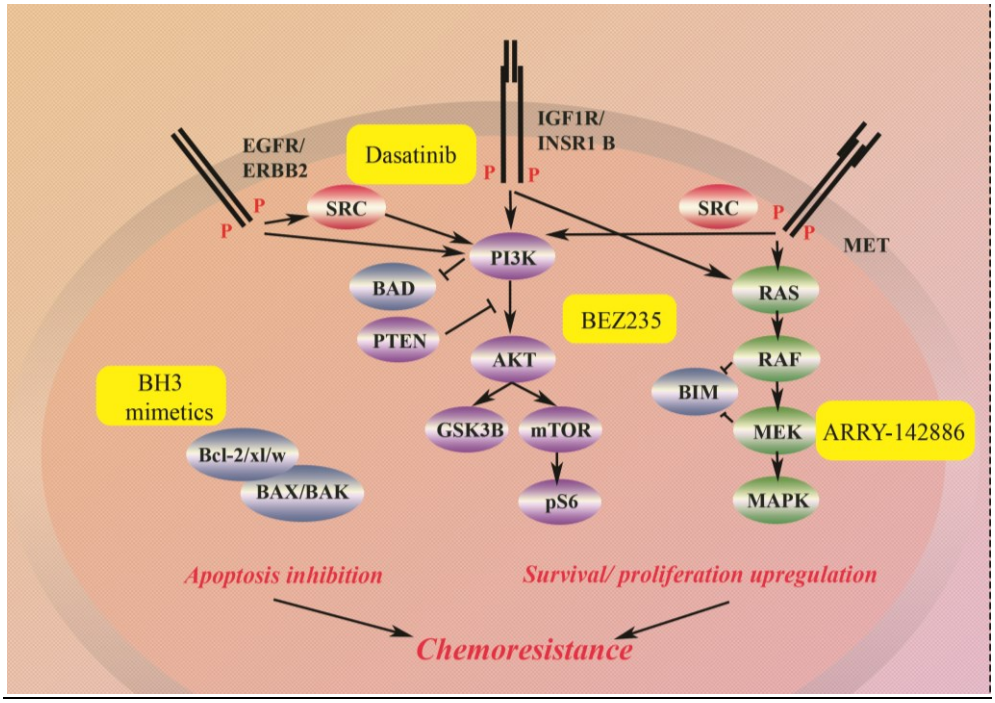

Figure 9.2. Interplay of survival and apoptosis pathways in chondrosarcoma. Activation of EGFR, IGF1R, and MET receptor tyrosine kinases (RTKs) were found using RTK profiling. Further investigation revealed activity of downstream PI3K/mTOR and MAPK pathways. Kinome profiling had previously revealed Src, PI3K, and AKT activity, and immunohistochemistry confirmed high mTOR signaling in human chondrasarcom tissues. The MAPK pathway was found to be activated in a subset of chondrosarcomas due to activating NRAS mutations, therefore downstream targeting with a MEK inhibitor is warranted. Active PI3K/mTOR, Src, and MAPK signaling pathways can lead to increased cell survival, but also promote resistance to apoptosis. Inhibition of apoptosis and upregulation of survival and proliferation can lead to chemoresistance, and targeting these pathways with inhibitors (shown in yellow) was found to successfully inhibit proliferation and overcome chondrosarcoma chemoresistance mechanisms. RAF and MEK can inhibit the transcription of the activating BH3 protein BIM, and PI3K can inhibit the sensitizing BH3 protein BAD. Lack of presence of these BH3 proteins leaves anti-apoptotic Bcl-2 proteins free to sequester the pro-apoptotic proteins BAX and BAK, in which case apoptosis is inhibited. As upregulation of anti-apoptotic Bcl-2 proteins was found in combination with activation of these kinase pathways, a therapeutic approach targeting these pathways simultaneously is advised.

VII. Future prospects

The orthotopic mouse model (**chapter 4**), can be used to explore the *in vivo* efficacy of the combination strategies that were shown here as *in vitro* data suggests these compounds are successful candidates for clinical trials. Future studies might explore the combination of dual PI3K/mTOR inhibitors with MEK inhibition in combination with BH-3 mimetics. This thesis shows the therapeutic potential of PI3K/mTOR inhibitors with MEK inhibitors (**chapter 8**) and of BH3 mimetics (**chapter 5&6**), and recently such an approach was shown to induce apoptosis in RAS mutated cells (7).
To further unravel the role of apoptosis and survival mechanisms in chemoresistance, in the final year a synthetic lethal siRNA screen with doxorubicin and cisplatin has been optimized and performed. The siRNA screen has been performed using the dharmacon libraries for ~80 apoptosis genes and a ~800 kinases. The results of this screen will identify the key players in the pathways described in this thesis and will increase our understanding of the complicated nature of chemoresistance of chondrosarcoma. Moreover, in the future, a similar approach can be used to investigate the resistance to radiotherapy, which will provide answers as to whether this resistance is mediated by similar pathways or that a distinct resistance mechanism is in place. In the coming years, the results from the apoptosis and kinase screen will need to be validated using shRNA, and protein expression of identified genes will be examined on human chondrosarcoma tissue using tissue microarrays. Using 2D cell culture and the orthotopic mouse model, inhibitors will be evaluated for their efficacy targeting the key players identified. This project was designed to corroborate and expand on earlier findings, and the ultimate goal will be proceed to clinical trials. The completion of the bench to bedside pipeline as shown here will hopefully aid in the rapid clinical implementation of effective targeted therapy for chondrosarcoma.

References

(1) Monderer D, Luseau A, Bellec A, David E, Ponsolle S, Saiagh S, Bercegeay S, Piloquet P, Denis MG, Lode L, Redini F, Biger M, Heymann D, Heymann MF, Le BR, Gouin F, Blanchard F. New chondrosarcoma cell lines and mouse models to study the link between chondrogenesis and chemoresistance. Lab Invest 2013.

(2) Schrage YM, Briaire-de Bruijn IH, de Miranda NFCC, van Oosterwijk JG, Taminiau AHM, van Wezel T, Hogendoorn PCW, Bovée JVMG. Kinome profiling of chondrosarcoma reveals Src-pathway activity and dasatinib as option for treatment. Cancer Res 2009;69(15):6216-22.

(3) Donzelli S, Fontemaggi G, Fazi F, Di AS, Padula F, Biagioni F, Muti P, Strano S, Blandino G. MicroRNA-128-2 targets the transcriptional repressor E2F5 enhancing mutant p53 gain of function. Cell Death Differ 2012; 19(6):1038-48.

(4) Huang Y, Jeong JS, Okamura J, Sook-Kim M, Zhu H, Guerrero-Preston R, Ratovitski EA. Global tumor protein p53/p63 interactome: making a case for cisplatin chemoresistance. Cell Cycle 2012;11(12):2367-79.

(5) Bosco R, Rabusin M, Voltan R, Celeghini C, Corallini F, Capitani S, Secchiero P. Anti-leukemic activity of dasatinib in both p53(wild-type) and p53(mutated) B malignant cells. Invest New Drugs 2012;30(1):417-22.

(6) Amrein L, Hernandez TA, Ferrario C, Johnston J, Gibson SB, Panasci L, Aloyz R. Dasatinib sensitizes primary chronic lymphocytic leukaemia lymphocytes to chlorambucil and fludarabine in vitro. Br J Haematol 2008;143(5):698-706.

(7) Tan N, Wong M, Nannini MA, Hong R, Lee LB, Price S, Williams K, Savy PP, Yue P, Sampath D, Settleman J, Fairbrother WJ, Belmont LD. Bcl-2/Bcl-xL Inhibition Increases the Efficacy of Mek Inhibition Alone and in Combination with PI3 Kinase Inhibition in Lung and Pancreatic Tumor Models. Mol Cancer Ther 2013

Chapter 10

Nederlandse Samenvatting

I. De brug van basaal onderzoek naar therapie

Het chondrosarcoom is een kwaadaardige kraakbeenvormende tumor in het bot en na het osteosarcoom de meest voorkomende kwaadaardige bottumor in de mens. Chondrosarcomen zijn resistent tegen conventionele radio- en chemotherapie. In **hoofdstuk 1** wordt het belang van translationeel onderzoek naar chondrosarcomen beschreven. Modelsystemen zijn noodzakelijk om resultaten die gevonden zijn in het laboratorium te vertalen naar patiënten en indien mogelijk nieuwe therapieën te ontwikkelen. De toepassing van modelsystemen en het belang van de juiste vertaling van de resultaten wordt beschreven in **hoofdstuk 2**, waar ook recente resultaten in pre-klinisch onderzoek naar chondrosarcomen worden toegelicht. Uit onderzoek wordt de rol van EXT en IDH mutaties in tumorgenese, alsook de mogelijkheden voor een gerichte therapie, duidelijk. In dit proefschrift wordt de ontwikkeling van twee modelsystemen, zowel *in vitro* (cellijnen, 2D and 3D kweken) als *in vivo* (orthotopische muismodellen) beschreven, om het onderzoek naar nieuwe behandelmethoden voor chondrosarcomen te ondersteunen. Deze modelsystemen werden vervolgens gebruikt om de rol van apoptose- en overlevings signaaltransductiecascades in chemoresistentie te bestuderen.
Aangezien het translationeel onderzoek zich richt op de patiënt, is het verzamelen van tumor materiaal (ingevroren, in paraffine of in celkweken) zeer belangrijk. Ingevroren materiaal kan worden gebruikt voor DNA, RNA en eiwit analyse.In paraffine bewaard weefsel kan worden gebruikt voor immunohistochemische analyse. Wanneer tissue micro-arrays (een paraffineblokje waarin meerdere kleine stukjes tumor van verschillende patienten worden geplaatst) worden gemaakt (**hoofdstuk 6-8**), kan gelijktijdig de immunohistochemische analyse van meerdere weefsels worden uitgevoerd. Het verzamelen van cellen voor celkweken en het gebruik van cellijnen (**hoofdstuk 3**) zijn essentieel voor het translationele onderzoek naar chondrosarcomen. Het *invitro* gedrag van tumorcellen kan worden bestudeerd in 2D en 3D kweken (**hoofdstuk 5**) evenals de reactie op medicijnen (**hoofdstuk 5-8**). Daarnaast kunnen stabiele cellijnen worden gebruikt voor injectie in muismodellen (**Hoofdstuk 4**) om xenograften te creëren. Deze *invivo*modellen maken het mogelijk om het effect van medicijnen te beoordelen waarbij rekening kan worden gehouden met omgevingsfactoren. Indien een behandeling veilig en effectief blijkt in muismodellen kan het resultaat gebruikt worden voor de ontwikkeling van klinische studies. Hiermee wordt de kans op succes verhoogd. Aangezien chondrosarcomenzeldzaam zijn is het alleen dankzij europese netwerken zoals EuroBoNet en EuroSARC mogelijk studies met grotere patientenpopulaties uit te voeren.

II. Cellijnen als modelsysteem om chondrosarcomen te onderzoeken

Om representatieve modellen te ontwikkelen, waarbij de grote verscheidenheid aan chondrosarcomen recht wordt gedaan, wordt in **hoofdstuk 3** beschreven hoe het

bestaande cellijn-panel voor chondrosarcomen kan worden uitgebreid. Het kweken van chondrosarcoom cellen is lastig en leidt vaak tot een overmaat aan fibroblasten. Bij het begin van het onderzoek beschreven in dit proefschrift stonden vier stabiele chondrosarcoom cellijnen ter beschikking, welke allen afkomstig waren van conventionele centrale chondrosarcomen. Gedurende het onderzoek werd een additionele cellijn afkomstig van conventioneel centraal chondrosarcoom gegenereerd en tevens twee cellijnen afkomstig van gededifferentieerd chondrosarcoom. Daarnaast werden zes cellijnen ontwikkeld door andere onderzoeksgroepen (1). Deze cellijnen zijn representatief voor de genetische verscheidenheid van chondrosarcomenaangezien drie cellijnen IDH1 mutaties laten zien, twee cellijnen IDH2 mutaties en vijf TP53 mutaties. Bovendien treedt bij alle cellijnen onderdrukking van p16 op (**hoodstuk 3, tabel 3**). Het belang van een set cellijnen die representatief is voor de verscheidenheid van chondrosarcomen wordt duidelijk gemaakt in zowel **hoofdstuk 7** als **hoofdstuk 8**. In **hoofdstuk 7** wordt beschreven dat cellijnen metTP53 mutaties gevoeliger zijn voor tyrosine kinase inhibitie in combinatie met doxorubicine dan cellijnen zonder TP53 mutaties. **Hoofdstuk 8** beschrijft het verschil in receptor tyrosine kinase activering tussen de verschillende cellijnen. Zo was bijvoorbeeld alleen de cellijn SW1353 bijzonder gevoelig voor MEK-inhibitie hetgeen verklaard kan worden uit de aanwezigheid van een NRAS mutatie. Deze mutatie was ook aanwezig in 12% van de conventionele centrale chondrosarcomen. Deze resultaten benadrukken het belang van een brede en uitgebreide set van cellijnen welke representatief zijn voor de onderlinge verschillen tussen de chondrosarcoom cellijnen.

III. Orthotopische muis modellen ter bestudering van chondrosarcomen

Hoewel cellijnen informatie kunnen verschaffen over het gedrag van tumorcellen, moet men voor de ontwikkeling van nieuwe therapeutische mogelijkheden ook rekening houden met de invloed van de omgeving op de tumorcel. De natuurlijke omgeving voor chondrosarcomenis het bot. De relatie tussen gezond weefsel en de tumorcel en de invloed van bloedtoevoer en het immuunsysteem op de ontwikkeling van tumorcellen kan echter niet worden bestudeerd bij het gebruik van cellijnen. Een betrouwbaar muismodel voor het menselijke chondrosarcoom is noodzakelijk om antwoorden te krijgen over de relatie tussen *in vivo* tumor gedrag en de respons op specifieke behandelingsmethoden. Tevens kan het een brug slaan tussen cellijn onderzoek en klinische studies.
In **hoofdstuk 4 wordt** de ontwikkeling van een dergelijk orthotopischmuismodel beschreven. Hiervoor werden een graad II cellijn, met IDH2 en TP53 mutaties, en een graad III cellijn, wild type voor IDH en TP53, gebruikt. Luciferasegetransformeerde cellijnen werden in de tibiae geinjecteerd. Hierdoor kon de groei van de tumor in het bot gemonitordworden gedurende het beloop van het experiment.

IV. Apoptose signaaltransductie cascade in conventionele en zeldzame vormen van chondrosarcomen

Hoofdstuk 5 beschrijft hoe 2D en 3D modellen kunnen worden gebruikt om de onderliggende oorzaken van chemoresistentie in conventionele chondrosarcomen te onderzoeken. Als eerste is aangetoond dat de resistentie niet afhankelijk is van de extracellulaire matrix of van de multidrug resistentiepompen. Aangezien de literatuur een hoge activiteit van de anti-apoptotische eiwitten Bcl-2 en Bcl-w in hooggradige conventionele chondrosarcomen laat zien, is de rol van Bcl-2 eiwitten verder onderzocht in cellijnen met behulp van de Bcl-2 remmer ABT-737. Tussentijdse combinatie behandeling, gebruik makend van doxorubicine of cisplatine, liet een dramatische reductie in de gebruikte concentraties zien en veroorzaakte apoptose in alle gebruikte cellijnen. Dit toont aan dat Bcl-2 anti-apoptotische eiwitten belangrijk zijn in chemoresistentie en dat inhibitie van Bcl-2 eiwitten chondrosarcoom cellen gevoelig maakt voor behandeling met traditionele chemofarmaca.
In **hoofdstuk 6** werd onderzocht of de eiwitexpressie van de verschillende zeldzame subtypes(gedifferentieerd, mesenchymaal, en clear cell chondrosarcoom) overeenkwam met de verschillende stadia van de groeiplaat. Voor dit doeleinde is een tissue microarray(een paraffineblokje waarin meerdere kleine stukjes tumor van verschillende patienten worden geplaatst) gemaakt. In tegenstelling tot de verwachting, kwam de expressie van de eiwitten in de verschillende subtypes niet overeen met de verschillende stadia in de groeiplaat waarmee ze morfologisch overeenkwamen. In alle subtypes werd sterke expressie van de anti-apoptotische Bcl-2 eiwitten gevonden, suggestief voor een specifieke opregulatie van anti-apoptotische eiwitten in chondrosarcomen, onafhankelijk van subtype. Van één van de zeldzame subtypes, gededifferentieerd chondrosarcoom, waren twee cellijnen beschikbaar. Combinatie behandeling met ABT-737 en doxorubicine of cisplatine liet een reductie in cel activiteit zien, wat wijst op eenzelfde resistentie mechanisme als in conventioneel chondrosarcoom. De overeenkomst die werd geobserveerd in de reactie op combinatie van Bcl-2 eiwit inhibitie en chemotherapie met betrekking tot een stop in cel proliferatie, suggereert dat deze strategie een sterke therapeutische kandidaat is voor de behandeling van chondrosarcomen.

V. Overlevings signaaltransductie cascade in conventionele chondrosarcomen

In de hoofdstukken 7 en 8 wordt onderzocht in hoeverre toegenomen kinase activiteit bijdraagt aan de overlevingskansen van chondrosarcoom cellen en eventuele resistentie tegen chemotherapie. Eerder is beschreven dat de Src signaaltransductie cascade actief is in het chondrosarcoom (2) en de rol van dit mechanisme bij chemoresistentie wordt bestudeerd in **hoofdstuk 7**. Aangezien TP53 mutaties eveneens een rol spelen bij chemoresistentie (3;4) is ook

onderzocht in hoeverre deze mutaties de respons op therapie beïnvloeden. Cellijnen met gemuteerd TP53 bleken extra gevoelig voor de combinatie van doxorubine met Src inhibitie door middel van dasatinib (Src inhibitie). Het is echter aangetoond dat monotherapie met dasatinib ook in staat is chemoresistentie te overwinnen in andere kwaadaardige tumoren, ondanks TP53 mutaties (5;6). Dus ook in het chondrosarcoom kunnen mechanismen actief zijn die met behulp van dasatinib geblokkeerd kunnen worden. Tevens werd gevonden dat Src inhibitie de migratie blokkeert bij alle gebruikte cellijnen, hetgeen suggereert dat migratie en chemoresistentie volgens verschillende mechanismen verlopen.
In **hoofdstuk 8** is het panel van chondrosarcoom cellijnengebruikt om de activatie van tyrosine-kinase receptoren (RTK) te onderzoeken, welke de onderlinge verschillen tussen de verschillende cellijnen bevestigde. Daarnaast werd door mutatie analyse aangetoond dat één cellijn een NRAS mutatie bevatte (SW1353), welke kon worden bevestigd in 12% van de conventionele chondrosarcomen. Ondanks verschillen in RTK activatie lieten alle cellijnen activatie van PI3K/mTOR zien. Activatie van het mTOR mechanisme kon worden aangetoondin 69% van de conventionele en 44% van de gededifferentieerde chondrosarcomen. Zowel bij het gebruik van cellijnen als bij muismodellen werd aangetoond dat de tumorgroei succesvol kan worden afgeremd door het gebruik van PI3K/mTOR inhibitoren.
In 2D celkweken bleek een gecombineerde aanpak van PI3K/mTOR remmers met MEK remmers het meest effectief, in het bijzonder in NRAS gemuteerde cellen. Echter, zowel in dit onderzoek als uit de literatuur blijkt dat bij RAS mutaties dit niet tot apoptose leidt.

VI.Mogelijkheden voor nieuwe therapeutische strategieën

Het is gebleken dat de mechanismen voor chemoresistentie in chondrosarcomen complex zijn. In dit proefschrift worden de rol van apoptose- en de overlevings signaaltransductie cascades in chemoresistentie onderzocht. In alle bestudeerde cellijnen leidde blokkering van Bcl-2 in combinatie met chemotherapie tot een duidelijke afname van de celgroei.Src-inhibitie door middel van dasatinib was met name succesvol in cellijnen met een TP53 mutatie indien dit gecombineerd werd met doxorubicine. Daarnaast werd aangetoond dat in alle cellijnen de PI3K/mTOR signaaltransductie cascade geactiveerd is, welke gebruikt kon worden om de verscheidenheid van de RTK activering te omzeilen. Bovendien laten voorlopige data zien dat mTOR afremming in combinatie met doxorubicine de mogelijkheid biedt om chemoresistentie te overwinnen (van Oosterwijk et al, ongepubliceerde resultaten). Dit biedt daarmee een derde mogelijkheid voor de behandeling van het inoperabele chondrosarcoom. Het belang van Bcl-2, Src-kinase en het PI3K/mTOR mechanisme als mogelijke aangrijpingspunten voor behandeling is daarmee aangetoond. Daarnaast kan op basis van *in-vitro* studies worden geconcludeerd dat

een combinatie van middelen succesvol kan zijn, met name in die gevallen waar één van de geactiveerde routes de cel gevoeliger maakt voor chemotherapie.

VII. Toekomstmogelijkheden

Het orthotopische muismodel (**hoofdstuk 4**) kan worden gebruikt om *in vivo* de effectiviteit te onderzoeken van de combinatie van behandelmethoden die als mogelijke kandidaten uit *in vitro* onderzoek naar voren gekomen zijn. Toekomstig onderzoek kan zich dan richten op duale PI3K/mTOR inhibitie in combinatie met MEK afremming. Dit proefschrift laat de therapeutische mogelijkheden van zowel PI3K/mTOR gecombineerd met MEK-remmers (**hoofdstuk 8**) alsook van Bcl-2 inhibitors zien (**hoofdstuk 5 en 6**). Recent is aangetoond dat een benadering waarbij deze therapieën gecombineerd worden leidt tot apoptose in cellen met RAS-mutaties (7).
In het laatste jaar van het onderzoek beschreven in dit proefschrift is nog een "synthetic lethal siRNA screen", gebruik makend van doxorubicine en cis-platina, geoptimaliseerd en uitgevoerd om verdere opheldering van de rol van de apoptose- en de overlevings signaaltransductie cascade bij chemoresistentie te verkrijgen. Hierbij is gebruik gemaakt van de Dharmacon bibliotheek (ca 80 apoptose genen en ca 800 kinases). Verwacht wordt dat op basis van deze screening het mogelijk zal zijn om de belangrijkste componenten voor de beschreven mechanismen te identificeren, wat tot een beter begrip van de onderliggende factoren zal leiden. In de toekomst zal deze methode ook worden gebruikt om de resistentie voor radiotherapie in het chondrosarcoom te onderzoeken. Dit kan dan inzicht geven in de resistentie voor radiotherapie en of dit op dezelfde mechanismen berust of dat hier een heel ander mechanisme een rol speelt. In de komende periode zullen de resultaten van apoptose en kinase screening gevalideerd moeten worden door middel van short hairpin RNAs (shRNA). Doormiddel van het introduceren van shRNA in een cel kan specifiek gen expressie worden onderdrukt. Hiermee geïdentificeerde targets kunnen vervolgens met gebruik van de pijplijn beschreven in dit proefschrift gevalideerd worden. In combinatie met de hier beschreven resultaten wordt hopelijk snel een weg gebaand naar implementatie van doelgerichte therapie voor inoperabel of gemetastaseerd chondrosarcoom.

Referenties

(1) Monderer D, Luseau A, Bellec A, David E, Ponsolle S, Saiagh S, Bercegeay S, Piloquet P, Denis MG, Lode L, Redini F, Biger M, Heymann D, Heymann MF, Le BR, Gouin F, Blanchard F. New chondrosarcoma cell lines and mouse models to study the link between chondrogenesis and chemoresistance. Lab Invest 2013 August 19.

(2) Schrage YM, Briaire-de Bruijn IH, de Miranda NFCC, van Oosterwijk JG, Taminiau AHM, van Wezel T, Hogendoorn PCW, Bovée JVMG. Kinome profiling of chondrosarcoma reveals Src-pathway activity and dasatinib as option for treatment. Cancer Res 2009;69(15):6216-22.

(3) Donzelli S, Fontemaggi G, Fazi F, Di AS, Padula F, Biagioni F, Muti P, Strano S, Blandino G. MicroRNA-128-2 targets the transcriptional repressor E2F5 enhancing mutant p53 gain of function. Cell Death Differ 2012;19(6):1038-48.

(4) Huang Y, Jeong JS, Okamura J, Sook-Kim M, Zhu H, Guerrero-Preston R, Ratovitski EA. Global tumor protein p53/p63 interactome: making a case for cisplatin chemoresistance. Cell Cycle 2012;11(12):2367-79.

(5) Bosco R, Rabusin M, Voltan R, Celeghini C, Corallini F, Capitani S, Secchiero P. Anti-leukemic activity of dasatinib in both p53(wild-type) and p53(mutated) B malignant cells. Invest New Drugs 2012;30(1):417-22.

(6) Amrein L, Hernandez TA, Ferrario C, Johnston J, Gibson SB, Panasci L, Aloyz R. Dasatinib sensitizes primary chronic lymphocytic leukaemia lymphocytes to chlorambucil and fludarabine in vitro. Br J Haematol 2008;143(5):698-706.

(7) Tan N, Wong M, Nannini MA, Hong R, Lee LB, Price S, Williams K, Savy PP, Yue P, Sampath D, Settleman J, Fairbrother WJ, Belmont LD. Bcl-2/Bcl-xL Inhibition Increases the Efficacy of Mek Inhibition Alone and in Combination with PI3 Kinase Inhibition in Lung and Pancreatic Tumor Models. Mol Cancer Ther 2013.

Curriculum Vitae

Jolieke Gerdy van Oosterwijk was born in Leiden, the Netherlands, on April 15th 1984. She attended preuniversity school (gymnasium) at the international school "Het Rijnlands Lyceum" in Oegstgeest, the Netherlands, where she received Bilingual Education obtaining the International Baccalaureate English A2 certificate. After graduating in 2002, she attended the Utrecht International Honours College "University College Utrecht" where she followed the pre-med track with a minor a psychology. During this time Jolieke participated in an EAP exchange program at the University of California at Berkeley. Jolieke wrote a Bachelor's thesis on identifying proteins in head and neck tumors using Mass Spectrometry at the department of Mass Spectrometry/Proteomics, Netherlands Proteomics Insitute, Utrecht University, under the supervision of Dr. M Slijper. Extracurricularly Jolieke became a certified freelance photographer, and she graduated as a Bachelor of Science with honors in 2005. Jolieke continued her studies in Berlin, Germany at the Charité Medical School, where she entered the International Elite Master Programme, Molecular Medicine, from which she graduated in 2008. Her master's thesis was written in the lab of Prof. Dr. rer. nat. Eva Klopocki and led to the discovery of a novel mutation in noncoding elements 5' of SOX9 and a publication in Nature Genetics. Immediately after finishing her master's thesis, Jolieke started her PhD education, at the Department of Pathology, LUMC, under supervision of Prof. dr. J.V.M.G. Bovée, of which the results are described in this thesis. In June 2013, Jolieke started as a postdoctoral fellow in the laboratory of Sharyn Baker, PharmD, at the Department of Pharmaceutical Sciences of St Jude Children's Research Hospital, Memphis, TN, USA.

List of Publications

- van Oosterwijk JG, Anninga JK, Gelderblom H, Cleton-Jansen AM, Bovée JVMG. Update on targets and novel treatment options for high grade osteo- and chondrosarcoma *Hem/Onc Clinics of North America*

- van Oosterwijk JG, de Jong D, van Ruler MAJH, Hogendoorn PCW, Dijkstra PDS, van Rijswijk CSP, Machado I, Llombart-Bosch A, Szuhai K, Bovée JVMG. Three new chondrosarcoma cell lines: one grade III conventional central chondrosarcoma and two dedifferentiated chondrosarcomas of bone. *BMC Cancer*

- van Oosterwijk JG, Plass JRM, Meijer D, Que I, Karperien M, Bovée JVMG. Orthotopic mouse model for chondrosarcoma of bone: an *in vivo* tool for drug testing. *Submitted*

- van Oosterwijk JG, Herpers B, Meijer D, Briaire de Bruijn IH, Cleton-Jansen AM, Gelderblom H, van de Water B, Bovée JVMG. Restoration of chemosensitivity for doxorubicin and cisplatin in chondrosarcoma in vitro: Bcl-2 family members cause chemoresistance *Annals of Oncology*

- van Oosterwijk JG, Meijer D, van Ruler MAJH, van den Akker BEWM, Oosting J, Krenács T, Picci P, Flanagan AM, Liegl-Atzwanger B, Leithner A, Athanasou N, Daugaard S, Hogendoorn PCW, Bovée JVMG. Screening for potential targets for therapy in mesenchymal, clear cell, and dedifferentiated chondrosarcoma reveals Bcl-2 family members and TGFbeta as potential targets. *American Journal of Pathology*

- van Oosterwijk JG, van Ruler MAJH, Briaire- de Bruijn IH, Herpers B, Gelderblom H, van de Water B, Bovée JVMG. Src kinases in chondrosarcoma chemoresistance and migration: dasatinib sensitizes to doxorubicin in TP53 mutant cells. *Britisch Journal of Cancer*

- Zhang Y-X, van Oosterwijk JG, Sicinska E, Moss S, Remillard SP, van Wezel T, Bühnemann C, Hassan AB, Demetri GD, Bovée JVMG, Wagner AJ. Functional profiling of receptor tyrosine kinases and downstream signaling in human chondrosarcomas identifies pathways for rational targeted therapy. *Clinical CancerResearch*

- Schrage YM, Briaire-de Bruijn IH, de Miranda NF, van Oosterwijk JG, Taminiau AH, van Wezel T, Hogendoorn PCW, Bovée JVMG. Kinome profiling of chondrosarcoma reveals SRC-pathway activity and dasatinib as option for treatment. *Cancer Research*

- Waaijer CJ, de Andrea CE, Hamilton A, van Oosterwijk JG, Stringer SE, Bovée JVMG. Cartilage tumour progression is characterized by an increased expression of heparan sulphate 6O-sulphation-modifying enzymes. *Virchows Archive*

- Pansuriya TC, van Eijk R, d'Adamo P, van Ruler MA, Kuijjer ML, Oosting J, Cleton-Jansen AM, van Oosterwijk JG, Verbeke SL, Meijer D, van Wezel T, Nord KH, Sangiorgi L, Toker B, Liegl-Atzwanger B, San-Julian M, Sciot R, Limaye N, Kindblom LG, Daugaard S, Godfraind C, Boon LM, Vikkula M, Kurek KC, Szuhai K, French PJ, Bovée JVMG. Somatic mosaic IDH1 and IDH2 mutations are associated with enchondroma and spindle cell hemangioma in Ollier disease and Maffucci syndrome. *Nature Genetics*

- Kurth I, Klopocki E, Stricker S, van Oosterwijk JG, Vanek S, Altmann J, Santos HG, van Harssel JJ, de Ravel T, Wilkie AO, Gal A, Mundlos S. Duplications of noncoding elements 5' of SOX9 are associated with brachydactyly-anonychia. *Nature Genetics*

Acknowledgements

It is my distinct honor to be able to thank all of you who have supported me throughout the years. Realizing that to do so with words does not do it justice, and that I am bound to forget some, I will be brief. I owe much gratitude to prof. dr. J.V.M.G. Bovée, thank you for making this work possible, Judith, thank you for the endless opportunities and preparing me to pursue my scientific career. Prof. P.C.W. Hogendoorn , Pancras, thank you for taking me into your lab and providing a scientific environment and always being enthusiastic. Prof. Dr. A.J. Gelderblom, Hans, you have been a wonderful collaborator and I have enjoyed working with you. To all the people in the lab, both those that have left and have joined, I have enjoyed working with all of you, it has been a great experience. In particular I will have to mention Maayke, we started on the same day and worked side by side for 4 years, it was sad to see you leave. Inge, you have been wonderful, I will never forget you. Marieke, you were a great roommate. To my family, I could not have done any of this without your everlasting belief in me.